IMMUNE RESPONSES TO HUMAN CYTOMEGALOVIRUS (HCMV) REACTIVATION IN ALLOGENEIC HAEMATOPOIETIC STEM CELL TRANSPLANTATION (HSCT)

by

NORFARAZIEDA HASSAN

A thesis submitted to
the University of Birmingham
for the degree of
DOCTOR OF PHILOSOPHY

Institute of Cancer and Genomic Sciences
College of Medical and Dental sciences
The University of Birmingham
September 2019

UNIVERSITY OF
BIRMINGHAM

University of Birmingham Research Archive

e-theses repository

This unpublished thesis/dissertation is copyright of the author and/or third parties. The intellectual property rights of the author or third parties in respect of this work are as defined by The Copyright Designs and Patents Act 1988 or as modified by any successor legislation.

Any use made of information contained in this thesis/dissertation must be in accordance with that legislation and must be properly acknowledged. Further distribution or reproduction in any format is prohibited without the permission of the copyright holder.

ABSTRACT

Allogeneic haematopoietic stem cell transplantation (allo-HSCT) is commonly used to treat a range of haematological malignancies with Human cytomegalovirus (HCMV) reactivation as one of the major risk factors. HCMV reactivation is crucial as it can lead to HCMV disease and increase mortality. The CMV serostatus of the recipient and donor in the HSCT setting plays a role in determining the risk of the patient getting viral reactivation. Recent studies have also suggested that CMV reactivation after HSCT is associated with faster immune reconstitution and reduction of leukaemia relapse. This project studied the phenotype kinetics of immune cells including Natural Killer (NK) cells, $CD4^+$, $CD8^+$ and TCRγδ T cells in HSCT patients after CMV reactivation. Also, the tetramer technique was used to study CMV specific $CD8^+$ and $CD4^+$ T cells responses reconstitution in these HSCT patients. Our data show that CMV reactivation gives significant impact on immune reconstitution of allo-HSCT by imprinting the immune cells with phenotypes specific to CMV. One major impact on NK cells seen in allo-HSCT with CMV reactivation is the huge expansion of $CD56^{dim}CD16^{bright}$ $NKG2C^+$ NK cells or the controversial 'memory-like' NK cells. The expansion of this NK population results in enhanced cytokines production after stimulation. In overall, the study of CMV reactivation in HSCT will ultimately give some insight of how to modify the clinical practice to target CMV reactivation and improve the overall clinical outcome.

ACKNOWLEDGEMENTS

First and foremost, I would like to express my sincere gratitude to my main supervisor, Professor Paul Moss for his continuous support and opportunity in doing my PhD study and with the huge and immense knowledge sharing throughout this long journey. Then, I would like to thank my co-supervisor, Dr Jianmin Zuo for his advice, encouragement and patience in guiding me to be a good scientist.

Specifically, I would like to thank Jane Nunnick for helping me with the collection of samples and clinical data from QE hospital; the Transplant group, Dr Suzy Eldershaw, Christine Stephens, Tanuja Rai, Uzma Altaf, Dr Kriti Verma, Dr Luke Maggs and Dr Francesca Kinsella for helping me with the patients' samples and lab work, especially Suzy who mostly involved in the initial part of my study, Jusnara Begum and Sara Barbieri from CMV group for helping me with recruitment of healthy donors and some experiments, Jimmy Van Hear for being my lab partner for gd T cell work, and also Dave Greenwood and Dr Wayne Croft for helping me with clinical data and statistical and R analysis. I also would like to thank Dr Hayden Pearce and Samantha Nicol for feeding me with biscuits and never stopped making me laugh with their weird jokes. In addition, I would like to acknowledge Amandeep Kaur, Dr Gokhan Tut, Megan Butler, Dr Guido Fermento, Dr Duncan Murray and Dr Rachel Bruton for the pep talk and help as well as the rest of the members of the Moss group for the 'fun' we had all these years.

My greatest gratitude also goes to the Ministry of Higher Education and Universiti Sains Malaysia for the financial support, as well as Bloodwise for the funding for the research and collaborators who contributed in this study. Last but not least, I would like to thank my family and friends for supporting me in the entire journey of my PhD. Thank you all.

TABLE OF CONTENTS

CHAPTER 1: INTRODUCTION 1
1.1. Haematopoietic stem cell transplantation (HSCT) 1
1.1.1. Allogeneic haematopoietic stem cell transplantation (allo-HSCT) 2
1.1.1.1. Human Leukocyte Antigen (HLA) typing and match 5
1.1.1.2. Minor Histocompatibility Antigens 7
1.1.1.3. The source of stem cell grafts 8
1.1.1.4. Transplant Conditioning 9
1.1.1.5. Donor lymphocyte infusion (DLI) 10
1.1.1.6. Chimerism 10
1.1.1.7. Graft versus host disease (GvHD) 11
1.1.1.8. Graft versus leukaemia (GvL) 12
1.1.2. Immune reconstitution after allogeneic HSCT 14
1.1.2.1. Natural Killer (NK) cells 17
1.1.2.2. $CD8^+$ and $CD4^+$ T cells 19
1.1.2.3. TCRγδ T cells 20

1.2. Human Cytomegalovirus (HCMV) 23
1.2.1. Introduction to HCMV 23
1.2.2. T cell response to CMV 24
1.2.3. The NK cells response to HCMV 25

1.3. CMV reactivation after allogeneic HSCT 26
1.3.1. Definition of 'CMV reactivation' 27
1.3.2. Prophylaxis and treatment for CMV reactivation 28
1.3.3. The importance of recipient and donor serostatus in CMV risk 29
1.3.4. CMV reactivation after autologous HSCT 31

1.4. The impact of CMV reactivation on patient outcomes after allogeneic HSCT 32
1.4.1. Expansion in adaptive or memory like $NKG2C^+$ NK cells 34
1.4.2. CMV-$CD8^+$ and $CD4^+$ T cell specific responses 36
1.4.3. Vδ1 T cells and the response to CMV reactivation 38

1.5. The potential association of CMV reactivation with reduced risk of leukaemia relapse 38
1.6. Hypothesis and objectives 40

CHAPTER 2: METHODOLOGY 42
2.1. Materials and reagents 42
2.1.1. Flow cytometry staining and cell culture 42
2.1.2. HLA typing PCR-SSP 44
2.1.3. CMV IgG ELISA 44
2.1.4. NK cell Intracellular cytokine staining 45

2.2. Study design 46
2.2.1. Patients 46
2.2.2. Healthy donors 47
2.2.3. Clinical data and patients' information 48

2.3. Samples processing 48
2.3.1. Isolation of Peripheral Blood Mononuclear Cells (PBMCs) 48
2.3.1.1. Cryopreservation and storage 49

2.3.1.2. Thawing of PBMCs 50
2.3.2. Serum collection for DNA extraction 50
2.3.3. Urine concentration for DNA extraction 50

2.4. HLA typing of healthy donors 51

2.4.1. Polymerase chain reaction-sequence specific primers (PCR-SSP) 51
2.4.2. Master mix preparation and PCR conditions 51
2.4.3. Gel electrophoresis 53

2.5. CMV IgG Enzyme linked Immunosorbant assay (ELISA) testing for healthy donors 54

2.5.1. Coating of plate with CMV lysate 54
2.5.2. Addition of IgG antibodies into the plate 54

2.6. Flow cytometry and PBMCs surface staining 57

2.6.1. Flow cytometry compensation 57
2.6.1.1. Compensation with antibody capture beads 57
2.6.1.2. Compensation with PBMCs 58
2.6.2. Flow cytometry plots analysis 58
2.6.3. Titration of newly purchased antibodies 59
2.6.3.1. PBMCs surface staining 60
2.6.4. T cell–HLA Class I and Class II tetramer staining 64
2.6.4.1. Tetramer assay and optimisation 64
2.6.4.2. Tetramer, $CD8^+$ and $CD4^+$ T cell staining 66

2.7. PBMCs and NK cell intracellular cytokines staining 70
2.8. Flow cytometric NK cytotoxicity assay 72

2.8.1. NK cells isolation 72
2.8.2. NK cells stimulation 73
2.8.3. PBMCs and NK purity test 74
2.8.4. K562 target cell lines 74
2.8.5. Effector and target ratios 74
2.8.6. Percentage of NK killing calculation 75

2.9. NK cell sorting and Antibody-Dependent Cellular Cytotoxicity (ADCC) assay 78

2.9.1. NK cell sorting 78
2.9.2. ADCC assay experiment set up 79

2.10. CMV viral load study in urine and serum 80

2.10.1. Optimisation of DNA extraction from urine and serum 80
2.10.1.1. DNA extraction from urine and serum by using QIAmp® Viral RNA Kit 81
2.10.1.2. DNA extraction from serum and urines by using High Pure Nucleic Acid Kit 82
2.10.2. In house CMV quantitative Polymerase Chain Reaction (qPCR) and DNA sequencing 83
2.10.2.1. Detection of CMV viral load by qPCR in urine and serum 83
2.10.2.2. qPCR viral load analysis and calculation 84
2.10.2.3. DNA sequencing of CMV viral genome 88

2.11. Statistical analysis 88

CHAPTER 3: 89
THE INCIDENCE AND CLINICAL SIGNIFICANCE OF CMV REACTIVATION AFTER HAEMATOPOIETIC STEM CELL TRANSPLANTATION 89
3.1. INTRODUCTION 89
3.2. OBJECTIVE 89
3.3. RESULTS 90

3.3.1. Frequency and cumulative incidence of CMV reactivation after allogeneic stem cell transplantation 90
3.3.2. Overall survival data in allo-HSCT 93
3.3.3. Incidence of CMV reactivation, graft versus host (GvHD) and relapse occurrence in relation with recipient-donor serostatus 96
3.3.4. Collection of blood samples for subsequent study within this thesis 99
3.3.5. Prophylaxis and treatment of CMV reactivation allo-HSCT patients 102
3.3.6. Control groups 105
3.3.6.1. Characteristics of healthy donors used in the study 105

3.4. DISCUSSION 107
3.5. CONCLUSION 111

CHAPTER 4: 112
NATURAL KILLER CELL PHENOTYPES AND FUNCTIONS IN CMV REACTIVATION AFTER ALLOGENEIC STEM CELL TRANSPLANTATION 112
4.1. INTRODUCTION 112
4.2. OBJECTIVES 113
4.3. RESULTS 113

4.3.1. NK cells gating strategy and analysis 113
4.3.2. Reconstitution of Natural Killer (NK) cells following an episode of CMV reactivation in patients undergoing allogeneic HSCT 115
4.3.2.1. The percentage of NK cells in healthy donors is not influenced by CMV serostatus 116
4.3.2.2. The number of NK cells increases in HSCT patients after CMV reactivation 117
4.3.2.3. The magnitude of CMV viral reactivation is correlated with the number and proportion of NK cell within peripheral blood 120
4.3.2.4. NK cells and viral loads in CMV risk group R+/D- with primary CMV infection 122
4.3.2.5. The influence of recurrent episodes of CMV viraemia on NK cell reconstitution . 126
4.3.3. Reconstitution of different subsets of NK cells following CMV reactivation after allogeneic HSCT 127
4.3.3.1. NK cell subsets in healthy donors 127
4.3.3.2. Evaluation of specific NK cell subsets in allo-HSCT patients with CMV reactivation and without reactivation 129
4.3.4. The pattern of expression of activating NKG2C^{+} and inhibiting NKG2A^{+} receptors on NK cells in relation to CMV reactivation after allo- HSCT 134
4.3.4.3. Flow cytometric analysis of NKG2C-positive NK cells 134
4.3.4.4. The proportion of CD56^{dim}CD16^{bright} NKG2C^{+} cells is increased in CMV seropositive healthy donors 136
4.3.4.5. Expansion of NKG2C^{+} and decrease in NKG2A^{+} cells within CD56^{dim}CD16^{bright} NK cell subset following CMV reactivation in patients after allo-HSCT 137
4.3.4.6. The ratio of NKG2C^{+} and NKG2A^{+} cells on CD56^{dim}CD16^{bright} in CMV reactivation patients 140
4.3.4.7. NKG2C^{+} and –NKG2A^{+} NK cells in different subsets of NK cells in CMV reactivation allo-HSCT 142
4.3.4.8. Comparison of NKG2C^{+} and NKG2A^{+} expression on NK cells in relation to CMV reactivation and CMV risk group 145
4.3.5. Examination of the extended phenotype of NK cells in patients following allo-HSCT and the impact of CMV reactivation 147
4.3.5.1. The pattern of CD57, KIR, PD-1 and KLRG1 expression on NK cells 147
4.3.5.2. Expression of CD69^{+} on CD56^{dim}CD16^{bright} NK cells 152
4.3.5.3. Comparison of CD57^{+}, KIR^{+} and CD69^{+} expression within CMV R+/D+ and R+/D- groups 154
4.3.6. NK cells retain cytotoxic function after CMV reactivation 155
4.3.6.1. NK cell cytotoxicity assay optimisation and gating strategy 155
4.3.6.2. NK cell killing properties in healthy donors and HSCT patients with CMV reactivation 158

4.3.6.3. The comparison of cytotoxicity function with NKG2C$^+$ NK and NKG2C$^-$ NK cells... 159
4.3.7. Cytokine production of NK cells from HSCT patients with CMV reactivation..... 160

4.4. DISCUSSION..... 163
4.5. CONCLUSION..... 174

CHAPTER 5: 175
THE PROFILE OF THE CMV-SPECIFIC T CELL IMMUNE RESPONSE AND OVERALL T CELL IMMUNE RECONSTITUTION IN RELATION TO CMV REACTIVATION AFTER ALLOGENEIC STEM CELL TRANSPLANTATION..... 175
5.1. INTRODUCTION..... 175
5.2. OBJECTIVES..... 176
5.3. RESULTS..... 177

5.3.1. CD8$^+$ and CD4$^+$ T cell..... 177
5.3.1.1. Gating strategies and analysis..... 177
5.3.1.2. CD8$^+$ and CD4$^+$ T cell in healthy donors..... 178
5.3.1.3. CD8$^+$ and CD4$^+$ T cell reconstitution in allo-HSCT patients with CMV reactivation.. 179
5.3.1.4. CMV specific CD8$^+$ and CD4$^+$ T cell reconstitution in allo-HSCT patients following CMV reactivation..... 183
5.3.1.5. CD57$^+$, CD38$^+$, PD-1$^+$ and CD28 null phenotypes from CD8$^+$ and CD4$^+$ T cells in healthy donors and CMV reactivation allo-HSCT..... 188
5.3.1.6. The profile of memory subsets of CD8$^+$ and CD4$^+$ T cells in healthy donors and transplant patients in relation to CMV reactivation..... 197
5.3.1.7. Kinetic changes in naïve and memory phenotypes of CD8$^+$ and CD4$^+$ T cells within HSCT patients in relation to CMV reactivation..... 203
5.3.1.8. Comparison of memory phenotypes of total CD8$^+$ and CD4$^+$ T cells in relation to CMV reactivation..... 207
5.3.1.9. Memory phenotypes of CD8$^+$ and CD4$^+$ T cells in relation to 'CMV risk group' after allo-HSCT..... 209
5.3.2. The reconstitution of unconventional T cells including γδ T cells in HSCT patients with CMV reactivation..... 212
5.3.2.1. Gating strategies and analysis..... 212
5.3.2.2. Pattern of CD8$^+$ and CD4$^+$ co-expression on T cells in healthy donors..... 214
5.3.2.3. Pattern of CD8$^+$ and CD4$^+$ co-expression on T cells in allo-HSCT patients..... 215
5.3.2.4. γδ T cells in healthy donors and transplant patients..... 216
5.3.2.5. The percentage distribution of CD8$^+$, CD4$^+$, CD8$^+$CD4$^+$ and CD8$^-$CD4$^-$ within TCRγδ cells in healthy donors and HSCT patients with or without CMV reactivation..... 221
5.3.2.6. Vδ2 negative and Vδ2 positive γδ T cell subsets in healthy donors..... 225
5.3.2.7. Vδ2-negative and Vδ2-positive γδ T cell subsets in HSCT patients with or without CMV reactivation..... 226
5.3.2.8. Vδ1$^+$Vδ2$^-$, Vδ1$^-$Vδ2$^+$ and Vδ1$^-$Vδ2$^-$ subsets in healthy donors and HSCT patients in relation to CMV reactivation..... 227

5.4. DISCUSSION..... 231
5.5. CONCLUSION..... 240

CHAPTER 6: 241
GENERAL DISCUSSION..... 241
6.1. DISCUSSION..... 241

REFERENCES..... 255
APPENDIX..... 273

LIST OF FIGURES

FIGURE 1.1.1. Summary diagram of allogeneic HSCT procedures. 4
FIGURE 1.1.2. Schematic representation of the function of the Major Histocompatibility Complex (MHC) (HLA) proteins.. 6
FIGURE 1.1.3. Missing self KIR in alloreactive NK cells.. 14
FIGURE 1.1.4. Different precursors of immune cells.. 15
FIGURE 1.1.5. Overview of the kinetics of immune reconstitution..... 16
FIGURE 1.1.6. TCRγδ T cells characterised by gamma and delta chains..... 22
FIGURE 1.3.1. CMV risk group in allogeneic stem cell transplant patients..... 31
FIGURE 1.4.1. Impacts of CMV reactivation on immune reconstitution in allo-HSCT.. 33
FIGURE 2.2.1. Sample collection schedule..... 47
FIGURE 2.3.1. Isolation of peripheral blood mononuclear cells (PBMCs) from whole blood. 49
FIGURE 2.5.1. Examples of CMV serum IgG ELISA calculation. 56
FIGURE 2.6.1. Example of NKG2A antibody titration from NK panel.. 59
FIGURE 2.6.2. Optimisation of tetramer staining.. 65
FIGURE 2.6.3. Optimisation of tetramer staining.. 65
FIGURE 2.10.1. Standard curves for CMV and β-2m and example of calculation..... 86
FIGURE 2.10.2. Example of amplification plots from CMV and β-2m genes standards.. 87
FIGURE 3.3.1. Frequency of CMV reactivation in allogeneic stem cell transplant patients consented to the BOOST trial in the 3 years between 2016 and 2018. 91
FIGURE 3.3.2. Cumulative incidence of CMV reactivation in patients in the 100 days post-HSCT (n=47) between 2016 and 2018)..... 92
FIGURE 3.3.3. The effect of recipient CMV status on overall survival of CMV positive and CMV negative allo-HSCT patients (n=89)..... 94
FIGURE 3.3.4. The effect of donor CMV status on overall survival of CMV positive and CMV negative allo-HSCT patients (n=89)..... 95
FIGURE 3.3.5. The effect of recipient/donor pair CMV serostatus on overall survival of CMV positive and CMV negative allo-HSCT patients (n=89). 96
FIGURE 3.3.6. Recipient-donor serostatus relationship with the occurrence of GvHD, relapse and CMV reactivation. 98
FIGURE 3.3.7. CMV viral loads detected in urine performed by in house qPCR. 104
FIGURE 4.3.1. NK cells in healthy donors..... 116
FIGURE 4.3.2. NK cells percentage and absolute number around the time of CMV reactivation and in non-reactivated control subjects.. 118
FIGURE 4.3.3. Comparison of the percentage and absolute number of NK cells in patients after SCT divided into those with an episode of CMV reactivation or not.. 120
FIGURE 4.3.4. Temporal association between the number and percentage of peripheral NK cells and the pattern of CMV viral load in CMV reactivation patients. 122
FIGURE 4.3.5. NK cell percentage and count following CMV reactivation in R+/D+ and R+/D- groups. 123
FIGURE 4.3.6. NK cells percentages and counts in R+/D+ and R+/D- groups associated with CMV viral loads 125
FIGURE 4.3.7. NK cell percentage and absolute count in patients who underwent CMV reactivation divided into those that had a single or multiple episode of viraemia. 126
FIGURE 4.3.8. General comparison of NK cells subsets in healthy donors, CMV reactivation and without reactivation allogeneic HSCT..... 128

FIGURE 4.3.9. NK cell subsets in healthy donors and in HSCT patients at various time points after CMV reactivation and in matched time points in patients without reactivation. 132
FIGURE 4.3.10. Comparison of NK cells subsets following allogeneic post HSCT and in relation to CMV reactivation or 'non-reactivation' as well as in healthy donors.. 133
FIGURE 4.3.11. NKG2C and NKG2A gating strategies. 135
FIGURE 4.3.12. $NKG2C^+$ and $NKG2A^+$ NK cells within the $CD56^{dim}CD16^{bright}$ subset in healthy donors according to CMV serostatus. 136
FIGURE 4.3.13. The proportion of $NKG2C^+$ and $NKG2A^+$ NK cells within the $CD56^{dim}CD16^{bright}$ population in HSCT patients with CMV reactivation (left) or without reactivation (right). 139
FIGURE 4.3.14. The ratio of $NKG2C^+$ and $NKG2A^+$ NK cells within the $CD56^{dim}CD16^{bright}$ NK cell population in HSCT patients with CMV reactivation and in healthy donors 141
FIGURE 4.3.15. Expression of NKG2C on different NK cell subsets, defined according to their profile of CD56 and CD16, in patients with viral reactivation. 143
FIGURE 4.3.16. Expression of NKG2A on different NK cell subsets, defined according to their profile of CD56 and CD16, in patients with viral reactivation. 144
FIGURE 4.3.17. $NKG2C^+$ and $NKG2A^+$ NK cells comparison with patients without reactivation and donors' serostatus (R+/D+ and R+/D-)..... 146
FIGURE 4.3.18. Examples of CD57, KIR (KIR2DL1/S1/S3/S5/KIR2DL2/DL3/KIR3DL1), PD-1 and KLRG1 expression on $CD56^{dim}CD16^{bright}$ NK cells in healthy donors and in patients after HSCT, distinguished by CMV reactivation or 'no-reactivation'..... 149
FIGURE 4.3.19. The pattern of CD57, KIR, PD-1 and KLRG1 expression on $CD56^{dim}CD16^{bright}$ NK cells in healthy donors. 150
FIGURE 4.3.20. Expression of $CD57^+$, KIR^+, $PD\text{-}1^+$ and $KLRG1^+$ on $CD56^{dim}CD16^{bright}$ NK cells after transplantation Significant changes in the proportion of CD57 and KIR were seen on $CD56^{dim}CD16^{bright}$ NK cells. 151
FIGURE 4.3.21. Example of CD69+ expression on $CD56^{dim}CD16^{bright}$ NK cells on healthy donors and patients with 'no reactivation' or CMV reactivation after allo-HSCT. 152
FIGURE 4.3.22. The distribution of $CD69^+$ expression on $CD56^{dim}CD16^{bright}$ NK cells in healthy donors according to CMV serostatus. 153
FIGURE 4.3.23. The expression of $CD69^+$ on $CD56^{dim}CD16^{bright}$ NK cells in relation to CMV reactivation after transplantation. 153
FIGURE 4.3.24. The pattern of $CD57^+$, KIR^+ and $CD69^+$ expression on NK cells according to CMV risk status. 154
FIGURE 4.3.25. Optimisation of NK killing assay using IFNα-pre-activated or control NK cells. 156
FIGURE 4.3.26. Comparison of NK cell lysis using effector cells from (a) CMV seronegative or (b) CMV seropositive healthy donors or (c) allo-HSCT patients following an episode of CMV reactivation. 157
FIGURE 4.3.27. NK cell lysis in healthy donors and in allo-HSCT patients after CMV reactivation. 159
FIGURE 4.3.28. Relative lytic activity by $NKG2C^+$ and $NKG2C^-$ NK cells..... 160
FIGURE 4.3.29. TNF-α and IFN-γ production from total NK cells and $NKG2C^+$ NK cells. 162
FIGURE 5.3.1. T cells gating strategies..... 178
FIGURE 5.3.2. Percentage of CD8 and CD4 T cells in healthy donors 179
FIGURE 5.3.3. The percentage and absolute number of $CD8^+$ T cells in allo-HSCT patients in relation to CMV reactivation or without reactivation. 181

FIGURE 5.3.4. The percentage and number of $CD4^+$ T cells after allo-HSCT in relation to CMV reactivation (n=26) and without reactivation allo-HSCT (n=25). 182
FIGURE 5.3.5. Example of tetramer staining on $CD8^+$ T cells on a CMV seropositive healthy donor and a transplant patient after CMV reactivation 184
FIGURE 5.3.6. Example of tetramer staining on $CD4^+$ T cells on a CMV seropositive healthy donor and a transplant patient after CMV reactivation. 185
FIGURE 5.3.7. CMV-specific $CD8^+$ and $CD4^+$ T cell responses following CMV reactivation after allo-HSCT 187
FIGURE 5.3.8. Examples of $CD57^+$, $CD38^+$, PD-1^+ and CD28 expression and histogram gating strategies on total $CD8^+$ T cells from CMV reactivation patients, no reactivation patients and healthy donors. 189
FIGURE 5.3.9. Examples of $CD57^+$, $CD38^+$, PD-1^+ and CD28 expression and histogram gating strategies on total $CD4^+$ T cells from CMV reactivation patients, no reactivation patients and healthy donors. 190
FIGURE 5.3.10. The percentage of $CD57^+$, $CD38^+$, PD-1^+ and $CD28^-$ on CD8 and CD4 T cells in healthy donors. 191
FIGURE 5.3.11. $CD57^+$, $CD38^+$, PD-1^+ and CD28 negative percentages from $CD8^+$ T cells in CMV reactivation and without reactivation patients. 195
FIGURE 5.3.12. The percentage of $CD57^+$, $CD38^+$, PD-1^+ and CD28- $CD4^+$ and CD8+ T cells in relation to CMV reactivation after transplant. 196
FIGURE 5.3.13. The percentage of $CD57^+$, $CD38^+$, PD-1^+ and CD28- $CD4^+$ and $CD8^+$ T cells in comparison between CMV reactivation (n=37) and 'without reactivation after transplant' (n=26). 197
FIGURE 5.3.14. Example of the memory phenotype of total $CD8^+$ and CMV-specific $CD8^+$ T cells in healthy donors and transplant patients according to CCR7 and CD45RA expression. 198
FIGURE 5.3.15. Example of the memory phenotype of total $CD4^+$ and CMV-specific $CD4^+$ T cells in healthy donors and transplant patients according to CCR7 and CD45RA expression. 199
FIGURE 5.3.16. Memory phenotypes of total $CD8^+$ and $CD4^+$ T cells from healthy donors. No differences in the percentages between CMV positive and CMV negative healthy donors for EM, EMRA, CM and Naïve T cells from both $CD8^+$ and $CD4^+$ T cells 200
FIGURE 5.3.17. Memory phenotypes of total and CMV-specific $CD8^+$ and $CD4^+$ T cells from healthy donors and HSCT patients with CMV reactivation or no reactivation. 202
FIGURE 5.3.18. EM, EMRA, CM and naïve T cell proportions within total $CD8^+$ from CMV reactivation and without reactivation patients 205
FIGURE 5.3.19. EM, EMRA, CM and naïve T cell proportions within total $CD4^+$ T cells from patients with CMV reactivation or 'no reactivation'. 206
FIGURE 5.3.20. EM, EMRA, CM and naïve T cell percentage within total $CD8^+$ and $CD4^+$ T cells in relation to CMV reactivation or 'no reactivation'. 208
FIGURE 5.3.21. EM and EMRA phenotypes comparison from $CD8^+$ T cells between R+/D- and R+/D+ CMV reactivation patients 210
FIGURE 5.3.22. EM and EMRA phenotypes comparison from $CD4^+$ T cells between R+/D- and R+/D+ CMV reactivation patients 211
FIGURE 5.3.23. TCRαβ and γδ T cells gating strategy 213
FIGURE 5.3.24. TCRαβ and γδ T cells (gated from αβ negative) $CD3^+$ population from healthy donor 214
FIGURE 5.3.25. Different T cells subset percentages in healthy donors according to $CD4^+$ and $CD8^+$ expression 215
FIGURE 5.3.26. T cells percentages in allo-HSCT patients without reactivation and with reactivation allo-patients according to $CD4^+$ and CD8+ expression 216

FIGURE 5.3.27. TCRαβ negative or γδ T cells plots gated from total $CD3^+$ population from healthy donors, CMV reactivation and no reactivation patients. γδ T cells were determined by TCRαβ negative population. 217
FIGURE 5.3.28. TCRαβ and γδ T cells (gated from αβ negative) $CD3^+$ population from healthy donors 218
FIGURE 5.3.29. TCRαβ and γδ T cell populations from healthy donors 218
FIGURE 5.3.30. The percentage and absolute count of TCRγδ cells after transplant in relation to CMV reactivation 220
FIGURE 5.3.31. Example of gating strategy of $CD8^+$, $CD4^+$, $CD8^+CD4^+$ and $CD8^-CD4^-$ subsets of TCRγδ T cells in healthy donors and transplant patients, with or without CMV reactivation. 222
FIGURE 5.3.32. $CD8^+$, $CD4^+$, $CD8^+CD4^+$ and $CD8^-CD4^-$ subsets of TCRγδ cells in healthy donors and HSCT patients, with or without viral reactivation 223
FIGURE 5.3.33. Percentages of $CD8^+$, $CD4^+$, $CD8^+CD4^+$ and $CD8^-CD4^-$ TCRγδ T cells in HSCT patients without CMV reactivation (n=25) or following CMV reactivation patients (n=37) 224
FIGURE 5.3.34. Examples of Vδ2 negative and Vδ2 positive plots in healthy donors, CMV reactivation patients and patients without reactivation 225
FIGURE 5.3.35. TCR Vδ2 negative and Vδ2 positive T cells in healthy donors (n=24) 226
FIGURE 5.3.36. Percentage of TCR Vδ2-negative and Vδ2-positive T cells in HSCT patients with or without CMV reactivation 227
FIGURE 5.3.37. Different TCR Vδ1 and Vδ2 T cells subsets in healthy donors and HSCT patients in relation to CMV reactivation 228
FIGURE 5.3.38. Different TCR Vδ1 and Vδ2 T cells subsets in healthy donors, no reactivation and CMV reactivation patients 229
FIGURE 5.3.39. Comparison between TCR Vδ1 and Vδ2 T cells subsets in CMV reactivation and no reactivation patients 230
FIGURE 6.1.1. Recovery and reconstitution of NK, CD8, CD4 and *γδ* T cells in CMV reactivation allo-HSCT 243
FIGURE 6.1.2. Correlation between NK $CD56^{dim}CD16^{bright}$ $NKG2C^+$ cells and $CD8^+$ EMRA T cells 249

LIST OF TABLES

TABLE 2.4.1. HLA primers with information specific alleles and concentrations used to prepare primer mixes for use in PCR-SSP 52
TABLE 2.4.2. Master mix preparation per 14x reaction.. 53
TABLE 2.4.3. PCR condition for HLA typing. 53
TABLE 2.6.1. NK panel 1 antibodies for surface staining. 61
TABLE 2.6.2. NK panel 2 (CD69) antibodies for surface staining. 62
TABLE 2.6.3. TCRγδ T cell panel and antibodies. 63
TABLE 2.6.4. Preparation of tetramer HLA Class I by using monomers.. 64
TABLE 2.6.5. List of HLA Class I and Class II tetramers used in T cell panels for the CMV reactivation allo-post HSCT samples.. 67
TABLE 2.6.6. CD8 T cell MHC Class I panel and antibodies. 68
TABLE 2.6.7. CD4 T cell MHC Class II panel and antibodies 69
TABLE 2.6.8. NK Intracellular cytokines panel and antibodies 71
TABLE 2.8.1. NK cells effector and K562 target ratios for NK killing assay. 75
TABLE 2.8.2. Calculation for live K562 cells/µl for each ratio for an example from one sample of healthy donor.. 76
TABLE 2.8.3. Calculation for killing of NK cells against K562 target cells.. 77
TABLE 2.9.1. NK cell sorting panel and antibodies. 78
TABLE 2.10.1. In house qPCR set up for CMV viral load detection. 84
TABLE 2.10.2. PCR cycles for CMV viral load detection. 84
TABLE 3.3.1. The demographic characteristics of patients who underwent CMV reactivation (n=41). 101
TABLE 3.3.2. Side effects of drugs used to treat CMV infection. 103
TABLE 3.3.3. Characteristics of patients with ‘no viral reactivation’ (n=26) 106
TABLE 6.1.1. Summary of NK and T cell phenotype in allo-HSCT patients after CMV reactivation as compared to control groups. 250

LIST OF ABBREVIATIONS

ADCC	Antibody-dependant cellular cytotoxicity
AF488	Alexa-fluor 488
AF700	Alexa-fluor 700
ALL	Acute Lymphoid Leukaemia
Allo-HSCT	Allogeneic Haematopoietic Stem Cell Transplantation
AML	Acute Myeloid Leukaemia
APC	Allophycocyanin
APC	Antigen Presenting Cell
ATG	Antithymocyte globulin
BM	Bone Marrow
BSA	Bovine Serum Albumin
CB	Cord blood
CD	Cluster of differentiation
CFSE	Carboxyfluorescein succinimidyl ester
CI	Confidence interval
CML	Chronic Myelogenous leukaemia
CMML	Chronic Myelomonocytic Leukaemia
CMV	Cytomegalovirus
CTL	Cytotoxic T lymphocyte
dH_20	distilled water
DLI	Donor lymphocyte infusion
DMSO	Dimethyl sulfoxide
DNA	Deoxyribonucleic acid
dNTP	Deoxyribonucleotide triphosphate
EBV	Epstein-Barr Virus
ECD	Phycoerythrin-Texas Red conjugate
EDTA	Ethylenediaminetetraacetic acid
ELISA	Enzyme-linked immunosorbent assay
FAM	Fluorescein amidites
FBS	Foetal bovine serum
FITC	Fluorescein isothiocyanate
FSC	Forward scatter
G-CSF	Granulocyte colony-stimulating factor

GvHD	Graft versus host disease
GvL	Graft versus leukaemia
HCl	Hydrochloric acid
HLA	Human leukocyte antigen
HRP	Horseradish peroxidase
HSCT	Haematopoietic stem cell transplantation
IFN	Interferon
LCL	Lymphoblastoid cell line
MA	Myeloablative
MDS	Myelodysplastic syndrome
mg	milligram
$MgCl_2$	Magnesium Chloride
mHAg	Minor Histocompatibility Antigen
MHC	Major Histocompatibility Complex
ml	millilitre
mM	milimolar
MUD	Matched Unrelated Donor
NGS	Next Generation Sequencing
NH_4	Ammonium
NHL	non-Hodgkin's Lymphoma
NK	Natural killer
NMA	Non-myeloablative
NRM	Non-relapse mortality
PB	Pacific blue
PBMC	Peripheral blood mononuclear cells
PBS	Phosphate Buffered Saline
PBSC	Peripheral blood stem cell
PCR	Polymerase Chain Reaction
PCR-SSP	PCR-Sequence Specific Primer
PD-1	Programmed cell death protein 1
PE	R-phycoerythrin
PE-Cy5	Phycoerythrin 5
PE-Cy7	Phycoerythrin 7
PerCPCy5.5	Peridinin chlorophyll protein complex-cyanin 5.5
PFA	Paraformaldehyde

qPCR	quantitative Polymerase chain reaction
RCMD	Refractory cytopenia with multilineage dysplasia
RIC	Reduced intensity conditioning
RPMI	Roswell Park Memorial Institute
TAMRA	Tetramethylrhodamine
TBE	Tris-Borate-EDTA
TCR	T cell receptor
TMB	Tetramethylbenzidine
TNF	Tumour necrosis factor
V500	Violet 500
µg	microgram
µl	microlitre

CHAPTER 1: INTRODUCTION

1.1. Haematopoietic stem cell transplantation (HSCT)

Haematopoietic stem cell transplantation (HSCT) is the transplantation of multipotent haematopoietic stem cells derived from bone marrow, umbilical cord or peripheral blood into patients as a potential curative treatment for a range of myeloid and lymphoid malignancies (Szyska and Na, 2016; Kolb, 2017; Niederwieser et al., 2016; Passweg et al., 2016). In some cases, HSCT is also used for non-malignant disorders such as immunodeficiency diseases, thalassemia and haemoglobinopathies (Shenoy and Boelens, 2015; Sureda et al., 2015). Haematopoietic stem cell transplantation is a highly complex procedure that requires specialist haematologists and highly trained nursing staff.

Stem cells are usually collected from peripheral blood by apheresis, however these may also be obtained from bone marrow and this explains the previous term for HSCT which was Bone Marrow Transplantation (BMT). The choice of HSCT procedure also depends on the condition of patients, as well as type of primary disease and source of stem cell donor (Perry and Linch, 1996). In the HSCT transplant setting, the patients (recipients) are given conditioning drugs along with immunosuppressive drugs which leads to reduced activity of their immune system and renders the patient prone to infections after transplant (Stern et al., 2018; Yang et al., 2018).

HSCT can be divided into autologous and allogeneic, depending on the source of the stem cell graft being infused into the patients. In autologous HSCT the patient is transplanted with their own stem cells, whilst in allogeneic transplantation the patient receives a graft from a different person (the donor). The donor could be a sibling (SIB) or a matched unrelated donor (MUD) (Sakaguchi et al., 2016). In some cases, the patient may receive a stem cell graft from another related donor such as a son, daughter or parent. With an autologous transplant the patient undergoes chemotherapy to reduce the tumour burden before their own stem cells are collected by apheresis or bone marrow aspiration procedures. These cells are then frozen prior to reinfusion into the patient following intensive conditioning to further reduce the tumour. This autologous treatment procedure is usually used to treat patients with myeloma, Hodgkin lymphoma or non-Hodgkin lymphoma (Stiff, 2015; Graff et al., 2015; Sureda et al., 2015).

1.1.1. Allogeneic haematopoietic stem cell transplantation (allo-HSCT)

There are a number of major risks to the recipient of the allogeneic HSCT, such as graft versus host disease (GvHD) and CMV reactivation that are either not observed, or much common, after autologous transplant. There are different risks in the autologous transplant setting such as transfer of residual cancer cells in the grafts. However, these will not be discussed in detail as the focus of this study is the allo-HSCT.

Allo-HSCT is a complex procedure that requires HLA matching of the recipient and donor, and for the patient to receive chemotherapy and conditioning before the day of transplant on Day 0 **(Fig. 1.1.1).** The choice of the stem cell graft can also be crucial in the transplant setting. Other factors that contribute to clinical risk in allo-HSCT include relative matching at Minor Histocompatibility Antigens (mHAg) loci and later complications such as 'mixed chimerism', which will be discussed in more detail in future sections.

Allo-HSCT is one of the most important therapeutic strategies for haemato-oncology and has the potential to cure some patients with chemotherapy-resistant disease. The curative potential of allo-HSCT is believed to mainly depend on the alloreactive immune response called the graft versus leukaemia (GvL) response. Overall survival at 5 years is around 50-60% with major complications such as relapse, graft versus host disease (GvHD) and infection (including CMV) dominating the mortality rate.

The mechanism of the GvL effect is not clear but is thought to be mediated through donor T cell recognition of mHAg mismatches between donor and patient. In allogeneic HSCT, GvHD and CMV reactivation are associated with significant morbidity and mortality (Ramanathan et al., 2016) and both events may be interrelated in the transplant setting (Jang et al., 2015). This study will focus on exploring the impact of CMV reactivation in allo-HSCT patients. Whilst CMV reactivation still constitutes a major risk in HSCT patients, other important factors such as the degree of HLA match between recipients and donors, the source of stem

cell grafts and the age of the patient are now arguably more significant. Nevertheless, screening for CMV reactivation is still used in almost all clinical centres (Majhail et al., 2012).

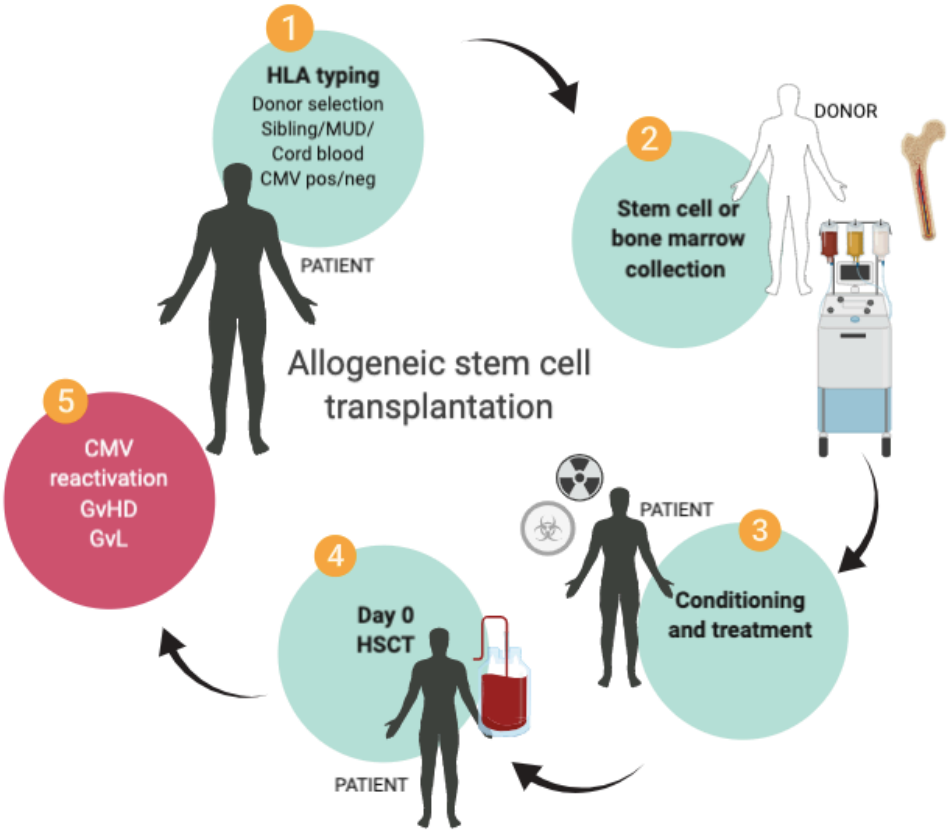


FIGURE 1.1.1. Summary diagram of allogeneic HSCT procedures. In allo-HSCT, the patient receives stem cell grafts from siblings, matched unrelated donors (MUD) or cord blood and the stem cells are collected either by apheresis or bone marrow aspiration procedures.

1.1.1.1. Human Leukocyte Antigen (HLA) typing and match

Prior to an allogeneic HSCT the recipients and prospective donors must be 'HLA typed' (Morishima et al., 2015). If a match is not found in a sibling, a matched unrelated donor (MUD) is usually requested from the worldwide stem cell donor registry (Anderlini et al., 2001). HLA testing is crucial and considered a major component in the allogeneic HSCT protocol in order to limit both GvHD and allograft rejection. HLA typing used to be determined by serological methods, however the laboratory testing has evolved with more complex and advanced technology being performed such as high resolution typing and next generation sequencing (NGS), although polymerase chain reaction (PCR) is still widely used and acceptable as the standard for laboratory testing (Chang et al., 2018a; Turner et al., 2018).

The Human Leukocyte Antigen system is also known as Major Histocompatibility Complex (MHC). It consists of a large family of genes of 4 Mbp on chromosome 6, located at the short arm 6p21.3. There are two main classes of HLA, HLA Class I, including HLA-A, HLA-B and HLA-C, and HLA Class II, which are HLA-DP, HLA-DQ and HLA-DR. The HLA genes encode proteins with important immune function and the genes are highly polymorphic, with HLA-B having the highest number of alleles (Kennedy et al., 2017).

HLA Class I protein is present on virtually all nucleated cells and presents peptides to $CD8^+$ T cells, whilst HLA Class II is found on antigen presenting cells (APC) and present peptide to $CD4^+$ T cells **(Fig. 1.1.2).** For each potential sibling donor,

the probability of a total HLA genetic match with the patient is 25% but the use of an HLA haploidentical-related donor is increasingly common. On the other hand, the probability of finding a match with an unrelated donor is about 30 to 90%, depending partly on the ethnicity of the patient. Cord blood transplants are usually available for >90% of patients (Besse et al., 2016).

Recipients and donors are usually tested for a potential '10/10' HLA allele match **(Fig. 1.1.2)** with high resolution allele typing at HLA-A, -B, -C, -DR and -DQ (Robinson et al., 2011; Marsh, 2017; Nunes et al., 2011). Some centres now also match at HLA-DP alleles as well. For a potential MUD the gold standard is a 10 out of 10 match and in most European populations this can be found for approximately 50% of patients, whilst a 9/10 matched donor can increase this by 20–30% (Tiercy, 2016).

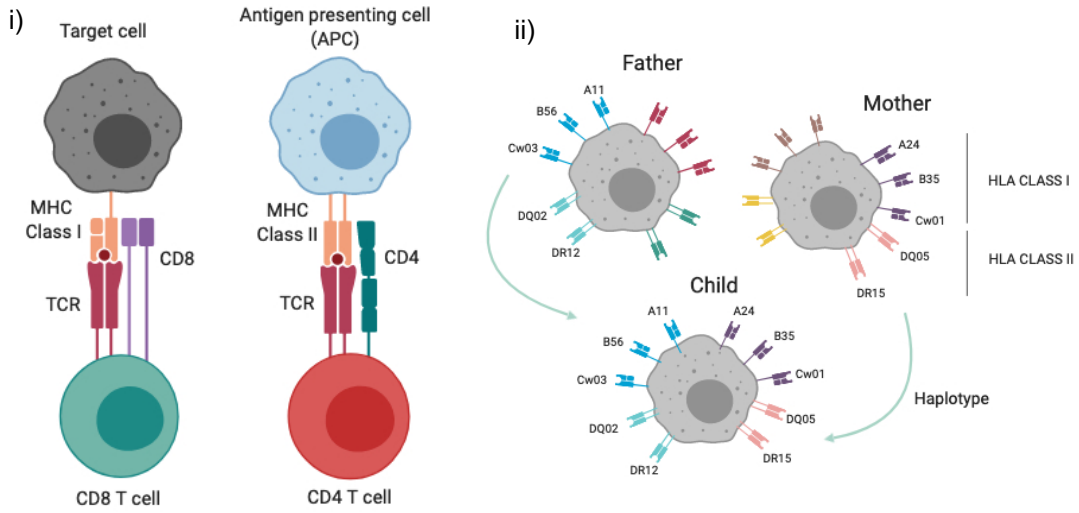


FIGURE 1.1.2. Schematic representation of the function of the Major Histocompatibility Complex (MHC) (HLA) proteins. (i) MHC proteins present peptides to the T cell receptor on $CD4^+$ or $CD8^+$ T cells (ii) An example of HLA haplotypes inherited by a child from its parents, and the potential utility of either as a haploidentical stem cell donor.

1.1.1.2. Minor Histocompatibility Antigens

Minor histocompatibility antigens (mHAg) are small peptides found on the surface of the cell and presented by MHC Class I or Class II proteins. mHAg can contribute to immunological alloreactive immune rejection in the allo-transplant setting due to their polymorphism where amino acid differences in the peptides can lead to recognition by donor T cells. mHAg can only be identified by T cells and their expression varies between tissues. To date approximately 54 different immunodominant mHAg have been identified by genomic sequencing (Spierings, 2014). 39 of these are associated with the most common HLA types in Caucasian patients and may be used as potential targets for immunotherapy in haematological cancers (Granados et al., 2016).

Most epidemiological studies have been done with the mHAgs HA-1, HA-8 and HY. HY mHAg mismatch is reported to be one of the factors that contributes to GvHD and is associated with decreased survival rate after allo-HSCT in some studies (Markiewicz et al., 2009). However, mismatch of mHAg is not as significant as the mismatch of an HLA locus. Strikingly, mHAg can also be a potential target for GvL and in the therapeutic setting the aim would be to maximise GvL while minimising GvHD (Martin et al., 2017). For example, HA-1 is an immunodominant mHAg whose expression is limited to hematopoietic cells and which is restricted through HLA-A2. $CD8^+$ T cells against this antigen may provide a potent GvL effect in HA-1^+ leukaemia patients without increasing the risk of GvHD. In our lab, we have conducted a first-in-man Phase I trial using a DNA vaccine to prime the immune response before boosting with a modified vaccinia Ankara virus (MVA).

The result showed that this vaccine can generate functional cytotoxic lymphocytes (CTL) that can specifically kill the HA-1 peptide positive target cells (manuscript in preparation).

1.1.1.3. The source of stem cell grafts

The sources of stem cell grafts for allogeneic HSCT can be from bone marrow (BM), peripheral blood stem cells (PBSC) or cord blood (CB). For PBSC the cells are collected by apheresis and normally the donor would be given granulocyte colony-stimulating factor (G-CSF) before harvesting to facilitate the mobilisation of haematopoietic stem cell progenitors from the bone marrow into the blood to increase the concentration of cells (Panch et al., 2017). Bone marrow has been used as a stem source since the development of HSCT but a study has shown a correlation between the use of PBSC and better outcome of allogeneic HSCT (Byrne et al., 2016). However, in contrast, PBSC has also been related to increased non-relapse mortality (NRM) and GvHD in paediatric HSCT when compared with BM as a source of stem cell grafts (Simonin et al., 2017). Normally, the volume of bone marrow that is collected is between 10-20 ml/kg, depending on recipient body weight, while from peripheral blood, the volume of apheresis is about 150 to 400 ml. In contrast, in umbilical cord blood the volume is from 80 to 160 ml. The collected stem cell grafts are also evaluated for the number of $CD34^+$ cells to ensure that sufficient stem cells are included for engraftment. A $CD3^+$ cell count may also be undertaken to assess the potential risk of GvHD, which is usually high in the stem cell source from peripheral blood (Czerw et al., 2016; Simonin et al., 2017).

1.1.1.4. Transplant Conditioning

Before allogeneic HSCT the patient must receive immunosuppressant and 'conditioning' drugs with the aim of minimising the cancer cell burden and establishing stem cell niches ('space') for restoration of haematopoiesis from donor cells. The conditioning regimens for allo-HSCT patients can be classified as myeloablative (MA) or non-myeloablative [NMA or 'reduced intensity' conditioning (RIC)]. MA may incorporate total body irradiation (TBI) and uses single or multiple drugs to ablate the stem cells of the recipients for autologous or allogeneic HSCT. Myeloablative conditioning for allo-HSCT recipients can also incorporate T cell depletion with ATG (anti-thymocyte globulin) or Alemtuzumab. Both ATG and alemtuzumab are also used in prophylaxis of GvHD, in which ATG (from rabbit) targeting various antigens on T lymphocytes while alemtuzumab targeting CD52 on the mature lymphocytes in T cell-depleted condition. The T cell-depletion method is most common in the UK while T cell-repletion allo-HSCT is most common in the US, and a study also has shown that the later has shown lower rate of TRM (Gokgoz and Arslan, 2018).

NMA incorporates a reduced chemotherapy regimen (Jethava et al., 2017; Atilla et al., 2017) and the choice follows standard protocols and guidelines from specialist clinicians. The age and morbidity of the patients, as well as their underlying disease, (Gyurkocza and Sandmaier, 2014) also have to be considered.

1.1.1.5. Donor lymphocyte infusion (DLI)

Donor lymphocyte infusion (DLI) is a post-transplant treatment where the recipient is infused with T cells from the original donor with the aim of eradicating residual cancer cells in a therapeutic manner. The aim is to achieve a successful GvL effect with minimal GvHD and the overall success is highly dependent on the primary disease (Deol and Lum, 2010; Stamouli et al., 2016).

DLI is also often used when there is an occurrence of mixed chimerism (see next section) to reduce the incidence of relapse (Schneidawind et al., 2019). Other than DLI, lymphocyte and cellular therapies such as the use of cytotoxic T lymphocytes (CTL), cytokine-induced killer cells (CIK), marrow and tumour-infiltrating lymphocytes (MIL) and chimeric antigen receptor T cells (CAR) are all on-going in clinical trials aiming to kill the residual cancerous cells after allo-HSCT (Dietz and Wayne, 2017).

1.1.1.6. Chimerism

Chimerism analysis is used to investigate the relative proportion of donor or residual host cells in the recipient post-transplant. The term chimerism originated from the Greek mythological creature called a Chimera and the term is widely used to describe the level of engraftment of stem cells from the donor in the recipient. The term ‘mixed chimerism’ is used when patients have a mixture of recipient and donor cells whilst ‘complete chimerism’ refers to a recipient with full donor engraftment. The analysis of chimerism is often done by assessment of short

tandem repeat (STR) or single nucleotide polymorphisms (SNPs) through analysing polymorphic regions in the genome of donor and recipient (Sanz-Piña et al., 2019).

Chimerism analysis in allo-HSCT patient is important as it has been reported that full chimerism in early post-HSCT is associated with lower risk of leukaemia relapse, particularly in myeloid disease (Chen et al., 2018a; Kinsella et al., 2019a). The study of chimerism in allo-HSCT has also been carried out within our group, where mixed chimerism was correlated with increased occurrence of relapse (Kinsella et al., 2019a). Data from our group has also shown that mixed chimerism is maintained predominantly by T regulatory cells (Kinsella et al., 2019b).

1.1.1.7. Graft versus host disease (GvHD)

Graft versus Host Disease (GvHD) remains a major complication in allogeneic HSCT. GvHD occurs when the T cells or NK cells of the donor attack the cells and tissue of the recipients. GvHD is normally classified into two types; acute GvHD (aGvHD) and chronic GvHD (cGvHD). aGvHD is defined as occurring before 100 days post-transplant while cGvHD occurs after 100 days post-transplant (Vigorito et al., 2009). Acute GvHD results from alloreactive recognition by donor T cells and factors such as increased age of the donor, use of high dose intensity regimen, choice of PBSC stem cell grafts and CMV serostatus can influence the risk. aGvHD predominantly affects the skin, liver and gastrointestinal tract (GIT) and the primary treatment is corticosteroids (Szyska and Na, 2016; Ghimire et al., 2017; Du and Cao, 2018).

Chronic GvHD can occur between 3 months and two years after transplant and, like aGvHD, the clinical manifestations can be seen in the skin, liver and GIT but it can also affect the eyes, oral mucosa, genitals and lungs. The incidence of cGvHD is around 50% and the pathogenesis is very complex and different from aGvHD, involving components of the innate and adaptive immune system. Similar to aGvHD, HLA match is considered as one of the major risk factors for cGvHD. The risk factors also include prior aGvHD, T replete stem cell grafts, use of male donors, and the age of the donor (Cooke et al., 2017).

The mechanism and pathophysiology of GvHD starts with the recognition of antigen-presenting cells (APC) of the recipient by T cells from the donor leading to alloreactive T cell response and production of inflammatory cytokines. The mechanism does not only involve T cells but may also include NK cells and potentially other immune effector cells such as neutrophils, macrophages as well as regulatory T cells (Treg) (Chang et al., 2018b; Ferrara et al., 2009). Chemokine ligands and receptors play an important role in regulating cell migration and work from our group has demonstrated the importance of CXCL10-CXCR3 interactions in the pathogenesis of both acute and chronic GvHD (Piper et al., 2007).

1.1.1.8. Graft versus leukaemia (GvL)

Whilst GvHD is a dangerous complication of allo-HSCT the opposite effect of allorecognition is observed in the action of the Graft versus leukaemia (GvL) effect. GvL provides curative potential within the graft where alloreactive lymphocytes transfused from the donor can act to eradicate host leukaemic cells. Many factors

influence the GvL effect including type of disease, the degree of HLA match and the degree of chimerism (Kolb, 2008). Several strategies have been used to manipulate lymphocytes to boost the effects of GvL whilst minimising GvHD. In clinical settings, the strategies to enhance GvL have included the use of DLI, leukaemia-specific T cells, NK cell infusion and CAR-T cells (Chang et al., 2018b). Other than T and NK cells, the effect of GvL can also be manipulated by TCRγδ T cells, which are likely to be less alloreactive than TCRαβ T cells and make them an important potential source of anti-tumour cells (Handgretinger and Schilbach, 2018).

The potential for manipulation of NK cells in grafts for a GvL effect in allo-HSCT has been shown by our group, with high numbers of NK cells associated with reduced risk of leukaemia relapse (Maggs et al., 2017). Unlike HLA typing which is a routine test in the allo-HSCT setting, killer immunoglobulin-like receptor (KIR) genotyping is not part of pre-transplant monitoring in most centres. Thus, the presence and potential roles of alloreactive NK cells from the graft of donors in rendering GvL effects may have been under recognised.

In the transplant setting it is the donors with a KIR-ligand mismatch described as 'missing-self' recognition **(Fig. 1.1.3)** that are thought to display high NK killing properties (Escudero et al., 2018; Moretta et al., 2009). The presence of specific types of KIR in allo-HSCT patients has also been correlated with protection against leukaemia relapse, however these were also associated with GvHD (Oevermann et al., 2014; Feuchtinger et al., 2009; Miller et al., 2007). Studies have been

extensively focusing on the inhibitory NK cell receptors KIR2DL1, KIR2DL2/3 and KIR3DL1 which bind to HLA-C/B group C1, C2 and Bw4 for potential adoptive and targeted immunotherapy (Becker et al., 2016). Strikingly, evidence has also shown that the CMV driven 'memory' NK cells can be manipulated to enhance GvL effect by tumour priming strategies (Pal et al., 2017).

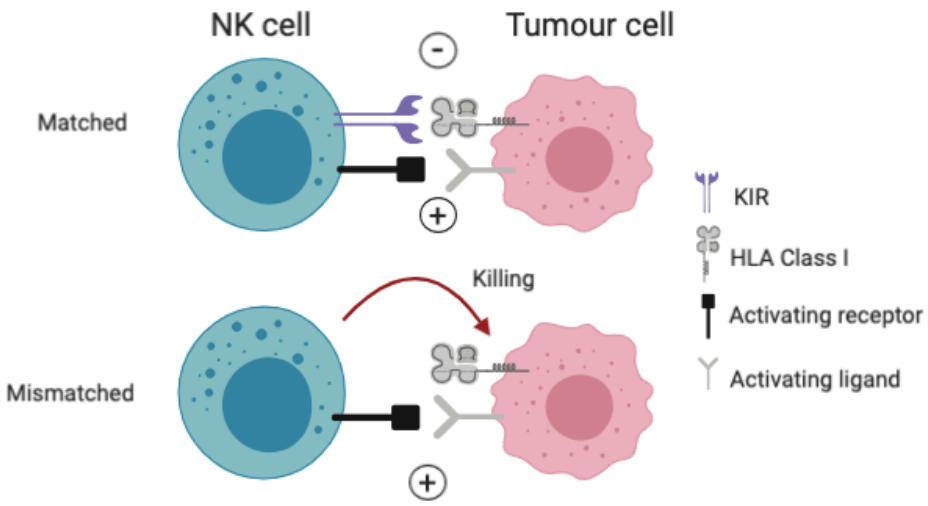


FIGURE 1.1.3. Missing self KIR in alloreactive NK cells. The absence of inhibitory KIR (mismatched) causing NK cell activation. On the other hand, when inhibitory KIR bind to HLA class I, NK cells were inactivated by inhibitory signals. Adapted from (Mahaweni et al., 2018).

1.1.2. Immune reconstitution after allogeneic HSCT

Following allo-HSCT the reconstitution of immune cells in recipients is dependent on cells infused from the donor graft, which are normally monitored for enumeration of $CD34^+$ cells (Rosenow et al., 2013). The source of the graft can contribute to the outcome of allo-HSCT, for example the number of nucleated cells is lower in umbilical CB compared to PB and BM. The immune cell recovery in allo-HSCT can be divided into innate and adaptive immunity. Innate cells include

the NK cells, dendritic cells, neutrophils, eosinophils and basophils while adaptive immune cells include mainly T cells and B cells **(Fig. 1.1.4).**

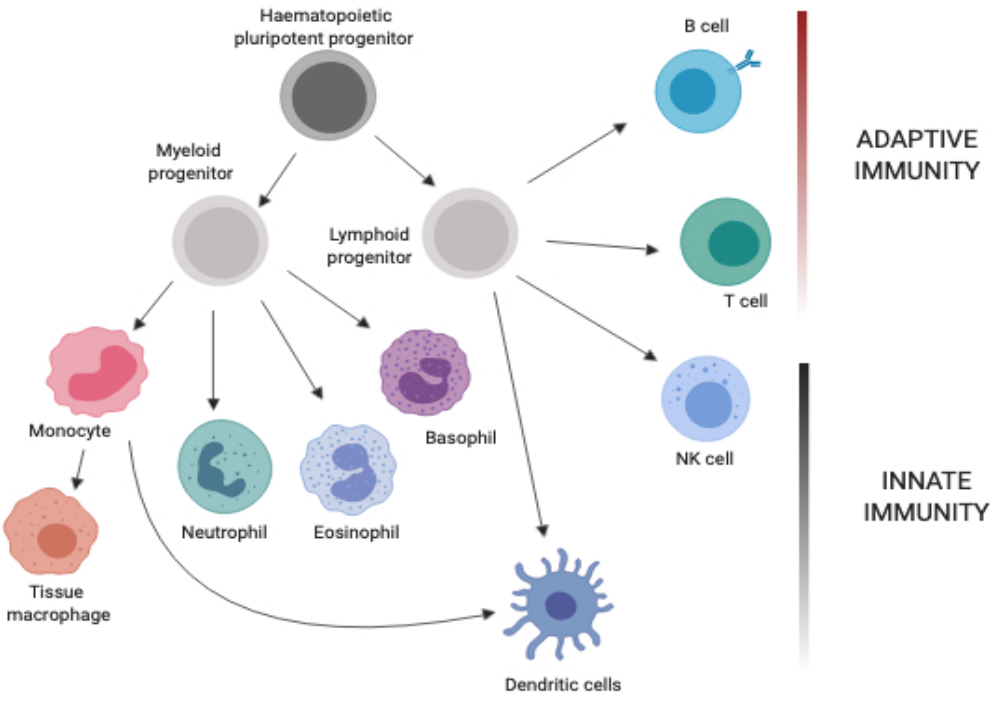


FIGURE 1.1.4. Different precursors of immune cells. Generally immune cells can be classified into innate and adaptive immunity. Adapted from (Ogonek et al., 2017a).

After allo-HSCT neutrophils are amongst the first immune cells to recover, followed by NK cells, T cells and B cells. The recovery of neutrophils takes about 14 to 30 days after allo-HSCT with different ranges depending on the source of the grafts **(Fig. 1.1.5).** On the other hand, NK cell reconstitution can take about 30 to 100 days, while around 100+ days are needed for T cell recovery with B cell reconstitution happening even later, up to 2 years post-transplant. Generally it is believed that $CD8^+$ T cell reconstitution is faster than $CD4^+$ T cell, but later than NK cells (Ogonek et al., 2017a; Stern et al., 2018).

The major challenge in the study of immune recovery after allo-HSCT is the assurance of safe transfer of immune cells from the donor into the patient with minimum GvHD effect and maximum GvL. This can be achieved through observation of reconstitution of different types of cells by flow cytometry and correlating with clinical outcome (Fry and Mackall, 2005; Auletta and Lazarus, 2005). Slow recovery of immune cells has been related to an increase in GvHD occurrence and mortality rate in allo-HSCT patients (Bejanyan et al., 2018). In various laboratories and transplant settings, a standard flow cytometry panel has been set up to monitor the recovery of immune cells in allo-HSCT patients. Patients usually monitored for total lymphocytes, T cells, B cells, NK cells, αβ T cells and γδ T cells using specific marker such as CD45, CD3, CD19, CD56 and CD16, TCRαβ and TCRγδ (Greco et al., 2018).

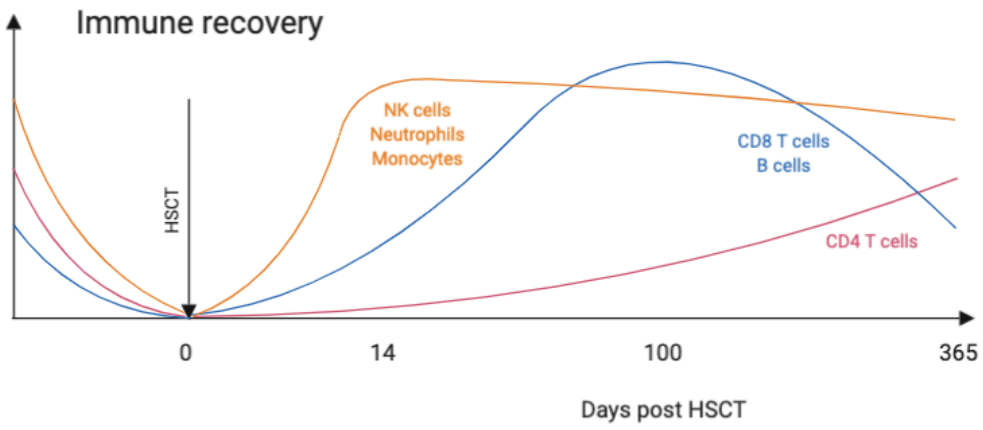


FIGURE 1.1.5. Overview of the kinetics of immune reconstitution. Adapted from (Stern et al., 2018).

Reconstitution of immune cells is believed to differ between autologous and allogeneic HSCT, with quicker lymphocyte recovery seen after autologous HSCT, within around 60 days after transplant (Wiegering et al., 2018). Also, studies have been carried out to manipulate the immune cell repertoire for transfusion by several advanced technologies, such as using αβ TCR and CD19 cell depletion and NK and T cell adoptive therapy (Neuenhahn et al., 2017; Stern et al., 2018; O'Reilly et al., 2016).

1.1.2.1. Natural Killer (NK) cells

Natural killer (NK) cells are part of the innate immune system forming part of the first line of defence and playing a key role in eradicating tumour cells and the killing of virally infected cells. As suggested by their name, NK cells kill the target cells 'naturally' and directly without prior antigen recognition. The activities of NK cells are mainly mediated by production of interferon-gamma (IFN-γ), tumour necrosis factor-alpha (TNF-α), interleukin 15 (IL-15), IL-12 and IL-18 inflammatory cytokines, as well as perforin and granzymes. Recently, NK cells have also been classified by their cytokine secretions, and belong to group 1 innate lymphoid cells (ILC) (Sivori et al., 2019; Zook and Kee, 2016).

NK cells have the ability to recognise 'missing self' target cells, as well as cells infected with virus and tumour cells which demonstrate downregulation of MHC class I, by several signalling pathways. As NK cells do not require antigen specificity like T and B cells, their activity and properties are highly dependent on the balance between germline encoded activating and inhibitory receptors (Lanier,

2008). NK cells reside in bone marrow, lymph nodes, skin, gut, tonsils, liver and lungs and are classified into cytotoxic, tolerant and regulatory dependent on their residency, phenotypes and functions (Wu et al., 2017; Abel et al., 2018).

NK cells are characterised as $CD56^{+}$ and $CD3^{-}$ in humans and they represent around 5 to 10% of lymphocytes in the peripheral blood. NK cells can also be classified into different populations according to their maturation stages and functional properties. For example $CD56^{dim}CD16^{bright}$ NK cells which circulate in the blood have high cytotoxic properties whilst $CD56^{bright}CD16^{negative}$ NK cells mainly reside in the secondary lymphoid organs and lymph nodes (Guillerey et al., 2016). In allo-HSCT, NK cells are the first lymphoid cells to reconstitute, with the majority of them being of the $CD56^{bright}CD16^{low/negative}$ subpopulation, such that the proportion of $CD56^{dim}$ to $CD56^{bright}$ cells is totally different in allo-HSCT patients compared to healthy donors (Huenecke et al., 2017). Studies within our group have shown that $CD56^{dim}$ NK cells increase slightly from day 0 to day 14 post-transplant and then started to drop. In contrast, $CD56^{bright}$ NK cells decrease from day 0 to day 14 and then start to expand. This observation reflects the emergence of newly generated immature NK at the transition time point of day 14 (Chan et al., 2018). Also, NK cells from day 14 were found to be donor-derived, highly proliferative and functional.

1.1.2.2. $CD8^+$ and $CD4^+$ T cells

T cells belong to the adaptive immune response and are characterised by their T-cell receptor (TCR) that recognises peptides loaded on the major histocompatibility complex (MHC) molecules of nucleated or antigen presenting cells. T cells are classified into cytotoxic T lymphocytes (CTL) or $CD8^+$ T cells and helper T lymphocytes or $CD4^+$ T cells. $CD8^+$ T cells recognise viral and mutated intracellular peptides presented by MHC Class I while $CD4^+$ T cells recognise peptides derived from extracellular pathogens presented by MHC Class II. $CD3^+$ TCR gene rearrangement and the development and differentiation of T cells into $CD8^+$ or $CD4^+$ occurs in the thymus (Zúñiga-Pflücker, 2004). The diversity and clonality of TCR on the T cells is crucial in protecting the host body against several pathogens (Takaba and Takayanagi, 2017).

After positive and negative selection in the thymus, naïve T cells generate different memory T cell subsets by travelling to secondary lymphoid organs where they encounter antigens presented by antigen presenting cells. The generation of different subsets of effector and memory T cells are described by distinct phenotypes and properties, including CCR7 expression. CCR7 is a chemokine receptor that controls the homing properties of the T cells. Most effector T cells die after antigen recognition, but some of them differentiate into memory T cells, such as central memory and effector memory which can subsequently be found in secondary lymphoid organs and non-lymphoid tissues. The memory phenotype of T cells can be characterised by CCR7 and CD45RA expression; effector memory ($CCR7^-CD45RA^-$), terminally differentiated memory ($CCR7^-CD45RA^+$), central

memory ($CCR7^+CD45RA^-$) and naïve T cells ($CCR7^+CD45RA^+$) (Mahnke et al., 2013; Sallusto et al., 1999; Masopust and Schenkel, 2013).

After allo-HSCT, T cell reconstitution is affected by several factors such as stem cell dose and HLA-match and is crucial in clinical outcome, with delays in the reconstitution causing significant transplant-related morbidity and mortality (de Koning et al., 2016). Moreover, early recovery of $CD8^+$ and $CD4^+$ T cells, specifically in patients receiving grafts from peripheral blood, are significant and are said to be predictive for the occurrence of GvHD (Waller et al., 2019).

T cell reconstitution post-transplant is also important for controlling infections such as CMV. Immune monitoring of CMV reactivation depends on the reconstitution of both $CD8^+$ and $CD4^+$ CMV specific responses to immunodominant CMV peptides, such as pp65, pp50, glycopreoteins-1 (IE-1) and IE-2 (Blyth et al., 2016). No differences have been found in CMV specific T cell recovery for either $CD8^+$ or $CD4^+$ cells in the allo-HSCT setting, however reconstitution occurs later in allo-HSCT than in auto-HSCT. The CMV-specific T cells are also thought to originate from either the donor, recipient or both (Widmann et al., 2018).

1.1.2.3. TCRγδ T cells

T cells can also be characterised by their surface expression of either αβ or γδ chains, known as αβ T cells or γδ T cells. Whilst both of these lymphocyte subsets undergo development in the thymus, the αβ T cells reside in the secondary lymphoid organs while γδ T cells are mainly found at epithelial surfaces (Fahl et

al., 2014). Unlike αβ T cells, γδ T cells do not recognise peptides presented on MHC but instead respond to a broad range of antigens directly, having naïve properties in the thymus and eventually acquire effector functions in the periphery (Fahl et al., 2014). The specific mechanism of γδ T cell development has not been well described, however they are believed to develop and differentiate from $CD8^-$ $CD4^-$ double negative common precursors (Hayday and Pennington, 2007).

There are three main γδ T cell subsets in humans based on their Vδ and Vγ chains. The Vδ1 subset can recognise different types of antigens and is found mainly in the thymus and peripheral tissues while Vδ2 subset, which is almost always associated with the Vγ9 subset, is predominantly found in the peripheral blood. Vγ9 T cells recognise phosphoantigens and non-peptide metabolites from intracellular pathogens (Lawand et al., 2017). Studies have indicated that γδ T cells can be classified into innate and adaptive (Bonneville et al., 2010; Vantourout and Hayday, 2013; Melandri et al., 2018), with a recent study showing that $Vγ9^+Vδ2^+$ T cells are an innate subset, whilst $Vγ9^-Vδ2^+$ T cells belong to the adaptive immune response. $Vγ9^+Vδ2^+$ T cells are present from birth, presenting public Vγ domains and responding to phosphoantigens while $Vγ9^-Vδ2^+$ T cells undergo differentiation and clonal expansion from naïve T cells and might respond to CMV (Davey et al., 2018b; Willcox et al., 2018). In contrast, Vδ1 T cells are said to have adaptive features **(Fig. 1.1.6)** and can be differentiated into naïve and effector phenotypes with upregulation of peripheral homing receptors and downregulation of lymphoid homing receptors (Davey et al., 2018a, 2017).

In the allogeneic transplant setting where TCR αβ and CD19 B cells are depleted, the naïve Vδ2 T cell subset reconstitutes as early as day 20 post-HSCT which suggests that the γδ T cells originate from both stem cell donors as well as recipients. These TCRγδ T cells are also believed to be functional having cytotoxic properties and expressing granzyme B, perforin and IFN-γ (Airoldi et al., 2015). In some other allo-HSCT setting, high number of γδ T cells have been correlated with higher survival rate and lower incidence of GvHD in the patients. These γδ T cells also are said to express NK cell receptors and mediate GvL effects (Minculescu and Sengeløv, 2015).

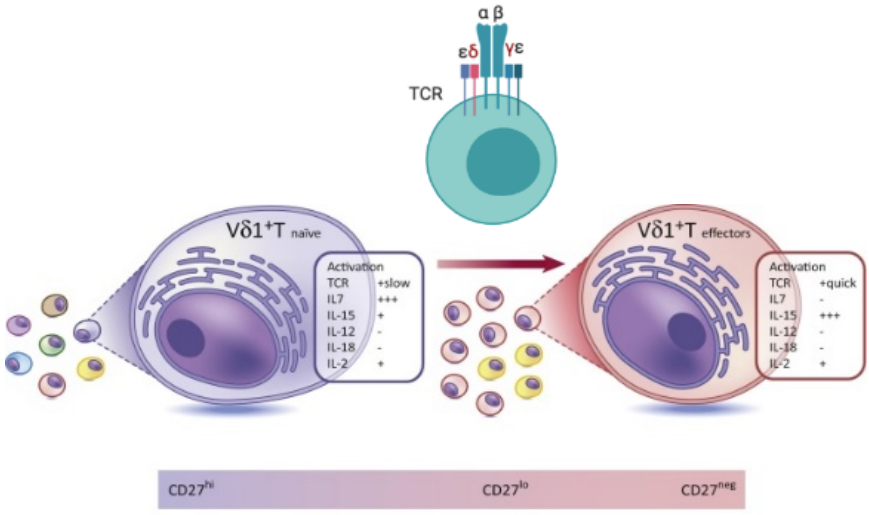


FIGURE 1.1.6. TCRγδ T cells characterised by gamma and delta chains. Vδ1 is the example of the common subset in the thymus, classified into innate and adaptive and undergone clonal expansion upon CMV infection or CMV reactivation. Adapted from (Davey et al., 2018a).

1.2. Human Cytomegalovirus (HCMV)

1.2.1. Introduction to HCMV

Human cytomegalovirus or HCMV is a herpesvirus (HHV-5) with a double-stranded linear DNA genome of approximately 235 kb. The virus is transmitted by exposure to infected saliva, urine, breast milk and body fluids. In healthy donors with a competent immune system the infection is asymptomatic. CMV is normally acquired in the early stages of life, mainly in new born infants or during childhood and once a person has been infected the virus is never completely cleared from the body, remaining latent in the host for the rest of their life. Although CMV is also believed to be replicated periodically to maintain and expand the infection (Boeckh, 2017; Wills et al., 2015), studies have shown that CMV resides in cells of the myeloid lineage with $CD34^+$ and dendritic cells upon reactivation (Sissons and Wills, 2015; Sinclair and Reeves, 2013). However, no evidence describing the residency of latent CMV in allo-HSCT has been reported due to the complexity of the mixed recipient-donor immune cells. In healthy donors, CMV genes can be detected mostly in the lungs, spleen, bone marrow and also lymph nodes, with evidence showing an abundance of CMV specific T cells found in lung (Gordon et al., 2017).

A meta-analysis study has described how CMV infection has 83% prevalence globally, with high rates of infection in Eastern countries when compared to European countries. CMV prevalence is most common in individuals with low socioeconomic status and also in women of reproductive age (Zuhair et al., 2019).

CMV infection has been associated with immunosenescence in some studies but the specific pathogenesis and mechanisms underlying this relationship remains unclear (Sansoni et al., 2014; Moss, 2019).

Data published by our group has also described how the CMV viral load burden increases in older healthy donors, probably due to the impaired immune system affecting the ability to control viral replication (Parry et al., 2016). Furthermore, the ability of CMV to evade, disseminate and replicate in the human host may relate to several encoded microRNA and peptides whose roles are still being debated and is taken into account (Jackson et al., 2017a). CMV DNA can be detected in the urine of some healthy donors, with a correlation found between CMV viral genes with production of IFN-γ T cell specific responses to the virus. However, no correlation was found between cytokine production in older people even though CMV has known to change the T cell repertoire (Jackson et al., 2017b).

1.2.2. T cell response to CMV

In humans, CMV is known to alter the phenotypes and functions of peripheral $CD8^+$ T cells, causing an expansion of memory cells that are believed to reflect expansion of cells following recognition of CMV-derived peptides. These changes in the T cell profile persist over time and may cause exhaustion following recurrent activation (Klenerman and Oxenius, 2016). Infection in healthy donors causes expansion of CMV-specific $CD8^+$ and $CD4^+$ T cells specific for a wide range of viral proteins and this can increase with aging. These CMV-specific T cells are typically polyfunctional, with the ability to produce several inflammatory cytokines

such as IL-2, TNF-α, IFN-γ, perforin as well as CD107a (Chiu et al., 2016). This data has been supported by findings from our group, which has described that CMV infection elicits memory inflation in older people, and a recent report showing that this was particularly marked for cells restricted to HLA-Cw*0702 epitopes. Similar to previous findings, this memory expansion was found to be functional with active secretion of IFN-γ and TNF-α (Hosie et al., 2017).

CMV infection is also known to cause the expansion of TCR Vδ2-negative T cells in healthy donors and the increase in this population is more significant in the elderly. However, no correlation was found between CMV-specific $CD8^+$ and $CD4^+$ T cells and the magnitude of the Vδ2-negative expansion (Alejenef et al., 2014).

1.2.3. The NK cells response to HCMV

In healthy donors CMV infection changes the profile of NK cell phenotype and distribution, causing the expansion of cells bearing the CD94/NKG2C activating receptor and an increase in both co-expression of inhibitory KIR (Muntasell et al., 2013c; Guma et al., 2006) and acquisition of the terminally differentiated marker CD57 (Bayard et al., 2016; Rölle and Brodin, 2016; Heath et al., 2016; Wu et al., 2013). The expansion of $NKG2C^+$ NK cells upon CMV infection is simultaneous with the downregulation of CD94/NKG2A, and cells show high cytotoxic properties upon HLA-E recognition on target cell lines (Bigley et al., 2016). The exposure of NK cells to CMV also causes the increase in the expression of the

activation marker CD69 on NK cells along with active IFN-γ production (Muntasell et al., 2013a). The high expression of CD94/NKG2C NK cells also has been related to the NKG2C genotype (Muntasell et al., 2013b).

CMV infection is also known to change the KIR repertoire on NK cells with a prolonged stable imprint being seen in healthy donors which may reflect self-education of NK cells upon viral stress (Beziat et al., 2013). The potential influence of CMV on immunosenescence in healthy donors has also been seen on NK cells, in which association has been found in $NKG2C^{+}CD57^{+}$NK cells in different subsets, most particularly within the $CD56^{dim}CD16^{bright}$ population (Campos et al., 2014).

1.3. CMV reactivation after allogeneic HSCT

CMV reactivation and disease are considered as one of the most important complications following HSCT and will be discussed extensively throughout the following chapters. In healthy donors CMV viral genes are barely detectable in peripheral bloods by quantitative PCR (Dioverti et al., 2017; Roback et al., 2003). However, immunosuppressed allo-HSCT patients are prone to the development of CMV reactivation, or primary infection if a seronegative patient receives a graft from a CMV seropositive donor (Emery et al., 2013). In some instances GvHD and CMV reactivation happen simultaneously which leads to poor transplant outcome (Ozdemir et al., 2007; Jang et al., 2015). CMV reactivation can develop at either an early or late stage post-transplant with the possibility of patients experiencing

multiple episodes of reactivation, mainly because of poor immune reconstitution. Overall, CMV reactivation occur in approximately 37% (median rate) of all patients after allo-HSCT with highest rate seen in CMV seropositive patients, regardless of the donor CMV serostatus (Styczynski, 2018).

1.3.1. Definition of 'CMV reactivation'

Monitoring for CMV reactivation is crucial in allo SCT patients as the complication can cause multiorgan diseases in the patients leading to significant morbidity and mortality (Boeckh and Ljungman, 2009; Atilla et al., 2017; Ramanathan et al., 2016; Teira et al., 2016). However, there are no standardised methods for detecting CMV DNA in peripheral blood as most laboratories use 'in house' quantitative polymerase chain reaction (qPCR) for CMV viral load testing. With different laboratories using different sets of primers that target different part of CMV genomes in the qPCR. According to the Stem Cell Transplant Unit, University Hospitals Birmingham guidelines (2017), CMV reactivation is defined as more than 200 copies/ml of CMV DNA detected in peripheral blood of allo-HSCT patients by qPCR. In comparison, the viral genes are barely detectable by qPCR in the peripheral blood of healthy donors (Dioverti et al., 2017; Roback et al., 2003). As there is no gold standard in the detection of CMV viral loads in transplant patients, the methods keep changing and evolving over time, with some controversial issues in determining the best source of samples for CMV viral load testing, either from plasma or from the whole blood (Emery et al., 2013; Ljungman et al., 2019).

In addition some labs have been using CMV culture rather than qPCR to diagnose primary CMV infection and CMV reactivation (Ljungman et al., 2011). Due to the complexity of the culture method, qPCR is generally considered to be sufficiently reliable and sensitive for viral load testing and monitoring for CMV reactivation in transplant patients. Indeed, since 2004, the antigenemia assay and PCR have been widely used all over the world for screening and pre-emptive therapy strategies in HSCT. Although the pp65 antigenemia test is adequate for CMV monitoring in pre-emptive therapy, the assay has several drawbacks such as the requirement for isolation of circulating neutrophils, which could be a problem in transplant where numbers are low, and the fact that the assay has to be processed quickly to retain sensitivity (Green et al., 2012; Chen et al., 2018b).

1.3.2. Prophylaxis and treatment for CMV reactivation

The treatment and prophylaxis strategies used in allo-HSCT aim to control and reduce CMV disease by following international standard criteria. These include the monitoring of viral load weekly for at least 12 weeks post-transplant, or indeed longer if the patient develops chronic GvHD. Treatment for CMV infection is generally undertaken using ganciclovir, valganciclovir, foscarnet or cidofovir as anti-viral agents following the guidelines being set up by each transplant centre (Hammerstrom et al., 2018; Emery et al., 2013). This pre-emptive therapy however has some disadvantages, due to the toxic effects of the antiviral drugs, such as ganciclovir which is associated increased risk of myelosuppression (Chen et al., 2018b). Nevertheless, despite these strategies to reduce CMV disease in allo-HSCT patients, CMV reactivation is still believed to be correlated with considerable

financial and morbidity implications for patients after allogenic HSCT (Webb et al., 2018; Robin et al., 2017).

1.3.3. The importance of recipient and donor serostatus in CMV risk

In the transplant setting the serological status of the donor and recipient remain crucial factors for the subsequent risk of CMV disease (Ljungman et al., 2011). There are four possible combinations of CMV serostatus pairs; CMV seropositive recipient and seropositive donor (R+/D+), seropositive recipient and seronegative donor (R+/D-), seronegative recipient and seropositive donor (R-/D+) and seronegative recipient and seronegative donor (R-/D-) **(Fig. 1.3.1).** The maximum risk for CMV occurs in an R+/D- transplant and is referred to as a *'primary infection'*. This is because the T cells transfused from the seronegative donor have never experienced CMV antigens before and therefore there are no CMV-specific memory T cells within the repertoire and the immune system must mount a primary immune response **(Fig. 1.3.1).** CMV within recipient cells remains unchecked by the graft or donor T cells until this immune response develops and this is exacerbated by immune suppression within the recipient. Nevertheless, even though R+/D- status is considered to be a high risk CMV group, patients within the R+/D+ pairing are even more likely to develop CMV reactivation, potentially due to the latent CMV burden within the patients' own stem cells (Wills et al., 2015; Jaskula et al., 2012; Krawczyk et al., 2018).

Patients within the R-/D- risk group rarely develop CMV infection although this may happen, potentially reflecting false attribution of serological status or primary infection from the external environment or third party blood products. As such it is unclear if this should be classified as either CMV reactivation or primary infection, although high viral load copy number is often detected within blood.

In most transplant protocols an R-/D+ transplant pair is avoided, where possible. CMV seronegative donors are selected where possible for CMV seronegative patients whilst CMV seropositive donor may be advantageous for CMV seropositive patients. According to recent guidelines (2013), risk-adapted strategies are necessary when monitoring patients within the CMV risk group R+/D- (Emery et al., 2013). This CMV risk group also possess a further risk as the pairing has been associated with increased potential for development of resistance to antiviral treatment (Servais et al., 2016).

CMV seropositive recipients undergoing HLA haploidentical unrelated cord blood allogeneic transplants receiving grafts from CMV seropositive donors (R+/D+) have been reported to show improved overall survival compared to the R+/D- group (Ramanathan et al., 2016). Another study has also described that poor survival rate in the R+/D- pairing whereas improved survival and transplant related mortality can be seen in R+/D+ patients (Ljungman et al., 2003). It has also been reported that the $CD3^+$ content within the graft and the use of a male donor also contribute to the risks of CMV disease in allogeneic HSCT (Webb et al., 2018; Ljungman et al., 2010).

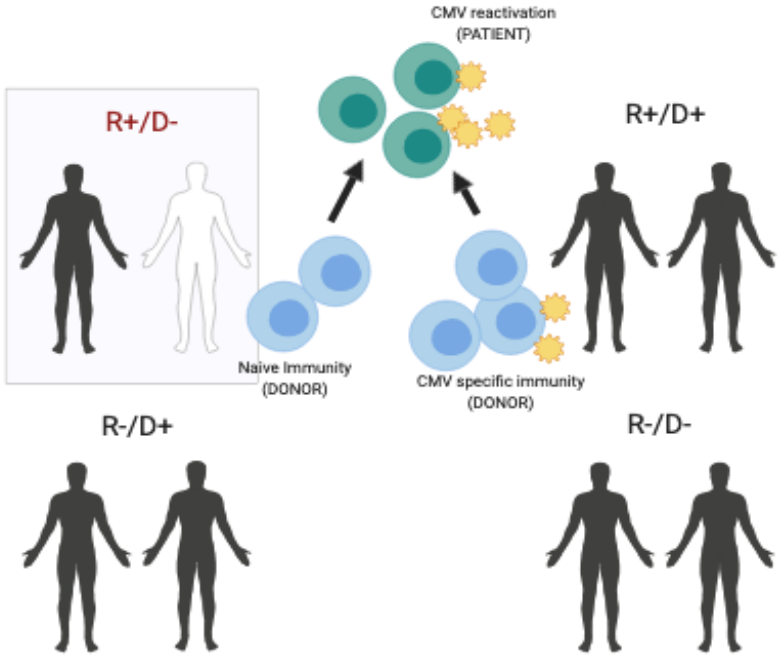


FIGURE 1.3.1.CMV risk group in allogeneic stem cell transplant patients. R+/D- pair possess a major risk in HSCT as compared to R+/D+, R-/D+ and R-/D- groups.

1.3.4. CMV reactivation after autologous HSCT

Unlike allo-HSCT, CMV reactivation is not a major concern after autologous HSCT. Although patients can still develop CMV reactivation due to immune suppression, this occurrence is much lower than seen in allo-HSCT, estimated at around 12% in some studies, and is also less severe in outcome (Styczynski, 2018). Nevertheless CMV reactivation can still contribute to morbidity (Marchesi et al., 2015) and CMV surveillance and viral load monitoring is recommended in some settings (Kaya et al., 2017).

1.4. The impact of CMV reactivation on patient outcomes after allogeneic HSCT

As discussed before, many studies have documented the harmful effects of CMV reactivation in allo-HSCT patients. Paradoxically, however, some reports have also described a potential clinical benefit from CMV reactivation, mainly in reducing the risk of leukaemia relapse. Even though the mechanisms on eradication of leukaemic cells by CMV induced immune cells are not clear, many believe that the effects are mediated by cell types such as NK and T cells. In this study, it was of interest to describe the potential roles of NK cells, as well as $CD8^+$, $CD4^+$ and γδ T cells, in controlling CMV reactivation in allo-HSCT patients **(Fig. 1.4.1).** The impact of viral load at the time of reactivation and the significance of the R+/D+ and R+/D- risk groups was also explored, to understand the importance of the transfer of naïve or CMV-immune donor cells.

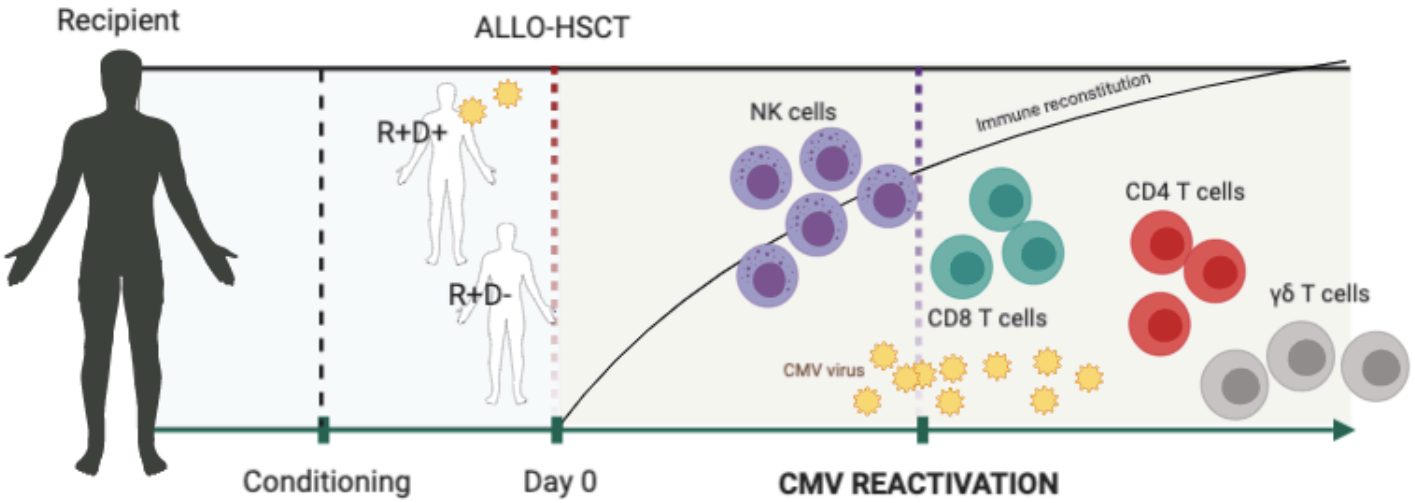


FIGURE 1.4.1. Impacts of CMV reactivation on immune reconstitution after allo-HSCT. The effects of CMV reactivation in allo-HSCT was studied on NK cells, $CD8^+$ T cell, $CD4^+$ T cells and γδ T cells.

1.4.1. Expansion in adaptive or memory like NKG2C$^+$ NK cells

NK cells play an important role in controlling the initial phase of CMV reactivation and, as their reconstitution happens much earlier than that of T cells and B cells after HSCT, we were particularly interested to assess how they responded to CMV reactivation. In addition, studies have shown that although NK cells belong to the innate immune system they also exhibit features of adaptive immunity and have memory properties which are driven specifically by CMV infection (Newhook et al., 2017; Paust et al., 2017). The reconstitution of these adaptive or 'memory-like' NK cells is said to favour an improved clinical outcome after allo-HSCT and is also influenced by the treatment regimen received by the patients, being increased after non-myeloablative conditioning (Cichocki et al., 2019).

One study reported the association of NK cell expansion with reduction in leukaemia relapse after HSCT and showed that this effect correlated with the mature and adaptive-like CD56^{dim}NKG2C$^+$CD57$^+$ NK population. This report also demonstrated that this subset of NK cells can produce high levels of the inflammatory cytokines TNF-α and IFN-γ in response to K562 myeloid leukaemia target cells. It was suggested that the mechanism of tumour killing might be due to switching of the NKG2A inhibitory marker to the NKG2C activating molecule in response to engagement with classical HLA-E (Cichocki et al., 2016). Remarkably, the clonal-like expansion of adaptive NKG2C$^+$ NK cells is said to be driven by the polymorphic CMV peptides specifically on UL40 which are presented by the HLA-E molecules on the infected cells (Hammer et al., 2018a). Even though the mechanism of adaptive NK cells expansion is still unknown, NKG2C$^-$ and NKG2C$^+$

NK cells are found to express the co-stimulatory molecule CD2 following the ligation of antibody-coated CD16 upon activation (Liu et al., 2016b). As well as producing high levels of TNF-α and IFN-γ, the NKG2C^{+} NK cell expansion also results in high levels of IL-18 being produced, in the absence of IL-12, in response to the target cells (Hammer et al., 2018b).

CD94/NKG2C and CD94/NKG2A are heterodimeric C-type lectin family activating and inhibiting receptors respectively which are related to killer-cell immunoglobulin like receptor (KIR) genes and appear homologous to Ly49H in mouse (Huygens et al., 2014; Pegram et al., 2011). It is reported that 4% of the human population carries a homozygous deletion of NKG2C (*NKG2C*$^{-/-}$; also known as the *KLRC2* gene) although it appears that increased expression of CD2 may partially overcome this functional deficiency within this population (Liu et al., 2016b).

The expansion of NK 'memory-like' NKG2C^{+} cells has been described in different allo-HSCT settings (Foley et al., 2012a, 2012b). Interestingly, after cord blood transplantation, the NKG2C genotype of the grafts can act as a biomarker in the prediction of CMV infection, with those grafts containing fewer NKG2C genes being associated with increased risk of subsequent reactivation, and this may be useful in prophylaxis and pre-emptive monitoring (Cao et al., 2018). CMV seropositivity in healthy people is associated with the presence of a population of adaptive NK cells with the classical CD56^{dim}CD16^{+}NKG2C^{+}CD57^{+} phenotype (Bayard et al., 2016; Lopez-Sejas et al., 2016; Malmberg et al., 2012). The KIR

genotype of the transplant donor is known to influence the rate of CMV reactivation (Cook et al., 2006) and studies have also have investigated the expression of inhibitory and activatory KIRs. Inhibitory KIR genes were associated with higher rate of CMV reactivation whereas the activatory ones were seen to reduce this risk. Somewhat unexpectedly, this profile was only observed when the HLA-C ligand was absent from the donor/recipient genotype (Davis et al., 2015; Behrendt et al., 2013).

1.4.2. CMV-CD8$^+$ and CD4$^+$ T cell specific responses

CMV has been reported to be able to stimulate very broad T cell responses and these T cell responses are important for controlling CMV reactivation (Lidehall et al., 2005; Sylwester et al., 2005). In allogeneic HSCT, the CMV specific CD8$^+$ and CD4$^+$ responses post-transplant have been reported to correlate with protection from CMV and are useful for the prediction of subsequent risk of CMV disease occurrence (Ljungman et al., 2011). Most of the studies looking at CMV T cell specific responses in post-HSCT have used HLA Class I tetramers (Liu et al., 2016a; Suessmuth et al., 2015; Borchers et al., 2011; Pourgheysari et al., 2009; Link et al., 2016) with only one study reporting on T cell specific responses using Class II tetramers (Raeiszadeh et al., 2015). In allo-HSCT setting, the CMV specific CD8$^+$ T cells can also be characterised by different avidity binding (Ogonek et al., 2017b), with high production of IFN-ɣ crucial in controlling the high viral load (Ciáurriz et al., 2017).

It was also observed that patients who failed to develop $CD4^+$ and $CD8^+$ CMV specific responses within 100 days post-HSCT were predisposed to late viral reactivation (Pourgheysari et al., 2009). Specifically, late recovery of CMV specific $CD8^+$ central memory T cells has been associated with increased risk of CMV recurrence (Liu et al., 2016a). In another study, CMV reactivation caused the inflation of $CD8^+$ effector memory (EM) and effector memory RA (EMRA) T cells after a period of one year in allo-HSCT (Lugthart et al., 2014). These memory T cells can also be transferred from the donor to the recipient, with antigen specific immunity in R+/D- recipient-donor pair predominantly derived from the recipient (Krawczyk et al., 2018). The impact of $CD4^+$ T cells is less well studied in allo-HSCT, but early recovery of $CD4^+$ T cells together with KIR3DL1 NK cells has been shown to be associated with lower incidence of CMV reactivation (Drylewicz et al., 2016). Studies into CMV specific responses have been further extended to include TCR sequencing and repertoire analysis in HSCT on TCRα and TCRβ, and specifically on HLA-A*2402 restricted epitopes (Suessmuth et al., 2015; Nakasone et al., 2013; Link et al., 2016).

1.4.3. Vδ1 T cells and the response to CMV reactivation

Unlike NK, $CD8^+$ and $CD4^+$ T cells, descriptions of γδ T cell reconstitution in allo-HSCT are less well described. A report by de Witte et al (2018) describes the expansion of the $V\delta1^+$ T cell subset upon CMV reactivation, whilst the Vδ2 subset remained as major γδ T cells population (de Witte et al., 2018). These $V\delta2^-$ cells have also be shown to be able to recognise tumour cells and expression of CD8αα co-stimulatory molecules may also be a feature (Scheper et al., 2013).

A recent study of γδ T cells reconstituted early after allo-HSCT used the next-generation sequencing (NGS) approach to determine the T-cell receptor (TCR) repertoire after CMV reactivation and concluded that this was broadly stable after transplant. Gamma chain genes (*TRG)* showed more sharing of sequence between individuals ('public' profile) whilst the delta sequences (*TRD*) were more variable or 'private' (Ravens et al., 2017). Of note, CMV reactivation did have a significant influence on the profile of the total γδ T cell reconstitution.

1.5. The potential association of CMV reactivation with reduced risk of leukaemia relapse

In recent years CMV reactivation has been shown to carry a potential clinical benefit for allo-HSCT patients as shown by a reduced rate of leukaemia relapse in different transplant settings and patient cohorts. However, this remains somewhat controversial, with different observations in different patient cohorts, and the mechanisms mediating this advantage remain unclear. A meta-analysis to probe

CMV advantage in transplant would require a large cohort of allo-HSCT patients with high incidence of CMV reactivation because several other parameters have to be taken into account, including type of disease and conditioning received in the allo-HSCT setting.

In most cases CMV reactivation has been associated with a negative outcome in HSCT, with a significant association with higher non-relapse mortality (NRM) and contribution to the occurrence of GvHD. Nevertheless, a substantial decrease in leukaemia relapse has been reported in different patient cohorts in patients with disorders such as AML and myeloproliferative disorders (MPD) (Inagaki et al., 2016; Takenaka et al., 2015; Green et al., 2013; Hilal et al., 2017; Peric et al., 2018). After cord blood allo-HSCT, no association has been found between CMV reactivation and relapse of AML or ALL leukaemia despite the analysis of a large patient cohort (Ramanathan et al., 2016).

The mechanism underlying a potential association between CMV reactivation and reduced rate of leukaemia relapse is not well defined. Studies have described the potential anti-tumour effects of immune cells which are expanded following CMV reactivation and this effect is predominantly observed with the NK cells. Nevertheless, there remains controversy in the field. Björklund et al., (2016) have shown that a more 'naïve' NK cell repertoire within the donor, with an increased proportion of $NKG2A^{+}CD57^{+}NKG2C$ cells, is strongly associated with protection from leukaemia relapse, potentially due to increased numbers of NK cells which

lack 'self-reactive' inhibitory KIR expression and are thus better able to kill tumour cells (Björklund et al., 2016).

Anti-leukaemic activity from CMV-induced NKG2C^{+} NK cells may depend on interaction with HLA-E and this is retained in the tumour cells whilst there is a downregulation of classical HLA-Class I. This has been described following analysis of a large patient cohort, in which a significant correlation was found between the reduction of leukaemia relapse and the expansion of NK cells with specific mature phenotypes, CD56^{dim}NKG2C^{+}CD57^{+} (Cichocki et al., 2016). The mechanism of tumour killing in allo-HSCT could also be mediated through γδ T cells, referring to a report saying the beneficial role to be played by the Vδ2 negative γδ T cells through the interaction with T-cell receptor (TCR) (de Witte et al., 2017; Litjens et al., 2018).

1.6. Hypothesis and objectives

We hypothesised that CMV reactivation will have a significant impact on allogeneic HSCT by imprinting the immune cells with phenotypes specific to CMV. Even though CMV reactivation has traditionally been thought to be associated with impaired outcome after allo-HSCT, this work may provide a better understanding of the roles of different immune cells in both controlling CMV reactivation and potentially eradicating leukaemic blasts. In addition, the study may identify a potential early biomarker to predict recurrence of CMV reactivation or infection which could improve the outcome of allo-HSCT. By comparing immune recovery

from CMV seronegative or seropositive transplant donors we will also be able to contrast the relative importance of transfer of immune memory.

The objectives were:

1. To observe the effect of CMV reactivation on the recovery and reconstitution of NK and T cells after allo-HSCT
2. To study the immune phenotypes of immune cells in relation to CMV reactivation after allo-HSCT
3. To interrogate the correlation between the changes in NK and T cell immune cell phenotypes and clinical outcome
4. To analyse the potential beneficial impact of CMV reactivation after allo-HSCT through the killing of leukaemic cells

CHAPTER 2: METHODOLOGY

2.1. Materials and reagents

2.1.1. Flow cytometry staining and cell culture

Wash media

RPMI-1640 Medium (Sigma, Cat #R8758)

50 U/ml Penicillin (Gibco™ Cat #15070063)

50 µg/ml Streptomycin (Gibco™ Cat #15070063)

Growth media

RPMI-1640 (Sigma, Cat #R8758)

10% FBS (Sigma, Cat #F7524)

50 U/ml Penicillin (Gibco™ Cat #15070063)

50 µg/ml Streptomycin (Gibco™ Cat #15070063)

2 mM L-Glutamine (Gibco™, Cat #25030024)

Growth media 20

RPMI-1640 (Sigma, Cat #R8758)

20% FBS (Sigma, Cat #F7524)

50 U/ml Penicillin (Gibco™ Cat #15070063)

50 µg/ml Streptomycin (Gibco™ Cat #15070063)

2 mM L-Glutamine (Gibco™, Cat #25030024)

Freezing media

FBS (Sigma, Cat #F7524)

10% DMSO (Sigma, Cat #D2650)

MACS buffer

1x PBS
(University of Birmingham or Oxoid™ / Thermo Scientific™ Cat #BR0014G)

0.5% BSA (Sigma, Cat #A7906)

2 mM EDTA (Sigma, Cat #S8045)

K562 cell lines (ATCC® CCL-243™)

CML K562 cell lines were maintained in growth media 20 in Corning® 25 cm^2 cell culture flask (Sigma, Cat #CLS430639)

EBV-transformed LCL cell lines (ATCC® CRL-5965)

Lymphoblastoid cell lines also were maintained in growth media 20 in Corning® 25 cm^2 cell culture flask.

2.1.2. HLA typing PCR-SSP

PCR buffer

2.6x NH_4 buffer (Bioline, Cat #BIO-21040)

0.52 mM dNTP Mix (Bioline, Cat #BIO-39025)

5.2 mM $MgCl_2$ (Sigma, Cat #M2670-100G)

0.06% (v/v) Glycerol (Sigma, Cat #G8773)

0.15 mg/ml Cresol Red (Sigma, Cat #11448)

Nuclease free water

1x TBE buffer

10x TBE buffer (Geneflow, Cat #B9-0020)

dH_20

2.1.3. CMV IgG ELISA

Coating buffer

Carbonate-Bicarbonate capsule (Sigma, Cat #C3041)

Sterile dH_20

Dilution buffer

0.05% Tween 20 (Cat #P1379)

1% BSA

1x PBS

Wash buffer

0.05% Tween 20

1x PBS

2.1.4. NK cell Intracellular cytokine staining

Paraformaldehyde, PFA

4.0% Paraformaldehyde (Sigma, Cat #158127)

dH_20

Saponin

0.5% Saponin (Sigma, Cat #47036)

dH_20

2.2. Study design

2.2.1. Patients

The population studied in this project including the patients who undergone allo-HSCT in the Queen Elizabeth Hospital, Birmingham, within West Midlands area. Patients were recruited from the QE hospital and samples taken following written, informed consent under the Biological Correlates of Outcomes from Stem Cell Transplant (BOOST) trial (RG 13-172).

Up to 60 ml of peripheral blood in sodium heparin (BD Vacutainer®, Cat. #367876) and 6 ml of clotted blood (BD Vacutainer®, Cat. #367837) were collected from allo-HSCT patients diagnosed with CMV reactivation for the first four weeks after their reactivation diagnosis. Up to 25 ml of urine was also collected from the patients during this period. Up to 36 ml of heparinised and 6 ml of clotted blood were also collected pre-transplant, pre-reactivation and for up to two years post-transplant **(Fig. 2.2.1).**

In addition, up to 36 ml of heparinised and 6 ml clotted peripheral blood were collected from patients (either CMV positive or negative) undergoing allogeneic transplant but without CMV reactivation at equivalent time points pre and post-transplant for use as controls. This group of patients were also followed for up to 2 years post-transplant.

Patients were routinely monitored under pre-emptive therapy for active CMV by quantitative polymerase chain reaction (qPCR) and reactivation diagnosed following a result of more than 200 copies/ml of CMV DNA in whole blood which has been tested in laboratory of Heartlands Hospital Birmingham. The test was done by using 'in house' qPCR assay and the details of the test are not accessible.

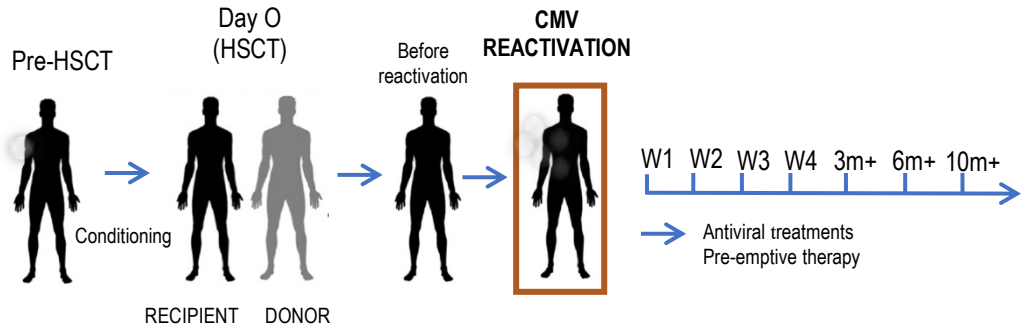


FIGURE 2.2.1. Sample collection schedule. Peripheral whole blood for isolation of PBMCs and serum was collected before transplant (Pre-HSCT), after conditioning pre-transplant (Day 0), at various time points post-transplant pre-reactivation, and post-reactivation for 4 weeks and at weeks and months thereafter up to two years. Urine samples were collected only within the four weeks post-reactivation. [W: week(s), m: month(s) after CMV reactivation].

2.2.2. Healthy donors

Healthy donors (HDs) who were either positive or negative for CMV were used as controls and were recruited from among the students and staff from the College of Medical and Dental Sciences, University of Birmingham following written informed consent under the BOOST trial (REC reference number 15/WM/0194) or CMV study (REC reference Number: 14/WM/1254). Up to 60 ml of peripheral blood was collected in sodium heparin tubes along with 6 ml of clotted blood. Where possible, HDs were selected who had been tested for CMV status previously by in house serum IgG ELISA. The CMV positive donors were typed for HLA

Class I and HLA Class II, with some of negative donors also typed for use in tetramer optimisation experiments.

2.2.3. Clinical data and patients' information

The characteristics of the patients with reactivation and without reactivation are described in more detail in Chapter 3. Additional patient information is shown in Appendix (Supp. Table 1a-e). The clinical data was obtained from the QE hospital and updated regularly in the database by research nurse assigned to the BOOST study. All patients were classified according to their CMV serostatus pairs; recipient positive and donor positive (R+/D+), recipient positive and donor negative (R+/D-), recipient negative and donor positive (R-/D+) and recipient negative and donor negative (R-/D). Donors with ambiguous CMV serostatus are classified as equivocal (R+/Dequi).

2.3. Samples processing

2.3.1. Isolation of Peripheral Blood Mononuclear Cells (PBMCs)

Peripheral Blood Mononuclear Cells (PBMCs) were isolated from heparinised blood by density gradient centrifugation over Lymphoprep^{TM} (Stem cell Technologies, Cat #07861) within 24 hours of collection. Peripheral blood was diluted 1:1 with wash media, layered on Lymphoprep^{TM} at a ratio of 2:1 and centrifuged at 2000 x g for 25 minutes (brake off). The buffy coat layer **(Fig. 2.3.1)** was harvested using a transfer pipette, resuspended in wash media and centrifuged

at 500 x g for 10 minutes to wash. The cell pellet was suspended in wash media according to the size of the pellet and the number of cells determined using a haemocytometer (Fast-Read 102®, Kova International, Cat #88010).

Cells were washed a final time in wash media and centrifuged at 500 x g for 10 minutes before being cryopreserved (described below).

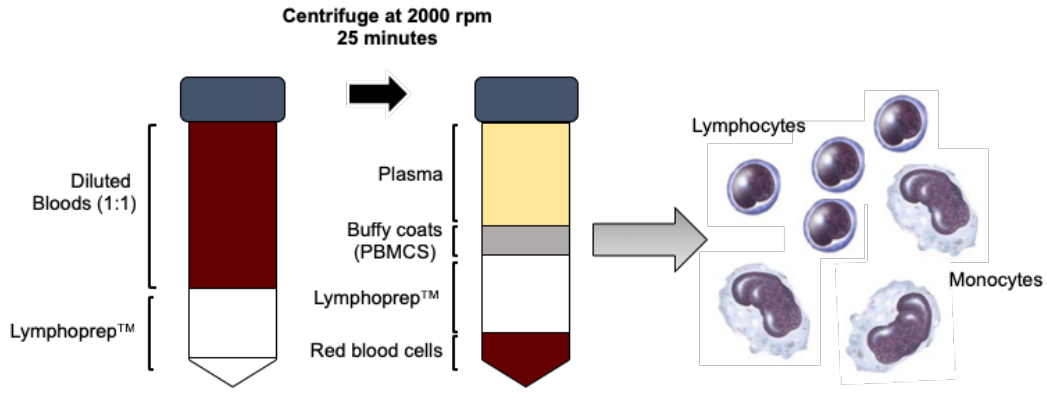


FIGURE 2.3.1. Isolation of peripheral blood mononuclear cells (PBMCs) from whole blood.

2.3.1.1. Cryopreservation and storage

Following the final wash step (described above) the cell pellet was resuspended in ice cold freezing media and transferred to cryovials (AlphaLabs, Cat #LW3532) in a Mr. Frosty™ Freezing Container containing isopropanol (Fisher Scientific, Cat #10674732) overnight to allow the cells to cool at a constant 1°C per hour. The vials were then transferred to either -80^{0}C or liquid nitrogen for longer term storage until required.

2.3.1.2. Thawing of PBMCs

Frozen cells were recovered by rapid thawing at 37°C in a water bath and centrifuging in pre-warmed growth media at 500 x g for 10 minutes. The cell pellet was re-suspended in 10 ml of growth media and a cell count performed. At this step, the visible and massive cell clumps were filtered by using EASYstrainer™ Cell Sieves, 70 µm (Greiner Bio-One, Cat #89508-344) into a 50 ml tube. PBMCs were again spun at 500 x g for 10 minutes and re-suspended in MACS buffer, centrifuged as at 500 x g and 5 minutes and the supernatant poured off.

2.3.2. Serum collection for DNA extraction

Whole blood collected in vacutainers containing clotting factor were centrifuged at 900 x g for 5 minutes, the cell free supernatant was harvested, transferred to 2 ml cryovials (Nunc™, Cat #377267) and stored at -80^{0}C for future use.

2.3.3. Urine concentration for DNA extraction

Urine samples were received weekly in the 4 weeks following CMV reactivation. Between 20 and 25 mls of urine were concentrated and filtered using the Microsep™ Advance Centrifugal Devices (PALL, Cat. #MCP100C46) according to the manufacturer's protocol. Four ml of urine was poured into the column and centrifuged for 3000 x g and 15 minutes. The concentrated urine from the filter was then suspended in 700 µl of PBS. The concentrated urine was transferred to 1.5 ml Eppendorf tubes and stored at -80^{0}C for future use (DNA extraction).

2.4. HLA typing of healthy donors

2.4.1. Polymerase chain reaction-sequence specific primers (PCR-SSP)

HLA typing was performed using the in-house PCR-SSP method using a set of HLA primers for specific alleles as described by Bunce et al., (1995). DNA from HDs were extracted from PBMCs using the DNeasy Blood & Tissue Kits (Qiagen, Cat #69504) according to the manufacturers' instructions. CMV positive HDs were typed for common HLA Class I (Eg: A2, A24, B7, B8 and B35) and Class II (Eg: DR7) using primers listed in **Table 2.4.1.**

2.4.2. Master mix preparation and PCR conditions

A 14x PCR master mix was prepared (see **Table 2.4.2**) for each donor tested and 9 µl aliquots divided into each of fourteen 0.2 ml PCR tubes (StarLab, Cat #14026700) and each of the fourteen primer mixes (forward and reverse) listed in **Table 2.4.1** was added to the appropriate tube (1-14). The PCR tubes were loaded into the thermocycler (GeneAmp® PCR System 9700) and run according to the programme in **Table 2.4.3.**

TABLE 2.4.1. HLA primers with information specific alleles and concentrations used to prepare primer mixes for use in PCR-SSP (Bunce, et al. 1995). The stock HLA primers concentration was 50 μM.

No	HLA specific alleles	Forward primer	Sequence	Final concentration (mM)	Reverse primer	Sequence	Final concentration (mM)	Product Size (bp)
1	A*0101, 0102	286F	CGACGCCGCGAGCCAGAA	2.7	431R	AGCCCGTCCACGCACCG	2.7	629
2	A*0201-17	296F	GTGGATAGAGCAGGAGGGT	3.4	302R	CCAAGAGCGCAGGTCCTCT	3.4	489
3	A*0301, 0302	291F	AGCGACGCCGCGAGCCA	1.3	299R	CACTCCACGCACGTGCCA	3.4	628
4	A*1102, 1102, 6601	290F	ACGGAATGTGAAGGCCCA	1.0	167R	GAGCCACTCCACGCACCG	1.7	552
5	A*01, 11, 3601, 8001, 3402	367F	TACTACAACCAGAGCGAGGA	1.2	394R	CCACGTCGCAGCCATACATT	1.2	300
6	B*0702-0705, 8101	193F	GGAGTATTGGGACCGGAAC	3.4	221R	TACCAGCGCGCTCCAGCT	3.4	300
7	B*0703	312F	ACACAGATCTACAAGACCAAC	3.4	221R	TACCAGCGCGCTCCAGCT	3.4	600
8	B*0801,0802, B51GAC, B*4406	195F	GACCGGAACACACAGATCTT	3.4	212R	CCTCCAGGTAGGCTCTGTC	3.4	543
9	B*0801, 0802	195F	GACCGGAACACACAGATCTT	3.4	220R	CCGCGCGCTCCAGCGTG	3.4	602
10	B*3501-3504	193F	GGAGTATTGGGACCGGAAC	3.4	223R	GCCATACATCCTCTGGATGA	3.4	369
11	B35*3501-13	188F	GCCGCGAGTCCGAGGAC	3.4	237R	GCGCAGGTTCCGCAGGC	3.4	128
12	B35*3501-3509,3511, 5301	195F	GACCGGAACACACAGATCTT	3.4	213R	GAGGAGGCGCCCGTCG	3.4	389
					277R	GGAGGAAGCGCCCGTCG	3.4	340
13	B*4402-06	202F	GGGGAGCCCCGCTTCATT	3.4	393R	GTCGTAGGCGTCCTGGTC	34	546
		272F	CGCCACGAGTCCGAGGAA	3.4	285R	CGTCGTAGGCGTACTGGTC	3.4	481
14	DRB1*0701	48F	CCTGTGGCGGGTAAGTATA	3.4	49R	CCCGTAGTTGTGTCTGCACAC	3.4	231
15	Control*	63F	TGCCAAGTGGAGCACCCAA	0.1	64R	GCATCTTGCTCTGTGCAGAT	0.1	796

TABLE 2.4.2. Master mix preparation per 14x reaction. Master mix was prepared as described below.

Master mix (14x)	Volumes (µl)
PCR buffer	70.9
Nuclease free water	35.0
Control primer mix*	14.0
BIOTAQ™ DNA polymerase (5 units/µl) (BIOLINE BIO-21040: 500 units)	0.75
DNA 28 ng/µl (140 ng/5µl)	5.0

TABLE 2.4.3. PCR condition for HLA typing.

Stage	Temperature	Time	Cycles
1	96°C	1 min	
2	96°C	25 sec	5
	70°C	45 sec	
	72°C	45 sec	
3	96°C	25 sec	21
	65°C	50 sec	
	72°C	45 sec	
4	96°C	25 sec	4
	55°C	60 sec	
	72°C	120 sec	
	4°C ∞		

2.4.3. Gel electrophoresis

Agarose gels were prepared by dissolving 1% (w/v) agarose powder (Bioline, Cat #BIO-41025) in 1x TBE buffer and heating in the microwave. The agarose was allowed to cool before the addition of Ethidium Bromide (Sigma, Cat #E-2515) solution at a final concentration of approximately 0.5 µg/ml. The agarose was poured into gel casting tray with appropriate size combs. The gel was allowed to set for about 30 minutes before being submerged in 1x TBE buffer in the gel tank. PCR products were loaded into the wells by mixing 13 µl of samples from the 14

reactions with 10x loading buffer and then carefully pipetted into the wells (1:1 ratio). 100 bp of ladder (5 µl) (Bioline, HyperLadder™ 100bp Cat #BIO-33029 200 lanes) was also added into a well and gel was run for 75 minutes at 70V. PCR products were viewed and recorded using a UV gel documentation system (GeneFlash, Syngene Bio Imaging).

2.5. CMV IgG Enzyme linked Immunosorbant assay (ELISA) testing for healthy donors

2.5.1. Coating of plate with CMV lysate

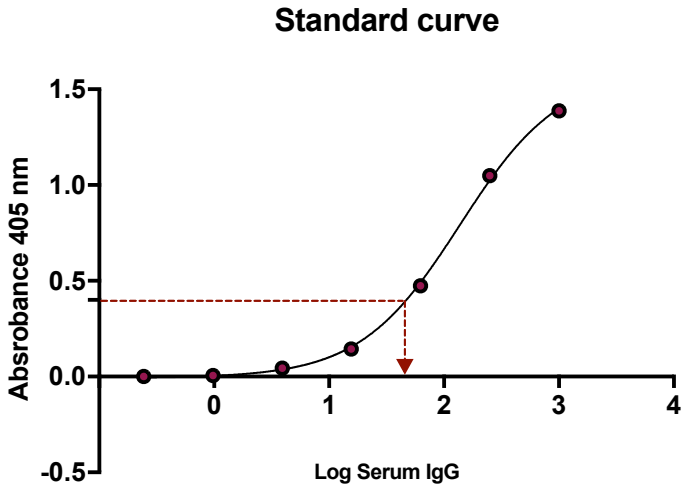
CMV serostatus of the HDs were determined by 2-day in house CMV ELISA that has been established in the lab. On day one, 96 well plate (NUNC MaxiSorp™, Cat #44-2404-21) was coated with 50 µl of mock or lysate, covered and left overnight in 4^0C in the fridge. Mock lysate and lysate from infected fibroblasts (UV-inactivated) which served as negative and positive fractions were prepared by diluting 1 µl of lysate in 4 ml of coating buffer.

2.5.2. Addition of IgG antibodies into the plate

On the next day, plasma samples of HDs were diluted 1:60 in a separate 96 well plate. On the same plate, standard wells were also prepared by serial dilution, by adding 80 µl of dilution buffer into the first well and 75 µl were added into remaining seven wells in the first column. The standard (20 µl) was added into the first well, mixed and then 25 µl were taken out and added into the second well and repeated until final well and 25 µl were discarded.

The coated plate with lysates from overnight incubation was then washed for 3 times with 200 µl wash buffer. Dilution buffer (90 µl) were added into each well of the plate and top up with 10 µl of diluted samples or serial diluted standards (final dilution of samples will be 1:600). All samples and standards were prepared in duplicates. The plate was then incubated for 1 hour at room temperature and then washed 3 times with 200 µl of wash buffer. After incubation, 100 µl CMV IgG conjugate antibody (goat anti-human IgG-HRP, SouthernBiotech Cat #2040-05) was added into the plate, incubated for an hour and the antibody was prepared by diluting 1.25 µl into 10 ml of dilution buffer (1:8000). After this step, the plate was washed 3 times and 100 µl TMB solution (1 step™ Ultra TMB-ELISA, Cat #34029) was added into each well and incubated for 15 minutes in the dark at room temperature. Finally, the reaction was stopped by adding 100 µl of 1M HCl (Hydrochloric acid, Sigma, Cat #43,557-0) and the absorbance 450 nm was then read with ELISA plate reader (Bio-Rad, iMark™ Microplate Reader).

Data was analysed by getting the value of average lysate and mock lysate, and the value of average mock is subtracted by mean value of lysate for both standards and serum samples. The values of standard curve were analysed by using GraphPad prism and transformed into X=log(X). Average readings from serum samples were determined from the standard curve. For example, in the graph it is shown that S1 is CMV seropositive with more than 10 U/ml and S2 is seronegative **(Fig. 2.5.1).**



	Mock	Mock	Average mock	Lysate	Lysate	Average lysate	Lysate-mock	IgG titre
S1	0.058625	0.055712	0.057169	0.423911	0.405289	0.41460	0.357431	40.69866
S2	0.071768	0.067266	0.069517	0.069548	0.072239	0.070893	0.001377	0.723687

FIGURE 2.5.1. Examples of CMV serum IgG ELISA calculation. CMV IgG detected from serum was determined from standard curve as shown by S1, more than 10 U/ml IgG detected is considered as positive.

2.6. Flow cytometry and PBMCs surface staining

2.6.1. Flow cytometry compensation

2.6.1.1. Compensation with antibody capture beads

Optimisation of the flow cytometry panels, and staining were done by using the Gallios™ Flow Cytometer (Beckman Coulter, Inc.) provided with 4 lasers (Blue, Red, Violet and Green) and 10 colour systems. Set up panels were performed on the Gallios following the compensation protocols from VersaComp Antibody Capture Bead Kit (Beckman Coulter Inc., Cat #B22804). One drop of each negative and positive beads was added into twelve 5 ml Falcon™ FACS tube (Cat #352063). 100 µl of sterile MACS buffer was added and spun for 500 x g and 1 minute to bring the beads to the bottom of tubes. A single colour antibody conjugate was added into individual labelled test tubes and vortexed immediately. Volumes of the antibodies used were according to the antibody titration.

The tubes were then incubated at room temperature in the dark for 30 minutes. Two ml of MACS buffer was added into each tube, vortexed and centrifuged at 2000 x g for 5 minutes. The supernatant was discarded carefully by using transfer pipettes and the beads were re-suspend in 400 µl of staining buffer. The compensation tubes were acquired on the Gallios to gain the compensation matrix and kept in 4^0C and reusable in 2 weeks' time. Compensation matrix was analysed by calculating the positive and negative beads using Kaluza software.

2.6.1.2. Compensation with PBMCs

The alternative way in compensation is by using HDs' PBMCs, which provide more accurate antibody bindings to the cells compared to the beads. The disadvantage from compensation by using PBMCs is that the acquisition has to be done quickly on the same day after staining to retain the viability of the cells. Compensation with PBMCs also solved the problems which occurred in setting up the panels by using the purchased recombinant antibodies (REAfinity™, Miltenyi Biotec) with mutated Fc region, as they did not have binding abilities on capture beads, similar to those tetramers and propidium iodide dye. In PBMCs compensation protocol, $1.0x10^5$ PBMCs or less were stained with antibody in each compensation tube and for T cell panels, a known CMV response HDs' PBMCs were used to assure tetramer binding. Compensation matrix was also analysed by using Kaluza software.

2.6.2. Flow cytometry plots analysis

All samples were run on the Gallios™ Flow Cytometer (Beckman Coulter, Inc.) which has 4 lasers (Blue, Red, Violet and Green). Data was analysed offline using Kaluza® Flow Analysis software version 2.1a (Beckman Coulter Inc.) or FlowJo® v10 (TreeStar Inc). Statistical analysis was done using GraphPad Prism 7 or IBM SPSS Statistics 24.

2.6.3. Titration of newly purchased antibodies

The newly purchased antibodies were titrated on $1.0x10^6$ HDs' PBMCs with different volumes, as well as with recommended volume by the manufacturer. Different volumes of antibodies were used for titration as shown from example of antibody titration plots **(Fig. 2.6.1)**, by staining PBMCs of HDs. Finalised volume required for the experiment was determined by the least amount of volume needed which has given the acceptable positive peak. For example, 3 µl of antibody was used in the NK panel as shown from the plots.

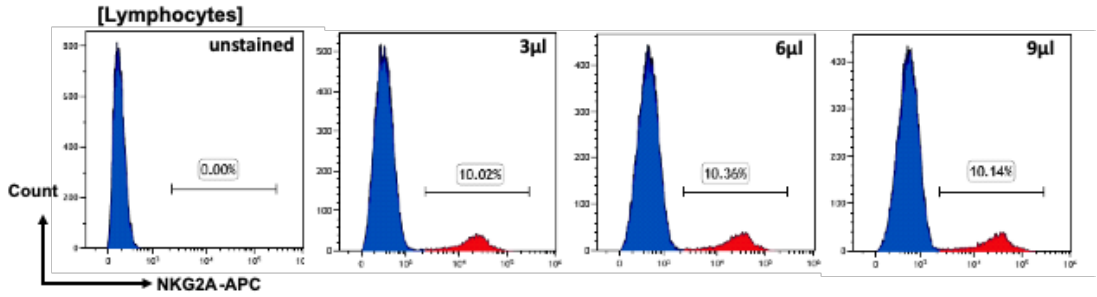


FIGURE 2.6.1. Example of NKG2A antibody titration from NK panel. PBMCs were stained with different volumes of NKG2A antibody on APC for titration and plots were gated from total lymphocytes.

2.6.3.1. PBMCs surface staining

Frozen cells were recovered as described above (section **2.3.1.3**). After the final wash cells were re-suspended in residual buffer and antibody panels added. The samples were incubated on ice for 20 to 30 minutes protected from light before being washed in MACS buffer and centrifuged at 500 x g for 5 minutes. Cells were re-suspended in residual buffer and 100 µl of MACS buffer added to each sample. Just prior to running the samples on the flow cytometer, 1.5 µl of PI was added into each tube.

2.6.3.1.1. NK cell and γδ T cell surface staining

For the NK and γδ T cell panels between $2.0x10^5$ and $1x10^6$ cells/ml were stained depending on the number that could be recovered from the patients which could be low during the first few weeks post-transplant. The antibodies that were used for NK and γδ T cell can be found in **Table 2.6.1, Table 2.6.2** and **Table 2.6.3.**

TABLE 2.6.1. NK panel 1 antibodies for surface staining.

NK	Colour	Manufacturer	Cat #	Clones	Channel	Volumes (µl)
KIR2DL1 **KIR2DL2** **KIR3DL1**	FITC	BioLegend	339504 312604 312706	MA4 DX27 DX9	FL1	5
NKG2C	PE	R&D Biosystems	FAB138P	Mouse IGG1	FL2	10
CD14 **CD19** **Propidium Iodide**	ECD	Beckman Coulter Beckman Coulter Miltenyi Biotec	IM2707U A07770 130-093-233	RMO52 J3-119	FL3	5
CD3	PerCp-Cy5.5	BioLegend	300328	HIT3a	FL4	1.5
PD-1/CD279	PE-Cy7	BioLegend	329916	EH12.2H7	FL5	5
NKG2A	APC	Miltenyi Biotec	130-098-8123	REA110	FL6	3
CD56	AF700	BioLegend	318332	HCD56	FL7	2
KLRG1	APC-Vio770	Miltenyi Biotec	130-103-642	REA261	FL8	3
CD57 (1:10)	PB	BioLegend	322316	HCD57	FL9	2.5
CD16	V500	BD Biosciences	561394	3G8	FL10	5

TABLE 2.6.2. NK panel 2 (CD69) antibodies for surface staining.

NK	Colour	Manufacturer	Cat #	Clones	Channel	Volumes (µl)
NKG2C	PE	R&D Biosystems	FAB138P	Mouse IGG1	FL2	10
CD14 **CD19** **Propidium Iodide**	ECD	Beckman Coulter Beckman Coulter Miltenyi Biotec	IM2707U A07770 130-093-233	RMO52 J3-119	FL3	5
CD3	PerCp-Cy5.5	BioLegend	300328	HIT3a	FL4	1.5
CD69	PE-Cy7	BioLegend	310192	FN50	FL5	5
NKG2A	APC	Miltenyi Biotec	130-098-8123	REA110	FL6	3
CD56	AF700	BioLegend	318332	HCD56	FL7	2
CD57 (1:10)	PB	BioLegend	322316	HCD57	FL9	2.5
CD16	V500	BD Biosciences	561394	3G8	FL10	5

TABLE 2.6.3. TCRγδ T cell panel and antibodies.

TCRγδ T cell	Colour	Manufacturer	Cat #	Clones	Channel	Volumes (µl)
TCRVδ1	FITC	Miltenyi Biotec	130-118-362	REA173	FL1	2
TCRαβ	PE	Beckman Coulter	306708	IP26	FL2	1.5
CD14 **CD19** **Propidium Iodide**	ECD	Beckman Coulter Beckman Coulter Miltenyi Biotec	IM2707U A07770 130-093-233	RMO52 J3-119	FL3	5
CD56	PE-Cy7	BioLegend	318318	HCD56	FL5	3
TCRVγ9	APC	Miltenyi Biotec	130-107-435	REA470	FL6	10
TCRVδ2	AF700	BioLegend	331416	B6	FL7	5
CD4	APC/Cy7	BD Biosciences	557871	RPA-T4	FL8	2.5
CD3	PB	BD Biosciences	558117	UCHT1	FL9	5
CD8	VioGreen	Miltenyi Biotec	130-113-164	BW135/80	FL10	2.5

2.6.4. T cell–HLA Class I and Class II tetramer staining

2.6.4.1. Tetramer assay and optimisation

Tetramer staining initially was done and optimised by using available Class I monomers produced in the lab (NLV, VLE, TPR and RPH). In the protocol, Streptavidin on APC (Invitrogen^{TM} Cat #SA1005) was first diluted with PBS, then 2 µl was added with the monomers by following volumes listed in **Table 2.6.4.** The mixture of monomers and Streptavidin was then mixed and spun briefly and incubated in the dark at room temperature for 20 minutes. This step was repeated for 4 times and the produced tetramers were kept in 4^0C and can be used up to 1 month after.

TABLE 2.6.4. Preparation of tetramer HLA Class I by using monomers. Volumes used are depending on the concentration of the available monomers.

Monomers	HLA types	Volumes (µl)	Concentration (µg/ml)	Monomer in µg	Streptavidin-APC volumes (µ/ml) (Monomer in µg x 0.87 µl)	PBS volumes (µl)
NLV	A2	20	111.00	2.22	1.93	8.07
VLE	A2	20	60.00	1.20	1.04	8.96
TPR	B7	20	361.00	7.22	6.28	3.72
RPH	B7	20	338.00	6.76	5.88	4.12

Optimisation of the tetramer staining was carried out by using PBMCs of CMV positive HDs with known responses to specific CMV peptides **(Fig. 2.6.2** and **Fig. 2.6.3).** PBMCs were thawed as described above (section **2.3.1.3**) and re-suspended at 1.0x10^6 cells/ml in MACS buffer. Each tetramer to be tested (1 µl) was added to the cells, incubated at 37^0C in a water bath for 15 minutes before being washed in MACS buffer at 2000 x g for 5 minutes. The supernatant was removed, and cells

stained with surface antibodies to CD3, CD14, CD19, CD56 and CD8 and PI (from $CD8^+$ T cell panel, **Table 2.6.6**). The remaining washing steps were following surface staining procedures.

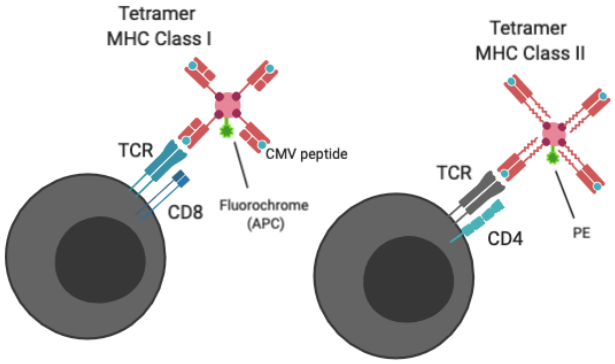


FIGURE 2.6.2. Optimisation of tetramer staining. PBMCs of HDs were stained with different types of HLA Class I tetramers; NLV, TPR and RPH.

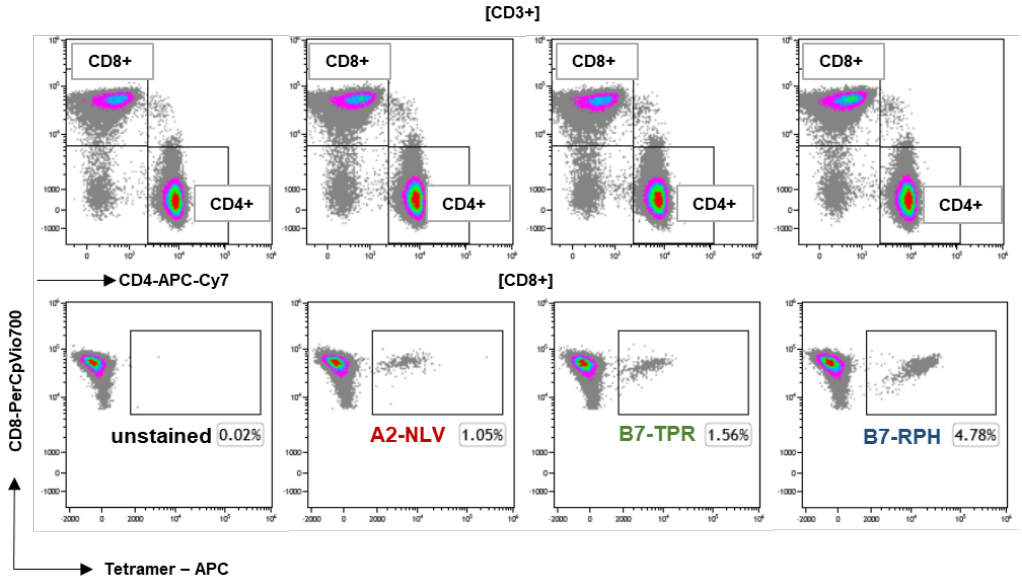


FIGURE 2.6.3. Optimisation of tetramer staining. PBMCs of HDs were stained with different types of HLA Class I tetramers; NLV, TPR and RPH.

2.6.4.2. Tetramer, $CD8^+$ and $CD4^+$ T cell staining

The tetramers used for HLA Class I and Class II tetramer staining for CMV-$CD8^+$ and CMV-$CD4^+$ T cell panels on CMV reactivation patients' samples were requested from the NIH Tetramer Core Facility, Emory University, United States **(Table 2.6.5)**. Tetramers were requested based on HLA types of CMV reactivation allo-HSCT patients **(Supplementary Table 1b).** Some of the tetramers requested from NIH were custom made and required peptides to be sent for production. Peptides were then purchased from AltaBioscience, United Kingdom. HLA Class I tetramers were requested on APC while Class II were on PE **(Fig. 2.6.2)**, and tetramers were also first tested on CMV positive HDs with known HLA types upon arrival and stored in 4^0C. However, some of the tetramers that were requested did not work and probably had degraded **(Table 2.6.5)** thus were excluded from staining and analysis. All seropositive HDs and CMV reactivation, as well as without reactivation PBMCs samples included in the analysis in this study were stained with NIH produced tetramers.

In finalised tetramer and T cell staining protocols, similar steps were used as those for in-house made tetramers staining, in which $1x10^6$ cells/ml PBMCs or less were re-suspended in MACS buffer, added with 1 µl tetramer, and incubated at 37^0C in water bath for 15 minutes. Cells were also washed in 4 ml MACS buffer and centrifuged at 2000 x g for 5 minutes. Then, the cells were stained with antibodies from either $CD8^+$ T cell panel for HLA Class I tetramers or $CD4^+$ T cell for HLA Class II (**Table 2.6.6** and **Table 2.6.7**) by following similar washing steps as in surface staining.

TABLE 2.6.5. List of HLA Class I and Class II tetramers used in T cell panels for the CMV reactivation allo-post HSCT samples. Tetramer HLA Class I were requested on APC while Class II on PE. *Tetramers that were not working.

HLA Restriction	Abb. code	Epitope sequence	Amino acid location	CMV protein (gene)	Concentration (mg/ml)
***HLA-A*01:01**	VTE	VTEHDTLLY	245-253	pp50 (UL44)	1.5
***HLA-A*01:01**	YSE	YSEHPTFTSQY	363-373	pp65 (UL83)	1.5
HLA-A*02:01	NLV	NLVPMVATV	495-503	pp65 (UL83)	1.4
HLA-A*02:01	VLE	VLEETSVML	316-324	IE-1 (UL123)	1.5
***HLA-A*03:01**	IMR	IMREFNSYK	683-691	gB (UL55)	1.5
***HLA-A*03:01**	TTV	TTVYPPSSTAK	945-955	pp150 (UL32)	1.5
***HLA-A*11:01**	SVL	SVLGPISGHVLK	13-24	pp65 (UL83)	1.5
HLA-A*24:02	QYD	QYDPVAALF	341-349	pp65 (UL83)	1.5
HLA-A*68:01	FVF	FVFPTKDVALR	185–195	pp65 (UL183)	1.5
HLA-B*07:02	TPR	TPRVTGGGAM	417-426	pp65 (UL83)	1.5
HLA-B*07:02	RPH	RPHERNGFTVL	265-275	pp65 (UL83)	1.5
HLA-B*08:01	ELR	ELRRKMMYM	199-207	IE-1 (UL123)	1.5
HLA-B*08:01	QIK	QIKVRVDMV	88-96	IE-1 (UL123)	1.5
HLA-B*35:01	FPT	FPTKDVAL	188-195	pp65(UL183)	1.5
HLA-DRB1*03:01	YQE	YQEFFWDANDIYR	188-195	pp65(UL83)	1.3
HLA-DRB1*07:01	DYS	DYSNTHSTRYV	217-227	gB (UL55)	1.4
HLA-DRB1*07:01	EPD	EPDVYYTSAFVFPTK	177-191	pp65 (UL183)	1.3
HLA-DRB5*01:01	NIE	NIEFFTKNSAFPKTT	221-225	IE-1 (UL123)	1.3

TABLE 2.6.6. $CD8^+$ T cell MHC Class I panel and antibodies.

$CD8^+$ T cell	Colour	Manufacturer	Cat #	Clones	Channel	Volumes (µl)
CCR7	FITC	R&D Biosystems	FAB197F	Mouse IgG2A	FL1	10
CD3	PE	Beckman Coulter	A07747	UCHT1	FL2	5
CD14 **CD19** **CD56-PECF594** **Propidium Iodide**	ECD	Beckman Coulter Beckman Coulter BD Biosciences Miltenyi Biotec	IM2707U A07770 562289 130-093-233	RMO52 J3-119 B159	FL3	5
CD8	PerCpVio700	Miltenyi Biotec	130-097-911	BW135/80	FL4	6
CD38	PE-Cy7	BioLegend	303516	Mouse IgG1, K	FL5	2.5
Tetramer	APC	NIH			FL6	1
CD45RA	AF700	BioLegend	304124	H1100	FL7	1
PD-1/CD279	APC-Cy7	BioLegend	329922	EH12.2H7	FL8	5
CD57 (1:10)	PB	BioLegend	322316	HCD57	FL9	2.5
CD28	BV510	BioLegend	302936	CD28.2	FL10	3

TABLE 2.6.7. CD4$^+$ T cell MHC Class II panel and antibodies

CD4$^+$ T cell	Colour	Manufacturer	Cat #	Clones	Channel	Volumes (µl)
CCR7	FITC	R&D Biosystems	FAB197F	Mouse IgG2A	FL1	10
Tetramer	PE	NIH			FL2	1
CD14 **CD19** **CD56-PECF594** **Propidium Iodide**	ECD	Beckman Coulter Beckman Coulter BD Biosciences Miltenyi Biotec	IM2707U A07770 562289 130-093-233	RMO52 J3-119 B159	FL3	5
PD-1/CD279	PerCp-Cy5.5	BioLegend	329914	EH12.2H7	FL4	5
CD38	PE-Cy7	BioLegend	303516	Mouse IgG1, K	FL5	2.5
CD4	AF647	BioLegend	317422	OKT4	FL6	5
CD45RA	AF700	BioLegend	304124	H1100	FL7	1
PD-1/CD279	APC-Cy7	BD Biosciences	329922	EH12.2H7	FL8	3
CD57 (1:10)	PB	BioLegend	322316	HCD57	FL9	2.5
CD28	BV510	BioLegend	302936	CD28.2	FL10	3

2.7. PBMCs and NK cell intracellular cytokines staining

Two million per ml PBMCs from patients with CMV reactivation, without reactivation and HDs were co-cultured with K562 cells overnight (1:1 ratio) in 37^0C incubator and suspended with 500 µl of growth media with 0.5 µl 10 mg/ml of Brefeldin A (Sigma, Cat #B5936). $2.0x10^6$ cells/ml of unstimulated PBMCs (without K562) were used as negative control.

The cells were spun at 500 x g for 5 minutes on the next day and washed with 2 ml of MACS buffer and the suspended cells were surface stained with antibodies as listed in **Table 2.6.8** for 20 minutes in ice. The cells were then washed with 2 ml of MACS buffer and spun again for 500 x g 5 minutes. 100 µl of 4% PFA was added for fixing and the tubes were mixed and incubated in the dark at room temperature for 15 minutes. The cells were then washed and spun for 2000 x g 5 minutes with MACS buffer. Supernatant was discarded and the cells were added with 12.5 µl of 0.5% Saponin, mixed gently and incubated in the dark at room temperature for 5 minutes. Cytokine antibodies (TNF-α and IFN-γ) were added into the tubes and again incubated for 30 minutes at room temperature in the dark, washed and run on the Gallios™.

TABLE 2.6.8. NK Intracellular cytokines panel and antibodies

NK Intracellular	Colour	Manufacturer	Cat #	Clones	Channel	Volumes (µl)
TNF-α	AF488	BioLegend	502917	Mab11	FL1	5
NKG2C	PE	R&D Biosystems	FAB138P	Mouse IGG1	FL2	10
CD14 **CD19**	ECD	Beckman Coulter Beckman Coulter	IM2707U A07770	RMO52 J3-119	FL3	5
CD3	PerCP-Cy5.5	BioLegend	300328	HIT3a	FL4	1.5
NKG2A/CD159a	APC	Miltenyi Biotec	130-098-8123	REA110	FL6	1
IFN-γ	AF700	BioLegend	502519	45.B3	FL7	2
CD56	APC/Cy7	BioLegend	318332	HCD56	FL8	3
Live/Dead	PB	Invitrogen	L34955	NA	FL9	2
CD16	V500	BD Biosciences	561394	3G8	FL10	5

2.8. Flow cytometric NK cytotoxicity assay

Optimisation of 3-day NK killing assay was performed by using few numbers of HDs' PBMCs and also by activating the NK cells with IFN-α, as well as without IFN-α stimulation. Experiments were set up by following established method in the lab and by using frozen HDs' PBMCs before proceeded with allo-HSCT patients. After testing with a number of samples, it was concluded that NK cytotoxicity assay was less effective with low number of isolated NK cells, as low as $2.0x10^5$ cells.

2.8.1. NK cells isolation

NK cells from HDs and patients were isolated from PBMCs using the negative selection EasySep™ Human NK Cell Enrichment Kit (Stem Cell™ Technologies, Cat #19055) and by following the manufacturer's instruction. About $2x10^7$ PBMCs of HDs were used, and the cells were counted and washed with growth media at 500 x g for 5 minutes. The PBMCs were then suspended in growth media in a suspension of $5x10^7$ cells/ml in a 15 ml tube. For example, $2.4x10^7$ cells were suspended in 480 µl of growth media ($2.4x10^6/5.0x10^7$ cells/ml). At this stage, some of the PBMCs were spared for purity test and transferred into a 5 ml polypropylene tube in the amount of $1.0x10^5$ cells/ml.

50 µl/ml of EasySep™ Human NK Cell Enrichment Cocktail was then added which contains antibodies that can recognise specific cell surface markers on non-NK cells in the 15 ml tube (For example, 24 µl of antibody cocktail was added into 480 µl

PBMCs suspension). The cell suspension in the tube was incubated for 10 minutes at room temperature and followed by addition of 100 µl/ml of EasySep™ D Magnetic Particles and incubated again at room temperature for 5 minutes. Beforehand, the magnetic particles tube was vortexed for 30 seconds before use. The PBMCs suspension was then added with 2.5 ml of MACs buffer and transferred into a 5 ml Falcon™ polystyrene FACS tube (Cat #352054). The tube was added into EasySep™ Magnet (Cat #18000) and left at room temperature for 2 to 3 minutes to allow the unwanted cells labelled with antibodies and magnetic particles, separated from NK cells. The NK cell suspension was then poured off (while in the magnet) into a new polystyrene tube and cell count on NK cell was performed. The NK cell suspension was washed at 500 x g for 5 minutes. The cells were then suspended again in growth media at $1.0x10^6$ cells/ml (For example, $2.2x10^6$ NK cells were suspended in 2.2 ml of growth media), and about $1.0x10^5$ cells were spared for a purity test.

2.8.2. NK cells stimulation

The isolated NK cells were activated overnight with 2 µg/ml of IFN-α (PeproTech, Cat #300-02A) at 37^0C in 5% CO_2. NK cells in growth media without IFN-α was also used as control. NK cells were transferred into Corning® 24 well plate (Sigma, Cat #CLS3526) and incubated overnight at 37^0C in 5% CO_2.

2.8.3. PBMCs and NK purity test

Both PBMCs and NK cells were stained with CD56, CD3, CD19, CD14 and PI as in NK panel for quality control check **(Table 2.6.1).** The tubes were washed in 2 ml of MACS buffer, spun for 500 x g 5 minutes and suspended in 100 µl MACS buffer, and run on the Gallios™.

2.8.4. K562 target cell lines

$2.0x10^6$ cells/ml of K562 were used in this experiment and washed in growth media for 500 x g 5 minutes. The cells were added to freshly prepared CFSE (eBioscience™, Cat #65-0850-84) in 1:50 dilution in the amount of 10 µl for labelling, in a 15 ml tube. K562 cells were then incubated in 37^0C for 10 minutes, suspended in 10 ml of growth media, and washed for 500 x g spinning at 5 minutes. Supernatant was poured off and added with 10 ml of growth media, incubated again in 37^0C for 30 minutes. The cell count was repeated, the tube was spun again for 500 x g and 5 minutes and the CFSE-labelled K562 cell lines were suspended in the amount of $5.0x10^5$ cells/ml.

2.8.5. Effector and target ratios

The stimulated and non-stimulated NK cells (effectors) and K562 cells (targets) ratios were prepared at 1:1, 0.5:1, 0.2:1 and 0.1:1 (E:T) and co-cultured *in vitro* overnight in 37°C in 5% CO_2, in round bottom Corning® 96 well plate (Sigma, Cat #CLS3799). CFSE-labelled K562 (100 µl) which should contain $5.0x10^4$ cells were

used as control and added with 100 µl of growth media to make up the final volume of 200 µl. Target cells (100 µl) were co-cultured with the effector NK cells dependent on the ratios **(Table 2.8.1).** Co-cultured cells in the wells were prepared in triplicate. The following day the samples were run on the Gallios™ flow cytometer following the addition of 12.5 µl of CountBright™ absolute counting beads (Life Technologies) and 1.5 µl of PI.

TABLE 2.8.1. NK cells effector and K562 target ratios for NK killing assay.

	NK (Effector)		K562 (Target)		Growth media
Control	None	None	100 µl	$5.0x10^4$	100 µl
0.1:1	10 µl	$5.0x10^3$	100 µl	$5.0x10^4$	90 µl
0.2:1	20 µl	$1.0x10^4$	100 µl	$5.0x10^4$	80 µl
0.5:1	50 µl	$2.5x10^4$	100 µl	$5.0x10^4$	50 µl
1:1	100 µl	$5.0x10^4$	100 µl	$5.0x10^4$	None

2.8.6. Percentage of NK killing calculation

The number of live K562 cells from the analysis from flow cytometry plots and the calculation for concentration per µl was determined by following **Table 2.8.2** and **Table 2.8.3.** The assigned bead counts used by using the CountBright™ was calculated depending on the concentration of beads and volume that was used for the assay. For example, for $0.54x10^5$ beads in 50 µl provided by the manufacturer, $1.35x10^4$ beads were used as assigned beads count (C) [12.5 µl x ($0.54x10^5$/50 µl)].

TABLE 2.8.2. Calculation for live K562 cells/µl for each ratio for an example from one sample of healthy donor. No of live K562 cells (A) and no of beads (B) were determined from flow cytometry analysis.

Replicate	Ratio	No of live cells - K562 (A)	No of beads (B)	(A)/(B) = X	Assigned beads count (C)	Volume of samples (µl) (D)	(C)/(D) = Y	Conc. of samples K562/µl (X) x (Y)	Mean (K562/µl)
1	Control	34529	3582	10	13500	200	67.5	650.7	714
2		33020	2896	11	13500	200	67.5	769.6	
3		31959	2987	11	13500	200	67.5	722.2	
1	0.1:1	26458	2930	9	13500	200	67.5	609.5	618
2		29194	3038	10	13500	200	67.5	648.6	
3		28183	3195	9	13500	200	67.5	595.4	
1	0.2:1	25537	3216	8	13500	200	67.5	536.0	523
2		24657	3046	8	13500	200	67.5	546.4	
3		23255	3225	7	13500	200	67.5	486.7	
1	0.5:1	17424	3407	5	13500	200	67.5	345.2	337
2		17515	3591	5	13500	200	67.5	329.2	
3		17340	3464	5	13500	200	67.5	337.9	
1	1:1	6667	3253	2	13500	200	67.5	138.3	139
2		7087	3453	2	13500	200	67.5	138.5	
3		7054	3422	2	13500	200	67.5	139.1	

TABLE 2.8.3. Calculation for killing of NK cells against K562 target cells. Mean number of live cells were determined from the average of cells from triplicate tubes. Percentage of killing was determined by the formula below.

Replicate	Ratio	No of live cells (mean) (X)	No of live cells control tubes (mean) (Y)	(X)/(Y)	Percentage %	Percentage % of killing
1	Control	33169	-	-	-	-
2						
3						
1	0.1:1	27945	33169	0.8	84.2	**15.8**
2						
3						
1	0.2:1	24483	33169	0.7	73.8	**26.2**
2						
3						
1	0.5:1	17426	33169	0.5	52.5	**47.5**
2						
3						
1	1:1	6936	33169	0.2	20.9	**79.1**
2						
3						

2.9. NK cell sorting and Antibody-Dependent Cellular Cytotoxicity (ADCC) assay

2.9.1. NK cell sorting

Unlike previous killing assay procedures, fresh PBMCs were isolated for NK cells in this assay to retain the viability of the cells by using similar isolation kit and protocols (using EasySep™ Human NK Cell Enrichment Kit). About 50 x 10^6 PBMCs from CMV seropositive HDs' with more than 20% NKG2C$^+$ expression on NK cells were used, isolated for NK cells and stained with NK antibodies in this experiment as listed in **Table 2.9.1.** Approximately 1.0 x 10^6 NK cells were successfully isolated and stained in 400 µl of sterile MACS buffer, then sorted for NKG2C positive and NKG2C negative populations in a sterile condition by using BD FACSMelody™ cell sorter. The sorted cells were collected in two tubes, separating the negative and positive NKG2C population in 500 µl of growth media. All procedures were following steps as in killing assay including NK purity check and IFN-α stimulation, otherwise stated below.

TABLE 2.9.1. NK cell sorting panel and antibodies.

NK antibodies	Colour	Manufacturer	Cat #	Clones	Volumes (µl)
NKG2C	PE	R&D Biosystems	FAB138P	Mouse IGG1	10.0
CD3	PerCP-Cy5.5	BioLegend	300328	HIT3a	1.5
CD56	APC/Cy7	BioLegend	318332	HCD56	3.0
Viability dye (1:10)	Cyan	eBioscience	65-0866-14	None	2.0

2.9.2. ADCC assay experiment set up

After overnight stimulation with IFN-α, NK cells with positive and negative NKG2C population were stained with 3 µl of purified anti-human CD16 antibody (BioLegend Cat #302002) for 15 minutes without washing the cells. Following the step, 10 µg/ml of rituximab was added into each well of K562 and EBV-transformed lymphoblastoid cell lines (LCL) ($5x10^4$ per well) and also incubated for 15 minutes, and rituximab was diluted beforehand from the stock solution (Roche, MabThera® 100 mg Rituximab 100 mg/ml) with growth media.

The experiment was not continued on due to time constraints, and because of difficulty in finding CMV positive HDs with high expression of NKG2C on NK cells. However, this experiment has been carried out on 4 HDs with more than 20% $NKG2C^+$ expression on their NK cells but still not enough to proceed with the assay due to low number of cells collection. Moreover, both K562 and LCL cells lines were briefly stained with FITC anti-human CD20 antibody (BioLegend, Cat #302304) and it was found out that CML blast crisis K562 cell lines do not express CD20 thus not conclusive for a successful ADCC assay which needed the binding of anti-CD20 rituximab on those target cells for killing activity to take place. CD20 in fact is expressed on LCL but was also not carried out as the experiment required a lot of optimisation.

2.10. CMV viral load study in urine and serum

2.10.1. Optimisation of DNA extraction from urine and serum

Urine samples were concentrated and filtered by using the Microsep™ Advance Centrifugal Devices according to the manufacturer's protocol as has been described before. DNA was extracted from the concentrated serum and urine using three different type of kits; QIAmp® DNA Micro Kit (Qiagen, Cat #56304), QIAmp® Viral RNA Kit (Qiagen, Cat #52904) and High Pure Viral Nucleic Acid kit (Roche, Cat #11858874001) by following manufacturer's instructions. DNA from urines and serum of HDs were not successfully extracted due to low availability of viral copy number detected from the serum and also urines of CMV seropositive HDs. However, 1 µl of CMV plasmid was added into concentrated urine or serum and used as positive control for the protocols. High Pure Viral Nucleic Acid kit has given the best and highest DNA concentration yields among all kits that have been tested, while QIAmp® DNA Micro Kit (which had been used for serum) barely detected any DNA.

2.10.1.1. DNA extraction from urine and serum by using QIAmp® Viral RNA Kit

In this protocol, 560 µl of Buffer AVL was transferred into 1.5 ml tubes and added with 140 µl of pre-warmed (in 37^0C) and thawed serum or concentrated urines and vortexed for more than 15 seconds to ensure complete lysis. The tube mixtures were then incubated at room temperature for 10 minutes. Ethanol (560 µl) (VWR, Cat #24102) was added into the tubes and vortexed, 630 µl of the mixtures were then transferred into sterile mini column by using micropipette and spun for 5500 x g for 1 minute (Eppendorf, Centrifuge 5418R). After spinning step, collection tubes were discarded, 500 µl of wash buffer (Buffer W1) was added and spun again for 5500 x g for 1 minute. At this step, collection tubes were discarded again, the mini columns were placed into new collection tubes and added with 500 µl of wash buffer 2 (Buffer W2). The columns added with buffer were then spun at high speed 14 500 x g for 3 minutes and collection tubes were discarded. Mini columns were placed into sterile 1.5 ml tubes and 60 µl of elution buffer was pipetted into the column, incubated at room temperature for 1 minute and spun for 5500 x g for 1 minute. The collected viral nucleic acid or DNA yields were then quantified (ng/µl) and checked for purity (A260/A280) with a 1.5 µl aliquot using NanoDrop™ UV spectrophotometer (Thermo Scientific™) and stored in -20^0C.

2.10.1.2. DNA extraction from serum and urines by using High Pure Nucleic Acid Kit

This protocol has given the highest concentration of DNA using small volumes of samples. Serum or concentrated urine (200 µl) were transferred into sterile 1.5 ml tubes, added with 200 µl of working solution, mixed and incubated at $+72^0$C for 10 minutes in the heat block. The working solution was prepared freshly by adding 50 µl of poly(A) carrier RNA with 2.5 ml of binding buffer. Following the step, 100 µl of binding buffer was added into the tubes, and then mixed again after being transferred into mini column with collection tubes by using micropipette. The columns were then spun for 8000 g for 1 minute, and the flow through from the collection tubes were discarded. The columns were placed into new collection tubes and 500 µl of inhibitor removal buffer was added and spun again for 8000 g for 1 minute. Next, the collection tubes were discarded and added with 450 µl of wash buffer, spun again for 8000 g for 1 minute and this step was repeated for one more time. After washing steps, the columns were placed into sterile 1.5 ml tubes and 50 µl of elution buffer was added and spun finally at 8000 g for 1 minute. Similar to previous DNA extraction procedures, collected DNA was then quantified by using NanoDrop™ spectrophotometer.

2.10.2. In house CMV quantitative Polymerase Chain Reaction (qPCR) and DNA sequencing

2.10.2.1. Detection of CMV viral load by qPCR in urine and serum

DNA (5 ng/µl or less) from serum and urine were tested using the in-house CMV qPCR assay targeting different regions of the HCMV genome with the human β-2 microglobulin gene used as a positive control. The qPCR and master mix components are listed in **Table 2.10.1** and with the qPCR cycle set up as following **Table 2.10.2**. All primers and probes stock concentration were 100 µM and 10 µM of primers were prepared by adding 50 µl of stock primers with 450 µl of nuclease free water, while 5 µM of probes were prepared by diluting 25 µl of stock probes with 475 µl of nuclease free water (Final volume 500 µl).

The standards were prepared in 6 tubes with 10 fold serial dilution with CMV standard 10^5, 10^4, 10^3, 10^2, 10^1 and 1 (copies/µl) **(Fig. 2.10.1** and **2.10.2).** CMV standard 10^5 was prepared by adding 20 µl of CMV 10^6/µl plasmid with 180 µl of nuclease free water (Final volume 200 µl), briefly mixed and quickly spun, and the steps were repeated for other standard tubes by adding 20 µl of CMV Standard 10^5 with 180 µl of nuclease free water and repeated until last tube. DNA samples (5 µl with 5 ng/µl) or CMV standards were added into PCR plate (BIOPlastics, Cat #ABA17500) with 20 µl of master mix **(Table 2.10.1)** and sealed with flat caps (BIOPlastics, Cat #B57821). The PCR plate was then spun at 1200 x g for 2 minutes before being placed and analysed in the 7500 Real-Time PCR System (Applied Biosystems®). β-2m probes were detected by FAM and TAMRA as detector dye and quencher while CMV probes were using FAM alone as the detector.

TABLE 2.10.1. In house qPCR set up for CMV viral load detection.

Primers/master mix	Volumes (µl)
2x TaqMan® Universal Master Mix II (Applied Biosystems®)	12.5
CMV/β-2m forward primers (10 µM) (Eurogentec) β-2m 5'GGA ATT GAT TTG GGA GAG CAT C 3' CMV 5' GCC GAT CGT AAA GAG ATG AAG AC 3'	2.5
CMV/β-2m reverse primers (10 µM) (Eurogentec) β-2m 5' CAG GTC CTG GCT CTA CAA TTT ACT AA 3' CMV 5' CTC GTG CGT GTG CTA CGA GA 3'	2.5
CMV/β-2 microglobulin probes (5 µM) (Eurogentec) β-2m 5' AGT GTG ACT GGG CAG ATC ATC CAC CTT C 3' CMV 5' AGT GCA GCC CCG ACC ATC GTT C 3'	1
Nuclease free water (DEPC-treated water, Invitrogen™, Cat #AM9906)	1.5
DNA (5 ng/µl) or CMV standards	5

TABLE 2.10.2. PCR cycles for CMV viral load detection. qPCR was run in 7500 Real-Time PCR System for 1 hour and 50 minutes.

Stage	Temperature	Time (mins)	Repeat	Ramp rate
1	50.0^0C	2:00	1	100
2	95.0^0C	10:00	1	100
3	95.0^0C	0:15	50	100
	60.0^0C	1:00		100

2.10.2.2. qPCR viral load analysis and calculation

qPCR analysis was done by Applied Biosystems® 7500 Real-Time PCR System, and standard curves for both CMV and β-2m were automatically plotted and analysed from the software. The number of viral copy numbers were extrapolated from the standard curve graphs **(Fig. 2.10.1).** Hence the values of viral copy numbers for each standard curve was determined by volumes of DNA plasmid that were used (Eg. Viral copy number for Standard 10^5: 5 µl x $1x10^5$ = 500 000 or $5x10^5$). The example also can be seen from **Fig. 2.10.1**, as the graph has shown that viral copy number extrapolated from Sample 1 has given the mean number of 757.3 viral copy number of CMV with 5372.59 or 5.4 x 10^3 β-2m control genes detected in urines. Calculation of viral copy number in ml was calculated as below;

Volume of urine being concentrated: 20 ml

Volume of concentrated urine used for DNA extraction: 40 µl

Viral copy number detected (from qPCR): 757.3 copies/ 5 µl

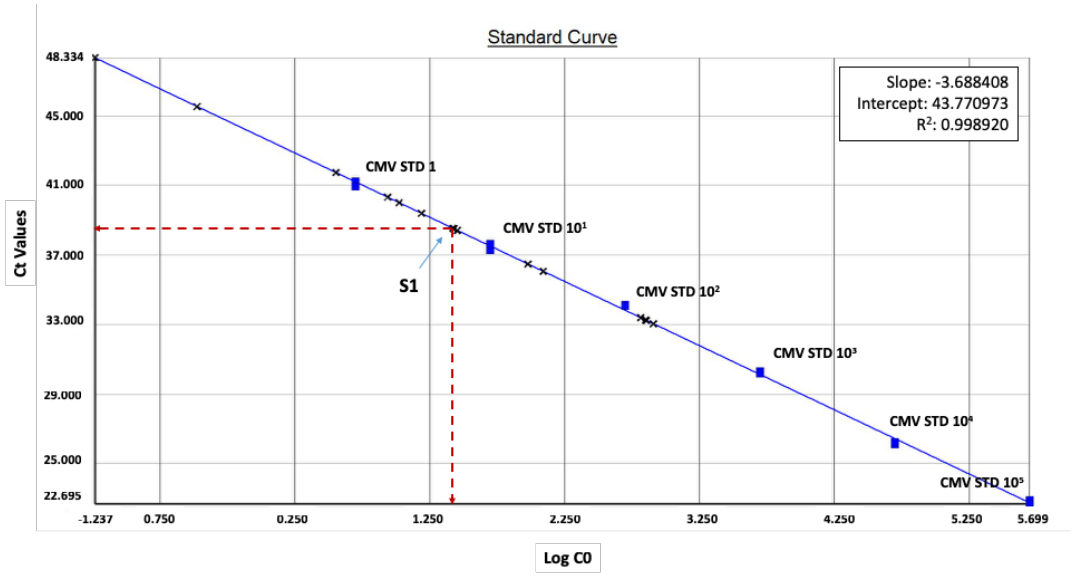
: 51.5 copies/µl

Volumes of viral copy number in urines

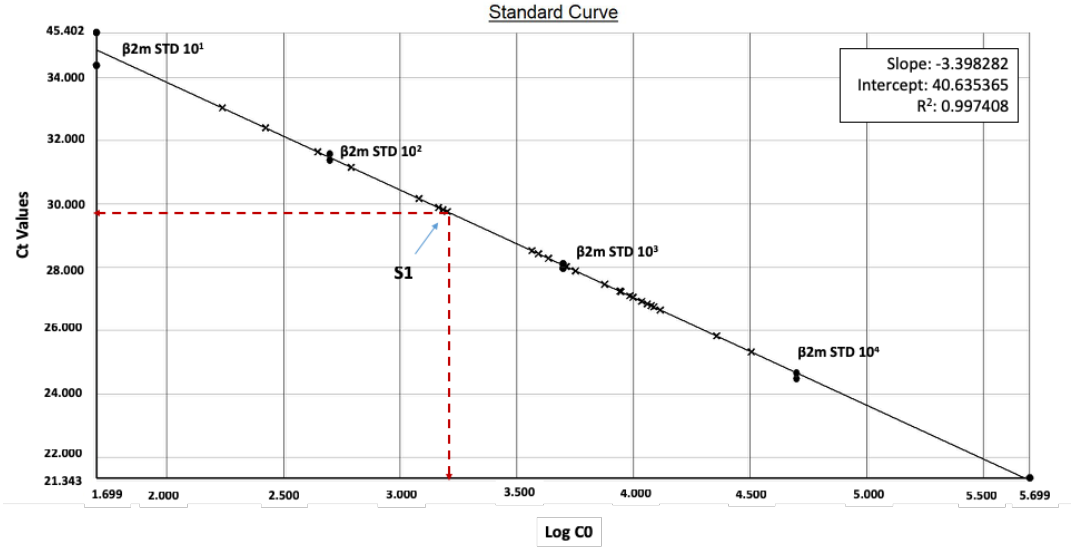
: 151.5 copies/µl x 140 µl

: 21210 copies in 20 ml

: **1060.5 copies/ml of viral DNA**



Sample Name	Detector	Task	Ct	StdDev Ct	Qty	Mean Qty	StdDev Qty
S1	CMV	Unknown	33.0474	0.152	807.935	757.279	71.6
S1	CMV	Unknown	33.2620	0.152	706.623	757.279	71.6



Sample Name	Detector	Task	Ct	StdDev Ct	Qty	Mean Qty	StdDev Qty
S1	B2M a	Unknown	29.8139	1.55	1.52898E+03	5.37259E+03	4.48808E+003
S1	B2M a	Unknown	29.8782	1.55	1.46375E+03	5.37259E+03	4.48808E+003

FIGURE 2.10.1. Standard curves for CMV and β-2m and example of calculation. Viral load copy number detected in urines per ml was determined by different calculation.

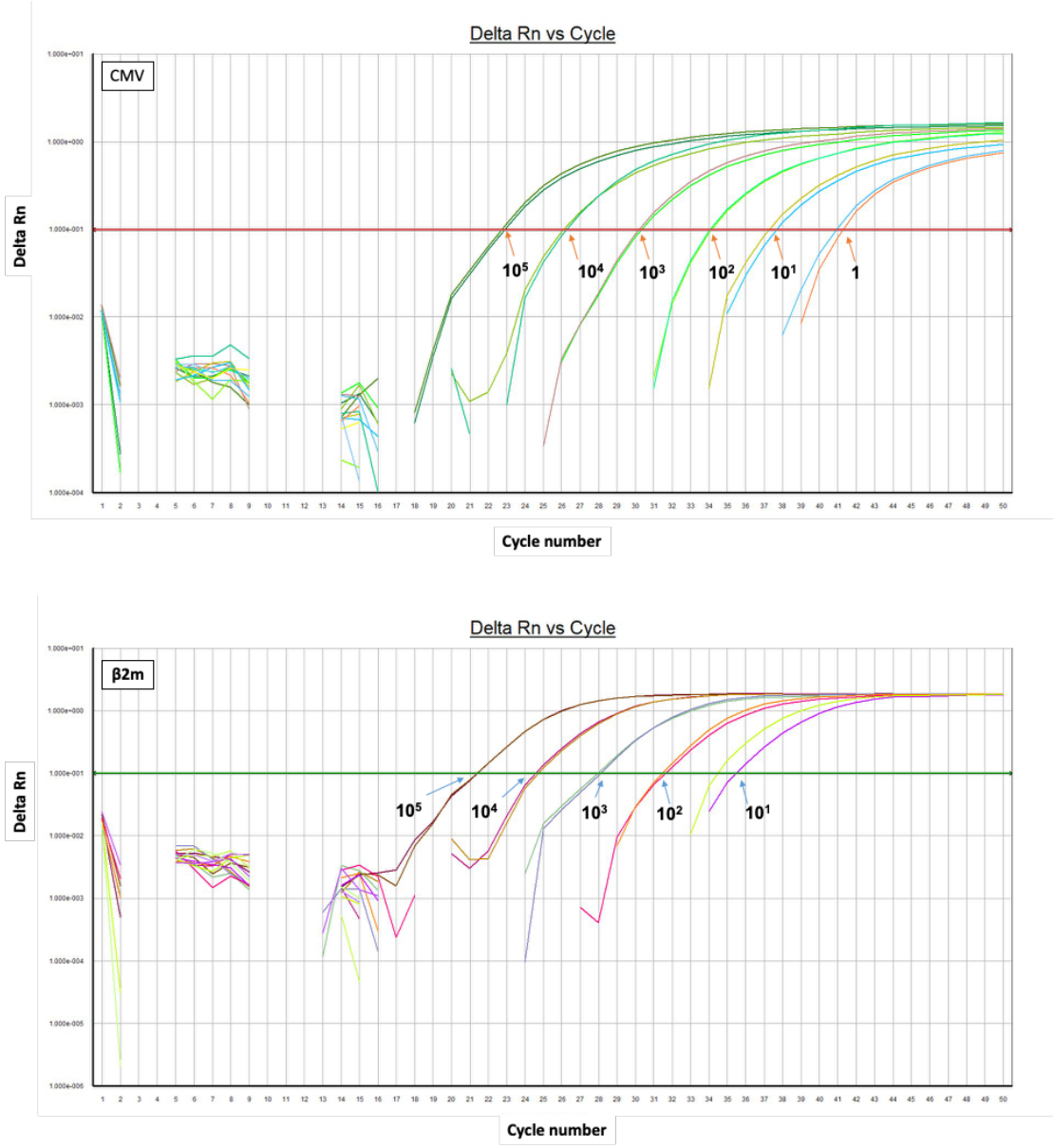


FIGURE 2.10.2. Example of amplification plots from CMV and β-2m gene standards. Standards were prepared by serial dilution method.

2.10.2.3. DNA sequencing of CMV viral genome

Some of the DNA samples that were extracted from QIAmp® Viral RNA Kit for serum and urine were sent for DNA sequencing to MRC-University of Glasgow Centre for Virus Research and DeutschesRheuma-Forschungszentrum, Germany. Unfortunately, CMV viral genome sequenced by MRC-University of Glasgow Centre for Virus Research could not be assembled and DNA sequencing was unsuccessful probably due to low viral load detected from urine and serum. CMV peptide sequencing was done in Germany as described by Hammer et al., (2018) and the information on the data and peptides sequences are available in Appendix (Supp. Table 5).

2.11. Statistical analysis

All data were analysed by using non-parametric test, Mann-Whitney for comparison between patients' groups and Wilcoxon sign rank test for different time-points within similar patients. Friedman test was used for comparison in more than two groups within similar group of patients. All sample sizes in the different time-points are small and treated as not normally distributed.

CHAPTER 3:

THE INCIDENCE AND CLINICAL SIGNIFICANCE OF CMV REACTIVATION AFTER HAEMATOPOIETIC STEM CELL TRANSPLANTATION

3.1. INTRODUCTION

This chapter will discuss the frequency and incidence of CMV reactivation in allo-HSCT patients consented to the BOOST trial at the QE hospital in the three years of study between 2016 and 2018. The impact of the CMV serostatus of both patients and donors was also investigated in relation to clinical outcomes of overall survival, GvHD, relapse and CMV reactivation within the same period of time. The patients' characteristics and demographics also will be discussed thoroughly in this chapter and compared to patients with no reactivation and healthy donors.

3.2. OBJECTIVE

The aim of this chapter was to assess the incidence of CMV reactivation in relation to patient and donor serostatus and to relate this to clinical outcome.

3.3. RESULTS

3.3.1. Frequency and cumulative incidence of CMV reactivation after allogeneic stem cell transplantation

The rate of CMV reactivation varies markedly in different allo-HSCT populations and is dependent on a range of factors. In a large recent study in the United States the cumulative incidence was 50-70% in CMV positive allo-HSCT patients (Boeckh, 2017). However, these numbers are heavily reliant on the nature of the diagnostic methods used in each study (Boeckh, 2017). This may partly explain the variation in reports with another example from a single institution study showing a total CMV reactivation incidence of only 33% (Melendez-Munoz et al., 2018).

Currently there are limited data on the incidence of CMV reactivation in patients in the United Kingdom using current transplant protocols. We studied CMV reactivation in 176 patients undergoing allo-HSCT at the Queen Elizabeth Hospital who were consented into the BOOST clinical study from 2016 to 2018. Before transplant, recipient and donor CMV serostatus was assessed by IgG and IgM ELISA and at day 0 and qPCR was then used for CMV viral load screening of recipients after transplant. 47 patients (26.7% [n=47/167]) developed CMV reactivation within the 3-year period of the study. A trend was seen towards a reduction in reactivation rate over time. In 2016, 28 out of 61 patients (45.9%) developed reactivation but this gradually reduced to 15 out of 61 (24.6%) in 2017 and only 4 of 54 (7.4%) in 2018 **(Fig. 3.3.1).**

Between 2016 and 2018, 53.2% of allo-HSCT patients with CMV reactivation (n=47) were of R+/D+ status and 38.3% within the R+/D- group. Surprisingly, 6.4% were initially typed as R-/D- and 2.1% were of the R+/'D equivocal' recipient-donor serostatus (graph not shown).

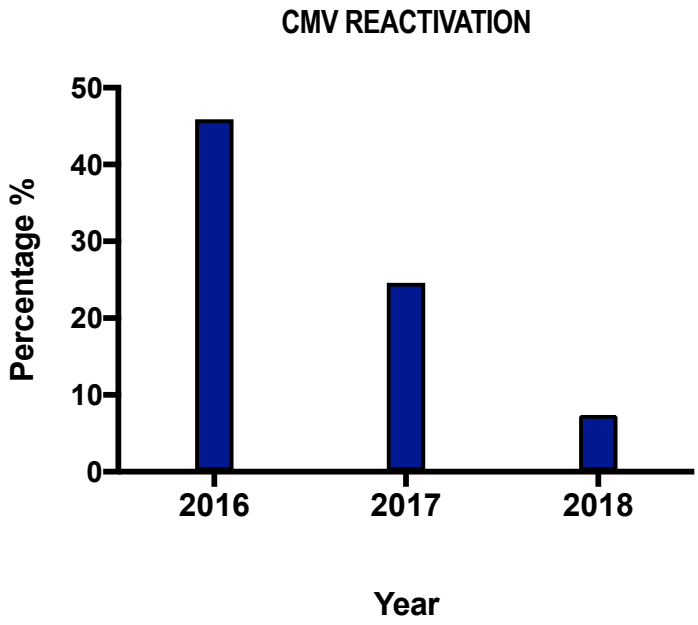


FIGURE 3.3.1. Frequency of CMV reactivation in allogeneic stem cell transplant patients consented to the BOOST study in the 3 years between 2016 and 2018. The percentage of patients with CMV reactivation in 2016 (45.9%; 28/61), 2017 (24.6%; 15/61) and 2018 (7.4%; 4/54) is shown.

The cumulative incidence of CMV reactivation in patients in the study (n=47) is shown in **Fig. 3.3.2** and also indicates that the median day for CMV reactivation is at day 40 post-transplant. When these patients were subdivided according to recipient/donor serotype the median cumulative incidence (%) of CMV reactivation in R+/D- pairs was 46 days compared to 36 days in the R+/D+ pair. However, the difference was not significant (p=0.1141) and greater patient numbers would be

needed to assess any effect of recipient/donor serostatus on the time to CMV reactivation.

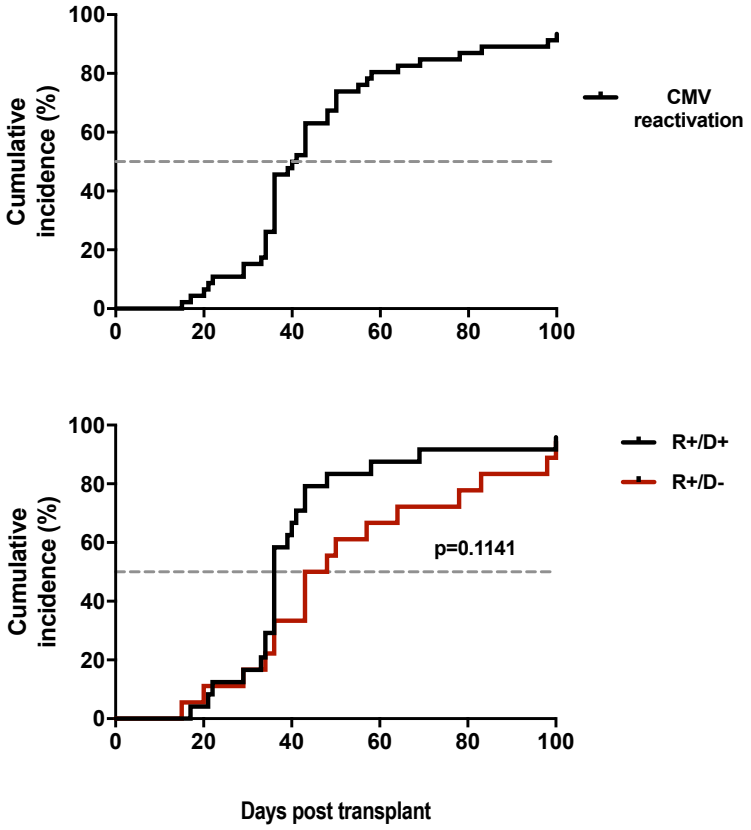


FIGURE 3.3.2. Cumulative incidence of CMV reactivation in patients in the 100 days post-HSCT (CMV reactivation n=47 / allo-HSCT n=176) between 2016 and 2018. The cumulative incidence (%) of CMV reactivation for R+/D+ (black line; median 36 days) and R+/D- (red line; 45.5 days) serostatus pairs for up to 100 days post-transplant (p=0.1141, ratio: 0.79 to 1.3, 95% CI: 0.43 to 2.3). Analysis was done by Kaplan–Meier survival analysis.

3.3.2. Overall survival data in allo-HSCT

The clinical follow up data from the allo-HSCT patients enrolled on the study was retrieved in order to investigate the effects of CMV on survival. Patients with Epstein-Barr (EBV) reactivation and with missing clinical data were excluded from the subsequent analysis, and of the remaining 89 allo-HSCT patients examined, 35 of them developed CMV reactivation. The allo-HSCT patients with EBV reactivation were excluded in this analysis to study the impact of recipient-donor CMV serostatus on overall survival without taking EBV reactivation as the cause of mortality. Similar to CMV reactivation, EBV reactivation is defined as more than 150 IU/ml EBV DNA by qPCR in the peripheral blood of allo-HSCT patients.

In the following graphs, the equivocal patients were treated and defined as seropositive. The overall survival data of allo-HSCT patients was analysed according to their CMV status (**Fig. 3.3.3,** n=89). The data shows no difference in the overall survival curves between the CMV positive and CMV negative allo-HSCT patients suggesting CMV serostatus of the recipient does not impact overall survival post-transplant (p=0.863, hazard ratio=1.08).

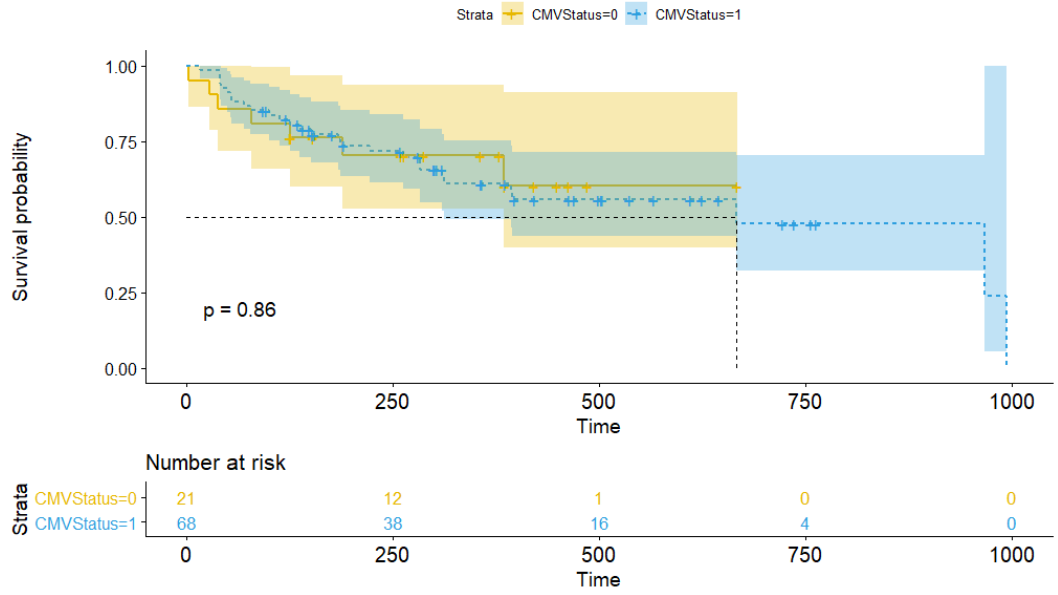


FIGURE 3.3.3. The effect of recipient CMV status on overall survival of CMV positive and CMV negative allo-HSCT patients (n=89). Survival probability of allo-HSCT patients was analysed according to whether they were CMV negative (CMV Status = 0, blue line) or CMV positive (CMV status = 1, yellow line). Survival probability analysis was done using R, p=0.863, hazard ratio=1.08.

The overall survival of allo-HSCT patients was then analysed according to the CMV serostatus of the donor (**Fig. 3.3.4,** n=89) and here a significant difference can be seen in the overall survival depending on whether the donor was CMV negative or CMV positive (p=0.011; hazard ratio: 2.4). The survival rate is lower in recipients receiving grafts from CMV positive donor (median: 393 days) as compared to patients receiving grafts from CMV negative donors (median: 994 days).

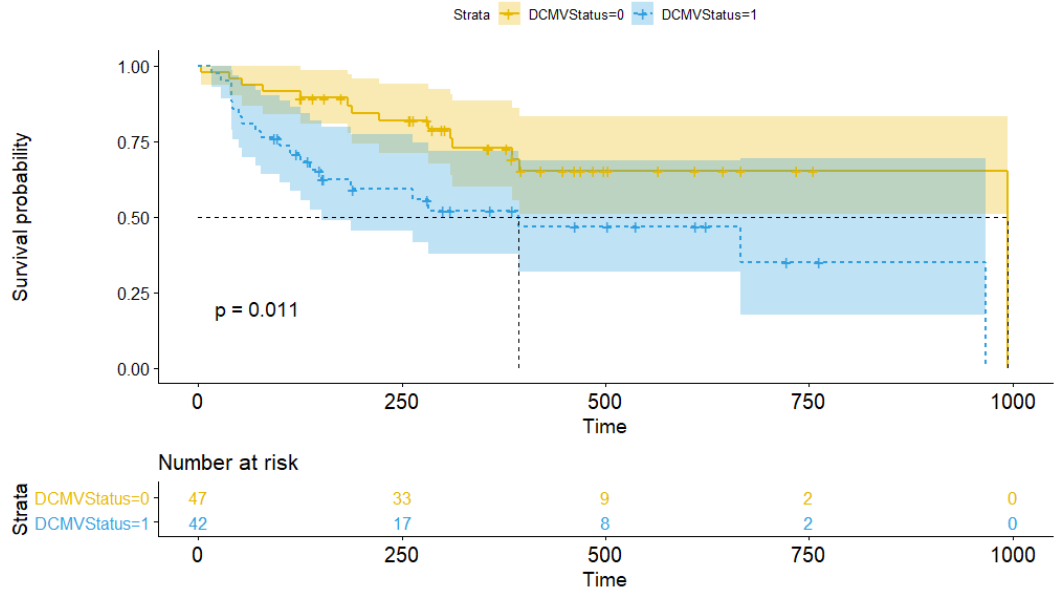


FIGURE 3.3.4. The effect of donor CMV status on overall survival of CMV positive and CMV negative allo-HSCT patients (n=89). Survival probability of allo-HSCT patients was analysed according to whether the stem cell donors were CMV negative (DCMV Status = 0, blue line) or CMV positive (DCMV status = 1, yellow line). Survival probability analysis was done using R, p=0.0133, hazard ratio: 2.408.

The impact of recipient-donor pairs on the overall survival of allo-HSCT patients was also examined (**Fig. 3.3.5,** n=89). The results show a significant difference in survival (p=0.045) between R+/D+, R+/D-, R-/D+ and R-/D- recipient/donor pairs, whilst a significant impact of donor serostatus can still be seen in overall survival of allo-HSCT patients (p=0.0097, hazard ratio=2.98). However, no effect on the survival rate of patients can be seen from CMV serostatus of recipient (p=0.28, hazard ratio: 0.58%). The median survival rate is also similar as in previous graphs, R+/D+ (median: 393 days) and R+/D- (median: 994 days).

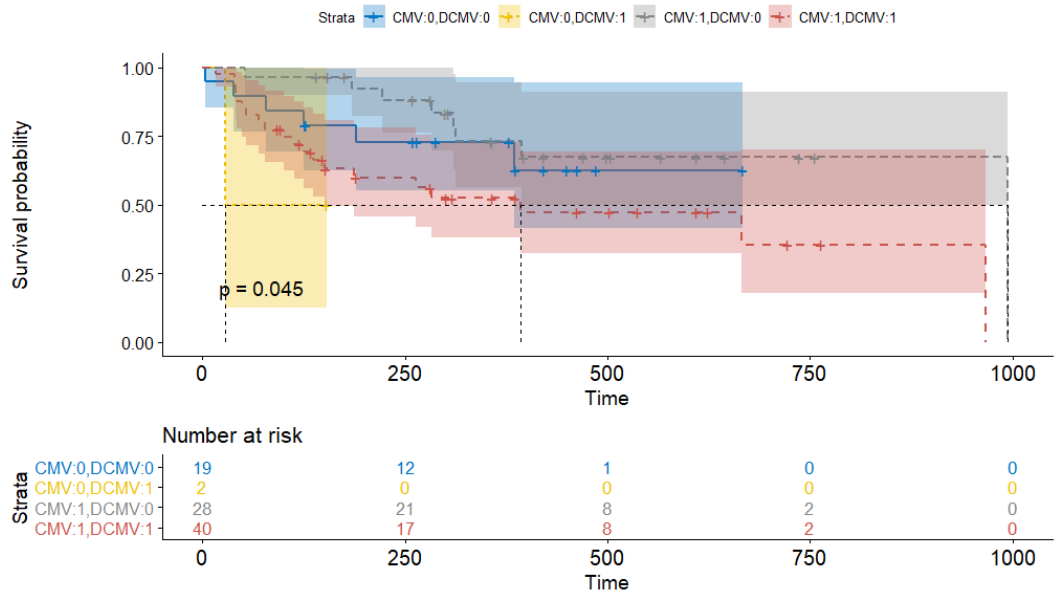


FIGURE 3.3.5. The effect of recipient/donor pair CMV serostatus on overall survival of CMV positive and CMV negative allo-HSCT patients (n=89). Survival probability of allo-HSCT patients was analysed according to their recipient/donor pair CMV status; R+/D+ (CMV:1, DCMV:1, red line), R+/D- (CMV:1, DCMV:0, grey line), R-/D+ (CMV:0, DCMV:1, yellow line) and R-/D- (CMV:0,DCMV:0, blue line). Survival probability analysis was done using R, p=0.045.

3.3.3. Incidence of CMV reactivation, graft versus host (GvHD) and relapse occurrence in relation with recipient-donor serostatus

Fig. 3.3.6 shows the influence of recipient-donor serostatus on the occurrence of CMV reactivation, GvHD and leukaemia relapse in the allo-HSCT patient cohort within similar period of time (2016 to 2018). Among these allo-HSCT patients, the event occurrence was analysed for aGvHD (n=116), cGvHD (n=76), CMV reactivation (n=117) and relapse (n=66). Discrepancies in the number of total patients in the group was due to missing data or the information was not available. Recipient/donor CMV serostatus was not a significant factor in relation to the development of acute or chronic GvHD (aGvHD: p=0.20, n=116, cGvHD: p=0.32, n=76, Global Fisher Exact test). The data however did not take an account for the impact of steroids that is used for the treatment of GvHD and grade which may

potentially affecting the analysis. On the other hand, significant difference can be seen in between R+/D+, R+/D-, R-D+ and R-/D- recipient-patient pairs which affecting the occurrence of CMV reactivation (p=0.0039, n=117). Surprisingly, the occurrence of leukaemia relapse within allo-HSCT patients was also affected by recipient-donor CMV serostatus (p=0.01084, n=66).



FIGURE 3.3.6. Recipient-donor serostatus relationship with the occurrence of GvHD, relapse and CMV reactivation. The occurrence of acute GvHD (n=116, p=0.2024) and chronic GvHD (n=76, p=0.3243) are not associated with recipient-donor serostatus however the occurrence of CMV reactivation (n=117, p=0.00392) and relapse (n=66, p=0.01084) are related with recipient-donor CMV serostatus in allo-HSCT patients. The analysis was done by Global fisher exact test by R.

3.3.4. Collection of blood samples for subsequent study within this thesis

Blood samples from patients who had experienced CMV reactivation have been collected from January 2016 to the end of December 2018. Amongst allo-HSCT patients being consented in the BOOST trial, only 41 CMV reactivation patients were included in this study, which also have included 4 patients who have had transplant in 2015. This include patients who had EBV reactivation. These frozen samples of patients without reactivation were available from the biobank and been used and analysed by following the guidelines from the BOOST ethics. The detailed information on the patients' demographics can be seen from **Table 3.3.1** and the additional information of the patients such as conditioning and HLA types can be found in Appendix (Supp. Tables 1a and 1b). The average day of CMV reactivation event in these patients (n=41) is on day 52±5 (Mean ± SEM) which is equivalent to week 6 or 7 post HSCT with median of day 43.

The median age of the study cohort was 59 years (range 20-70), of which 59% were male and 39% had a diagnosis of AML (39.0%). 61% had received a graft from a MUD **(Table 3.3.1).** The majority CMV reactivation patients included in the analysis had a R+/D+ CMV serostatus (54%), while the rest are the CMV risk group R+/D- (37%), recipient-donor negative matched, R-/D- (7.3%) or R+/'Dequivocal' (2.4%). R+/'Dequivocal' referred to a CMV serostatus that was ambiguous and could not be determined confidently by qPCR. The majority of the patients did not relapse (76%) but 59% of them were diagnosed with acute GvHD. Within the number of patients who had developed aGvHD (n=24), some patients (n=6) also

developed chronic GvHD. 36% of CMV reactivation patients had received the combination of Flu/Melph/Campath conditioning.

All patients who experienced CMV reactivation received some form of anti-viral treatment including acyclovir, valganciclovir, cidofovir, ganciclovir or foscarnet, depending on factors such as prophylactic or pre-emptive therapy and viral load. The patients received antiviral treatments (valganciclovir, ganciclovir, etc) as early as a day after high CMV viral loads have been detected from blood after been given acyclovir. 54% of patients only experienced one episode of viral reactivation.

TABLE 3.3.1. The demographic characteristics of patients who underwent CMV reactivation (n=41).

PATIENT DEMOGRAPHICS (CMV reactivation)	NUMBER (n=41)	PERCENTAGE (%)
Age range 20-70 years (median: 59 years) Reactivation days after transplant 52±5 (median: day 43) Range days (10 to 125 days)		
CMV serostatus (Recipient/Donor)		
R+/D+	22	53.7
R+/D-	15	36.6
R-/D-	3	7.3
R+/D equivocal	1	2.4
Sex		
Male	24	58.5
Female	17	41.5
Donor type		
Siblings	13	31.7
Matched unrelated donor (MUD)	25	61.0
Related donor (son)	1	2.4
Cord	2	4.9
Diagnosis		
AML	16	39.0
ALL	4	9.8
MDS	9	22.0
Others (CMML, NHL, RCMD, etc.)	12	29.3
Relapse incidence		
Relapse	10	24.4
Non-relapse	31	75.6
GvHD		
only aGvHD	24	58.5
only cGvHD	1	2.4
aGvHD and cGvHD	6	17.1
non-GvHD	16	39.0
Conditioning		
Flu/Melph/Campath	15	35.6
Flu/Bu/ATG	7	17.1
Flamsa/Bu	8	19.5
Beam/Campath	5	12.2
Others (Cyclo/Flu/TBI, Cyclo/TBI, TLI/ATG, Bu/Cy, Cy/TBI, Flu/beam/Campath)	6	14.6
Viral episodes		
Single viral episode	22	53.7
Multiple viral episodes	19	46.3

3.3.5. Prophylaxis and treatment of CMV reactivation allo-HSCT patients

The highest risk of CMV reactivation occurs in patients who are seropositive and receive T cell depleted-grafts from unrelated donor grafts (Camargo and Komanduri, 2017). According to local guidelines (2017), the CMV serostatus of patients and donors is important in the consideration of donor selection as a CMV seronegative donor will be selected wherever possible for a CMV seronegative patient. As such primary CMV infection is a relatively uncommon condition that occurs when seronegative recipients receive stem cell grafts from CMV seropositive HDs. Indeed, as seen from **Table 3.3.1**, none of the CMV reactivation patients were from the R-/D+ group. A much more common scenario was when a CMV seropositive patient received a graft from a CMV seronegative donor and as such the infused immune system was 'CMV naïve'. We took advantage of this mismatch to study the relative NK and T cell reconstitution from CMV naïve or seropositive donors.

For prophylaxis treatment all the patients were given daily acyclovir initially until 35 days of transplant. Afterwards, the patients were tested with CMV viral load by weekly routine qPCR and when there was evidence of CMV reactivation, the patients were given antiviral treatments dependent on the type of grafts received by the patients, either from HLA identical sibling or matched unrelated donor. In HLA identical sibling, the patients were given antiviral drugs, monitored twice weekly by qPCR for antiviral response until a decline is observed, or the virus has been cleared from the peripheral blood. The patients who received grafts from related

donor also received valganciclovir for the antiviral treatment. On the other hand, in the patients receiving grafts from MUD, they were monitored once weekly and received valganciclovir if the viral load was <10,000 copies/ml of CMV in peripheral blood, or ganciclovir if this was >10,000. Nevertheless, there are side effects and complications in the pre-emptive therapy and antiviral treatments in allo-HSCT patients, as shown from **Table 3.3.2**.

TABLE 3.3.2. Side effects of drugs used to treat CMV infection. Adapted from (Emery et al., 2013).

Drugs	Side effects	Treatments
Ganciclovir	Myelosuppression	Granulocyte colony-stimulating factor
Valganciclovir	Haemolysis Nausea/vomiting Fever Rash Mental state changes	Toxicity-specific dose reductions Regular twice daily 5HT3 inhibitors
Foscarnet	Electrolyte abnormalities Renal impairment Nausea/vomiting Genitourinary Urinary symptoms	Aggressive electrolyte replacement Fluid support Regular twice daily 5HT3 inhibitors Toxicity-specific dose reductions
Cidofovir	Renal impairment Nausea/vomiting Ocular	Probenecid Aggressive prehydration Regular twice daily 5HT3 inhibitors Ophthalmology review

3.2.4.1. CMV viral loads in urine and serum

Serum and urine samples from allo-HSCT patients with known CMV reactivation were analysed for CMV DNA by qPCR following DNA extraction using different types of kits (described in detail in Chapter 2). Beta-2 microglobulin (B-2m) gene expression was also assessed as a positive control (1511±770 copies/ml; **Fig. 3.3.7**). CMV DNA could only be detected in minority of urine samples (14±5 copies/ml**; Fig. 3.3.7**). The urine samples were randomly selected from time points within the first four weeks after reactivation. Unfortunately, the qPCR method was not able to detect the CMV DNA where serum was used as the DNA source (data not shown) and the list of samples used are available in the Appendix (Supp. Table 5). Similar samples were sent to MRC-University of Glasgow Centre for Virus Research and Deutsches Rheuma-Forschungszentrum, Germany for sequencing work.

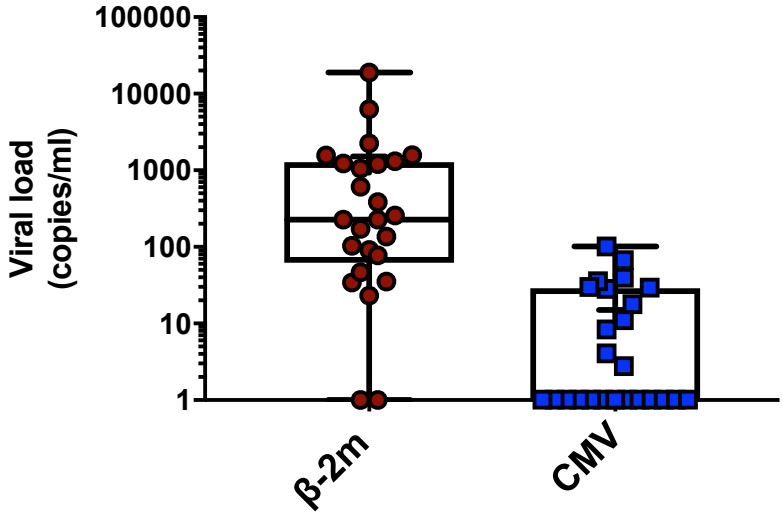


FIGURE 3.3.7. CMV viral load in urine. Samples were analysed by qPCR with β_2m used as a positive control. CMV copy number was detectable in only a minority of urine samples from CMV reactivation patients (n=25).

3.3.6. Control groups

In this study, two different control groups were used for comparisons for all data analysis that will be discussed in further chapters. The CMV reactivation allo-HSCT patients (n=41) were compared with allo-HSCT patients without CMV reactivation (n=26) and HDs. The number of HDs used for comparison varied dependent on the type of analysis, either for NK cells, $CD8^+$, $CD4^+$ or TCRγδ T cells.

All patients were monitored by CMV qPCR for 6 months after transplant. The characteristics of patients selected for comparison with the study group, with no CMV reactivation, is shown in **Table 3.3.3** and the list of patients is available within the Appendix (Supp. Table 1d, e). Unlike CMV reactivation patients, viral loads in patients without reactivation are below 200 copies/ml (undetectable) by routine qPCR. The patients' demographics are otherwise similar to the CMV reactivation patients. The patients are also classified according to CMV serostatus of recipient and donor, as shown from the **Table 3.3.1**. Unlike CMV reactivation allo-HSCT, peripheral blood samples were not collected weekly.

3.3.6.1. Characteristics of healthy donors used in the study

HDs were recruited, consented and collected among the staff and students from College of Medical and Dental Sciences. HDs were tested by serum IgG ELISA to distinguish between CMV seropositive and seronegative. Similar to patients without reactivation, viral loads in HDs were also undetectable by 'in house' CMV

DNA qPCR. The list of HDs used for the analysis are listed in the Appendix (Supp. Table 8).

TABLE 3.3.3. Characteristics of patients with 'no viral reactivation' (n=26).

PATIENT DEMOGRAPHICS (No reactivation)	**NUMBER (n=26)**	**PERCENTAGE (%)**
Age range 26-72 (median: 57.5 years)		
CMV serostatus (Recipient/Donor) R+/D+ R+/D- R-/D-	 8 2 16	 30.1 7.7 61.5
Sex Male Female	 15 11	 57.6 42.3
Donor type Siblings Matched unrelated donor (MUD)	 13 17	 31.7 61.0
Diagnosis AML ALL MDS Others (CMML, NHL, RCMD, etc.)	 7 2 8 9	 26.9 0.8 3.1 34.6
Relapse incidence Relapse Non-relapse	 10 31	 24.4 75.6
GvHD Only aGvHD Only cGvHD aGvHD and cGvHD non-GvHD	 11 1 4 10	 42.3 3.8 15.4 38.5
Conditioning Flu/Melph/Campath Flu/Bu/ATG Flamsa/Bu Cyclo/TBI Beam/Campath Flu/Cyclo	 7 7 5 4 2 1	 17.1 17.1 12.2 9.8 4.9 2.5

3.4. DISCUSSION

The incidence of CMV reactivation in allo-HSCT patients

Over the period of three years, 27% (n=47) of allo-HSCT patients being treated in the QE hospital had developed CMV reactivation, and the occurrence was the highest in R+/D+ allo-HSCT patients (n=25, 53%, graph not shown). Data in this study is somehow opposite to previous report that showing R+/D- recipient-donor allo-HSCT patients had the higher occurrence of CMV reactivation as compared to R+/D+ group (Vaezi et al., 2016). Comparison of the incidence or frequency of CMV reactivation could not be made with cohorts from the years before 2016 as no data was available, but the data is still comparable to from the United States (50-70% in R+) (Boeckh, 2017).

The incidence of CMV reactivation has decreased markedly over the past 3 years. The reasons for this are not entirely clear but may potentially include factors such as a reduction of viral seroprevalence within the transplant population, improved efficacy of prophylactic therapy or changes in the conditioning regimen. Indeed, an increase in the use of acyclovir from +35 to +100 days had been introduced during the period of study.

Of note, the number of patients included in the analysis does not represent all patients but only those that have been consented in the study. Furthermore, from the number of allo-HSCT patients who developed CMV reactivation between 2016 to 2018 only 21.0% (n=37) were included in the analysis in project. The major

reasons the patients were not included in the study were because either the patients difficult to bleed or requested to be taken out from the study (extra 36 ml of peripheral bloods and 25 ml of urine were taken within first four weeks after reactivation). As such the study is somewhat limited for statistical analysis because of the size of the study group.

Patients with documented CMV reactivation, as measured by the hospital assay, were also investigated for CMV viral loads within serum and urine. However, the methods were not able to detect CMV genes in the serum, probably due to the virus titres being too low or the DNA extraction kits that were used were not able to extract enough viral DNA (Qiagen and Roche DNA extraction kits). This suggests that our methodology was somewhat lower than that performed by the clinical laboratory. Nevertheless, the control β-2m genes can still be detected and amplified by similar methods signifying the methods were working. Some patients have been detected with CMV in the urine, but the viral copy number is also quantitatively low. Similar DNA samples from serum and urine were sent to MRC-University of Glasgow Centre for Virus Research for sequencing work, but CMV viral genomes were unsuccessfully identified and sequenced. Surprisingly, in total 6 out of 33 of DNA samples sent for viral UL40 peptide sequencing to Deutsches Rheuma-Forschungszentrum, Germany were successfully sequenced, as following the published work (Hammer et al., 2018) (Data available in Appendix).

Patient's demographics and healthy donors

In total, 41 patients have been included in the analysis which will be further discussed in the next few chapters. Four of them are the patients who had transplant in year 2015 and 2016. The availability of the samples was also dependent on whether patients were attending the haematology clinic for follow up treatment and monitoring. Patients developed reactivation at a median time of day 43 after transplant and therefore a 6 week timepoint post-transplant was chosen to compare week of reactivation (CMV reactivation allo-HSCT). A limitation of this study was that weekly blood samples were not available from this control group.

Overall survival probability in allo-HSCT patients

At 47, the number of patients with CMV reactivation between 2016 and 2018 is rather low to provide strong statistical power for an assessment of overall survival. CMV seroprevalence did not have an impact on overall survival although survival was better with donor CMV negative serostatus ($p=0.013$). This suggests an importance for donor serostatus in allo-HSCT outcome but is opposite to a large previous study which reported that lower survival rate and transplant-related mortality (TRM) in patients who receive a graft from a CMV seronegative donor (Ljungman et al., 2003). These discrepancies may arise from the fact that there are a limited number of patients in this study, as well as additional factors such as conditioning regimens and type of donor graft origin.

When the CMV serostatus of recipient and donor were analysed in pairs, significant differences were seen in the survival curves, with the lowest survival rate within the R+/D+ pair as compared to R+/D-, R-/D- and R-/D+ (p=0.045). A higher survival rate was seen in the R+/D- patients (median: 994 days, as compared to R+/D+ median: 393 days). Even though studies have described that CMV risk group R+/D- contributed to poor survival rate of patients (Ramanathan et al., 2016; Ljungman et al., 2003), our data has shown the opposite, also probably due to low number of allo-HSCT patients being analysed. However, another study has also shown that R-/D- group has the highest survival rate among as compared to R+/D+ and R+/D- (Schmidt-Hieber et al., 2013). However, the analysis has excluded the patients with no EBV reactivation which potentially contributed to bias in this study.

Occurrence of GvHD, CMV reactivation and relapse in allo-HSCT

As the number of CMV reactivation events was low, the effect of recipient-donor serostatus on the occurrences of GvHD and relapse was also analysed in the total cohort. The data has shown that occurrence of both acute and chronic GvHD in allo-HSCT in fact are not affected by recipient-donor serostatus **(Fig. 3.3.6)**. However, the occurrences of leukaemia relapse and CMV reactivation were strongly affected by recipient-donor CMV serostatus (relapse, p=0.011 and CMV reactivation, p=0.0039). Even though the number of occurrences is very small in each group, the data is giving an insight on the importance of CMV serostatus in CMV reactivation as well as leukaemia relapse. No studies have been found in

analysing the CMV recipient-donor pair serostatus on the association of leukaemia relapse.

3.5. CONCLUSION

In brief, this chapter has described the evaluation on the patients' demographics used in this study as well as the patients without reactivation and HDs. The small numbers of CMV reactivation allo-HSCT used in this study has been justified with the low incidence in a period of 3 years. The overall survival rate in the R+/D- is also higher in allo-HSCT patients as compared to R+/D+ patients, with strong impact of recipient-donor CMV serostatus on occurrence of CMV reactivation and leukaemia relapse.

CHAPTER 4:
NATURAL KILLER CELL PHENOTYPES AND FUNCTIONS IN CMV REACTIVATION AFTER ALLOGENEIC STEM CELL TRANSPLANTATION

4.1. INTRODUCTION

As discussed in the previous chapter, NK cells are the first lymphocyte population to undergo substantial immune reconstitution after HSCT. NK cells play a critical role in controlling HCMV infection in healthy people and CMV seropositive individuals undergo a permanent alteration in their peripheral NK repertoire. As such, given the clinical importance of CMV infection in patients after HSCT it was of interest to study the profile of NK cell phenotype and function following an episode of viral reactivation in this setting.

In order to undertake this analysis percentage and absolute count of total NK cells were monitored starting from the initial time of reactivation until a follow up period at several months thereafter. Comparison was made with two different control groups, allogeneic HSCT patients who did not suffer an episode of viral reactivation and HDs. Also, the effects of CMV reactivation on NK cell subpopulations were further explored through analysis of different subsets according to the profile of CD56 and CD16 expression. The expression of NKG2C and NKG2A, which are the important indicators of NK expansion after HCMV infection, have also been studied. CD57, KIR, PD-1, CD69 and KLRG1 expression was also explored.

Finally, the functional capacity of NK cells was assessed by analysis of cytotoxicity and cytokine production.

4.2. OBJECTIVES

The objective of this chapter was to study NK cell phenotype and function in the early period following CMV reactivation in allo-HSCT patients. Specifically, the aims were to assess how viral reactivation served to modulate the pattern of NK cell expansion, phenotype and function.

4.3. RESULTS

4.3.1. NK cells gating strategy and analysis

Flow cytometric gating for identification of NK cells was done according to methods and protocols established within the research group. PBMC were stained with a range of antibodies against proteins expressed on NK cell subsets (Chapter 2, **Table 2.6.1** and **2.6.2**) and single cells were gated according to FSH and FSA **(Fig. 4.3.1).** Doublet cells were excluded from all plots to avoid false positive analysis which maybe causing double positive cell readings. Then the lymphocytes were gated according to FSH and SSH and live cells identified using Propidium Iodide (PI). The monocytic (CD14) and B cell fractions (CD19) were also stained so that they could be excluded in the same channel as PI **(Fig. 4.3.1).** PI dye functions by penetrating the membrane of dead cells and therefore allowed identification of live populations. NK cells were identified within live cells by expression of $CD3^-$ and $CD56^+$ **(Fig. 4.3.1).**

Following identification of the total NK cell subsets four different subsets of NK cells were then identified by the pattern of CD56 and CD16 co-expression. These are the $CD56^{dim}$ $CD16^{bright,}$ $CD56^{dim}$ $CD16^{negative}$, $CD56^{bright}$ $CD16^{bright}$ and $CD56^{bright}$ $CD16^{negative}$ subsets which were gated according to intensity of surface expression **(Fig. 4.3.1)** $NKG2C^{+}NKG2A^{-}$ and $NKG2C^{-}NKG2A^{+}$ subsets were also determined, and the expression of these molecules is largely mutually exclusive **(Fig. 4.3.1).** All the other markers except CD56 and CD16 expression were studied using the NK cell $CD56^{dim}CD16^{bright}$ subset to exclude complication. The same gating strategies were used in the patient group and also the control subsets.

The calculation of the absolute cell count per µl was done by extrapolating the percentage of NK cells (gated from the product of the live and lymphocyte subsets, Appendix: Supp. Table 3 and 4) from the total lymphocyte count (in 10^9/L) which was obtained from the haematology laboratory in the local hospital. Unfortunately, no data were available on the absolute count from HDs and some of the absolute count values from patients were too low for analysis.

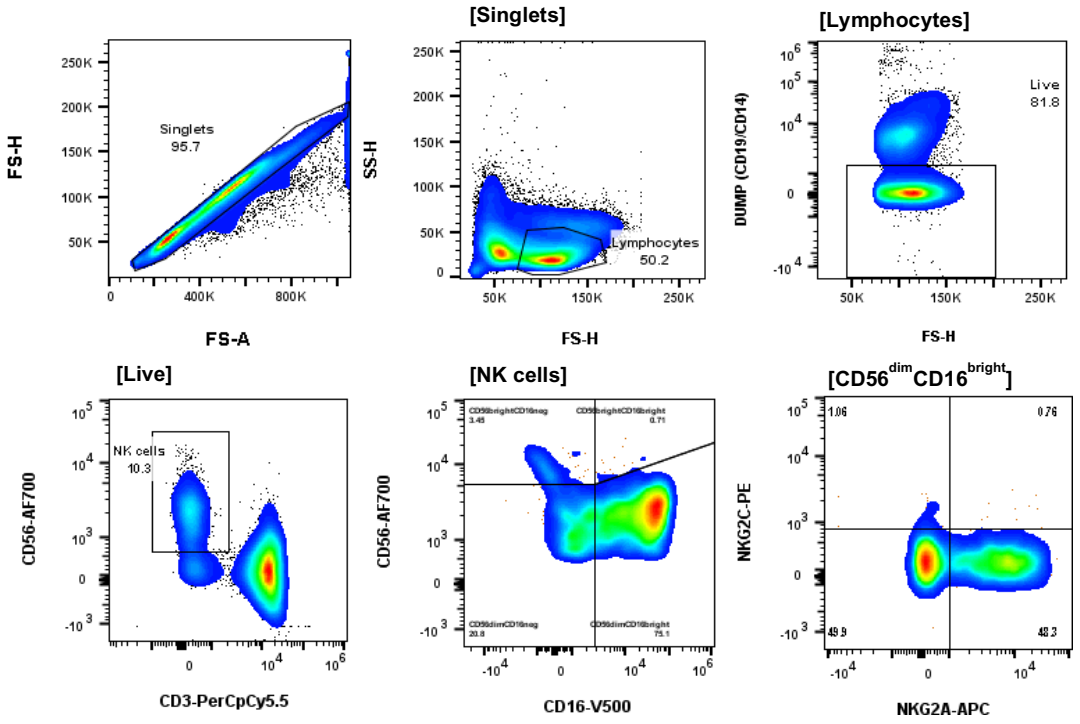


FIGURE 4.3.1. NK cell gating strategy. NK cells were gated from single cells (to exclude doublets) then lymphocytes and live cells by adding PI, CD19 and CD14 (excluding monocytes, B cells and dead cells). Total NK cells were gated from $CD56^{+}$ and $CD3^{-}$ population and further classified into four different subsets, allowing identification of the predominant $CD56^{dim/right}$ and CD16 $^{bright/negative.}$ The expression of NKG2A and NKG2C was also examined.

4.3.2. Reconstitution of Natural Killer (NK) cells following an episode of CMV reactivation in patients undergoing allogeneic HSCT

In initial studies the reconstitution of NK cells after HSCT was compared between patients who experienced an episode of CMV reactivation and a control group without CMV reactivation. A healthy donor cohort was also incorporated into analysis. As such the groups for comparison in the study included: 1) CMV seronegative HDs, 2) CMV seropositive HDs, 3) no reactivation allo-HSCT patients and 4) CMV reactivation allo-HSCT patients.

4.3.2.1. The percentage of NK cells in healthy donors is not influenced by CMV serostatus

CMV serostatus was determined in a cohort of 39 HDs using an in-house CMV serum IgG ELISA. The average percentage of NK cells within the whole lymphocyte (live cells) subset was 9.8±1.3% (n=39). The percentage of NK cells from CMV seronegative donors was 7.3±0.9% (Mean±SEM) compared to 12.2±7.3% from seropositive donors **(Fig. 4.3.2)** but this difference was not statistically significant (p=0.22, Mann-Whitney test). Analysis of the absolute count of NK cells on HD was not performed but the percentages of each individual subset were determined for comparison with data from HSCT patients.

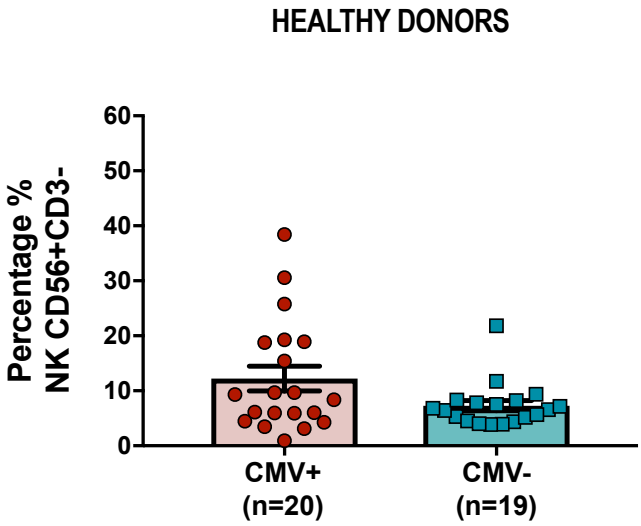


FIGURE 4.3.2. NK cells in healthy donors. No change was seen in the proportion of NK cells in CMV seropositive (12.2±7.3% [Mean±SEM]) and CMV seronegative (7.3±0.9%) HDs. The CMV serostatus of HDs was determined from serum IgG ELISA with 10 U/ml considered as CMV positive. Overall mean percentages for total HDs are 9.8±1.3% (n=39). No data were available on the absolute number of NK cells in HD.

4.3.2.2. The number of NK cells increases in HSCT patients after CMV reactivation

The initial studies addressed the impact of CMV reactivation on the frequency of NK cells in allo-HSCT by studying the proportion and absolute count of NK cells at different time points including pre-HSCT, pre-reactivation, at the time of reactivation and at weeks 1, 2, 3, 4 and months 3, 6 10 post-reactivation. For the non-reactivation group, the samples were collected from week 6 after HSCT as this was most similar in time to the median point of HCMV reactivation (average 43 days post HSCT).

The percentage of NK cells in both 'CMV reactivation' and 'non-reactivation' HSCT patients prior to transplant was not statistically different compared to HD (grey bar in the graph) **(Fig. 4.3.3).** However, after HSCT the percentage of NK cells in both groups increases markedly which reflects the fact that NK cells are the first lymphoid population reconstitution after HSCT.

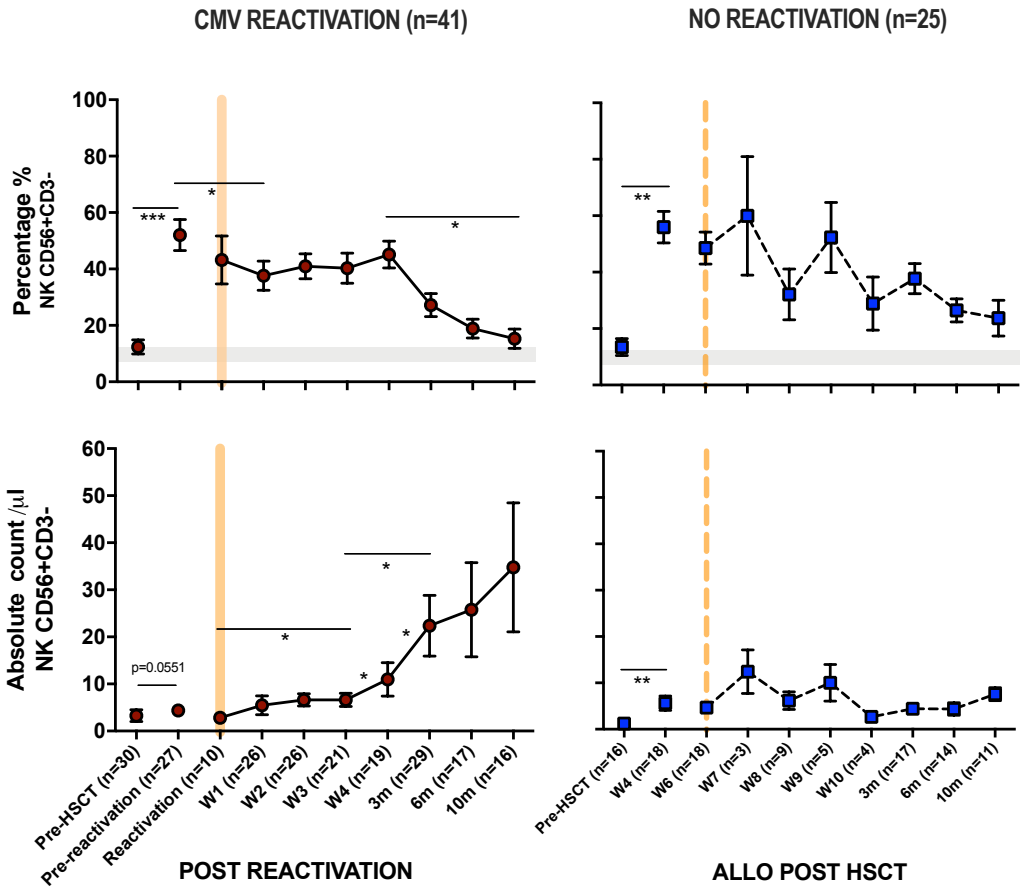


FIGURE 4.3.3. NK cells percentage and absolute number around the time of CMV reactivation and in non-reactivated control subjects. Patients were classified as undergoing an episode of CMV reactivation when viral load reached above 200 copies/ml. The time of viral reactivation is shown by the brown column and the time-matched point in 'non-reactivation' patients is indicated by the dashed vertical line. The grey line represents the range of total NK cells within CMV seronegative (7.3±0.9%) and CMV seropositive HDs 12.2±7.3% [Mean±SEM]). Analysis was done by Wilcoxon sign rank test (*p<0.05, **p<0.01, ***p<0.005). [W: week(s), m: month(s) after CMV reactivation/allo-HSCT].

The median time at viral reactivation was 43 days post-HSCT and week 6 was therefore taken as an appropriate matched time point for the 'non-reactivation' group. Interestingly the proportion of NK cells was maintained at a high level of the total lymphoid pool for 4 weeks after reactivation **(Fig. 4.3.3**, Friedman test, p=0.736), from 43% at the week of viral reactivation to 45% after 4 weeks. In contrast this value declined within the non-reactivation group over this period.

Even more striking observations were observed in relation to the influence of viral reactivation on the subsequent trajectory of the absolute number of NK cells. Following reactivation, the total count of NK cells went up 11-fold from 3 cells/µl at the time of reactivation to 35 cells/µl at the final time point of assessment at 10 months. In contrast, the NK cell number remained very stable over this period in patients who did not experience an episode of CMV reactivation **(Fig. 4.3.3).** As such CMV reactivation acts to greatly increase the number of NK cells within the peripheral circulation and these are likely to play an important role in the control of viral reactivation.

Statistical analysis of the proportion and total count of NK cells was then undertaken between the CMV reactivation and 'non-reactivation' groups **(Fig. 4.3.4).** The increase in the total number of NK cells after reactivation was strongly significant at 3, 6 and 10 months. Although an 11-fold increase was also seen at 4 weeks the statistical power at this time was somewhat limited by the size of the group.

Interestingly, this substantial increase in the NK cell number was not reflected in a parallel increase in the proportion of NK cells within the blood. Indeed, at months 3, 6 and 10 this value actually fell in the CMV reactivation group. As such, this indicates that viral reactivation must also drive an increase in the number of other lymphoid cells within the periphery. This was to become an important theme of the subsequent work.

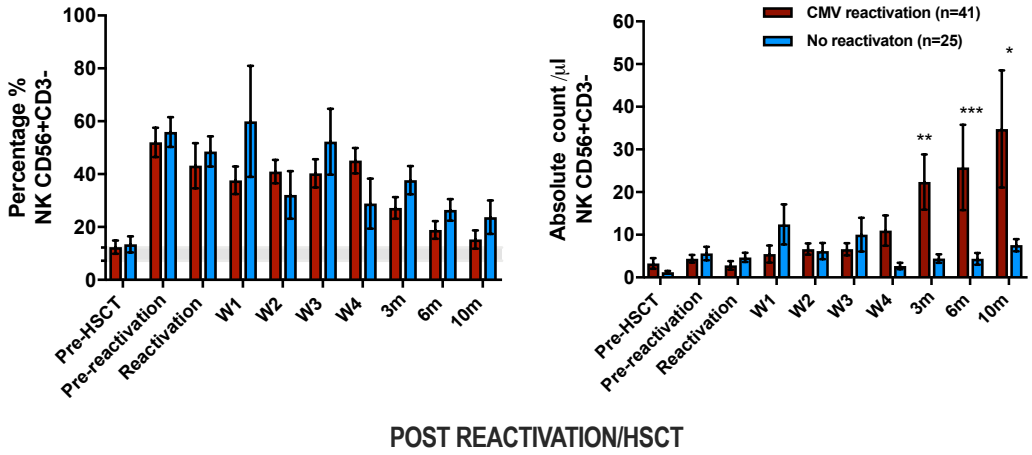


FIGURE 4.3.4. Comparison of the percentage and absolute number of NK cell in patients after HSCT divided into those with an episode of CMV reactivation or not. The absolute number of NK cells is increased at 3, 6 and 10 months after reactivation but no significant changes are observed in the relative proportion of NK cell within blood. Dotted lines represent the HD total NK cell range between CMV seronegative (7.3±0.9%) and CMV positive subjects (12.2±7.3%; Mean±SEM). No data were available on absolute count in the HD group. Analysis was done by Mann Whitney test (*p<0.05, **p<0.01, ***p<0.005). [W: week(s), m: month(s) after CMV reactivation/allo-HSCT].

4.3.2.3. The magnitude of CMV viral reactivation is correlated with the number and proportion of NK cell within peripheral blood

CMV viral load can be quantified by qPCR from the serum of HSCT patients. Therefore, how the peak load of viraemia was correlated with the pattern of NK cell reconstitution was assessed. The CMV viral load was monitored every week after CMV reactivation was initially detected (defined as >200 copy of CMV/ml) and this data was retrieved from the clinical virology laboratory in QE hospital. When

the CMV virus load fell to <200 copies/ml in the whole blood sample this was considered as a zero figure.

The range of viral load within the reactivation cohort was 228 to 18,990 copies/ml within blood with a mean value of 1960±490 copies/ml at the time of reactivation **(Fig. 4.3.5).** The high SEM value indicates that viral load varies substantially from one individual to another. The CMV viral load peaked at two weeks after reactivation and then declined although a second smaller peak at week 4 after reactivation was seen in many patients **(Fig. 4.3.5).** The correlation between the total CMV viral load during reactivation and quantitative measure of NK cells within blood also was assessed. Generally, there was a correlation between CMV viral load and overall NK cell percentages ($p=0.0076$, Spearman correlation, Appendix) while no association was found with the NK absolute count ($p=0.15$). Specifically, the correlation between NK cell percentages from week 2 and viral load ($p=0.04$) also was found. This shows that the magnitude of viraemia during reactivation acts to drive the size of the subsequent NK response within blood.

As discussed above, the proportion of NK cells within PBMC remained high within the first four weeks after reactivation and this is coincident with the period of high CMV virus load **(Fig. 4.3.5).** The viral load became virtually undetectable when the absolute NK count rose above 20/ml suggesting that this may represent a potential biomarker for effective control of viraemia. However, the NK cell count continued to rise during this period suggesting that even low levels of CMV load may be enough to stimulate the NK cell proliferation **(Fig. 4.3.5).**

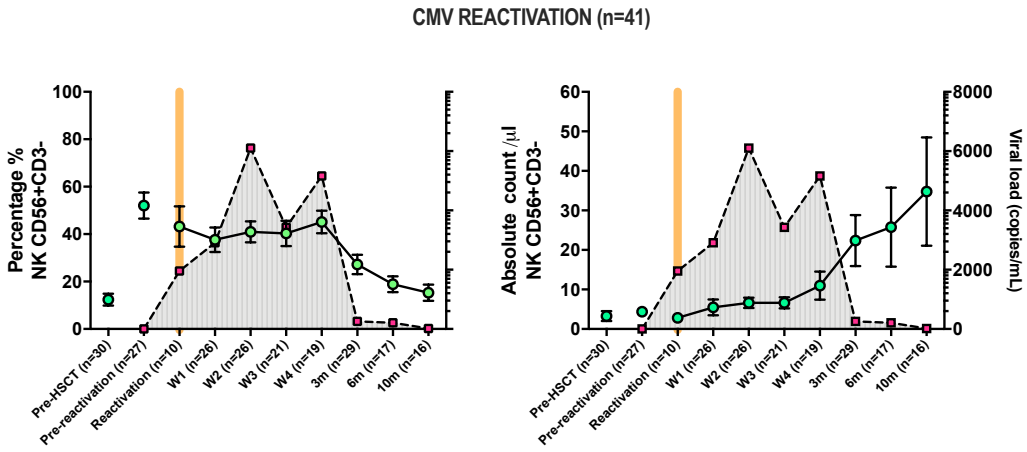


FIGURE 4.3.5. Temporal association between the number and percentage of peripheral NK cells and the pattern of CMV viral load in CMV reactivation patients. The mean value for detectable virus from week of reactivation in peripheral bloods is 1956±484 copies/ml (range; 228 to 18,994 copies/ml, n=41). [W: week(s), m: month(s) after CMV reactivation/allo-HSCT].

4.3.2.4. NK cells and viral loads in CMV risk group R+/D- with primary CMV infection

An important consideration at this point was that some transplant donors are already CMV seropositive at the time of donation and therefore in this situation CMV-specific lymphoid effector/memory cells would be infused into the patient at the time of stem cell donation. In contrast, some donors do not carry persistent CMV infection ('CMV seronegative') and so their immune cells are responding to CMV reactivation for the first time (as a primary immune response) when there is viral reactivation from the patient's cells. This difference could have a major impact on the profile of NK cell expansion at the time of viral reactivation.

As such the impact of CMV reactivation on NK reconstitution was next investigated in these two patient and donor group pairs which termed as R+/D+ and R+/D-. In R+/D- group the CMV positive patients received stem cells from individuals with 'CMV naïve' immune status.

Interestingly, any significant difference was not observed in either the proportion or number of NK cells after viral reactivation between these two groups **(Fig. 4.3.6).** However, the kinetics of NK expansion show that the percentage of NK cells was somewhat lower from W2 to W3 after reactivation in patients with primary CMV infection (R+/D-) but started to increase, and indeed overtake, the R+/D+ group after W4 **(Fig. 4.3.6).** In term of the total count of NK cells, there was little difference between these two groups until the total NK cell count was higher in the primary CMV infection (R+/D-) compared to the R+/D+ group at 10 months after reactivation.

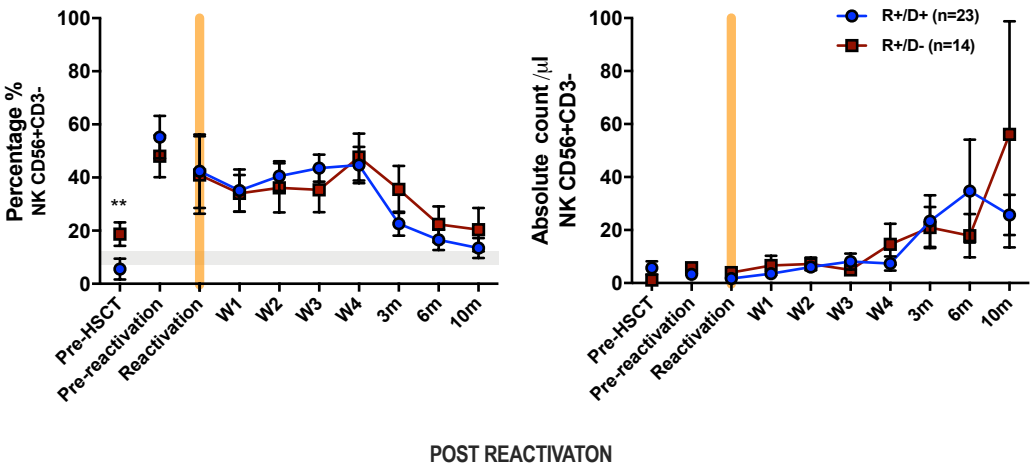


FIGURE 4.3.6. NK cell percentage and count following CMV reactivation in R+/D+ and R+/D- groups. No significant differences were observed between these two groups apart from the NK cells percentage prior to transplant. Grey line is the HD total NK cells range between CMV seronegative (7.3±0.9%) and CMV positive 12.2±7.3% [Mean±SEM]), no data available on HD absolute count. Analysis was done by Mann Whitney test (*p<0.05, **p<0.01, ***p<0.005). [W: week(s), m: month(s) after CMV reactivation/allo-HSCT].

Next, the kinetics and magnitude of the viral load following reactivation between the R+/D+ and R+/D- groups were compared. This was also related to both the NK cell percentage and absolute count **(Fig. 4.3.7).** Interestingly, the initial viral load at the time of CMV reactivation was markedly higher in R+/D+ patients, at 2350 ±810 copies/ml, compared to a value of 897±270 copies/ml in the R+/D- patients (p=0.05, Mann Whitney test). The reason for this is not clear but may potentially suggest that virus introduced into the patient within donor monocytic cells may contribute to viraemia. It is also possible that donor mediated CMV specific immunity acts, perhaps via induction of an inflammatory environment, to increase the initial viral load at the time of reactivation whilst subsequently proving able to bring this under control.

In contrast the peak viral load was considerably higher in the R+/D- cohort compared to R+/D+ patients, indicating a role for existing CMV-specific immunity in partially controlling this variable (**Fig. 4.3.7**). A further point of interest was that the profile of viral load in the R+/D- cohort demonstrated two separate peaks which occurred between weeks 2 and 4. Indeed the second peak of viral load was higher than the primary value. This was not seen in R+/D+ patients and suggests that the initial control of viral replication during a primary immune response, potentially mediated through NK cells, may need subsequent support from alternative arms of the immune system such as B or T cell adaptive responses.

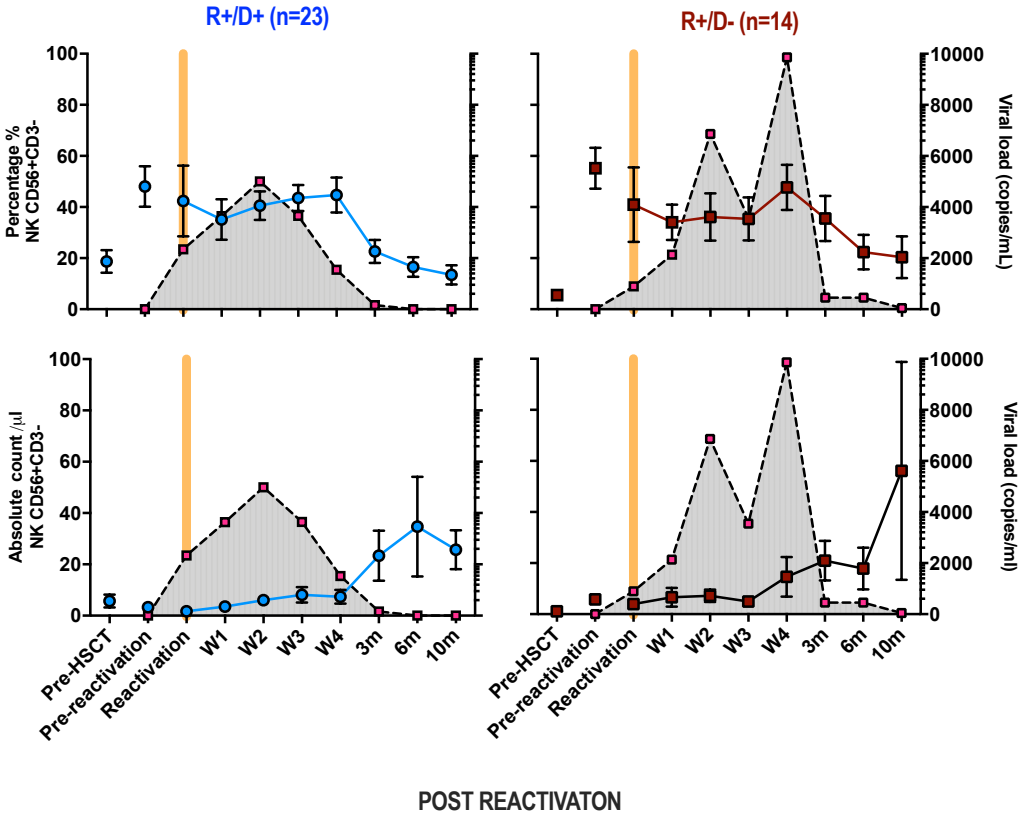


FIGURE 4.3.7. NK cells percentages and counts in R+/D+ and R+/D- groups associated with CMV viral loads. Mean value for detectable virus from week of reactivation in R+/D+ group is 2346±808 copies/ml (n=23) while in R+/D- group is 897±274 copies/ml (n=14). [W: week(s), m: month(s) after CMV reactivation/allo-HSCT].

4.3.2.5. The influence of recurrent episodes of CMV viraemia on NK cell reconstitution

The pattern of CMV viraemia after HSCT can be very variable and may be observed as a single event that is subsequently well controlled, primary uncontrolled viraemia or recurrent episodes. 19 of the patients in this study underwent two or more episodes of viraemia whilst 22 experienced only a single reactivation (n=22).

Interestingly, there was no significant difference in the proportion or total count of NK cells between these two groups **(Fig. 4.3.8)** although a trend was observed towards an increased proportion of NK cells from W3 to 3 months after reactivation in patients with single viral episode compared to those with multiple episodes.

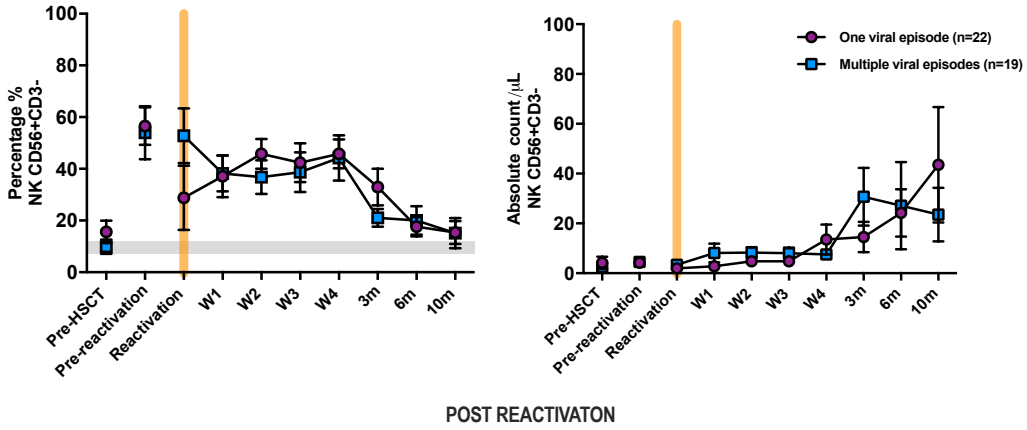


FIGURE 4.3.8. NK cell percentage and absolute count in patients who underwent CMV reactivation divided into those that had a single or multiple episode of viraemia. Grey line is the HD total NK cells range between CMV seronegative (7.3±0.9%) and CMV positive 12.2±7.3% [Mean±SEM]). No data was available on HD absolute count. Analysis was done by Mann Whitney test (*p<0.05, **p<0.01, ***p<0.005). [W: week(s), m: month(s) after CMV reactivation/allo-HSCT].

4.3.3. Reconstitution of different subsets of NK cells following CMV reactivation after allogeneic HSCT

4.3.3.1. NK cell subsets in healthy donors

Classically, NK cells are identified as two major populations: $CD56^{dim}CD16^{bright}$ and $CD56^{bright}CD16^{negative}$. CD16 is the FcγRIII molecule whilst CD56 is involved in homotypic adhesion. $CD56^{dim}$ is expressed on approximately 90% of NK cells while the $CD56^{bright}$ subpopulation represents around 10% of cells in HDs. However, it is now clear that the composition of NK cells is much more complicated than previously thought. Indeed, the relative expression of CD56 and CD16 can separate NK cells into four groups: $CD56^{dim}$ $CD16^{bright,}$ $CD56^{dim}$ $CD16^{negative}$, $CD56^{bright}$ $CD16^{bright}$ and $CD56^{bright}$ $CD16^{negative}$. Several reports have shown that these four groups are functionally different and as such it was of interest to study their reconstitution after HSCT and the potential relationship to CMV reactivation.

To set the baseline, the composition of these four groups was studied initially within HD. This showed that approximately 80% of NK cells in HD express the $CD56^{dim}CD16^{bright}$ (77.6±1.9% [Mean±SEM]) phenotype which is considered as a marker of mature and cytotoxic NK cells (Amand et al., 2017) **(Fig. 4.3.9).** This was followed by other NK cells subsets; $CD56^{dim}CD16^{negative}$ at 12.2±1.6%, $CD56^{bright}CD16^{negative}$ at 7.7±0.9% and $CD56^{bright}CD16^{bright}$ at only 2.4±0.3% of the NK population. After this study with HDs, the exact same gating strategies were then applied to HSCT patients, with or without CMV reactivation.

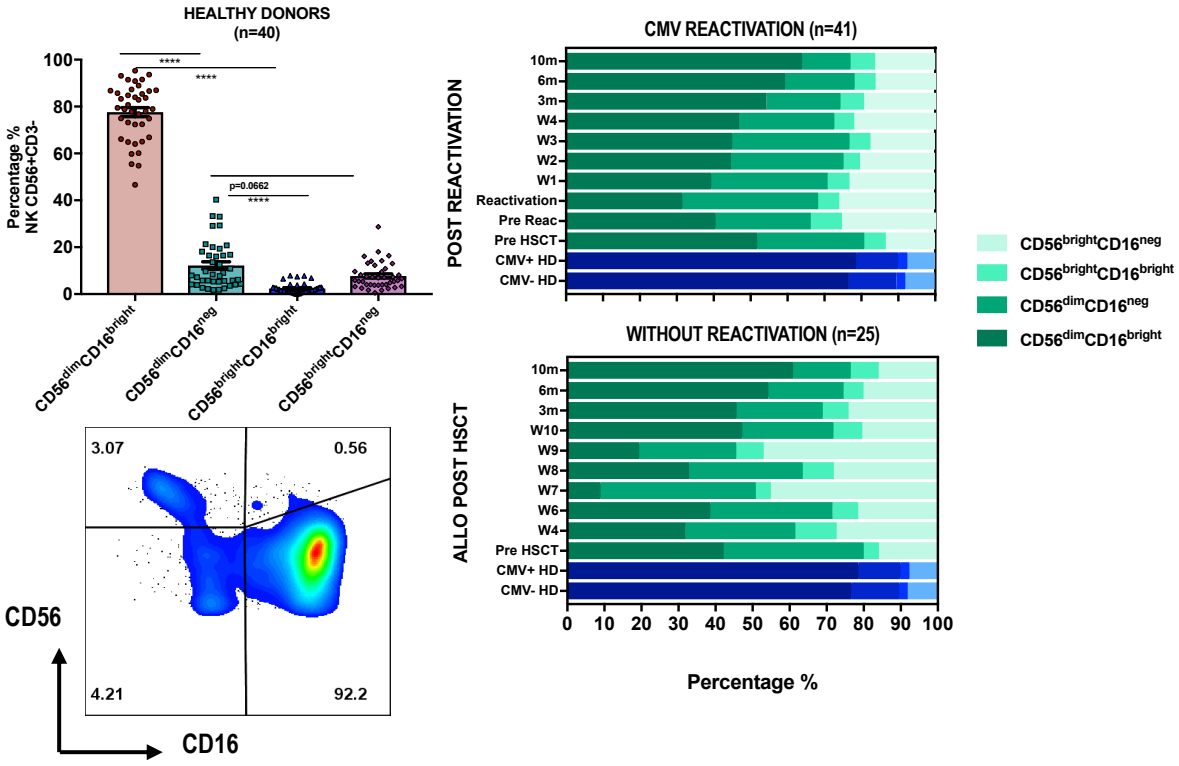


FIGURE 4.3.9. General comparison of NK cell subsets in healthy donors, CMV reactivation and without reactivation allogeneic HSCT. Majority of HD NK cells are comprised of $CD56^{dim}CD16^{bright}$ (77.6±1.9% [Mean±SEM]), while $CD56^{dim}CD16^{neg}$ constitute about 12.2±1.6%, $CD56^{bright}CD16^{bright}$: 2.4±0.3% and $CD56^{bright}CD16^{neg}$: 7.7±0.9%. Total NK cells gated from lymphocytes constitute about 9.8±1.3% in HDs (n=39). No differences in NK subsets in CMV negative (n=20) and CMV positive HDs (n=20), and in patients with reactivation and without reactivation. Analysis was done by Wilcoxon sign rank test and Mann Whitney test. (*p<0.05, **p<0.01, ***p<0.005). [W: week(s), m: month(s) after CMV reactivation/allo-HSCT].

4.3.3.2. Evaluation of specific NK cell subsets in allo-HSCT patients with CMV reactivation and without reactivation

4.3.3.2.1. $CD56^{dim}CD16^{bright}$

This NK subset is by far the dominant NK subset in HDs and no differences were seen between CMV seronegative HDs (77%±2.4%, n=20) and seropositive individuals (78.6±3.0%, n=20) (p=0.4135, Mann Whitney test) **(Fig. 4.3.10).** Following allo-HSCT this population was generally decreased compared with HDs, in both CMV reactivation and non-reactivation patients, particularly before HSCT and in the early post-transplant period. This could reflect the conditioning treatment given to the patients prior to transplant. However, this NK subset did start to expand from W3 after HCMV reactivation (p=0.0112, Mann Whitney test) and increased further thereafter **(Fig. 4.3.11).**

Interestingly, the percentage of this $CD56^{dim}CD16^{bright}$ cytotoxic population is always higher in the CMV reactivation group compared with the non-reactivation group, and this was most pronounced at W3 after reactivation (p=0.0112, Mann Whitney test). This indicates a likely role for CMV reactivation in driving reconstitution of this subpopulation. Indeed, in CMV reactivation patients this $CD56^{dim}CD16^{bright}$ population doubled from 32% (±6.2%) at the time of viral reactivation to 64% (±5.4%) after 10 months (**Fig. 4.3.10**, p=0.0312, Wilcoxon sign rank test), whilst the expansion in non-reactivation patients occurred only at late time points and was less marked.

4.3.3.2.2. $CD56^{dim}CD16^{negative}$

The $CD56^{dim}$ and $CD16^{negative}$ NK population was the second largest NK subset in HDs and no differences were seen between CMV seropositive and seronegative HDs (**Fig. 4.3.10,** p=0.29, Mann Whitney test). Interestingly a big increase of this population was seen after HSCT in both the CMV reactivation and 'non-reactivation' patients. Indeed, at the time of reactivation, or at W6 in the time point-matched non-reactivation patients, this population represents nearly 40% of whole NK population. After this highpoint the population starts to decrease in both groups and is almost the same as HDs by the time of 10 months **(Fig. 4.3.10).** No significant changes were seen when the $CD56^{dim}CD16^{negative}$ population was compared between reactivation or 'non-reactivation' patients **(Fig. 4.3.11).**

4.3.3.2.3. $CD56^{bright}CD16^{bright}$

The proportion of $CD56^{bright}CD16^{bright}$ NK cells is the lowest of the NK cell subsets and barely detectable within HDs (2.4±0.3%, n=40) **(Fig. 4.3.10).** This population was slightly higher within HSCT patients compared to HDs at the pre-HSCT, pre-reactivation and W1 and W2 after CMV reactivation/matched time points **(Fig. 4.3.11).** Similar percentages of $CD56^{bright}CD16^{bright}$ cells were seen within patients with CMV reactivation and without reactivation **(Fig. 4.3.10** and **Fig. 4.3.11).**

4.3.3.2.4. $CD56^{bright}CD16^{negative}$

The last subset of NK cells to consider was the $CD56^{bright}CD16^{negative}$ population, which is thought to represent non-cytotoxic and cytokine-producing NK cells. Overall this population was higher in the HSCT patients compared with HDs, independent of CMV reactivation. In both patient groups there is also an expansion of this population after HSCT compared with pre-HSCT, which demonstrates that expansion is due to NK reconstitution **(Fig. 4.3.11).** There was a trend towards a lower subset of these cells in the CMV-reactivation group compared with 'non-reactivation' patients in the early time points after reactivation, particularly at week 1 and week 3 **(Fig. 4.3.11).** Of note, the $CD56^{bright}CD16^{negative}$ NK cells that circulate after allo-HSCT are believed to be early differentiated subsets of NK cells that have originated from the bone marrow.

Combined with the previous observation that the $CD56^{dim}CD16^{bright}$ population is higher after CMV reactivation, these finding demonstrate that CMV acts to drive an increased cytotoxic profile of peripheral NK cells.

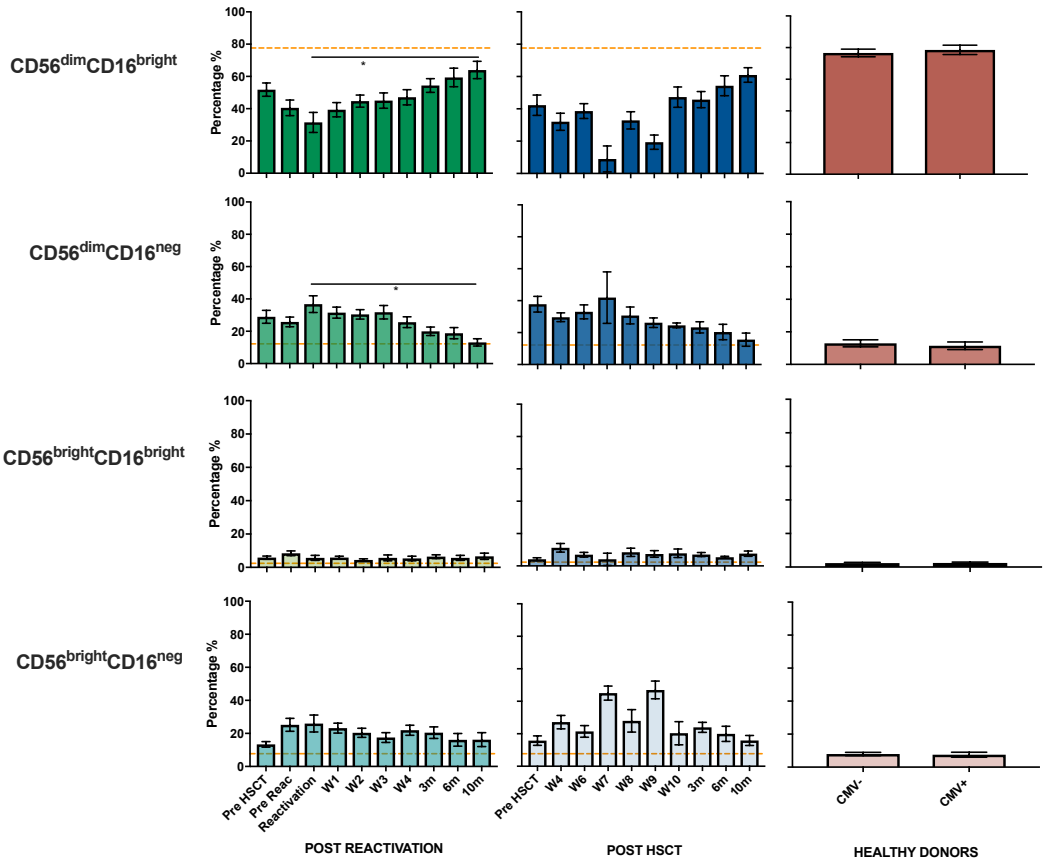


FIGURE 4.3.10. NK cell subsets in healthy donors and in HSCT patients at various time points after CMV reactivation and in matched time points in patients without reactivation. Orange dotted lines represent the average percentage of NK subsets in HDs: $CD56^{dim}CD16^{bright}$ (77.6±1.9% [Mean±SEM]), $CD56^{dim}CD16^{negative}$ (12.2±1.6%) $CD56^{bright}CD16^{bright}$ (2.4±0.3%) and $CD56^{bright}CD16^{negative}$ (7.7±0.9%). No differences in NK subsets in CMV negative (n=20) and CMV positive HDs (n=20). Analysis was done by Wilcoxon sign rank test and Mann Whitney test (*p<0.05, **p<0.01, ***p<0.005). [W: week(s), m: month(s) after CMV reactivation/allo-HSCT].

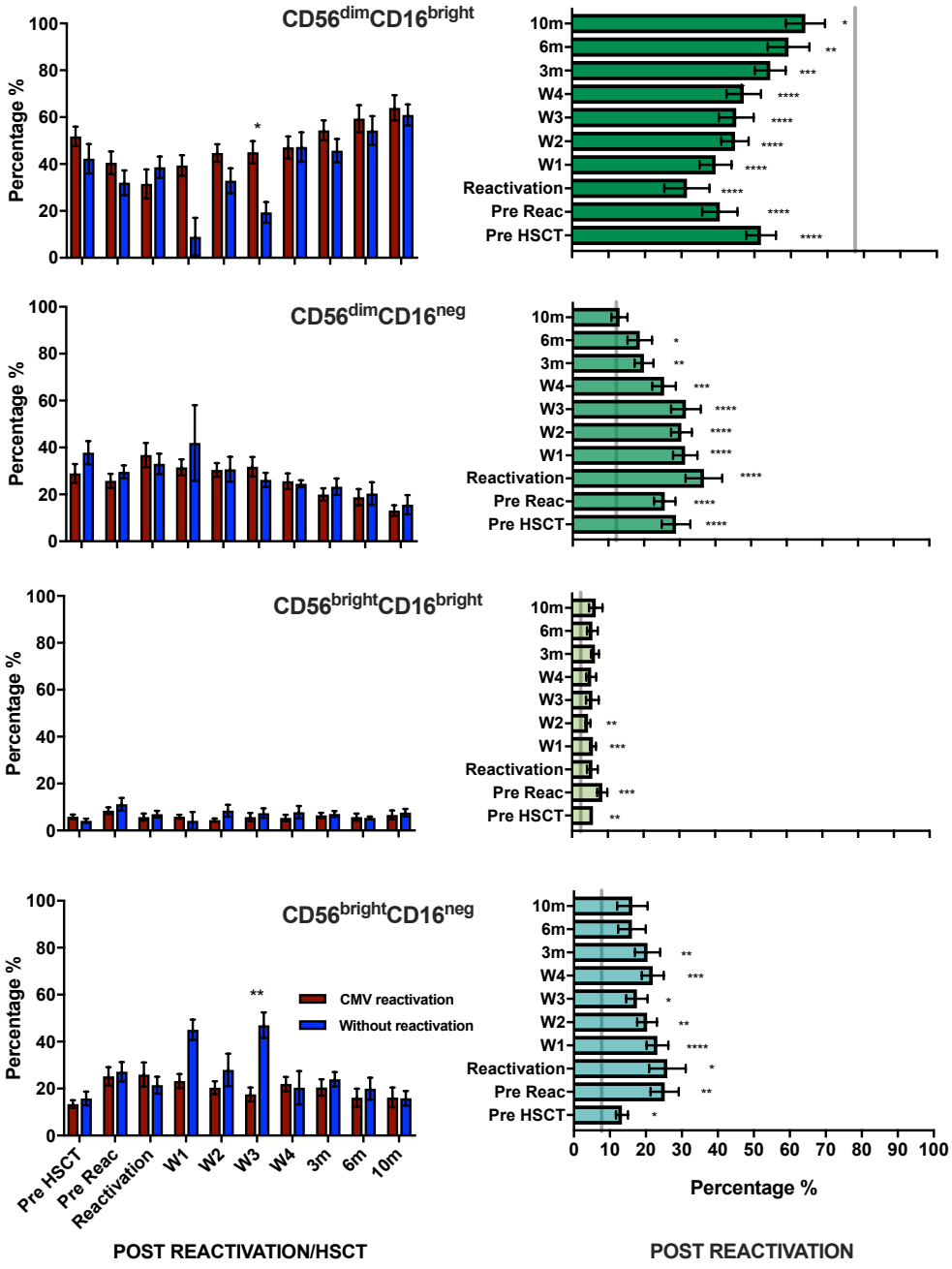


FIGURE 4.3.11. Comparison of NK cell subsets following allogeneic post HSCT and in relation to CMV reactivation or 'non-reactivation' as well as in healthy donors. Grey lines (right) represent the percentage of subsets in HDs: $CD56^{dim}CD16^{bright}$ (77.6±1.9% [Mean±SEM]), $CD56^{dim}CD16^{negative}$ (12.2±1.6%) $CD56^{bright}CD16^{bright}$ (2.4±0.3%) and $CD56^{bright}CD16^{negative}$ (7.7±0.9%). No differences in NK subsets in CMV negative (n=20) and CMV positive HDs were seen (n=20). Comparisons on the right were made between CMV reactivation allo-HSCT and HDs. Analysis was done by Mann Whitney test (*p<0.05, **p<0.01, ***p<0.005). [W: week(s), m: month(s) after CMV reactivation/allo-HSCT].

4.3.4. The pattern of expression of activating NKG2C$^+$ and inhibiting NKG2A$^+$ receptors on NK cells in relation to CMV reactivation after allo- HSCT

4.3.4.3. Flow cytometric analysis of NKG2C-positive NK cells

Both the NKG2C and NKG2A receptors are able to form a heterodimer with CD94. NKG2C is normally believed to be an activating receptor and is expressed on a highly differentiated NK population. In contrast, NKG2A is a largely inhibitory receptor and acts as a marker of more immature NK cells. CD94/NKG2C and CD94/NKG2A both belong to the CD94/NKG2 family although, unlike other NKG2 molecules, NKG2D does not form a heterodimer with CD94 (Lian et al., 2002). NKG2C$^+$ NK cells represent a 'memory' like NK cell that is known to be expanded following CMV infection and also known as the maturation marker (Nerreter et al., 2017). The subset has been studied quite extensively within HDs, and following allo-HSCT, although any studies that investigate this cell in the immediate period after viral reactivation is not aware of. A multistep gating approach was used to identify this population **(Fig. 4.3.1, Fig. 4.3.12** and to characterise the NKG2C$^+$NKG2A$^-$ and NKG2C$^-$NKG2A$^+$ populations. NKG2C$^+$NKG2A$^-$ and NKG2C$^-$NKG2A$^+$ NK cells were gated by flow cytometry from within the main NK subset and also the mature and cytotoxic CD56^{dim}CD16^{bright} subset.

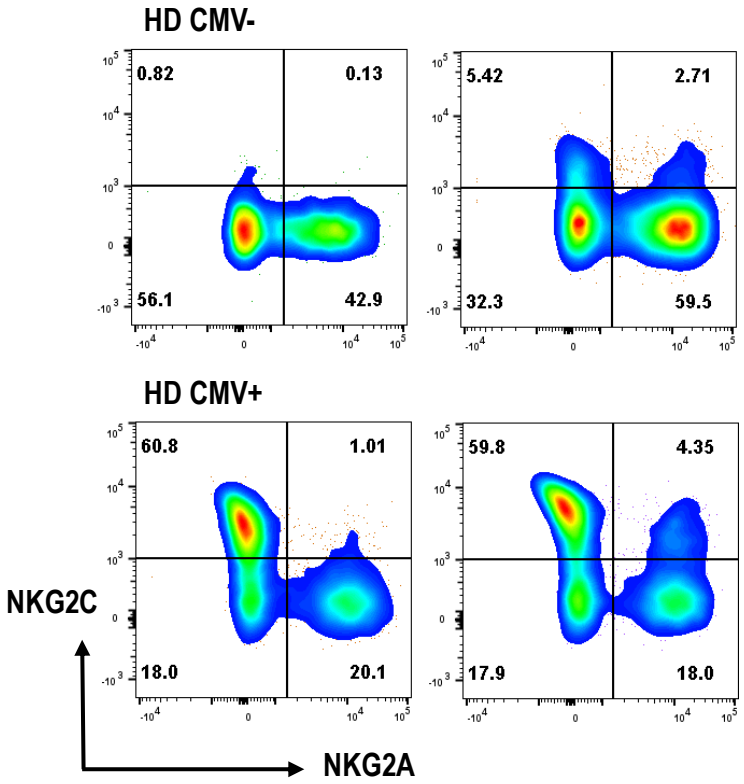


FIGURE 4.3.12. NKG2C and NKG2A gating strategies. NKG2C^{+} cells were gated from the major subset of NK cells and the CD56^{dim}CD16^{bright} subsets from CMV seropositive and seronegative HDs, and also patients subdivided by CMV reactivation or 'non-reactivation' allo-HSCT.

4.3.4.4. The proportion of $CD56^{dim}CD16^{bright}$ $NKG2C^+$ cells is increased in CMV seropositive healthy donors

In HDs the average percentage of $NKG2C^+$ cells within the mature $CD56^{dim}CD16^{bright}$ population from CMV seronegative and seropositive HDs was 1.4% (±0.2) and 10.9% (±3.5%) respectively ($p<0.0001$, Mann Whitney test). Meanwhile, $NKG2A^+$ cells gated from the same NK subset constituted 50% (±2.6%) and 40% (±3.2%) respectively (**Fig. 4.3.13,** $p=0.0065$, Mann Whitney test). This confirms a previous body of information that CMV infection increases the proportion of circulating $NKG2C^+NKG2A^-$ NK cells with an associated decrease in the $NKG2C^-NKG2A^+$ pool.

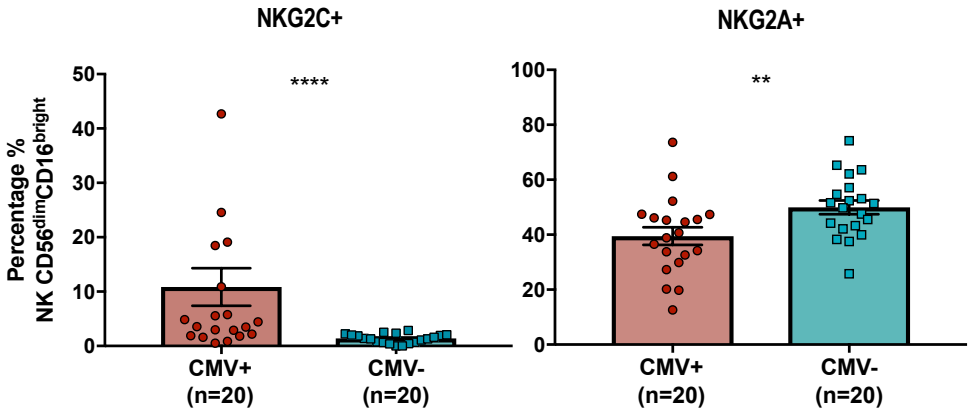


FIGURE 4.3.13. $NKG2C^+$ and $NKG2A^+$ NK cells within the $CD56^{dim}CD16^{bright}$ subset in healthy donors according to CMV serostatus. Significant changes in the proportion of $NKG2C^+$ cells in CMV seropositive (1.4±0.2 to 10.9±3.5% [Mean±SEM]) and CMV seronegative (50.0±2.6 to 39.5±3.2%) donors were observed. Analysis was done by Mann Whitney test (*$p<0.05$, **$p<0.01$, ***$p<0.005$).

4.3.4.5. Expansion of NKG2C^{+} and decrease in NKG2A^{+} cells within CD56^{dim}CD16^{bright} NK cell subset following CMV reactivation in patients after allo-HSCT

Having established the proportion of NKG2A and NKG2C expression in CMV seropositive and seronegative HDs, HSCT patients were next studied. Blood samples were taken at the same time points as previous analyses, including pre-HSCT, pre-reactivation, reactivation point, weeks 1, 2, 3 and 4 post reactivation and at month 3, 6 10 after reactivation. Equivalent time points from the 'non-reactivation' group were also identified, as mentioned before.

At the pre-HSCT, pre-reactivation and CMV-reactivation/matched time points the percentage of NKG2C^{+} NK cells were the same as in CMV seropositive HDs in both CMV reactivation and non-reactivation groups **(Fig. 4.3.14).** However, interestingly, a rapid expansion of the NKG2C^{+}CD56^{dim}CD16^{brigh} NK subset was seen in the immediate post-reactivation period which can be seen as early as day 7 after viral reactivation **(Fig. 4.3.14).** As such a marked increase in this cell subset could be seen as a potential biomarker for CMV reactivation. Furthermore, the NKG2C^{+} NK population continued to expand even after the CMV reactivation had been cleared. Indeed, at 10 months after initial reactivation the NKG2C^{+} cell proportion had increased to represent up to 36% of the total NK cell pool, which is far higher than the normal range in CMV seropositive HDs (grey shades) **(Fig. 4.3.14).** This relentless increase of NKG2C^{+} NK cells over 10 months could represent a clonal expansion from NK cells that are activated at the time of

reactivation or may imply that there is low level and subclinical ongoing CMV reactivation after the initial episode.

The NKG2C^{+}CD56^{dim}CD16^{bright} NK subset also expanded post-HSCT in patients who did not suffer an episode of CMV reactivation. This was observed from month 3 to month 10 after transplant but to nowhere near the scale that was observed in patients that had undergone an episode of CMV reactivation. In fact, the proportion of these cells within this 'no-reactivation' group remained the same as that seen within CMV seropositive HDs. This further confirms that the big expansions that had been detected after CMV reactivation are driven directly by that episode **(Fig. 4.3.14).** Despite the overall increase in the proportion of NKG2C^{+} NK cells, a small and non-significant decrease was observed between 21 and 28 days after CMV reactivation **(Fig. 4.3.14).**

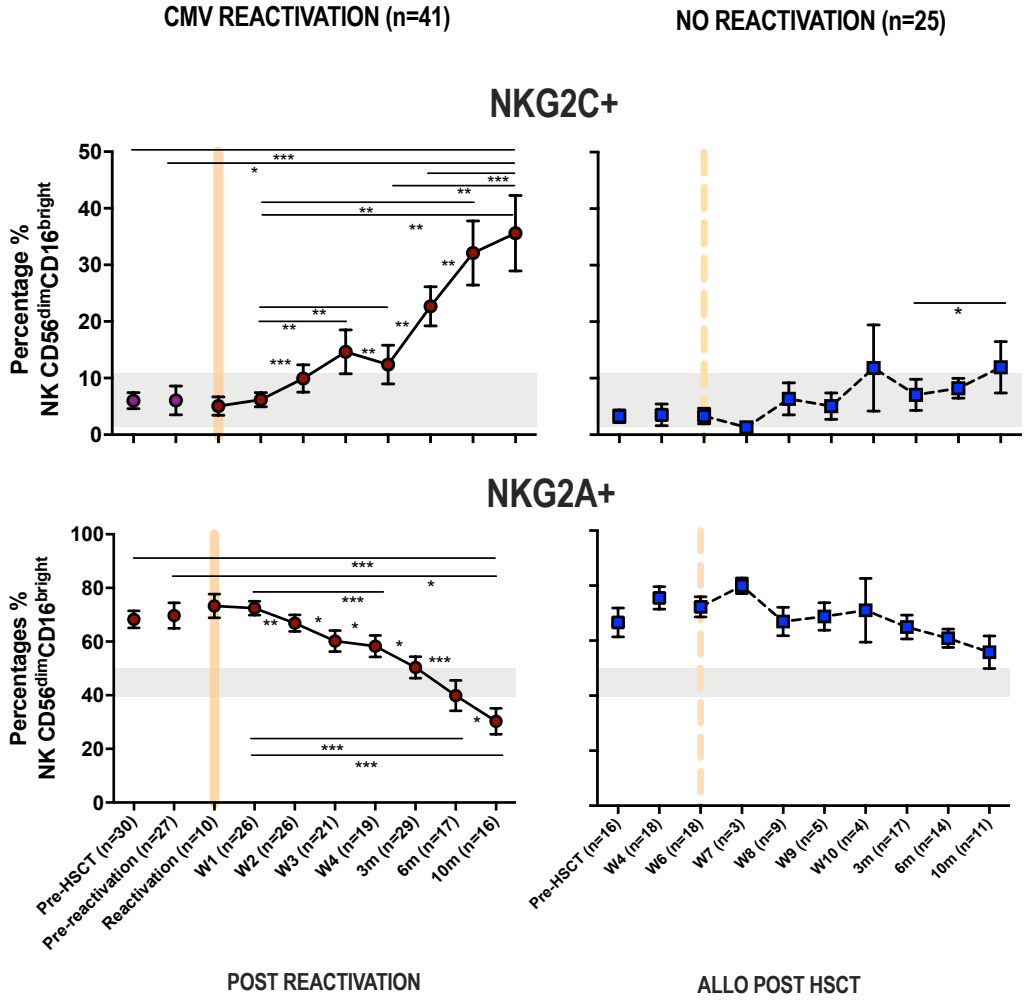


FIGURE 4.3.14. The proportion of NKG2C$^+$ and NKG2A$^+$ NK cells within the CD56^{dim}CD16^{bright} population in HSCT patients with CMV reactivation (left) or without reactivation (right). Grey lines represent the range of NKG2C$^+$ cells in CMV seropositive or seronegative HDs (10.9 ±3.5% vs 1.4 ±0.2% [Mean±SEM]) and also the NKG2A$^+$ subset (40 ±3.2% vs 50 ±2.6% respectively). *Statistical analysis was done by Wilcoxon sign rank test for matched time points (*p<0.05, **p<0.01, ***p<0.005). [W: week(s), m: month(s) after CMV reactivation/allo-HSCT].

The expression of NKG2A and NKG2C appears to be largely mutually exclusive on NK cells (Bigley et al., 2016) although a few double positive cells were seen in the HSCT patients **(Fig. 4.3.12).** The proportion of NKG2A$^+$ cells in HSCT patients was far above the range seen in HDs (grey line) until the latest time point of examination at 10 months after HSCT. This is likely to reflect a significant increase

in immature NKG2A$^+$ NK cells during the natural period of NK reconstitution after transplantation. CMV reactivation acts to accelerate the process of NK cell maturation, and the proportion of NKG2A$^+$ cells decreased by almost 5% between day 7 and day 14 alone (from 72 to 67%), before continuing to drop to a level of around 30% at month 10, below that seen in HDs **(Fig. 4.3.14).**

4.3.4.6. The ratio of NKG2C$^+$ and NKG2A$^+$ cells on CD56^{dim}CD16^{bright} in CMV reactivation patients

As the data had shown an apparently reciprocal relationship between the proportion of NKG2C$^+$ and NKG2A$^+$ NK cells, NKG2C$^+$/NKG2A$^+$ NK cell ratio at different time points were next compared. In CMV seronegative HDs the NKG2C$^+$: NKG2A$^+$ ratio is very small (0.03:1) compared to that in seropositive HDs (0.3:1) **(Fig. 4.3.15).** At the time of initial CMV reactivation this ratio remained at 0.1:1 from the pre-HSCT baseline up until W2 after reactivation. However, from W3 to 3 months after reactivation the ratio started to increase to 0.2—0.5:1 and was comparable with the value seen in CMV seropositive HDs. Moreover, at 10 months the NKG2C$^+$ cell percentage became larger than the NKG2A$^+$ cell subset such that the ratio reached 1.2:1.

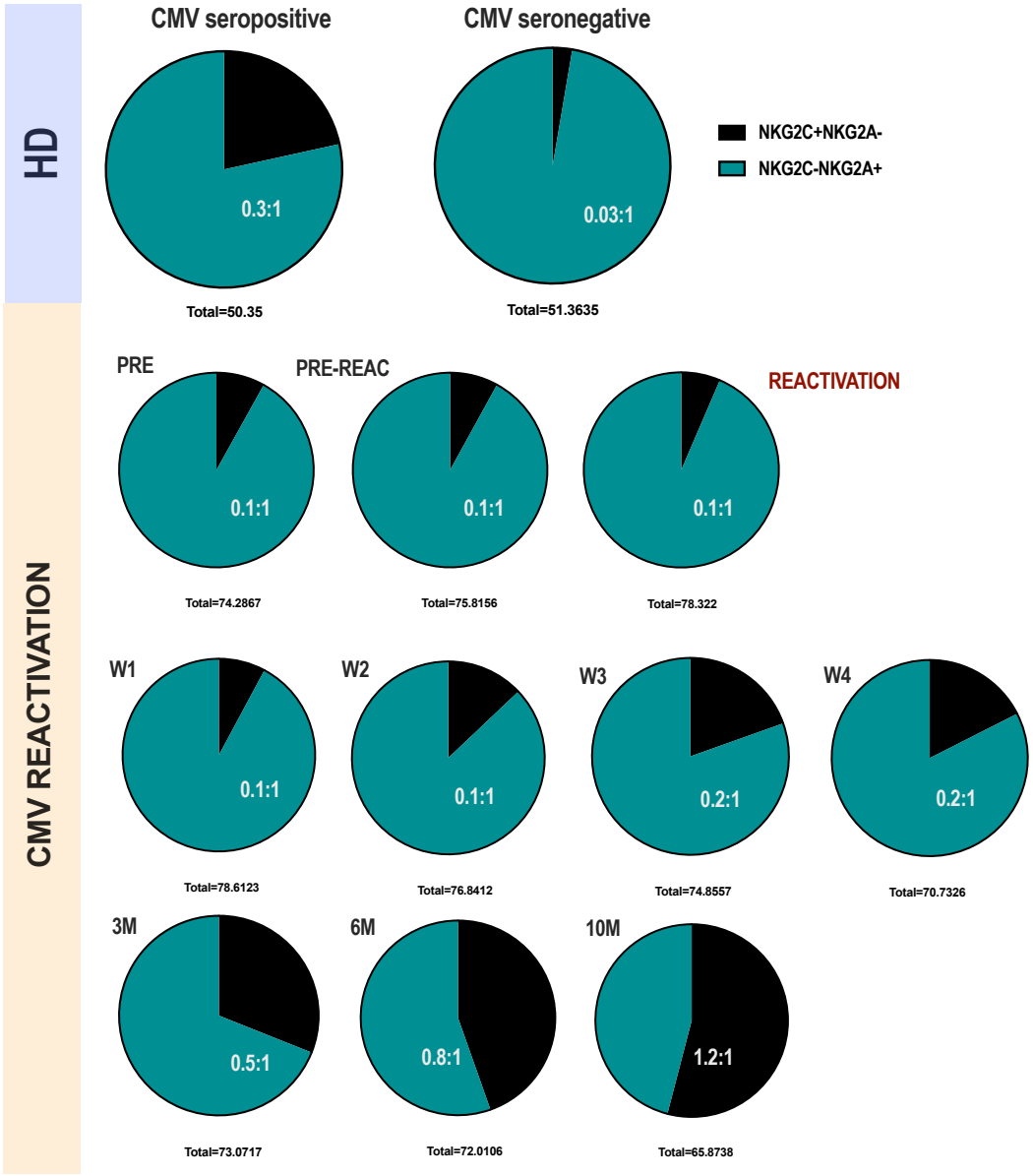


FIGURE 4.3.15. The ratio of NKG2C^{+} and NKG2A^{+} NK cells within the CD56^{dim}CD16^{bright} NK cell population in HSCT patients with CMV reactivation and in healthy donors.

4.3.4.7. NKG2C^{+} and –NKG2A^{+} NK cells in different subsets of NK cells in CMV reactivation allo-HSCT

The analysis of NKG2C and NKG2A expression described above was based solely on the numerically dominant cytotoxic CD56^{dim} CD16^{bright} NK subset. However, this study was repeated within the other three subsets of NK cells.

As such the profile of NKG2C and NKG2A expression on the CD56^{dim}CD16^{negative}, CD56^{bright}CD16^{bright} and CD56^{bright}CD16^{negative} NK cell subsets and the proportion of positive cells was compared with HDs was next examined **(Fig. 4.3.16** and **4.3.17).** Interestingly, the expression of NKG2C^{+} increased on all four different subsets within 2 weeks of viral reactivation with a substantial expansion observed at later time points from 3 to 10 months **(Fig. 4.3.16).** The magnitude of NKG2C expression was 3-4-fold higher on the two CD56^{dim} NK subsets, believed to represent the mature NK population, compared to the CD56^{bright} populations.

Simultaneous with the increase in NKG2C^{+} cells, a coordinate loss of NKG2A^{+} cells were also observed from all four different NK subsets **(Fig. 4.3.17).** The time course of this change closely mirrored that of NKG2C expansion, with initial changes being observed within 2 weeks but that a marked decline from months 3 to 10. Again, these changes were most marked within the CD56^{dim} population.

These comparable changes in activating NKG2C^{+} and inhibiting NKG2A^{+} cells from different NK subsets are notable and never been described in previous studies, particularly within these early periods following viral reactivation.

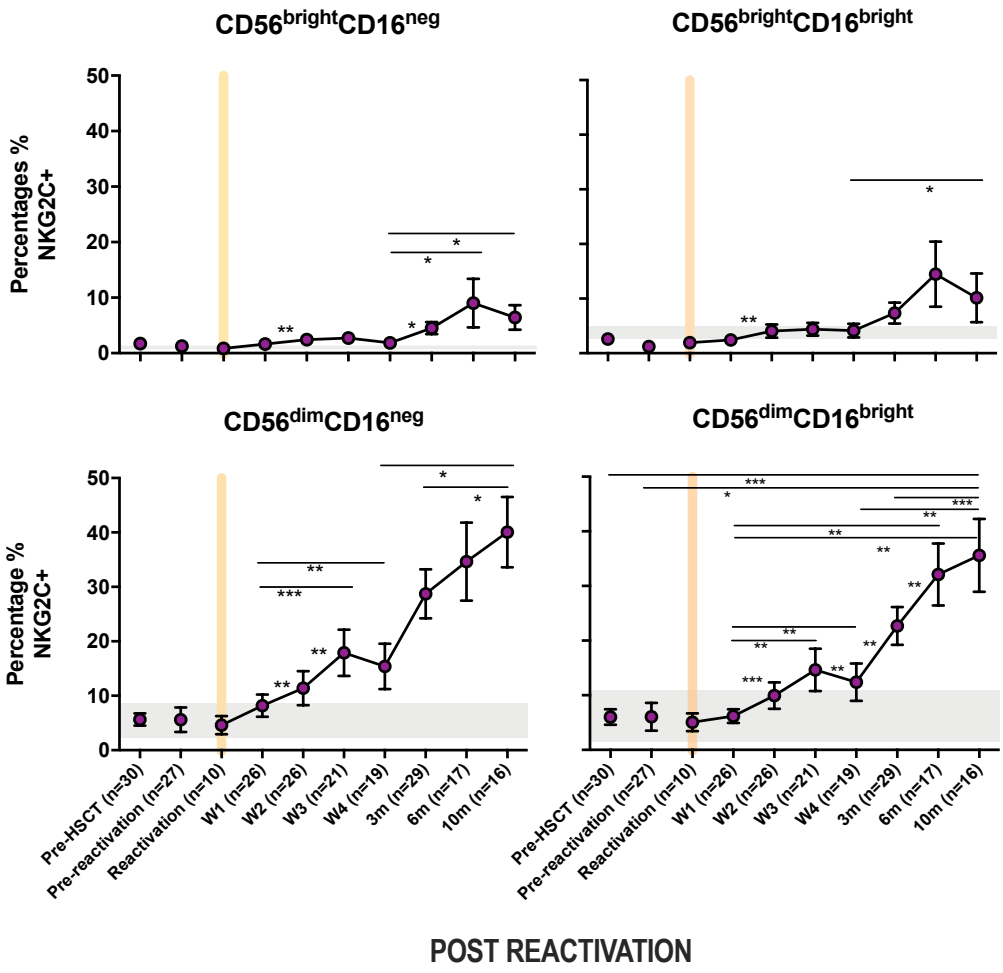


FIGURE 4.3.16. Expression of NKG2C on different NK cell subsets, defined according to their profile of CD56 and CD16, in patients with viral reactivation. Range of NKG2C^{+} NK cells from CMV seronegative to CMV seropositive HDs are from 2.2 ±0.4% (Mean±SEM) to 8.5 ±2.0% for CD56^{dim}CD16^{negative} (*p=0.0012), 2.7 ±0.7% to 5.0 ±1.7% in CD56^{bright}CD16^{bright} (p=0.28) and 0.9 ±0.2% to 1.1 ±0.3% in CD15^{bright}CD16^{negative} (p=0.70).*Statistical analysis was done by Wilcoxon sign rank test for matched time points (*p<0.05, **p<0.01, ***p<0.005).

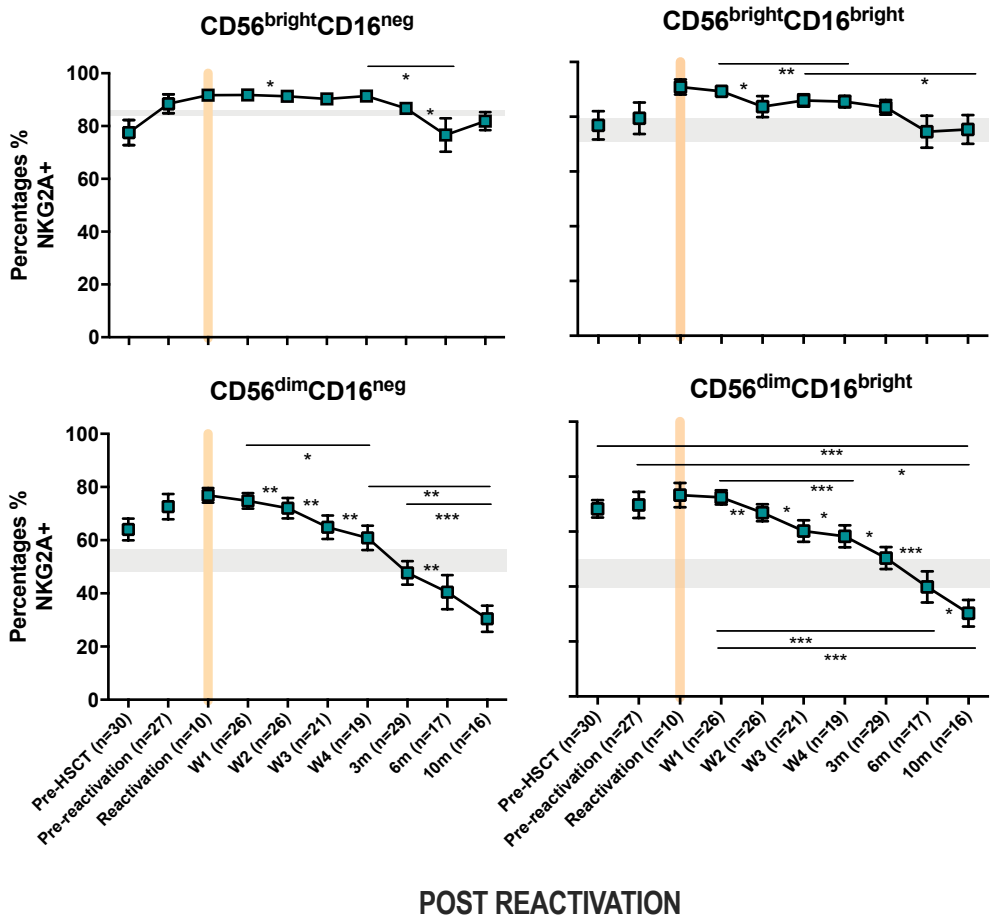


FIGURE 4.3.17. Expression of NKG2A on different NK cell subsets, defined according to their profile of CD56 and CD16, in patients with viral reactivation. Range of NKG2A^{+} NK cells from CMV seronegative to CMV seropositive HDs are from 56.4 ±2.9% (Mean±SEM) to 47.9 ±2.6% for CD56^{dim}CD16^{negative} (*p=0.0460), 79.5 ±1.9% to 70.9 ±4.8% in CD56^{bright}CD16^{bright} (p=0.3107) and 85.9 ±1.0% to 83.7 ±2.0% in CD15^{bright}CD16^{negative} (p=0.4491).*Statistical analysis was done by Wilcoxon sign rank test for matched time points (*p<0.05, **p<0.01, ***p<0.005). [W: week(s), m: month(s) after CMV reactivation/allo-HSCT].

4.3.4.8. Comparison of NKG2C$^+$ and NKG2A$^+$ expression on NK cells in relation to CMV reactivation and CMV risk group

The point to point comparison between CMV reactivation and no reactivation groups have been analysed in similar graphs for both NKG2C$^+$ and NKG2A$^+$ CD56^{dim}CD16^{bright} NK cells **(Fig. 4.3.18).** When compared with patients without reactivation, the significant expansion of NKG2C$^+$ NK cells is also prominent even from the first to second week after CMV reactivation. Then the striking expansion of NKG2C$^+$ NK cells also can be seen starting from 3 months until after 10 months observation period **(Fig. 4.3.18).** On the other hand, the NKG2A loss works in a delayed manner, and no changes in the proportion can be seen from the first week for NKG2A$^+$ NK cells, but was observed from 3 months to 10 months reactivation period.

The CMV risk group R+/D- reflects an episode of primary CMV reactivation as the transplant donor does not have CMV-specific immune memory. The proportion of NKG2C$^+$ NK cells was somewhat lower during the first 4 weeks after reactivation in R+/D- patients which suggests that NKG2C$^+$ 'memory-like' NK cells are transferrable from donor to recipient. Reciprocal changes were observed for NKG2A$^+$ NK cells which were consistently higher in R+/D- patients from the point of reactivation until 6 months thereafter. This data suggests that the kinetics of decrease of NKG2A expression is slower than R+/D- group.

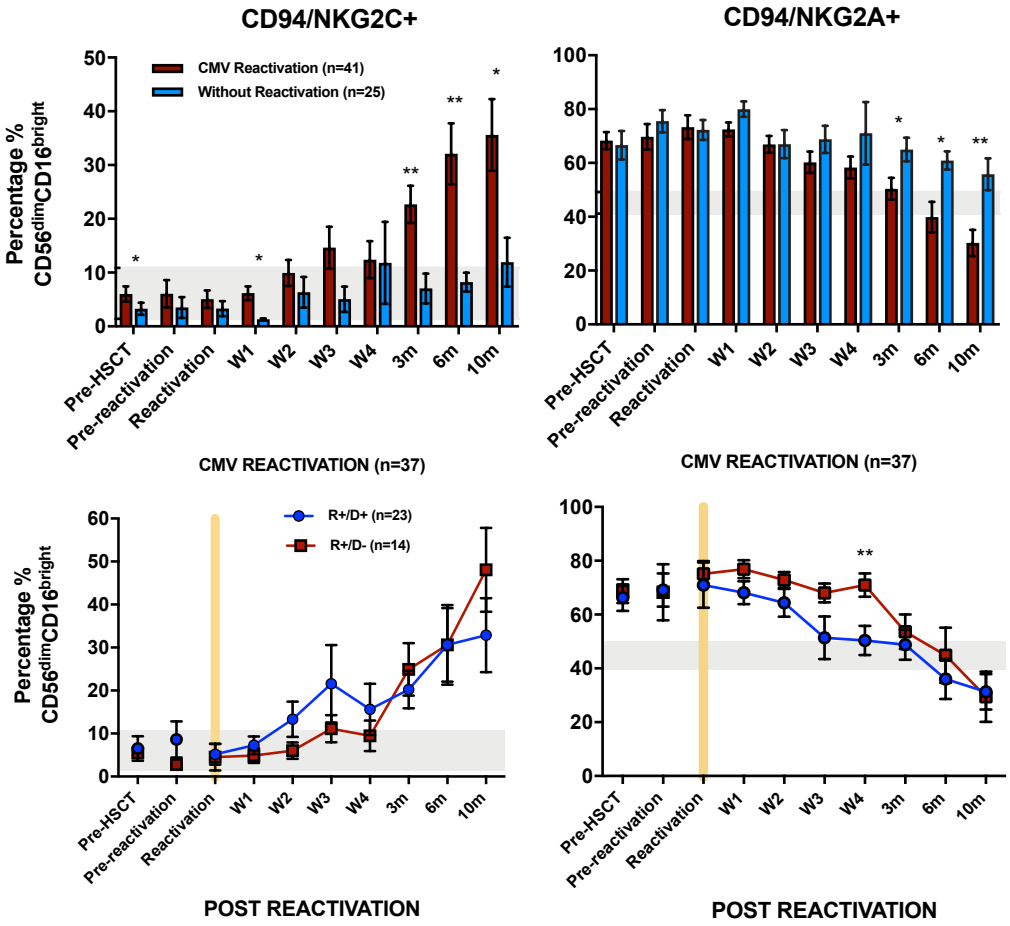


FIGURE 4.3.18. NKG2C$^+$ and NKG2A$^+$ NK cells comparison with patients without reactivation and donors' serostatus (R+/D+ and R+/D-). Changes in the proportion on NKG2C$^+$ NK cells can be seen from first four weeks (not statistically significant). However, significant changes can be seen on NKG2A$^+$ NK cells' proportion from W4 after reactivation or allo-HSCT. Dotted lines showing the ranges of NKG2C$^+$ on HDs (CMV- 1.4 ±0.2%, n=20 CMV+ 10.9 ±3.5%, n=20) NKG2A$^+$ (CMV+ 39.5 ±3.2%, n=20 CMV- 49.9 ±2.5%, n=20). *Data was analysed with Mann Whitney test. (*p<0.05, **p<0.01, ***p<0.005). [W: week(s), m: month(s) after CMV reactivation/allo-HSCT].

4.3.5. Examination of the extended phenotype of NK cells in patients following allo-HSCT and the impact of CMV reactivation

4.3.5.1. The pattern of CD57, KIR, PD-1 and KLRG1 expression on NK cells

In order to understand more about the biology of NK subsets after HSCT, and the impact of viral reactivation, the pattern of expression of a range of membrane proteins was next examined.

Four different surface proteins were chosen to be studied. CD57 is a marker of mature NK cells, KIR proteins are major regulators of NK cell activity, PD-1 is a strong inhibitory 'checkpoint' protein and KLRG1 has been associated with relative senescence. $CD57^{+}$ and several inhibitory and activating KIR^{+} phenotypes have been used previously to distinguish NK 'memory-like' cells that have been observed in CMV seropositive HDs and in various transplant settings (Foley et al., 2012a, 2012b; Cichocki et al., 2016). However, no studies have previously elaborated the potential importance of PD-1 or KLRG1 in this setting. This study further takes the advantage of this cohort of HSCT patients with CMV reactivation and the very early time points after reactivation. All data was analysed on the major cytotoxic $CD56^{dim}CD16^{bright}$ NK subset and KIR expression was analysed using different KIR-specific antibodies that identify both activating and inhibitory receptors. **Fig. 4.3.19** shows examples of the expression pattern of these four molecules in different settings, including HD and HSCT patients.

The initial analysis focused on the pattern of CD57 expression. No changes were seen in the percentage of $CD57^+$ NK cells between CMV seronegative and seropositive HDs ($CD57^+$: 56 ±3.1% to 63 ±4.4%) **(Fig. 4.3.20).** However, the percentage of $CD57^+$ NK cells was lower in the HSCT patients before transplant in both 'CMV reactivation' and 'non-reactivation' groups compared with HDs **(Fig. 4.3.21).** Interestingly, the percentage of $CD57^+$ NK cells started to go down after the CMV reactivation at W1 and remained low until W4 before it went back up to normal level 3 month after reactivation and finally reached higher level than HDs. In the 'non-reactivation' patients showed an increase in the proportion of $CD57^+$ NK cells can only be seen between 3 to 10 months post-transplant and the percentage never went higher level than HDs. Comparison of these two groups showed that the $CD57^+$ level was lower in the CMV reactivation group at the early time points after reactivation (particularly W2) before rising to a high level at month 10.

The pattern of KIR expression was studied in a similar way to CD57. Again, no changes were seen between CMV seropositive and seronegative HDs (47±2.9% to 51±3.5% respectively) **(Fig. 4.3.20).** Unlike CD57, the percentage of KIR^+ NK cells in HSCT patients before transplant was similar to HDs but, interestingly, the percentage of KIR^+ NK cells started to go down after the CMV reactivation at W1 before returning to normal levels at 3 weeks after reactivation finally reaching higher levels than the HD. No significant changes were observed in the percentage of KIR^+ NK cells in the 'non-reactivation' group. Of interest, significantly higher

levels of KIR^+ NK cells were seen in the CMV reactivation group from 3 months to 10 months after reactivation **(Fig. 4.3.21).**

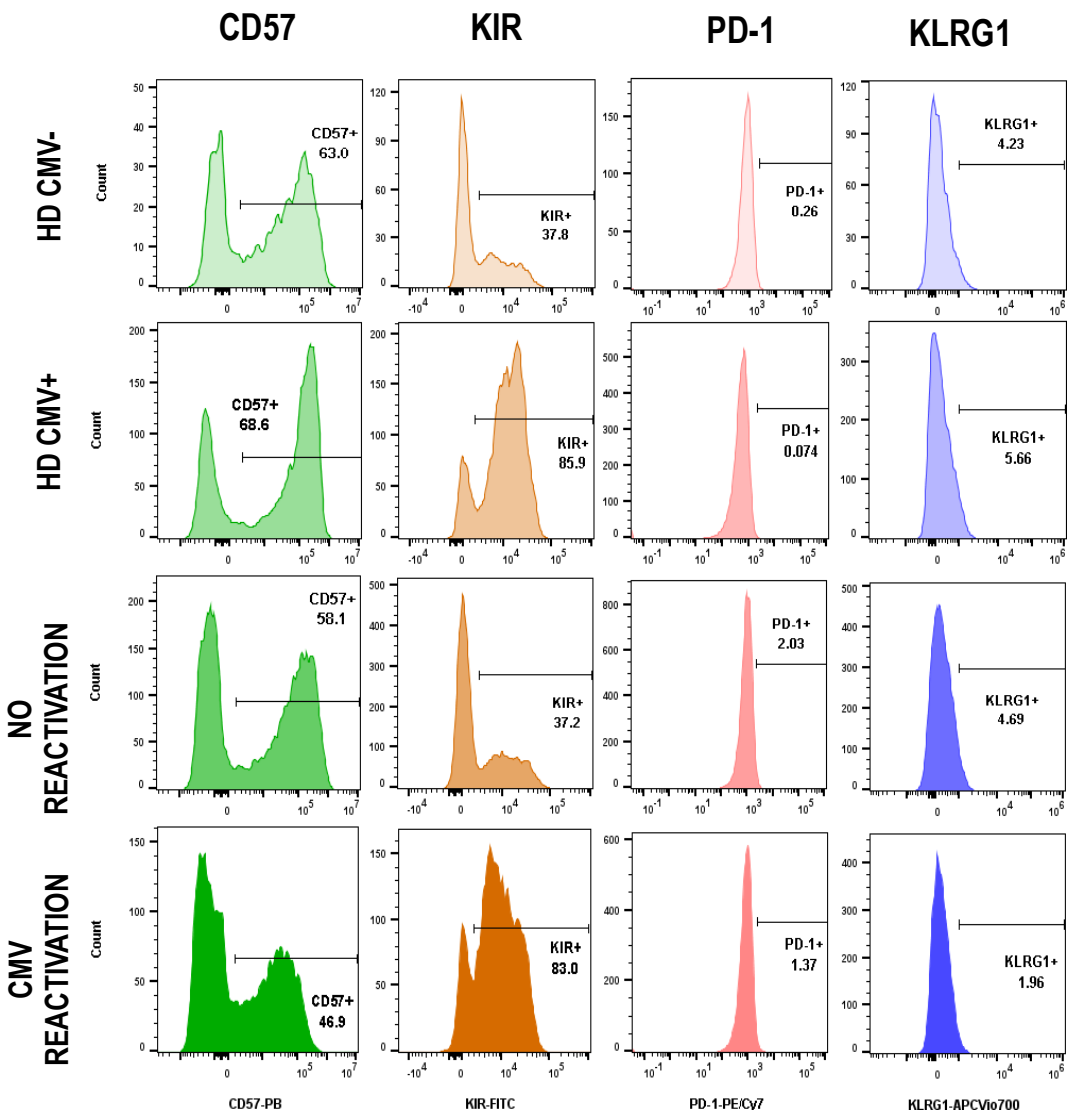


FIGURE 4.3.19. Examples of CD57, KIR (KIR2DL1/S1/S3/S5/KIR2DL2/DL3/KIR3DL1), PD-1 and KLRG1 expression on $CD56^{dim}CD16^{bright}$ NK cells in healthy donors and in patients after HSCT, distinguished by CMV reactivation or 'no-reactivation'. Similar gating strategies were applied for each marker to analyse each patient group.

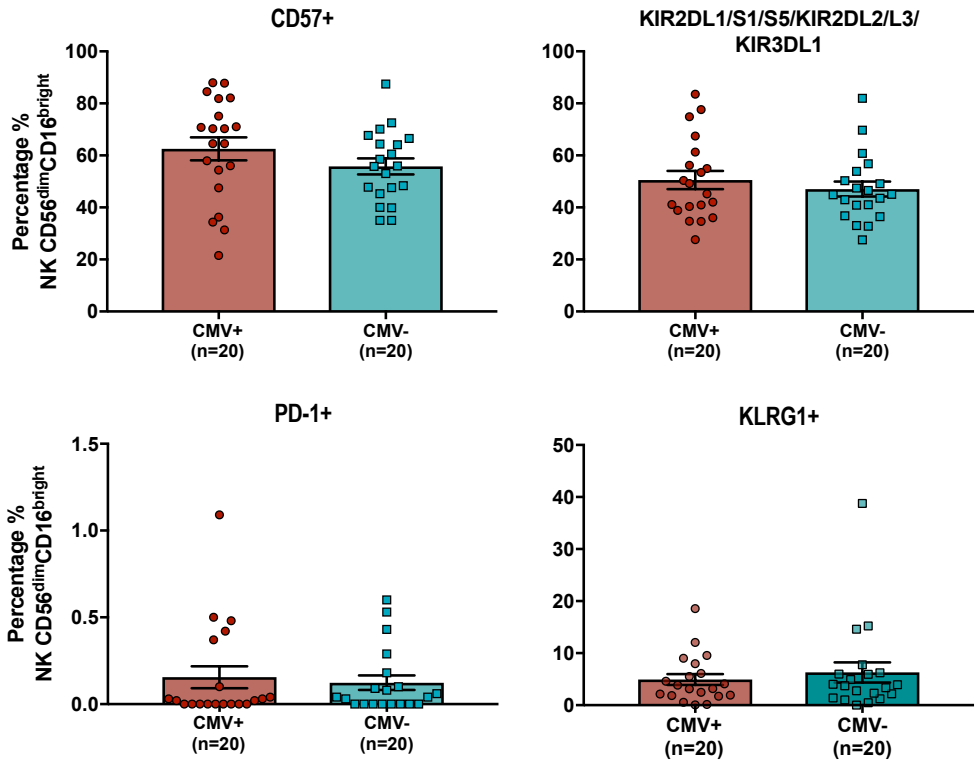


FIGURE 4.3.20. The pattern of CD57, KIR, PD-1 and KLRG1 expression on $CD56^{dim}CD16^{bright}$ NK cells in healthy donors. No differences can be seen in proportion of those markers in between seronegative and seropositive HDs. $CD57^{+}$ (CMV- 56 ±3.1%, CMV+ 63 ±4.4%, p=0.1344), KIR^{+} (CMV- 47 ±2.9%, CMV+ 51 ±3.5%, p=0.58), $PD\text{-}1^{+}$ (CMV- 0.12 ±0.04%, CMV+ 0.16 ±0.06%, p=0.65) and $KLRG1^{+}$ (CMV- 6.3 ±1.9%, CMV+ 4.9 ±1.0%, p=0.9254). All n=20. *Statistical analysis by Mann Whitney (*p<0.05, **p<0.01, ***p<0.005).

PD-1 and KLRG1 both function as inhibitory receptors on NK cells. PD-1 expression is generally very low on HD (CMV seronegative: 0.12 ±0.04%; CMV seropositive: 0.16±0.06%, **Fig. 4.3.20**) but was substantially increased at all time points after transplant. Although there were minor fluctuations in both groups, these values were not influenced significantly by CMV reactivation.

In contrast KLRG1^{+} expression on NK cells after transplant was low compared to HD (CMV seronegative: 6.3±1.9%, CMV seropositive: 4.9±1.0%), **(Fig. 4.3.20).** However, again no difference was observed between patients with or without CMV reactivation **(Fig. 4.3.21).**

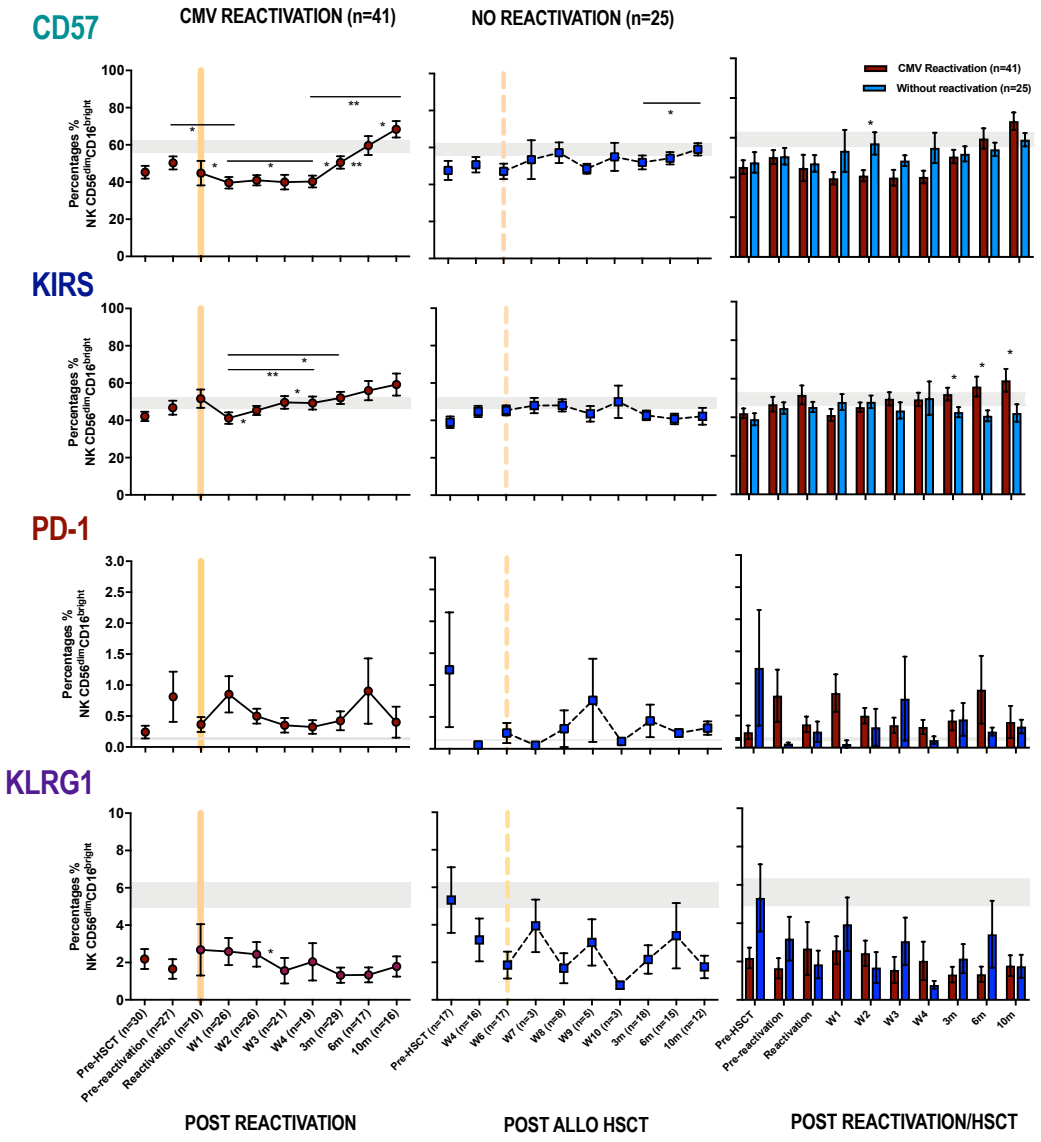


FIGURE 4.3.21. Expression of CD57^{+}, KIR^{+}, PD-1^{+} and KLRG1^{+} on CD56^{dim}CD16^{bright} NK cells after transplantation. Significant changes in the proportion of CD57 and KIR were seen on CD56^{dim}CD16^{bright} NK cells. Dotted lines show the ranges of CD57^{+} NK cells on HDs (CMV- 56 ±3.1%, CMV+ 63. ±4.4% p=0.1344); KIR^{+} (CMV- 47 ±2.9%, CMV+ 51 ±3.5%, 0.5831); PD-1^{+} (CMV- 0.12 ±0.04%, CMV+ 0.16 ±0.06%, p=0.6502) and KLRG1^{+} (CMV- 6.3 ±1.9%, CMV+ 4.9 ±1.0%, p=0.9254). *Statistical analysis was done by Wilcoxon sign rank test for matched phenotypes and Mann Whitney test (*p<0.05, **p<0.01, ***p<0.005). [W: week(s), m: month(s) after CMV reactivation/allo-HSCT].

4.3.5.2. Expression of CD69^{+} on CD56^{dim}CD16^{bright} NK cells

CD69 is a transient marker of activation on NK cells (Fogel et al., 2013) and the pattern of CD69 expression on CD56^{dim}CD16^{bright} NK cells was next assessed **(Fig. 4.3.22).** No differences were seen in the proportion of CD69^{+} NK cells between CMV seropositive and CMV seronegative HDs (p=0.41, Mann Whitney test**, Fig. 4.3.23**) and these values were represented by grey lines in the graph of HSCT patients with or without CMV reactivation **(Fig. 4.3.24).** Interestingly, the percentage of CD69^{+} NK cells was much higher in HSCT patients at virtually all time points after transplant. The highest expression was seen at the time of CMV reactivation and the percentage then started to fall over the next few weeks **(Fig. 4.3.24).** Unlike the CMV reactivation group, patients without reactivation did not show any difference in expression at individual time points. Overall the percentage of CD69^{+} NK cells was higher at the point of CMV reactivation but then fell such that it was actually lower than in the 'non-reactivation' group at 10 months post HSCT.

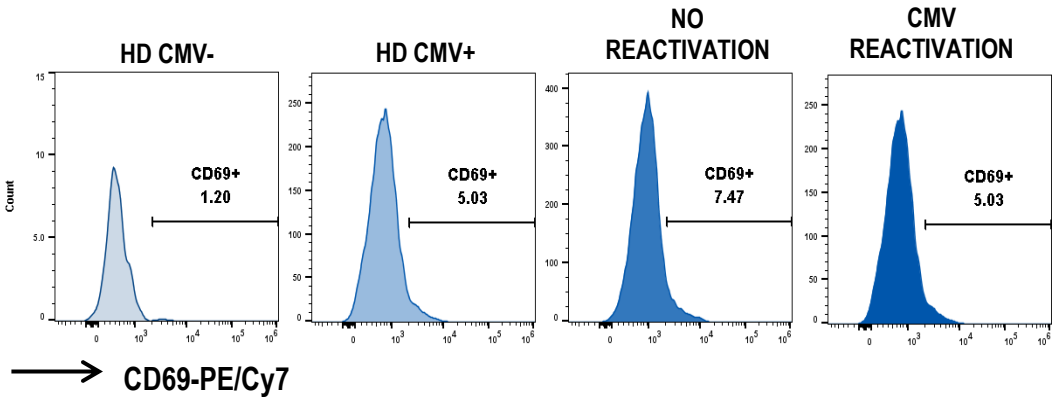


FIGURE 4.3.22. Example of CD69^{+} expression on CD56^{dim}CD16^{bright} NK cells on healthy donors and patients with 'no reactivation' or CMV reactivation after allo-HSCT.

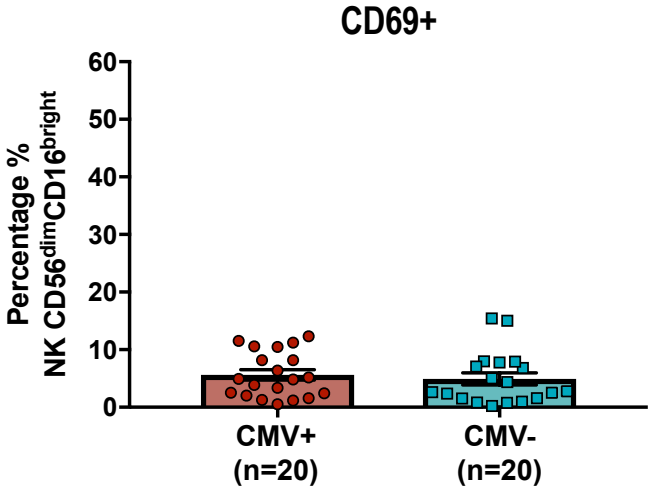


FIGURE 4.3.23. The distribution of CD69^{+} expression on CD56^{dim}CD16^{bright} NK cells in healthy donors according to CMV serostatus. No significant changes were observed in the proportion CD69^{+} cells in HDs (CMV- 4.9 ±1.0%, CMV+ 5.6 ±0.8%, p=0.41, n=20). CMV serostatus of HDs were determined from serum IgG ELISA with 10 U/mL considered as CMV positive. Analysis was done by Mann Whitney test (*p<0.05, **p<0.01, ***p<0.005).

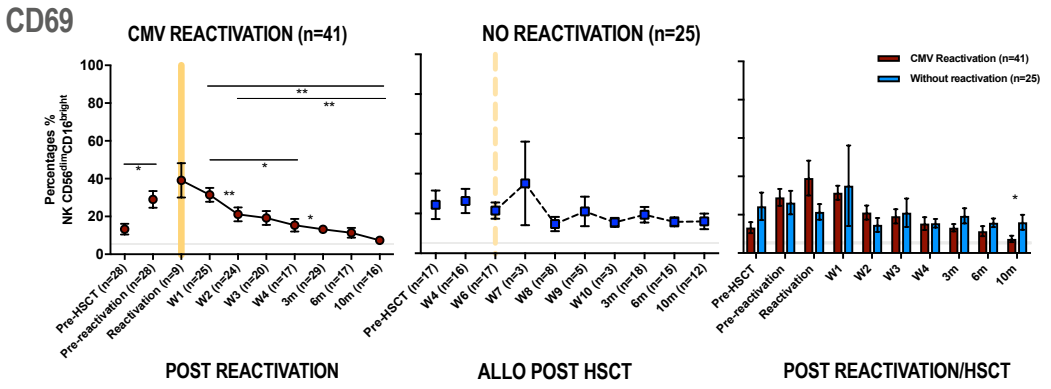


FIGURE 4.3.24. The expression of CD69^{+} on CD56^{dim}CD16^{bright} NK cells in relation to CMV reactivation after transplantation. Significant changes can be seen from various time points after reactivation, but not in without reactivation allo-HSCT. Dotted lines showing the ranges of HDs (CMV- 4.9 ±1.0%, n=20 CMV+ 5.6 ±0.8%, n=20, p=0.4115). *Statistical analysis was done by Wilcoxon sign rank test for matched phenotypes and Mann Whitney test (*p<0.05, **p<0.01, ***p<0.005). [W: week(s), m: month(s) after CMV reactivation/allo-HSCT].

4.3.5.3. Comparison of CD57$^+$, KIR$^+$ and CD69$^+$ expression within CMV R+/D+ and R+/D- groups

The work had shown that significant changes are seen in the expression of CD57, KIR and CD69 on NK cells in relation to CMV reactivation. Therefore, these values were compared between the R+/D+ and R+/D- groups **(Fig. 4.3.25).**

The pattern of CD57$^+$ and KIR expression resembled that which had been seen for NKG2C$^+$. In particular, expression was slightly higher at early time points in R+/D+ patients but then was overtaken by values in the R+/D- patients later on **(Fig. 4.3.25).** The opposite pattern was seen for CD69$^+$ expression within the two subsets.

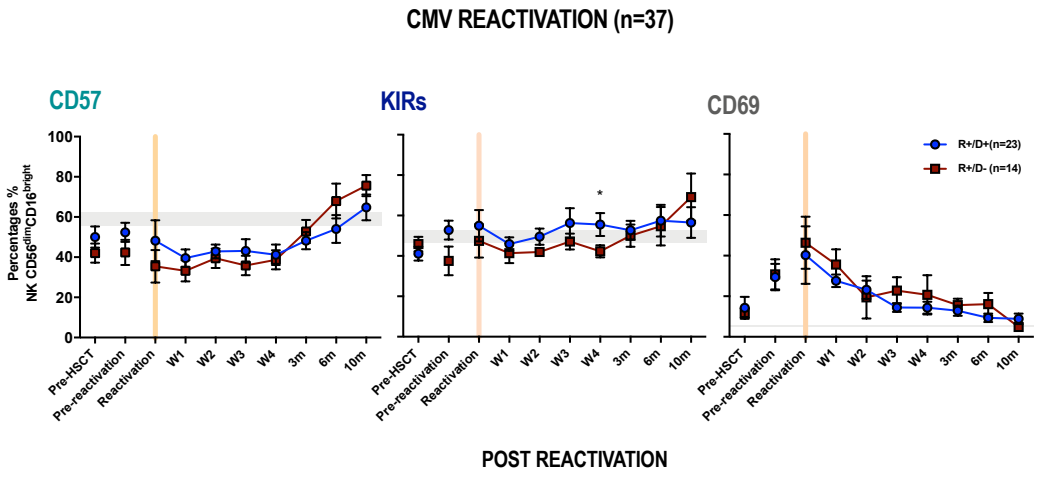


FIGURE 4.3.25. The pattern of CD57$^+$, KIR$^+$ and CD69$^+$ expression on NK cells according to CMV risk status. *Statistical analysis was done by Mann Whitney test (*p<0.05, **p<0.01, ***p<0.005). [W: week(s), m: month(s) after CMV reactivation/allo-HSCT].

4.3.6. NK cells retain cytotoxic function after CMV reactivation

4.3.6.1. NK cell cytotoxicity assay optimisation and gating strategy

Flow cytometric analysis had revealed that both the period of immune reconstitution after HSCT and the development of CMV reactivation influenced the phenotype of NK cells. As such it was next interesting to see if there was also any functional difference in the activity of the NK cell populations.

A flow cytometric-based NK cytotoxicity assay was optimised using HD PBMC whereby the percentage of killing was determined by the proportion of live K562 cells (Chapter 2, **section 2.8**). Experimental variables included with or without overnight pre-activation with IFN-α.

Pre-activation of NK cells with IFN-α led to a modest but non-significant increase in target cell lysis **(Fig. 4.3.26).** Briefly, NK cells were enriched with magnetic beads, the purity of NK cells was checked using flow cytometry staining and then they were activated with IFN-α overnight. NK cells were co-cultured with CFSE-labelled K562 cell overnight before the whole culture was harvested and analysed on flow cytometry with beads added for validation. Bead count, as well as K562 and NK cell number and percentage, were then determined **(Fig. 4.3.27).** The live and CFSE positive K562 were counted using beads as standard. The assay also was prepared with different NK: K652 (effector: target) ratios from 0.1 to 1.0 **(Fig. 4.3.27).**

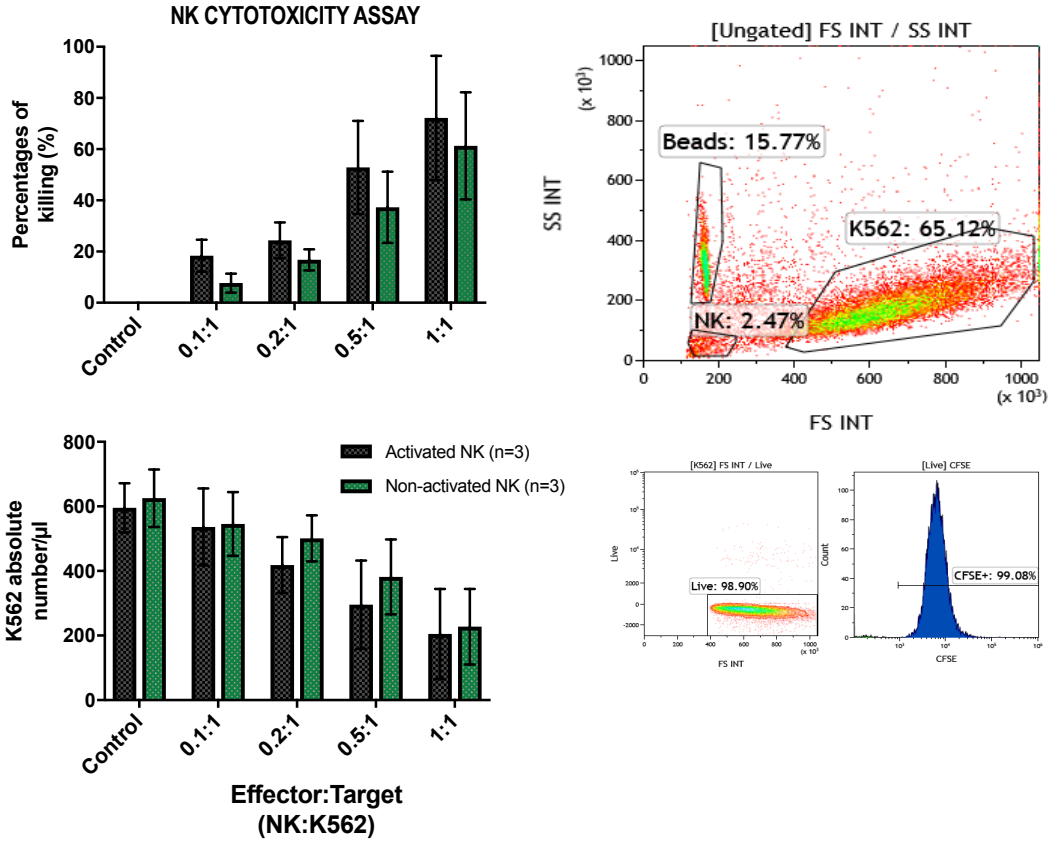


FIGURE 4.3.26. Optimisation of NK killing assay using IFN-α pre-activated or control NK cells. The percentage of killing and absolute number of target cells were determined by the number of live and dead cells, by following the calculation as in method section, Chapter 2. *Statistical analysis was done by Mann Whitney test (*p<0.05, **p<0.01, ***p<0.005).

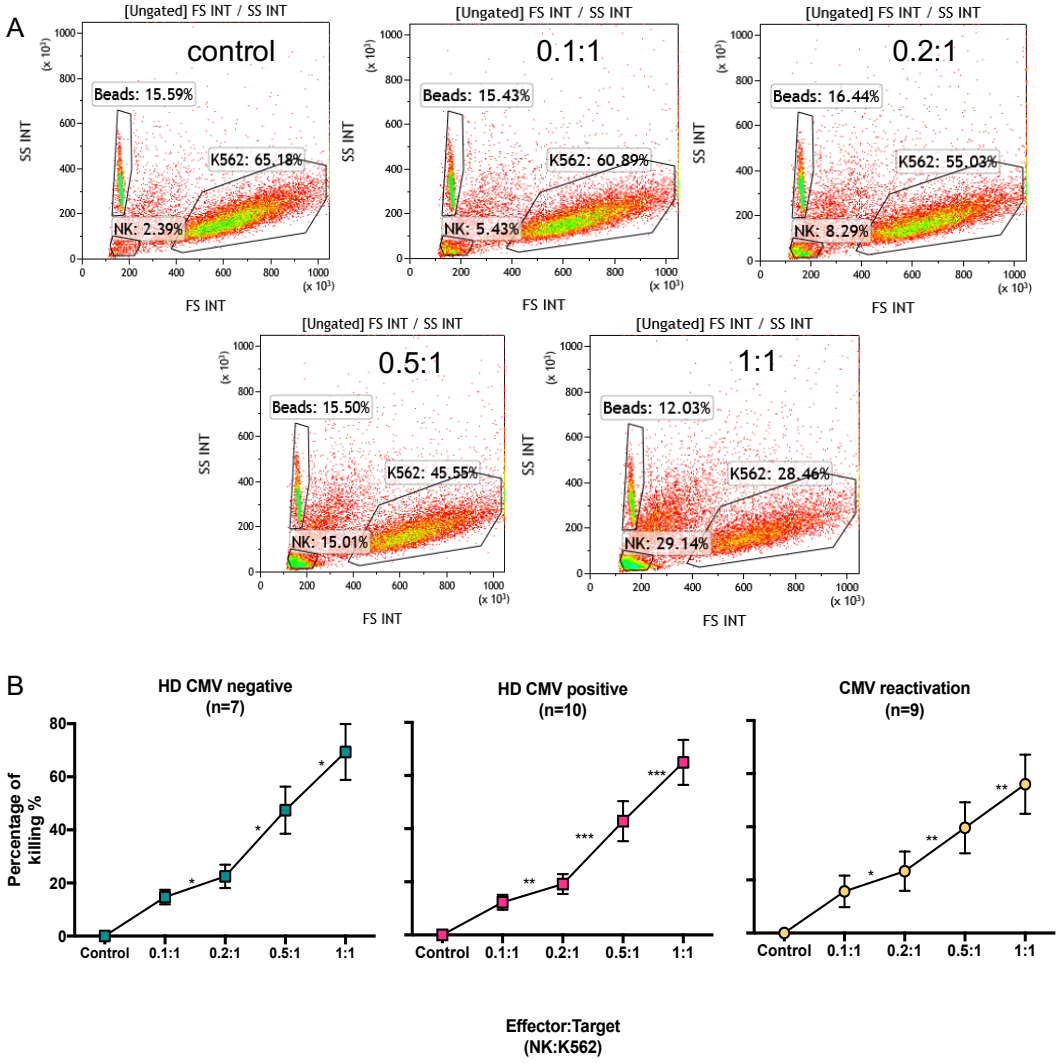


FIGURE 4.3.27. Comparison of NK cell lysis using effector cells from (a) CMV seronegative or (b) CMV seropositive healthy donors or (c) allo-HSCT patients following an episode of CMV reactivation. The percentage of target cell lysis is strongly correlated with the number of effector cells in the assay. *Statistical analysis was done by Wilcoxon sign rank test (*p<0.05, **p<0.01, ***p<0.005).

4.3.6.2. NK cell killing properties in healthy donors and HSCT patients with CMV reactivation

NK cell lysis was next compared using effector cells from HDs who were CMV seronegative or seropositive, and compared this to cells from allo-HSCT patients that had undergone an episode of CMV reactivation **(Fig. 4.3.28).** In the allo-HSCT patients the effector cells were isolated from blood samples taken 10 months after the initial viral reactivation. Interestingly, the efficacy of NK cell lysis was similar between CMV seronegative and seropositive patients and was also maintained in the allo-HSCT cohort **(Fig. 4.3.28).**

As such, NK cells from HSCT patients with a prior episode of HCMV reactivation retain cytotoxic activity, but this is not more or less efficient compared to HDs. In order to examine this further, it was interesting to see if NKG2C expression might act to modulate NK cell lytic function. As such NK cell lysis between patients with high $NKG2C^+$ NK cell proportion (>20%) or those with a lower percentage (<20%) (n=13) was compared **(Fig. 4.3.28).** These samples were selected >10 months after CMV reactivation as the assay was not possible at early time points due to low volume of blood samples and low NK cell number. A modest, but non-significant, increase in NK cell lysis from patients with >20% $NKG2C^+$ NK cells was observed.

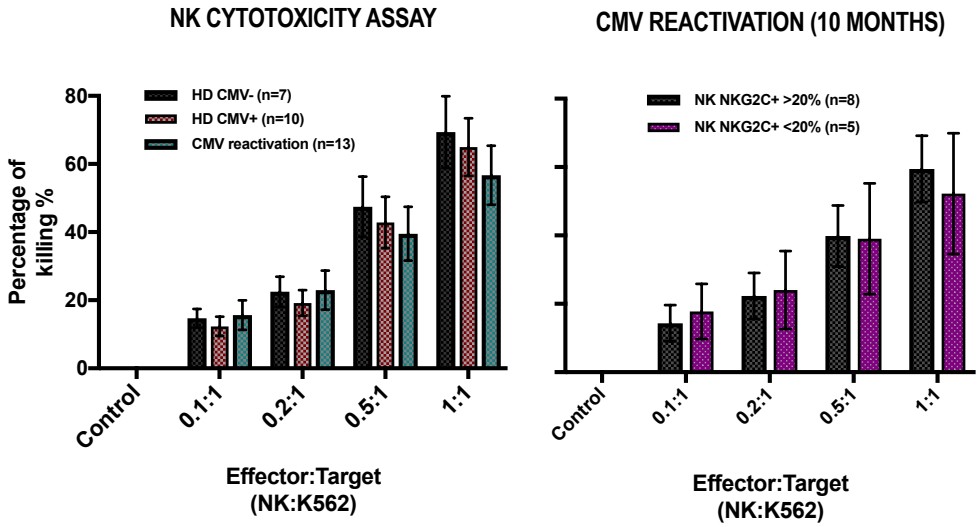


FIGURE 4.3.28. NK cell lysis in healthy donors and in allo-HSCT patients after CMV reactivation. No changes in the killing properties can be seen in when grouped into CMV- HD, CMV+ HD and CMV reactivation. No changes in the killing activities also was observed when the patients were classified into high NKG2C^{+} expression (higher than 20%) and low NKG2C^{+} expression (lower than 20%). *Statistical analysis was done by Mann Whitney test (*p<0.05, **p<0.01, ***p<0.005).

4.3.6.3. The comparison of cytotoxicity function with NKG2C^{+} NK and NKG2C^{-} NK cells

To further study whether NKG2C expression might act to modulate cytotoxic function, NK cytotoxicity was next assessed by sorting NKG2C^{+} and NKG2C^{-} cells from HDs with >20% of NKG2C^{+} NK cells within the global NK cell population (Effector: target ratio, 1:1, **Fig. 4.3.29**). This was a challenging technical approach but was feasible in two donors although no consistent patterns were observed in relation to the outcome.

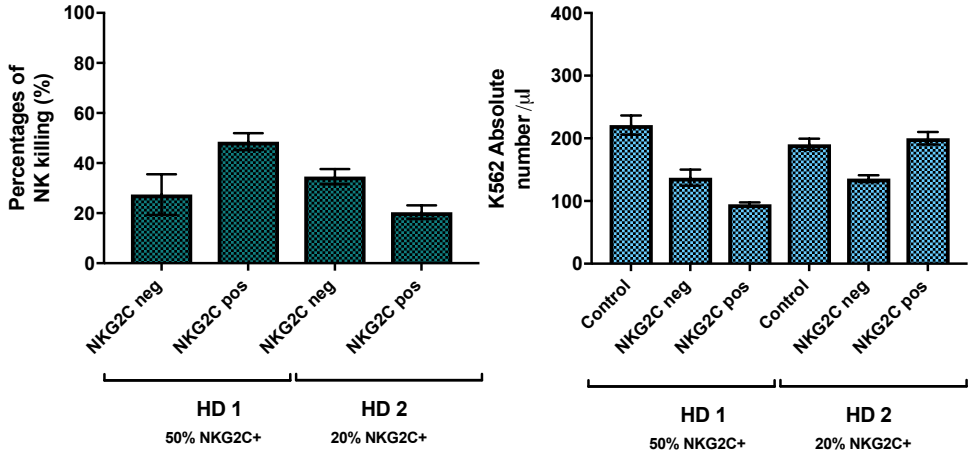


FIGURE 4.3.29. Relative lytic activity by NKG2C$^+$ and NKG2C$^-$ NK cells. No differences can be seen in the killing of these two different groups, and NKG2C$^+$ NK cells were sorted from two HDs. Effector: target (NK: K562) ratio was 1:1. *Statistical analysis was done by Wilcoxon sign rank and Mann Whitney test (*p<0.05, **p<0.01, ***p<0.005).

4.3.7. Cytokine production of NK cells from HSCT patients with CMV reactivation

Previous experiments had shown that NKG2C$^+$ NK cells retain cytotoxic activity and it was next decided to assess their profile of cytokine production. PBMC were co-cultured with K562 cells overnight and cytokine production was assessed by intracellular staining with antibodies specific for TNF-α or IFN-γ. Similar to the cytotoxic analysis, TNF-α and IFN-γ production by NK cells from the different groups were comparable.

As expected, within HDs a very low percentage (2.0%) of NK cells produced cytokine in absence of stimulation. Interestingly, a low level of cytokine production was observed in NK cells from HSCT patients in the absence of K562 stimulation, although this increase was not significant **(Fig. 4.3.30).** 8.7% of NK cells from HDs produced TNF-α after K562 stimulation. Remarkably, this value rose over 7-fold to reach 61.3% (p=0.0025, Mann Whitney test) within NK cells from HSCT

patients that had undergone a period of with CMV reactivation and to 21% those without CMV reactivation (p=0.059, Mann Whitney test). Similar differences were observed for IFN-γ production which was measured at 10.3% in the HD group compared to 73% and 25% in HSCT patients with or without CMV reactivation respectively (p=0.0025 and p=0.0159, Mann Whitney test). These observations reveal that CMV reactivation acts to prime NK for increased production of inflammatory cytokines following exposure to target cells.

In order to investigate the potential role of NKG2C expression on this pattern of enhanced cytokine secretion, the profile of cytokine production in $NKG2C^+$ and $NKG2A^+$ NK cells were next compared. No significant differences can be seen between $NKG2C^+$ and $NKG2A^+$ NK cell, probably due to the sample size in each group being very low. But there is a trend that points to the higher TNF-α production in $NKG2C^+$ NK cells compared with $NKG2A^+$ NK cells from both HSCT patients with or without CMV reactivation.

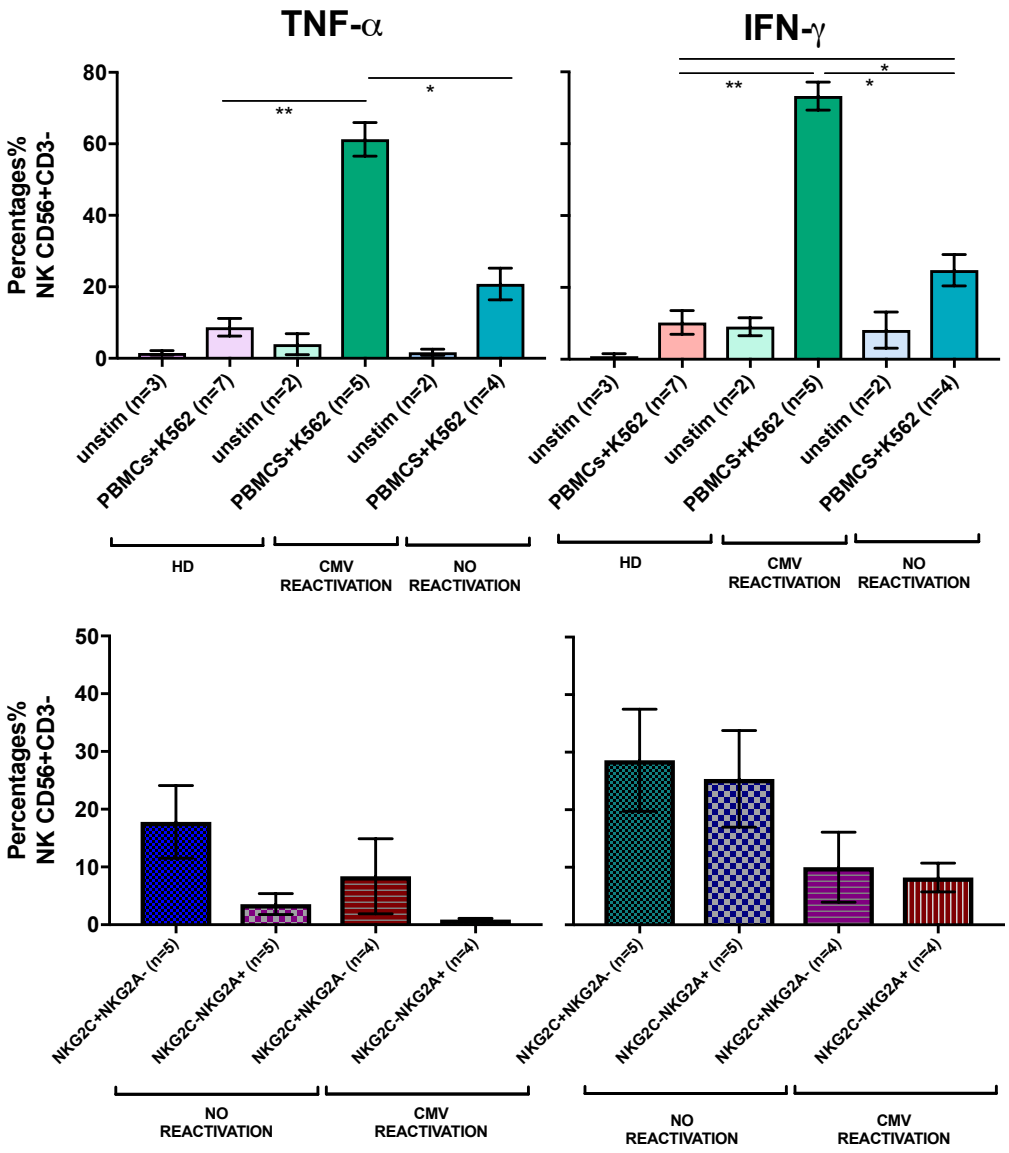


FIGURE 4.3.30. TNF-α and IFN-γ production from total NK cells and NKG2C^{+} NK cells. There is an increase in the TNF-α and IFN-γ secretion from NK cells in CMV reactivation group and allo-HSCT when compared with HDs and with unstimulated NK cells. *Statistical analysis was done by Wilcoxon sign rank and Mann Whitney test (*p<0.05, **p<0.01, ***p<0.005).

4.4. DISCUSSION

In this chapter the focus is on the phenotype and function of NK cells in the HSCT patients and how this is influenced by an episode of CMV reactivation. The novelty of this work is based primarily on the fact that very early time points after CMV reactivation, weekly for 4 weeks, were included and also added some long-term points such as months 3, 6 and 10 post-reactivations. The data analysed the percentage and total number of NK cells and the NK cell count was observationally increased after CMV reactivation compared to those patients without CMV reactivation. Interestingly, this coincided with a rapid expansion of $NKG2C^{+}$ $CD56^{dim}CD16^{bright}$ NK cells that continued until the final assessment at 10 months. An increase in $CD57^{+}$ and KIR^{+} NK cells was also seen after viral reactivation. The activating receptor CD69 was at the highest level at the point of CMV reactivation and then started to reduce to a normal state. Importantly, NK cells from HSCT patients with CMV reactivation retained lytic activity but showed enhanced production of cytokines.

NK cells reconstitution upon allo-HSCT patients with CMV reactivation

This chapter has examined immune reconstitution of total NK cells in CMV reactivation allogeneic HSCT. As reported before, NK cells recovered within 30 to 100 days after allo-HSCT (Ogonek et al., 2017a; Stern et al., 2018) and there is an increase of both NK cells percentages and absolute numbers in our patient cohort from the point before HSCT to the point before reactivation (average around week 4 post HSCT). The range of reactivation days in this patients' cohort is between 10

to 125 days (Mean: 52±5 days, Median: day 43) and the time points of pre-reactivation were randomly selected from weeks before reactivation took place.

The proportion of NK cells in HSCT patients with CMV reactivation and without reactivation are similar at early time points but become higher within one week of CMV reactivation and this pattern continues for 10 months. Interestingly, after four weeks of reactivation percentage of NK cells beings to decrease into a range comparable with HDs. This implies that reactivation also acts to boost the number of other lymphoid subsets and led to further work on T cells. This consistent increase of NK cells over 10 months took place despite no evidence of CMV reactivation as monitored by the clinical grade PCR test.

An important finding was that the NK cell percentage and absolute count correlated with the degree of viral load. This suggests that the absolute response of the NK pool is directly related to the degree of viraemia. The influence of CMV-specific immunity in the donor was also investigated. The initial viral load was actually higher in the R+/D+ group, a somewhat surprising observation which suggests that virus carried from the donor, or potentially CMV-specific immune responses, act to initially boost the viraemia. Indeed, a strong lymphocyte proliferation response to CMV prior to transplant has been previously associated with increased subsequent risk of reactivation (Barron, 2009). However, after this point the viral load was overall higher in the CMV-naïve donors, who also showed a pattern of dual peaks of viral reactivation.

Despite these patterns there was no significant difference between these two groups of patients in terms of the number or proportion of NK cells after reactivation. Also, no substantial differences were observed in patients who had a single or multiple episode of viral reactivation. This may reflect the fact that second reactivation events mostly occurred at later time points, typically after 3 months, the role of T cell immune responses may be more significant at this time.

Reconstitution of different subsets of NK cells in CMV reactivation allo-HSCT

NK cells can be divided into four major subsets: $CD56^{dim}CD16^{bright}$, $CD56^{dim}CD16^{neg}$, $CD56^{bright}CD16^{bright}$, $CD56^{bright}CD16^{neg}$. Classically, the $CD56^{dim}$ $CD16^{bright}$ is the dominant cytotoxic population whilst $CD56^{bright}CD16^{neg}$ cells predominantly express cytokines (Lajoie et al., 2017). Recent studies have shown that the $CD56^{dim}CD16^{neg}$ population can be expanded in cancer patients and can also produce cytokines (Vujanovic et al., 2019). Huenecke, et al. (2017) described the distribution of three different major NK subsets development with clear roles in predicting risk of viral infection after transplant (Huenecke et al., 2017). In term of function, Chan, et al. (2018) distinguished the $CD56^{dim}$ and $CD56^{bright}$ NK cells and showed a role for high IL-10 secretion from NK cells in suppressing aGvHD, whilst Helena, et al. (2017) have described the importance of IFN-γ secreted by $CD56^{dim}$ $CD16^{negative}$ NK cells in the context of immune reconstitution, and in controlling infection and killing cancer cells (Chan et al., 2018; Helena et al., 2017).

The $CD56^{dim}$ and $CD16^{bright}$ NK population is believed to play a major role in the control of CMV-infected cells (Bayard et al., 2016). In these studies, this population constituted the major NK subset after transplant, representing 32% of cells at the time of viral reactivation and increasing to 64% after 10 months. However, these numbers are still comparatively low when matched with HDs where values are typically around 78%. Interestingly, the percentage of $CD56^{dim}CD16^{negative}$ NK cells was high in this HSCT cohort but in parallel with the increase of $CD56^{dim}CD16^{bright}$ cells there was a decrease of $CD56^{dim}CD16^{negative}$ from similar time points. One possible explanation is that the mature $CD56^{dim}$ acquire cytotoxic properties by gaining expression of CD16 and that this is promoted by CMV reactivation. No significant increase of $CD56^{dim}CD16^{bright}$ or decrease of $CD56^{dim}CD16^{neg}$ cells was seen in the absence of CMV reactivation but the same trend remained.

In HDs, $CD56^{bright}$ NK cells constituted about 10% of NK cells in peripheral blood (Angelo et al., 2015) and is believed to be the immature NK subset and undergo maturation in secondary lymphoid organs (Michel et al., 2016). As the NK cells are recovering after allo-HSCT, immature $CD56^{bright}$ cells are expected to be higher than HDs and more likely circulating in peripheral blood of the patients, and these cells also are known to be less functional and secreting low levels of IFN-γ and TNF-α. Meanwhile, the mature $CD56^{dim}$ NK cells are more functional, mainly involved in antibody dependent cell mediated cytotoxicity (ADCC) while the immature $CD56^{bright}$ NK cells play a role as an active producer of cytokines IFN-γ and TNF-α with lower cytotoxicity properties (Pical-Izard et al., 2015; Ullrich et

al., 2016; Chan et al., 2018). Data from our patient cohort also showed that the $CD56^{bright}CD16^{negative}$ comprised of 7.7% NK cells in peripheral blood, whilst $CD56^{bright}CD16^{bright}$ was the least common population.

Expansion of NK memory-like $NKG2C^{+}$ NK cells within the $CD56^{dim}CD16^{bright}$ population

Several reports have shown that CMV infection drives the expansion of a 'memory-like' mature $CD56^{dim}NKG2C^{+}CD57^{+}$ population in both HDs and HSCT patients. Indeed, these cells show ability to kill leukemic blasts in allo-HSCT patients and may be associated with a reduction in disease relapse, even though the underlying mechanisms are still not clear (Cichocki et al., 2016; Foley et al., 2012a, 2012b). Recent studies have shown that expansion and differentiation of $NKG2C^{+}$ NK cells is modulated by different CMV strains that encode variable sequences of UL40-derived peptides, specifically on VMAPRTLIL, VMAPRTLLL and VMAPRTLVL (Hammer et al., 2018). In addition, expansion of this subset is largely specific for CMV reactivation rather than other infection (Hendricks et al., 2014). However, the subject of adaptive or memory-like NK cells is still controversial due to the fact that NK cells do not express germline rearranged receptors such as adaptive B and T cells, and thus belong to first line of immune defence and innate immunity. Despite this, evidence is now emerging that immune cells that belong to the innate immune response can display immunological memory in response to specific CMV antigens (Cerwenka and Lanier, 2016).

The kinetics study of 'memory-like' NK cell expansion after CMV reactivation was able to show for the first time that this is observed within the first month. This coincides with a reduction in the NKG2A^{+} pool and it will be of interest to see if this profile can be used in some way as a biomarker of reactivation. The expansion of NKG2C^{+} NK cells was also seen continuously after reactivation which is fascinating and may potentially reflect a continuous low level of CMV reactivation. Alternatively, it is possible that the initial episode of reactivation initiated a steady and inexorable clonal expansion of these cells over that period. A particular finding of interest was the observation that NKG2C^{+} expression on CD56^{bright} cells peaked at 6 months whilst that on the CD56^{dim} subset continued to increase at month 10. It is believed that CD56^{bright} cells mature into CD56^{dim} cells and as such this may indicate that clonal expansion of NKG2C^{+} cells moves through the NK cell maturation pathway with a 6-month peak. A modest increase in NKG2C^{+} NK cells was also observed in patients without CMV reactivation after 3 months post-transplant.

While about 5% of the healthy population have *NKG2C*$^{-/-}$ homozygous gene deletion, *NKG2C* zygosity also has been reported to correlate with the expansion of these 'memory-like' NK cells, in which both *NKG2C*$^{+/+}$ and *NKG2C*$^{+/-}$ CMV+ individuals have shown variable expansion of the CD56^{bright} NK cells (Muntasell et al., 2013b). This shows that the NKG2C host genotypes might be important and should be explored further in CMV reactivation allo-HSCT.

Both NKG2C^{+} and NKG2A^{+} form a heterodimer with CD94 on NK cells and their expression seemed largely mutually exclusive on NK cells. However, some cells did show intermediate expression of both receptors and may represent a population in transition between the two dominant states. The NKG2C^{+}: NKG2A^{+} ratio in CMV+ HDs is around 0.3:1 and a similar level of 0.2—0.5:1 was seen initially after reactivation but then increased after 6 months to 0.8—1.2:1. As such the high levels of CMV reactivation in the transplant patients lead to an 'overshoot' of the NKG2C^{+} pool by 10 months.

Evidence suggests that CMV reactivation drives the expansion of NKG2C^{+} NK cells within the mature CD56^{dim} subset (Della Chiesa et al., 2013b, 2013a) but we were able to show that the increase of NKG2C^{+} cells, and parallel decrease in NKG2A^{+} populations, is also seen within the immature CD56^{bright} NK cells. This further supports the idea that the study of NKG2C^{+} NK cells in the control of CMV reactivation should not be restricted to the CD56^{dim} pool (Wagner et al., 2017). This work also supported the idea that memory-like NK cells can be transferrable between CMV positive donors to a CMV positive recipient (Foley et al., 2012b) as a higher proportion of NKG2C^{+} cells was seen within first four weeks after reactivation in the R+/D+ group.

Evaluation of other significant phenotypes upon CMV reactivation

Some studies have described CMV-driven NK cells as mature NK cells rather than memory NK cells due to an extended phenotype characterised by KIR^{+}NKG2A^{-} NKG2C^{+}CD57^{+}Siglec7^{-} expression (Della Chiesa et al., 2013b, 2013a). The

expansion of this specific NK cell population has been observed after CMV reactivation following allo-HSCT but also in different transplant settings such as lung (Harpur et al., 2019) and kidney transplantation (Redondo-Pachón et al., 2017; López-Botet et al., 2017). We evaluated expression of CD57, KIR, PD-1, KLRG1 and CD69 in these studies and focused on the $CD56^{dim}CD16^{bright}$ pool. Of note, the proportion of both $CD57^{+}$ and KIR^{+} NK cells briefly fell after CMV reactivation and then started to rise continuously after 4 weeks of reactivation. This indicates that CMV reactivation induces the acquisition of CD57 on $CD56^{dim}CD16^{bright}$ NK cells. It is believed that $CD57^{+}$ NK cells are terminally differentiated, with reduced ability for proliferation and differentiation, and expression may also be a marker of senescence (Kared et al., 2016; Nielsen et al., 2013). It is not clear why expression was slightly reduced during the first month after reactivation, but it is conceivable that may reflect preferential recruitment of this subset into tissue.

The increase of inhibitory KIR expression is believed to be related with NK 'education' and licensing (Della Chiesa et al., 2014; Charoudeh et al., 2013; Behrendt et al., 2009; Foley et al., 2012b; Marcenaro et al., 2017; López-Botet et al., 2016; Juárez-Vega et al., 2017). One limitation in this study was that the panel of KIR-specific antibodies contained reagents against both inhibitory and activatory KIR proteins and as such it is difficult to assess how this pattern of increased expression that was observed in this study serves to modulate the activation state of the NK cell.

KLRG1 is upregulated upon NK cell activation (Robbins et al., 2002) whilst PD-1 expression is believed to be an inhibitory receptor on NK cells, with overall expression influenced by CMV infection (Della Chiesa et al., 2016). No significant changes were seen in expression of either of these markers following CMV reactivation. However, KLRG1 expression was massively downregulated on NK cells in all HSCT patients whilst PD-1 was substantially increased. These phenomena are likely to be related to the conditioning regimen of HSCT patients and may reflect the process of homeostatic proliferation that occurs when lymphocytes expand in a lympho-depleted environment.

Murine studies have shown that CD69 can be upregulated upon NK cell activation, alongside KLRG1 (Fogel et al., 2013). An association between CMV viraemia and $CD69^{+}IFN^{+}$ NK cell expansion has been seen in allo-HSCT (Barron et al., 2009). This result is in line with our data that the highest proportion of $CD69^{+}$ NK cells within the $CD56^{dim}CD16^{bright}$ subset can be observed at the reactivation time point, even though this proportion does decrease to normal state after weeks of reactivation. This data implies that CD69 on NK cells may represent a potential marker for very early CMV reactivation. Remarkably, the CD69 marker was highly expressed in HSCT patients with or without CMV reactivation compared to those HDs, suggesting that NK cells were highly activated, or potentially later 'exhausted', in allogeneic HSCT patients.

The function of NK cells in allo-HSCT patients following CMV reactivation

The properties of NK memory-like cells are interesting as their functional properties are believed to be enhanced due to the activatory phenotype of $NKG2C^+$ expression compared to NKG2A (Bigley et al., 2018). This may be important in understanding the correlation between CMV reactivation and a reduced rate of leukaemia relapse after HSCT (Cichocki et al., 2016). One suggestion has been that CMV-driven $NKG2C^+$ NK cells demonstrate enhanced antibody-dependent cell mediated cytotoxicity (ADCC) (Michelo et al., 2017; Holder et al., 2018; Muccio et al., 2018). Our data showed that NK cells in CMV reactivation allo-HSCT patients retained killing properties comparable to those NK cells of HDs. To investigate the potential role of NKG2C in enhancing the NK cytotoxicity, we have carried out the experiments in two ways. At first, the patients were grouped into two groups: one with NK cells with high $NKG2C^+$ expression (more than 20%) and one with low $NKG2C^+$ expression less than 20%. No significant differences were observed between these groups although cytotoxicity tended to be higher in the 'high NKG2C' subgroup compared to the 'low NKG2C' cohort. Secondly, the $NKG2C^-$ and $NKG2C^+$ NK cells from HDs (50% $NKG2C^+$ expression) were flow sorted, and their relative cytotoxic function then assessed. Again, no consistent differences were seen between these groups and future studies will be needed to extend these studies. It would be of particular interest to assess antibody dependent cell cytotoxicity in this work.

Cytokine production is another important function of NK cells and it is noteworthy that our previous research has shown that $CD56^{bright}$ NK cells can produce cytokine in the HSCT setting (Chan et al., 2018). This data also revealed that very large numbers of NK cells from HSCT patients with CMV reactivation were able to produce the intracellular cytokines TNF-α and IFN-γ. IFN-γ and TNF-α are markers of cytolytic function in NK cells and reinforce this dominant phenotype after viral reactivation (Wang et al., 2012). As such, enhanced cytokine production may be a further mechanism of reduced relapse rate after HSCT. The increase in the cytokines production was also further investigated through $NKG2C^+$ and $NKG2CA^+$ NK cells. TNF-α was reported to be highly produced from $NKG2C^+$ adaptive NK cells in CMV-induced HDs (Muntasell et al., 2013c). From our data, we also found that $NKG2C^+$ NK cells produce higher amount TNF-α than $NKG2C^-$ NK cells in both HSCT patients with or without CMV reactivation **(Fig. 4.3.30)** but no difference of IFN production was found.

4.5. CONCLUSION

In conclusion, this chapter has successfully demonstrated the kinetics of NKG2C^{+} NK cells expansion from the mature and cytotoxic CD56^{dim}CD16^{bright} NK cells following time points after CMV reactivation allo-HSCT, together with descriptions on other substantial markers that define memory-like NK cells, such as NKG2A, CD57 and KIR. Unlike previous studies, the descriptions on the expansion were monitored within first week of reactivation, and analysis on the other markers were done individually. It is concluded that NK cells in CMV reactivation patients retained functional capacities, with abilities in producing inflammatory cytokines and performing cytotoxic activities within immunosuppressive conditions. Moreover, the very prolonged expansion of NK cells following a single episode of CMV reactivation suggests that viraemia may act to programme long term expansion of mature NK cells from an NKG2C^{+} progenitor within the bone marrow.

CHAPTER 5:

THE PROFILE OF THE CMV-SPECIFIC T CELL IMMUNE RESPONSE AND OVERALL T CELL IMMUNE RECONSTITUTION IN RELATION TO CMV REACTIVATION AFTER ALLOGENEIC STEM CELL TRANSPLANTATION

5.1. INTRODUCTION

CMV infection can initiate very strong $CD8^+$ and $CD4^+$ T cell responses (Lidehall et al., 2005; Sylwester et al., 2005) and indeed, these are so marked as to influence the overall profile of the peripheral T cell repertoire. Furthermore, a relatively unique feature of CMV infection is that the magnitude of CMV-specific CTL can increase further during the period of persistent infection. In this chapter the immune reconstitution of $CD4^+$ and $CD8^+$ T cells in allo-HSCT patients and how this was influenced by the pattern of CMV reactivation are reported in this study. Comparisons were made with two different control groups, allogeneic HSCT patients with no CMV reactivation and HDs.

An important aim was to interrogate the kinetics of CMV-specific $CD8^+$ and $CD4^+$ T cells using HLA-Class I and HLA-Class II tetramers and to relate this to the pattern of CMV viral load. The phenotype of virus-specific cells was determined by the pattern of expression of CD57, CD38, PD-1 and CD28. Importantly, these profiles were also determined on the total T cell repertoire, including memory subgroups.

γδ T cells belong to a class of unconventional immune cells and exhibit features of both innate and adaptive immune cells. In this chapter, different subsets of γδ T cells are also examined at defined time points after CMV reactivation in allo-HSCT. This study is the first to evaluate the very early kinetics of virus-specific and total CMV reactivation during the first month of reactivation after allo-HSCT.

5.2. OBJECTIVES

Briefly, the objective of this chapter is to describe the effects of CMV reactivation on the reconstitution, phenotype and differentiation of $CD8^+$, $CD4^+$ and γδ T cells after allogeneic HSCT and its relationship to viral load. The aim is to determine if this information can help to guide clinical practice and provide insight into novel cellular immunotherapies for HSCT patients with CMV reactivation.

5.3. RESULTS

5.3.1. $CD8^+$ and $CD4^+$ T cell

5.3.1.1. Gating strategies and analysis

The examples of gating strategies as shown in the figures were from HDs. As shown in **Fig. 5.3.1**, lymphocyte populations were first determined from single cells to exclude false positive results from the double positive cells. Then live T cells which have excluded dead cells, monocytes, B cells and NK cells were gated from total lymphocytes. After this, the $CD3^+CD8^+$ lymphocytes were used to gate the $CD8^+$ T cell population and $CD3^+$ $CD4^+$ lymphocytes were used to gate $CD4^+$ T cell population. In this gating strategy, $CD56^+$ cells have been excluded in the dump channel, thus CMV specific T cells with CD56 expression might have been missed in the data analysis (Almehmadi et al., 2014).

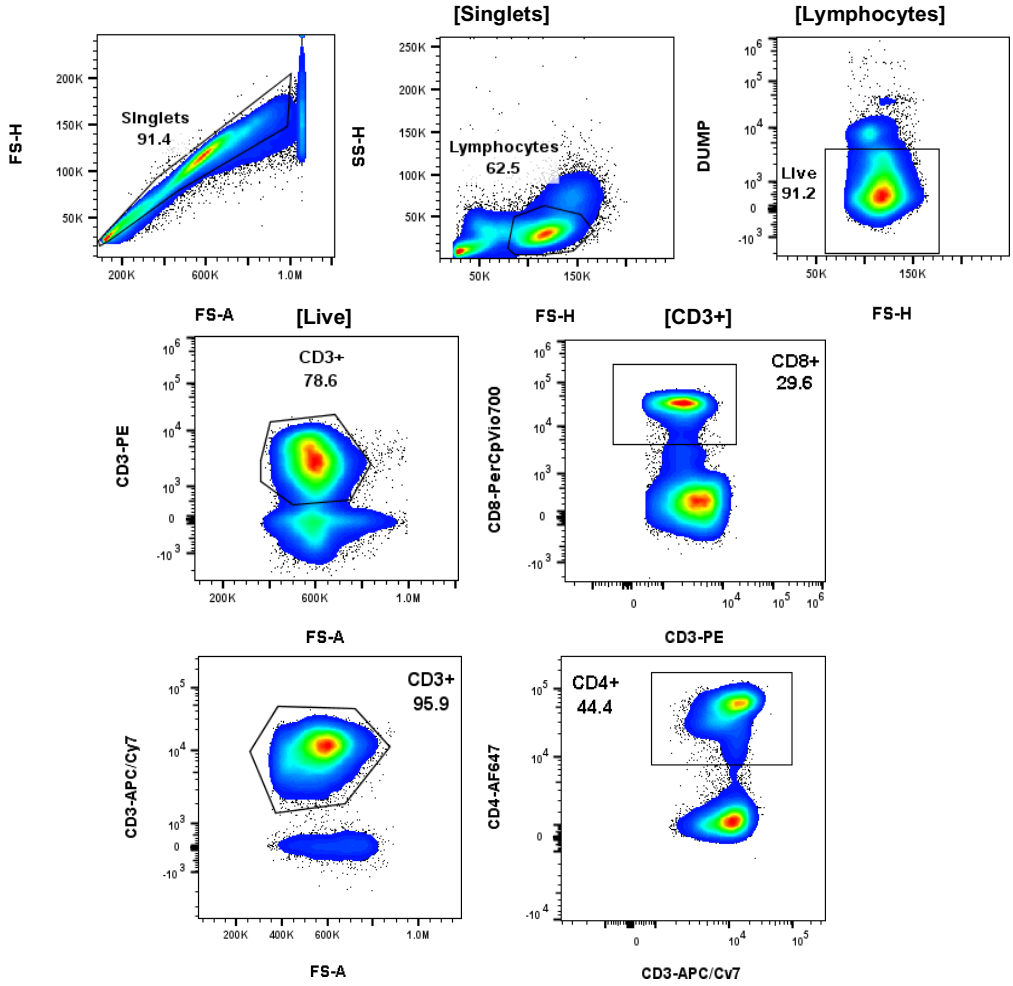


FIGURE 5.3.1. T cells gating strategies. $CD8^+$ and $CD4^+$ T cells were gated from single cells excluding doublets then lymphocytes and then live cells by staining of PI, CD19, CD14 and CD56 in dump channel (excluding monocytes, B cells, NK cells and dead cells). $CD3^+$ T cells were gated from live cells, then $CD8^+$ and $CD4^+$ T cells were then determined from total $CD3^+$ from different channels.

5.3.1.2. $CD8^+$ and $CD4^+$ T cell in healthy donors

At first, the proportion of $CD8^+$ and $CD4^+$ T cells was studied within HD to determine control values. No differences in the overall proportion of $CD8^+$ and $CD4^+$ T cells within the total T cell population were observed between CMV seropositive and CMV seronegative HDs. **Fig. 5.3.2** shows that the percentage of $CD8^+$ T cells is 26% ±2.0% and 29% ±2.1% in CMV seronegative and CMV

seropositive individuals respectively. Comparable values for CD4 T cells are 58% ±2.7% and 65% ±2.4% respectively **(Fig. 5.3.2)**. Analysis on the absolute lymphocyte count was not available in HDs. Overall, the average percentages of T cell in HDs regardless of CMV serostatus were 28% ±1.5% for $CD8^+$ T cells and 61% ±1.9% for $CD4^+$ T cells. These values were used to determine a normal range which is shown as a grey line in the future figures.

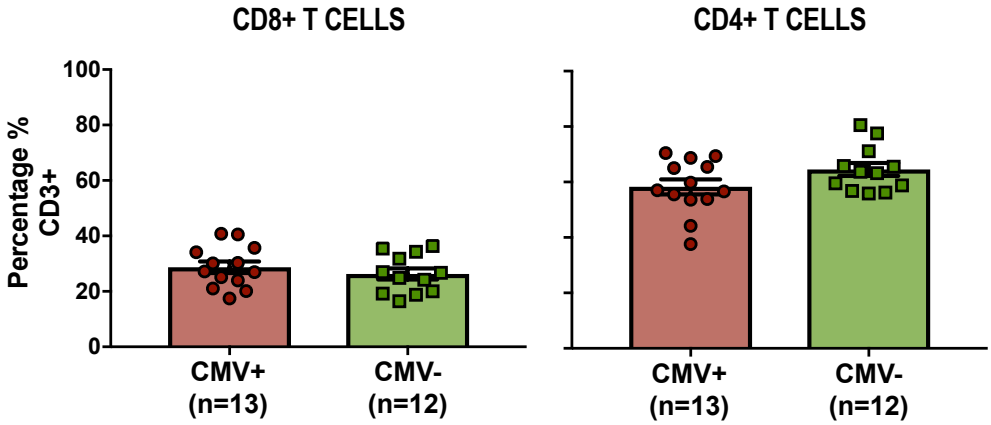


FIGURE 5.3.2. Percentage of $CD8^+$ and $CD4^+$ T cells in healthy donors. No differences in the proportion of $CD4^+$ or $CD8^+$ T cells were observed. Analysis was done by Mann Whitney test (*p<0.05, **p<0.01, ***p<0.005).

5.3.1.3. $CD8^+$ and $CD4^+$ T cell reconstitution in allo-HSCT patients with CMV reactivation

T cells reconstitute over a more prolonged period than NK cells following allogeneic stem cell transplantation and this kinetics are also influenced by immunosuppressive treatment and the lymphopenic environment. **Fig. 5.3.3** shows the percentage and absolute number of $CD8^+$ T cells in the blood of patients in the first 10 months following allo-HSCT. These values are shown in relation to the occurrence of an episode of CMV reactivation.

Of interest, the percentage of $CD8^+$ T cells is higher in all allo-HSCT patients compared to HDs although absolute cell counts remain low **(Fig. 5.3.3)**. Indeed, a profile of a reverted CD8:CD4 ratio has been observed in HSCT patients after transplant.

$CD8^+$ T cell reconstitution is very slow in those patients where there is no episode of CMV reactivation (**Fig. 5.3.3**). In contrast there is a marked increase in T cell number after viral reactivation, most notably at 3 months after CMV reactivation where it increases by 10-fold from week 4 to 10 months. As NK cells also had been observed in chapter 4, this pattern of $CD8^+$ T cell expansion continued for a long period even after a single episode of CMV reactivation. The percentage of $CD8^+$ T cells also increases from week 2 after reactivation until 3 months' time point.

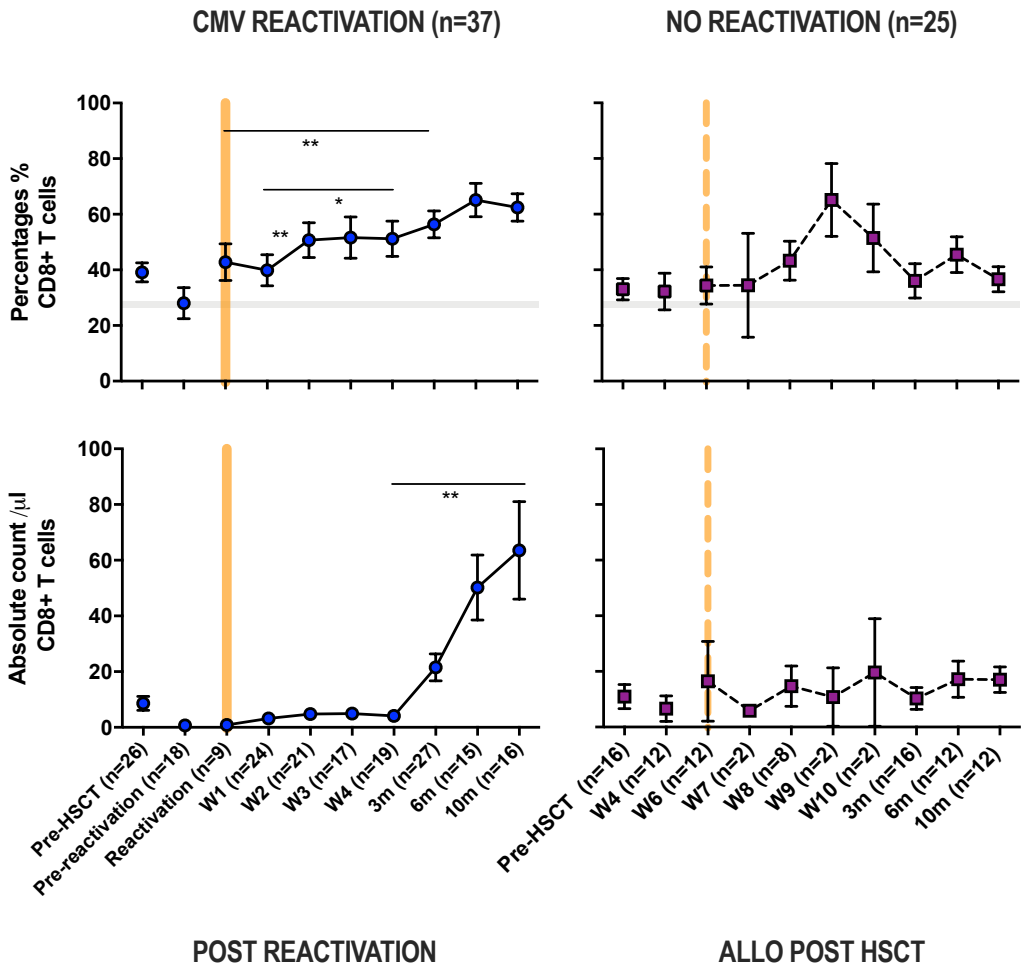


FIGURE 5.3.3. The percentage and absolute number of CD8$^+$ T cells in allo-HSCT patients in relation to CMV reactivation or without reactivation. CMV reactivation was defined as a viral load >200 copies/ml. The grey line represents values in HDs. Analysis was done by Wilcoxon sign rank test (*p<0.05, **p<0.01, ***p<0.005). [W: week(s), m: month(s) after CMV reactivation/allo-HSCT].

Similar findings were observed in relation to the reconstitution of CD4$^+$ T cells **(Fig. 5.3.4).** Overall, the percentage of CD4$^+$ T cells in all patients was generally lower compared with HDs (grey lines) which is compatible with the increased percentage of CD8$^+$ T cells that had been observed. There were no significant changes in either the percentage or count of CD4$^+$ T cells in the patients without CMV reactivation over the time course of this study. However, the percentage of CD4$^+$ T cells did decrease somewhat after CMV reactivation, particularly between

W1 and W2 and between 6 months and 10 months after reactivation. Furthermore, and similar to both NK and $CD8^+$ T cells, elevated numbers of CD4 T cells were seen from W3 to 10 months after CMV reactivation. As such CMV reactivation is seen to drive reconstitution of all major lymphoid subsets.

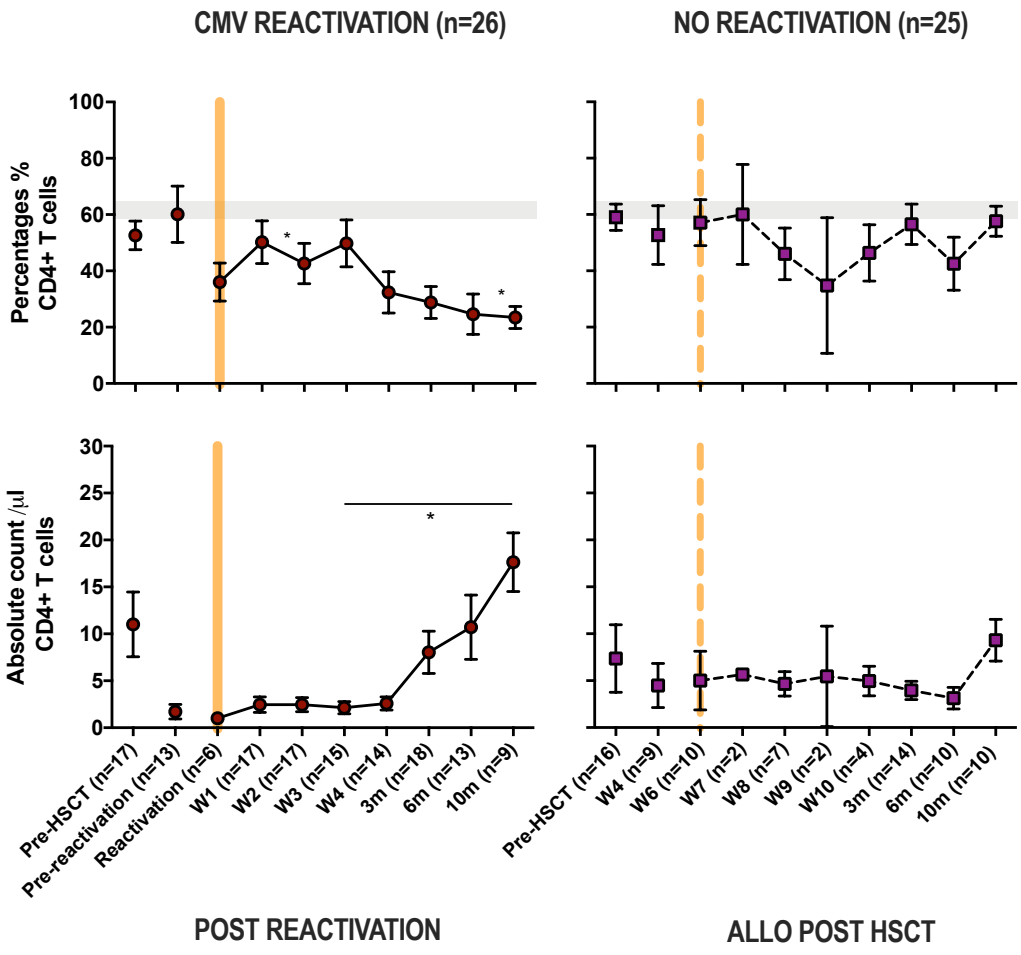


FIGURE 5.3.4. The percentage and number of $CD4^+$ T cells after allo-HSCT in relation to CMV reactivation (n=26) and without reactivation allo-HSCT (n=25). Grey line represents the range in HD. Analysis was done by Wilcoxon sign rank test (*p<0.05, **p<0.01, ***p<0.005). [W: week(s), m: month(s) after CMV reactivation/allo-HSCT].

5.3.1.4. CMV specific $CD8^+$ and $CD4^+$ T cell reconstitution in allo-HSCT patients following CMV reactivation

After this study of the whole T cell population it was also felt to be important to understand the kinetics of CMV-specific responses in relation to reactivation. This was achieved through the use of HLA-peptide tetramers. The percentage of CMV-specific $CD8^+$ and $CD4^+$ T cell populations was calculated from the total $CD8^+$ and $CD4^+$ T cell pool according to **Fig. 5.3.5** and **Fig. 5.3.6**. The advantage of using tetramers is that they can bind to the target T cells with more than one TCR with high affinity than monomer, while the disadvantage is the tetramer binding only restricted to certain CMV peptides and HLA types.

Tetramers were selected on the basis of patients' HLA genotype and we elected to combine all appropriate tetramers that could be used within each patient into a single assay (Chapter 2, **section 2.6.4.2**). This was due to the extremely low number of T cells available from early time points after transplant. Also, the detection of the CMV specific responses is dependent on the availability of individual tetramers and does not cover the whole range of HLA genotypes. As such, pooling the tetramers can maximise the statistical validity of the findings and make best usage of limited resources. A comparison with $CD8^+$ and $CD4^+$ tetramer responses from CMV seropositive HDs was not included in this study, as few donors of appropriate genotype were available, but there are many previous reports of tetramer staining in healthy people. HD blood samples were used for staining optimisation.

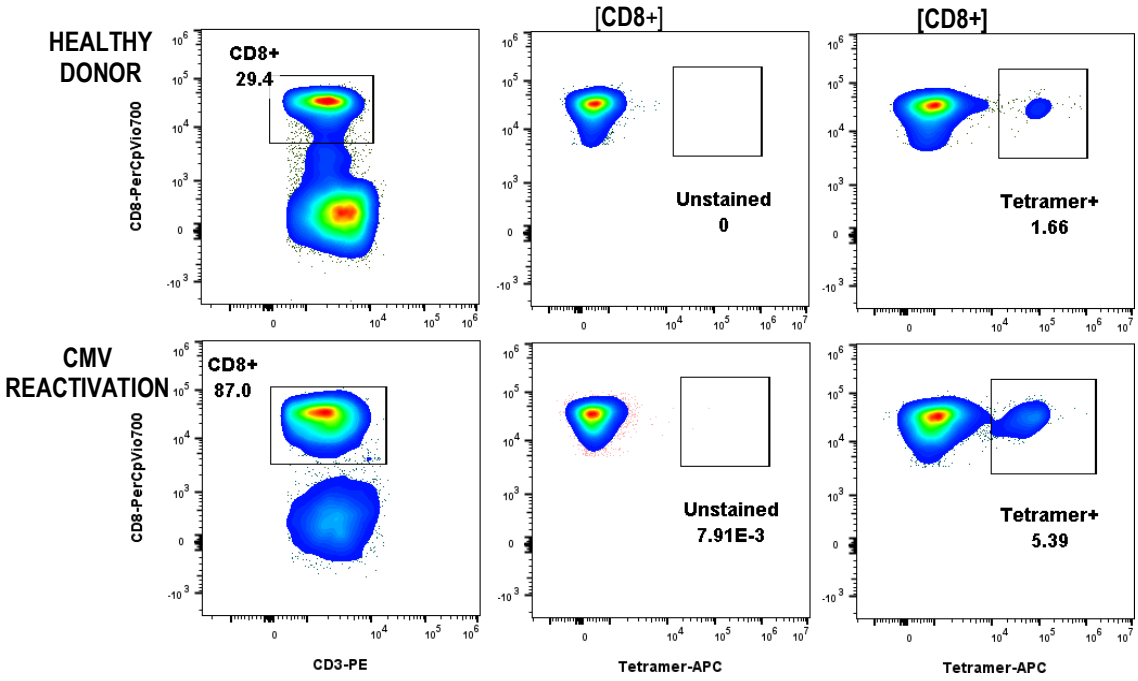


FIGURE 5.3.5. Example of tetramer staining on $CD8^+$ T cells on a CMV seropositive healthy donor and a transplant patient after CMV reactivation. Tetramer positive cells were determined from total $CD8^+$ T cells on patients with known HLA Class I types and tetramer unstained PBMCs used as negative control.

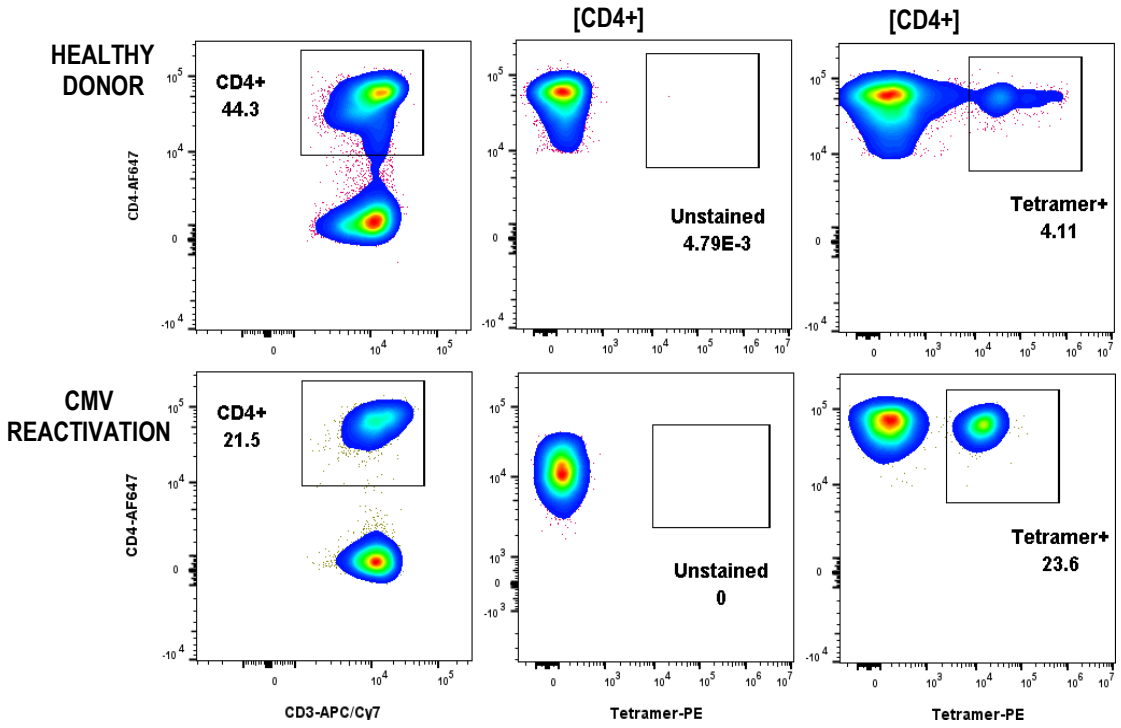


FIGURE 5.3.6. Example of tetramer staining on CD4$^+$ T cells on a CMV seropositive healthy donor and a transplant patient after CMV reactivation. Tetramer positive cells were determined from total CD4$^+$ T cells on patients with known HLA Class II types and tetramer unstained PBMCs used as negative control.

Importantly, CMV-specific T cells were detectable in most samples taken from the HSCT patients following an episode of CMV reactivation. As such, the kinetics of CMV-specific T cell responses can be studied and correlated with the profile of CMV virus load **(Fig. 5.3.7)**.

For CD8$^+$ CMV-specific responses the average percentage of tetramer-binding cells was around 1% of total CD8 population. This was increased relative to pre-reactivation frequency even at the initial time of reactivation. This increased further until week 3 after CMV reactivation before it decreased and became stable at around 3-months post-transplant. The kinetics of the CMV-specific CD8$^+$ T cell

response mirrored those of the CMV virus load, which fits the hypothesis that peptides released during CMV infection directly stimulate the proliferation of CMV-specific CD8 T cells. Indeed, a correlation was observed between the viral load and the $CD8^+$ response (Appendix, Supp. Fig. 1) (Of note, the slightly different kinetics of CMV virus load in the $CD4^+$ and $CD8^+$ graphs are due to the fact that 37 patients were included in the analysis for CMV-specific $CD8^+$ T cells and only 26 patients for CMV-specific $CD4^+$ T cells).

It is a completely different story for the pattern of the CMV-specific $CD4^+$ T cell response. Again, the average percentage response represented around 1% of the total $CD4^+$ repertoire. This increased substantially in the first 3 weeks after CMV reactivation and remained elevated until the final time point at 10 months after reactivation. No clear correlation between viral load and CMV-specific $CD4^+$ T cell response was observed (Appendix, Supp. Fig. 1).

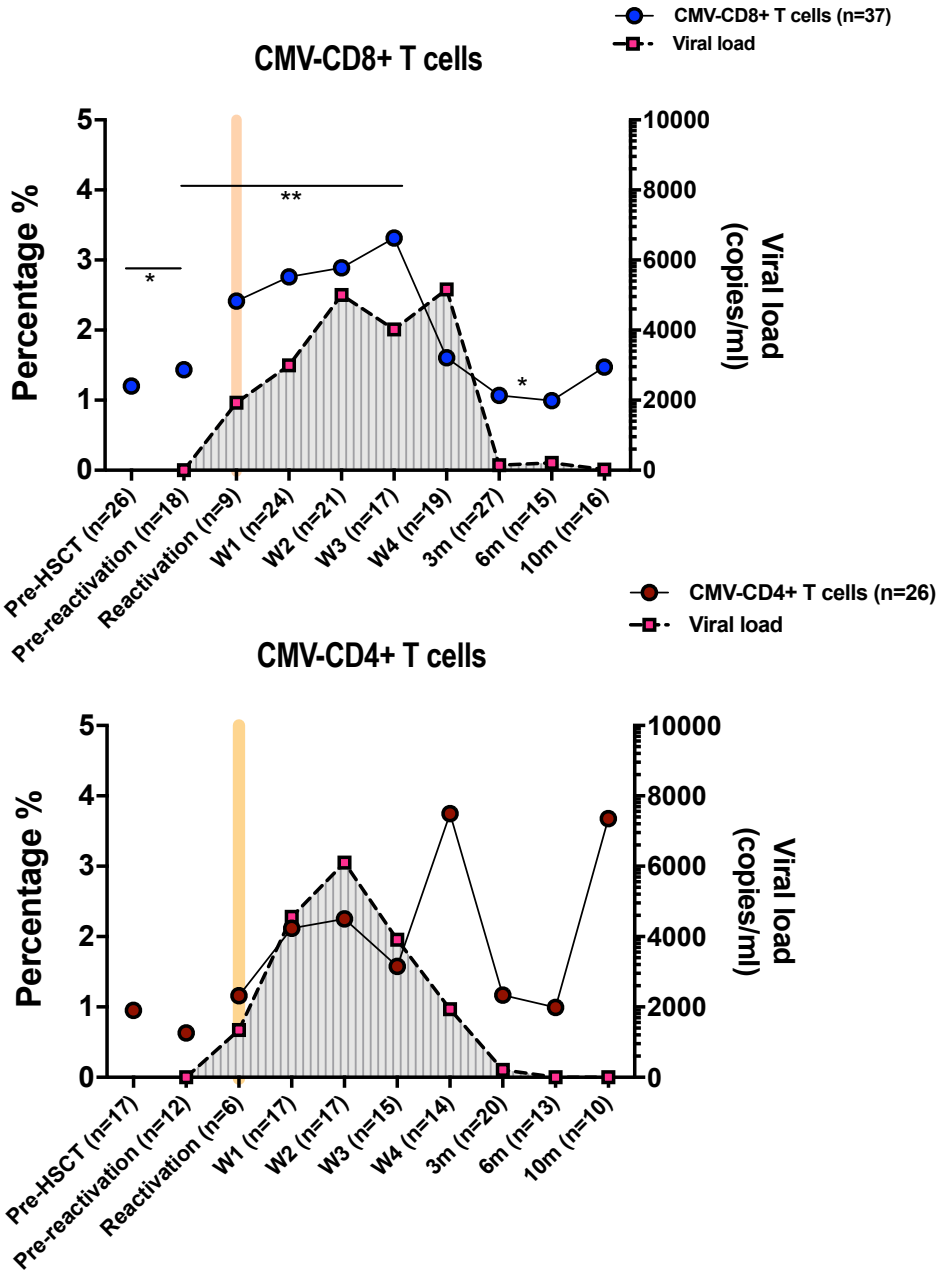


FIGURE 5.3.7. CMV-specific CD8$^+$ and CD4$^+$ T cell responses following CMV reactivation after allo-HSCT. Patients were classified as 'CMV reactivation' when viral load was >200 copies/ml. Orange bar represent the week of reactivation. [W: week(s), m: month(s) after CMV reactivation/allo-HSCT].

5.3.1.5. CD57$^+$, CD38$^+$, PD-1$^+$ and CD28 null phenotypes from CD8$^+$ and CD4$^+$ T cells in healthy donors and CMV reactivation allo-HSCT

In order to understand the changes in the phenotype of T cells in relation to CMV reactivation, the pattern of CD57$^+$, CD38$^+$, PD-1$^+$ and CD28$^-$ expressions were next assessed on the virus-specific CD8$^+$ and CD4$^+$ T cells. The analysis was done by looking at the percentage expression of each marker on the histogram plot (**Fig. 5.3.8** and **5.3.9)**. The data from HSCT patients with CMV reactivation included the total CD8$^+$ and CD4$^+$ population as well as the CMV-specific tetramer-positive T cells. The same gating was applied to all samples in different control groups and at different time points.

At first, the percentage of CD57$^+$, CD38$^+$, PD-1$^+$ and CD28$^-$ expression on total CD8$^+$ and CD4$^+$ T cells were compared between CMV seropositive and seronegative HDs **(Fig. 5.3.10)**. As mentioned before, tetramer staining on HDs was not included as not enough samples were available for analysis. An increase in the percentage of CD57$^+$ cells was seen on both CD8$^+$ and CD4$^+$ T cells in CMV seropositive HDs compared with CMV negative HDs (CD8$^+$ T cells; CMV positive: 28.6±4.8%, CMV negative: 15.9±1.9%, p=0.0257 and CD4$^+$ T cells; CMV positive: 6.0±1.4%, CMV negative: 1.9±0.3%, p=0.0118). This observation is in line with many previous reports showing that persistent CMV infection leads to an increased profile of CD57 expression on T cells. In contrast, the percentage of CD38$^+$, PD-1$^+$ and CD28$^-$ T cells were not different between CMV seropositive and seronegative HDs.

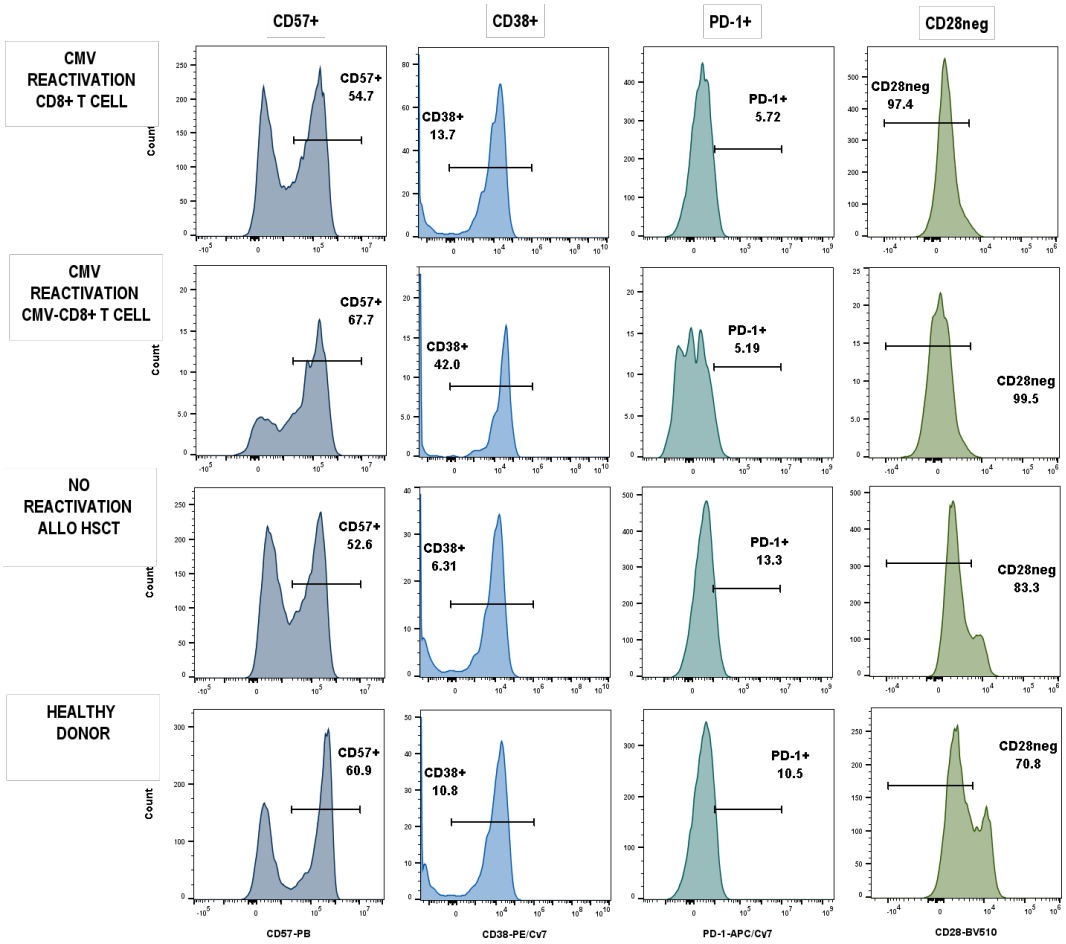


FIGURE 5.3.8. Examples of CD57$^+$, CD38$^+$, PD-1$^+$ and CD28 expression and histogram gating strategies on total CD8$^+$ T cells from CMV reactivation patients, no reactivation patients and healthy donors. CMV specific CD8$^+$ T cell analysis was also performed from 'CMV reactivation' patients. All gating was done on positive cells except for CD28 in which measured by the 'negative' cell population.

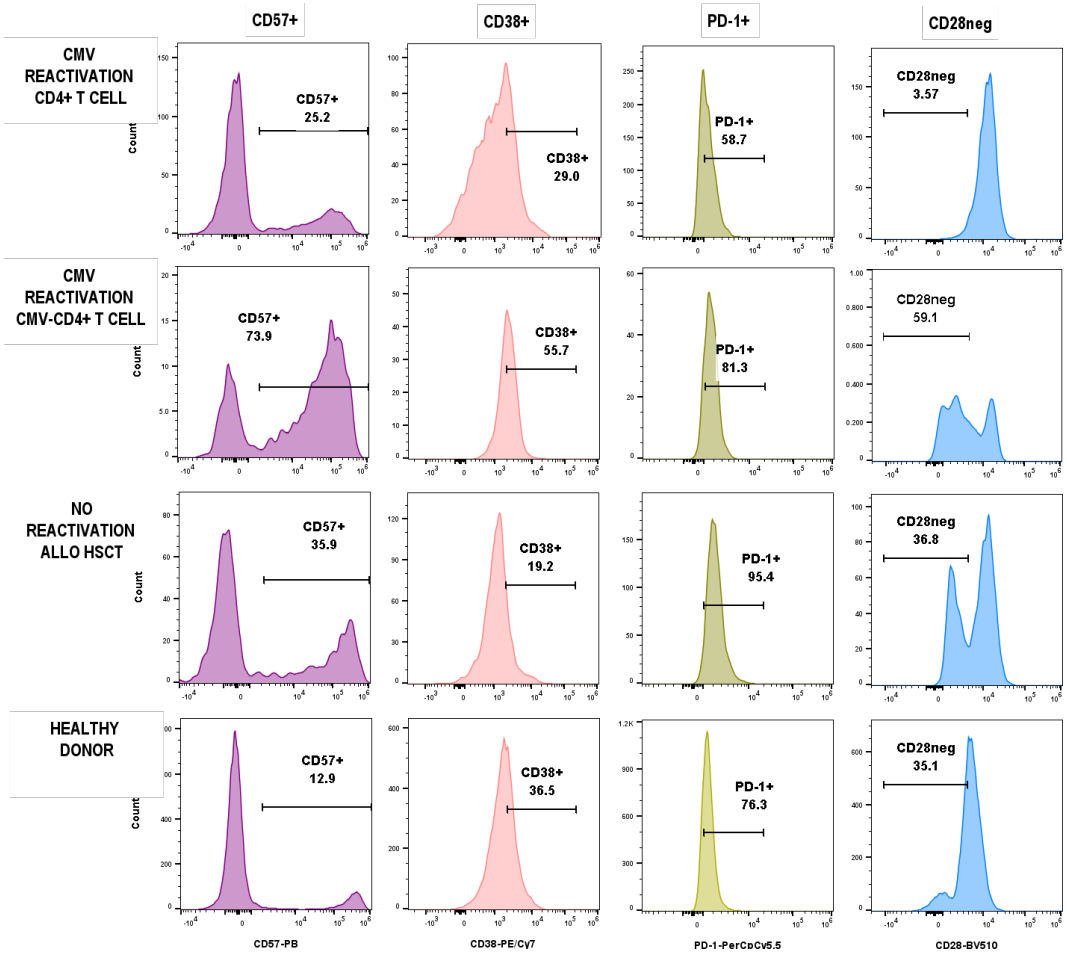


FIGURE 5.3.9. Examples of CD57$^+$, CD38$^+$, PD-1$^+$ and CD28 expression and histogram gating strategies on total CD4$^+$ T cells from CMV reactivation patients, no reactivation patients and healthy donors. CMV specific CD4$^+$ T cell analysis was also performed from 'CMV reactivation' patients. All gating was done on positive cells except for CD28 in which measured by the 'negative' cell population.

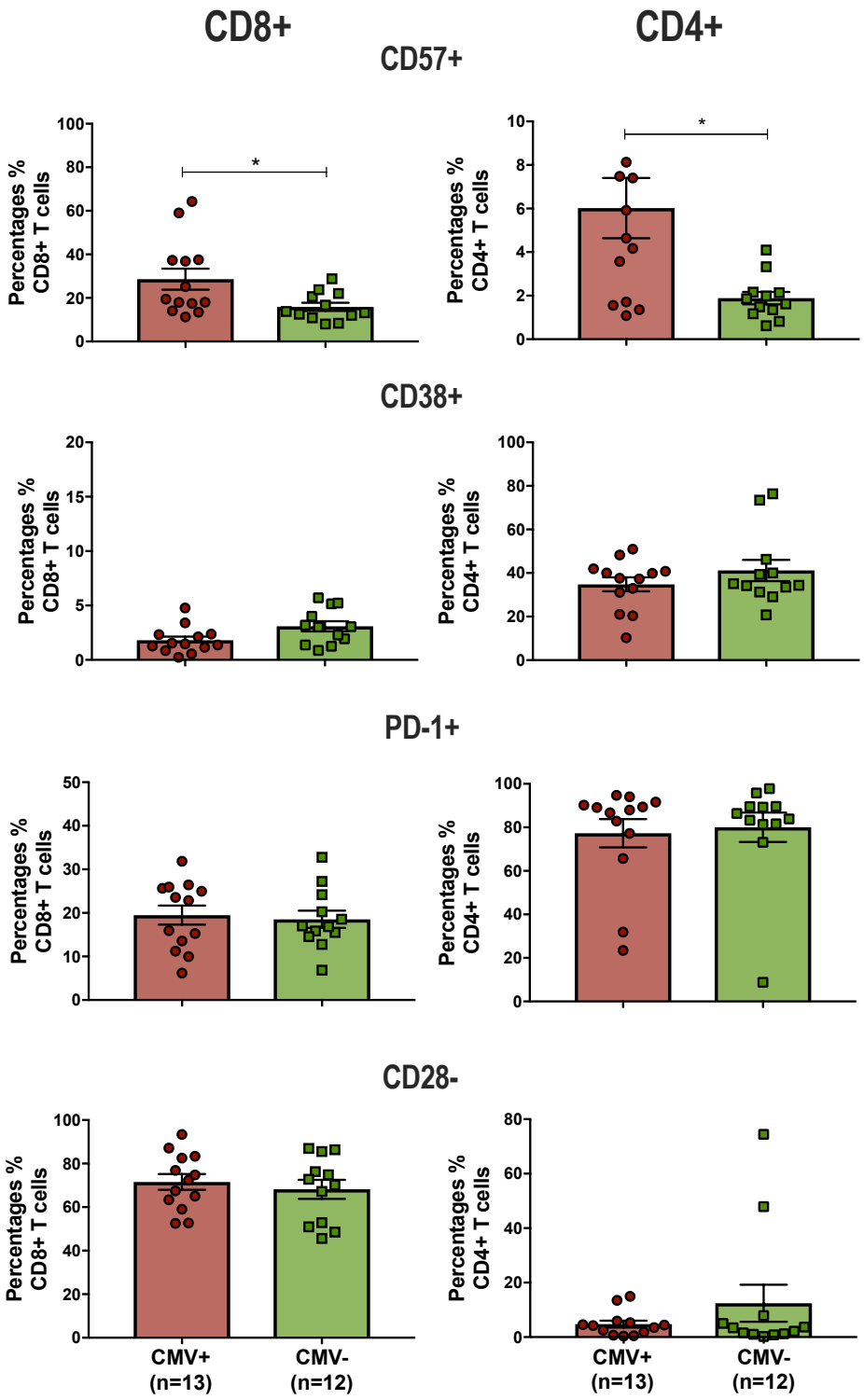


FIGURE 5.3.10. The percentage of CD57^{+}, CD38^{+}, PD-1^{+} and CD28^{-} on CD8 and CD4 T cells in healthy donors. Percentages on CMV seropositive or CMV seronegative donors were (CD8^{+}) CD57^{+}: 28.6±4.8% vs 15.9±1.9%; CD38^{+}: 1.8±0.3% vs 3.1±0.5%; PD-1^{+}: 19.5± 2.2% vs 18.5± 2.0% and CD28^{negative}: 71.6±3.6% vs 68.2± 4.4%. (CD4^{+}); CD57^{+}: 6.0±1.4% vs 1.9±0.3%, CD38^{+}: 34.8±3.2% vs 41.2±4.9%, PD-1^{+}: 77.3±6.5% vs 80.0±6.7% and CD28^{negative}: 4.8±1.3% vs 12.5±6.8%. Analysis was done by Mann Whitney rank test (*p<0.05, **p<0.01, ***p<0.005).

These markers were then applied to the study of HSCT patients. This data is shown in **Fig. 5.3.11** for $CD8^+$ T cells in **Fig. 5.3.12** for $CD4^+$ T cells. The expression of CD57 on $CD8^+$ T cells was slightly increased pre-reactivation in transplant patients compared to HDs but then increased markedly after CMV reactivation on both the total and the virus-specific populations and this continued until 10 months after reactivation **(Fig. 5.3.11).**

Interestingly, the kinetics of the increase of CD57 expression on CMV-specific $CD8^+$ T cells is delayed compared to the profile on the total $CD8^+$ pool. In particular, it remains stable for the first month after viral reactivation but then increases to reach the very high level seen in the global $CD8^+$ pool at 10 months. Patients who do not suffer an episode of viral reactivation also have levels of $CD57^+$ $CD8^+$ T cells that are above control levels, suggesting that the transplant protocol may be partly responsible for this effect, but the magnitude of increase is much greater in the patients with reactivation **(Fig. 5.3.13).** Unlike $CD8^+$ T cells, $CD57^+$ expression on total $CD4^+$ cells in HDs is very low (<10%) as shown from **Fig. 5.3.10**. The percentage of $CD57^+$ CD4 T cells from both total $CD4^+$ and CMV-specific $CD4^+$ T cells is higher expression through the time course in both CMV reactivated and non-reactivated patients compared to HDs, but there are no major changes across the time course **(Fig. 5.3.12).**

CD38 is an ectoenzyme that acts as an activation marker for T cells (Cockerham et al., 2014). In HDs, the expression of CD38 on total $CD8^+$ cells are also very low regardless of CMV serostatus **(Fig. 5.3.10).** Overall CD38 expression on the $CD8^+$

T cells from HSCT patients is higher than HDs **(Fig. 5.3.11).** In HSCT patients with CMV reactivation, significant increase of CD38 expression can be seen from the first week of reactivation to fourth week in both total $CD8^+$ and CMV-specific $CD8^+$ T cells. The expression level of CD38 reached the peak level at week 2 and started to go down until after 10 months to the comparable level to those of HDs **(Fig. 5.3.11, Fig. 5.3.13).**

Another interesting observation is that CD38 expression is consistently lower on CMV-specific $CD8^+$ T cells compared with the whole CD8 population. The percentage of $CD38^+$ $CD4^+$ T cells shows similar kinetic as $CD8^+$ T cells in HSCT patients with CMV reactivation **(Fig. 5.3.11 and 5.3.12).** There was an increase in CD38 expression at the point that CMV reactivation happened, and the CD38 expression peaked around 2 weeks after reactivation and then went back down to normal range as HDs **(Fig. 5.3.12).** Again, the CD38 expression was lower in CMV specific $CD4^+$ T cells than whole $CD4^+$ T cells population. The data from both $CD8^+$ and $CD4^+$ T cells has shown that CD38 can be used as an important activation marker in early CMV reactivation, as no comparable observational changes can be seen from HSCT patients with no reactivation.

PD-1 is expressed on recently activated T cells and is also the prototypic marker of T cell exhaustion (Dirks et al., 2013; McKinney et al., 2015). No differences in PD-1 expression was seen between HDs in relation to CMV serostatus **(Fig. 5.3.10).** Overall, the kinetics of PD-1 expression on $CD4^+$ and $CD8^+$ T cells in HSCT patients with CMV reactivation were similar to those for CD38 through the time

course of reactivation (**Fig. 5.3.11** and **Fig. 5.3.12**). PD-1 expression on $CD8^+$ T cells increased when the CMV reactivation happened, peaked around 2 weeks later and went back down to normal range around 10 months later. For the $CD4^+$ T cells, no clear increase of PD-1 expression was seen at reactivation, but the decrease of expression is significant at later time points. Interestingly, the PD-1 expression on total CD8/CD4 T cells and CMV specific CD8/CD4 T cells were not distinguishable (**Fig. 5.3.11** and **Fig. 5.3.12**).

Unlike other markers that have been discussed above, CD28 phenotype was analysed for the percentage of 'negative' cells, which have previously been shown to be boosted during persistent CMV infection (Dirks et al., 2013). In HSCT patients with CMV reactivation, the percentage of CD28-negative CD8 T cells was lower at the point before or just after CMV reactivation compared with HDs. However, the percentage of CD28-negative $CD8^+$ T cells then kept increasing after the CMV reactivation in HSCT patients. For the $CD4^+$ T cells, there was also a continual increase of CD28-negative population. Similar to other markers, no changes in the percentages were seen in HSCT patients without CMV reactivation. As such, these data clearly show that CMV infection leads to the expansion of the CD28-negative $CD8^+$ and $CD4^+$ T cells.

Overall comparisons between CD57, CD38, PD-1 and CD28 expressions on $CD8^+$ T cells pool between CMV reactivation and non-reactivation groups were shown in **Fig. 5.3.13.**

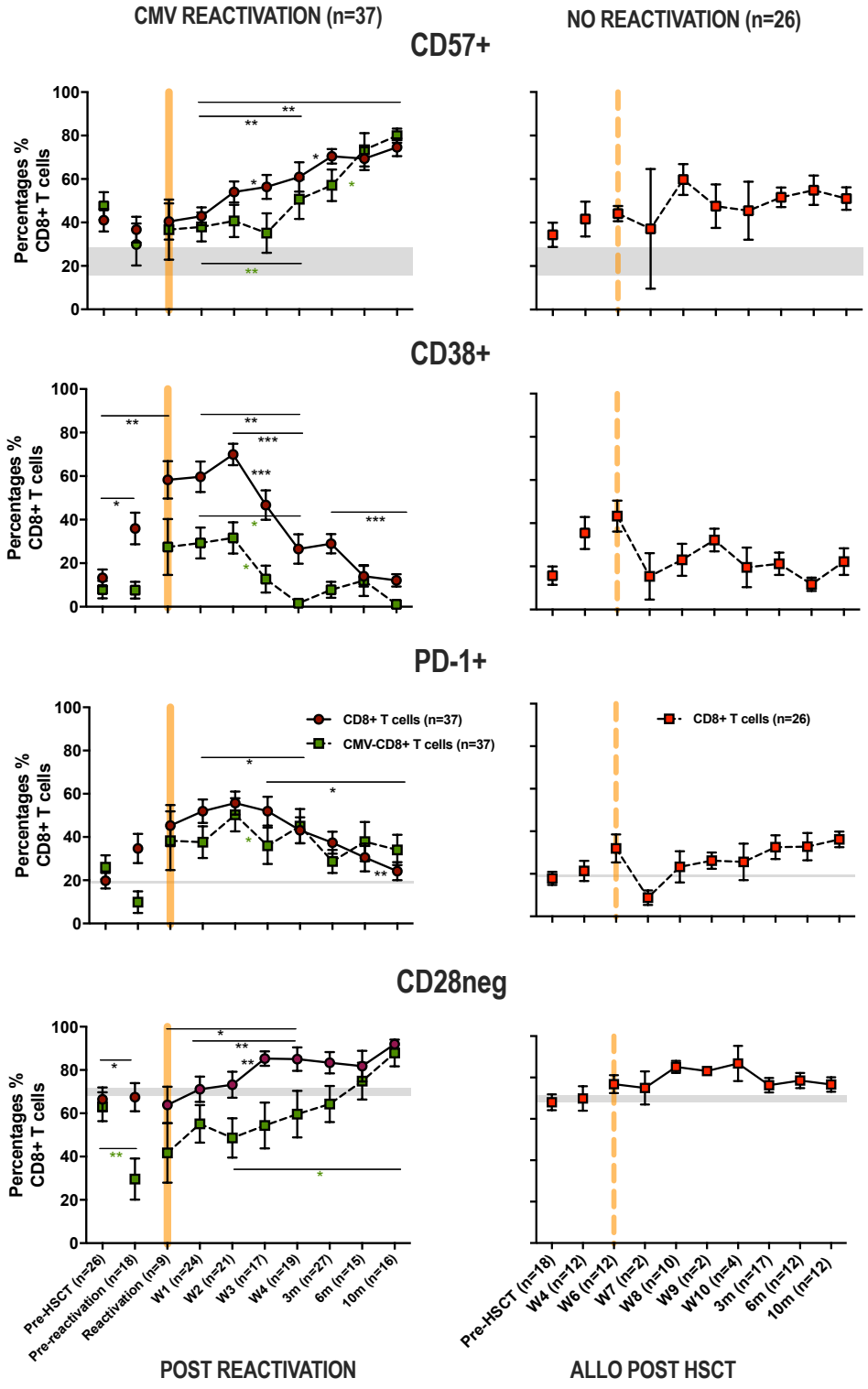


FIGURE 5.3.11. CD57^{+}, CD38^{+}, PD-1^{+} and CD28^{negative} percentages from CD8^{+} T cells in CMV reactivation and without reactivation patients. Brown circles represent whole CD8^{+} populations and green squares CMV-specific tetramer+ cells. Range of percentage of positive cells from CMV seropositive to CMV seronegative HDs are represented by grey lines. Analysis was done by Wilcoxon sign rank test (*p<0.05, **p<0.01, ***p<0.005). [W: week(s), m: month(s) after CMV reactivation/allo-HSCT].

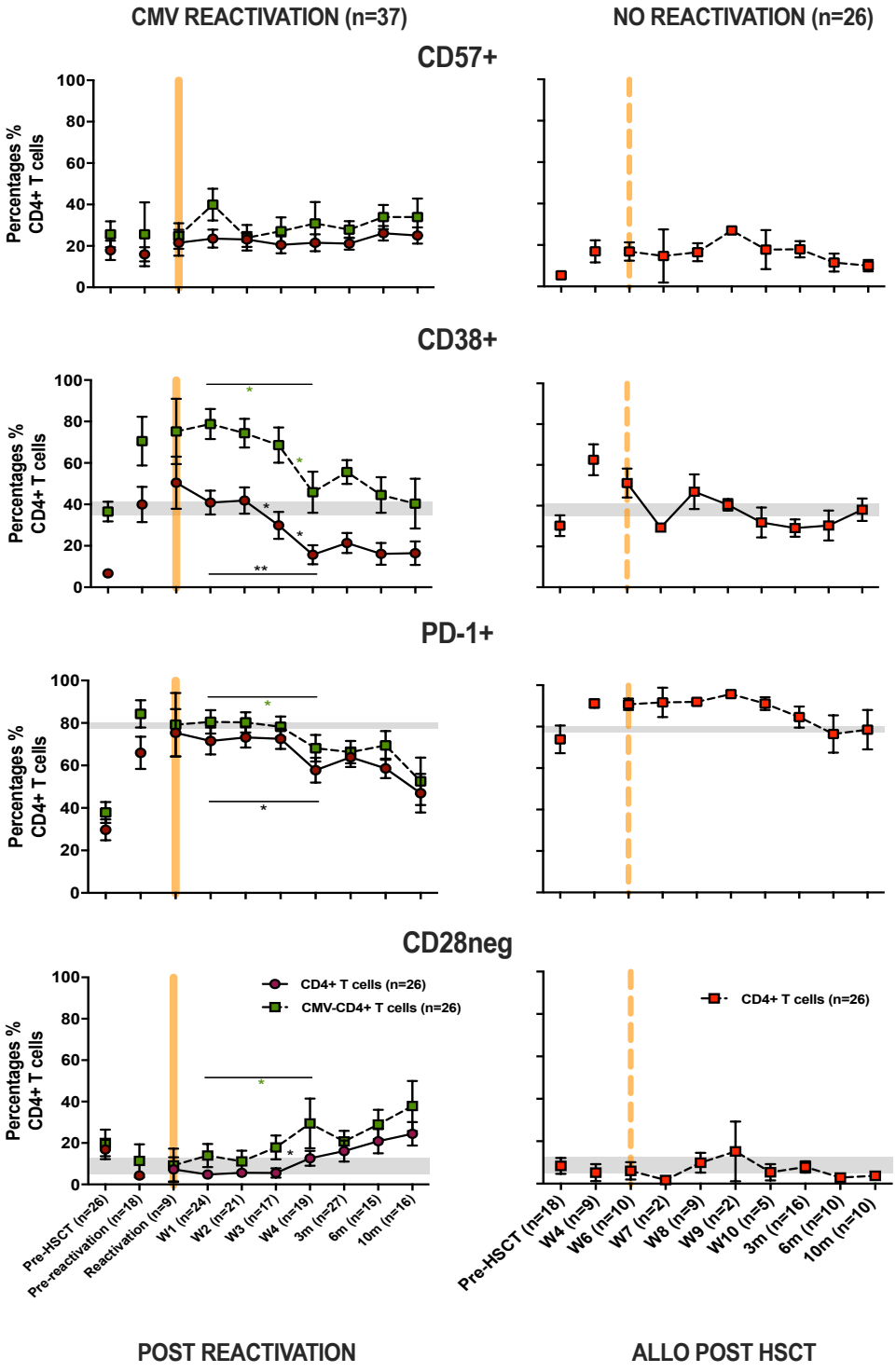


FIGURE 5.3.12. The percentage of CD57^{+}, CD38^{+}, PD-1^{+} and CD28^{negative} CD4^{+} T cells in relation to CMV reactivation after transplant. Brown circles represent whole CD4^{+} populations and green squares CMV-specific tetramer+ cells. Range of percentage of positive cells from CMV seropositive to CMV seronegative HDs are represented by grey lines. Analysis was done by Wilcoxon sign rank test (*p<0.05, **p<0.01, ***p<0.005). [W: week(s), m: month(s) after CMV reactivation/allo-HSCT].

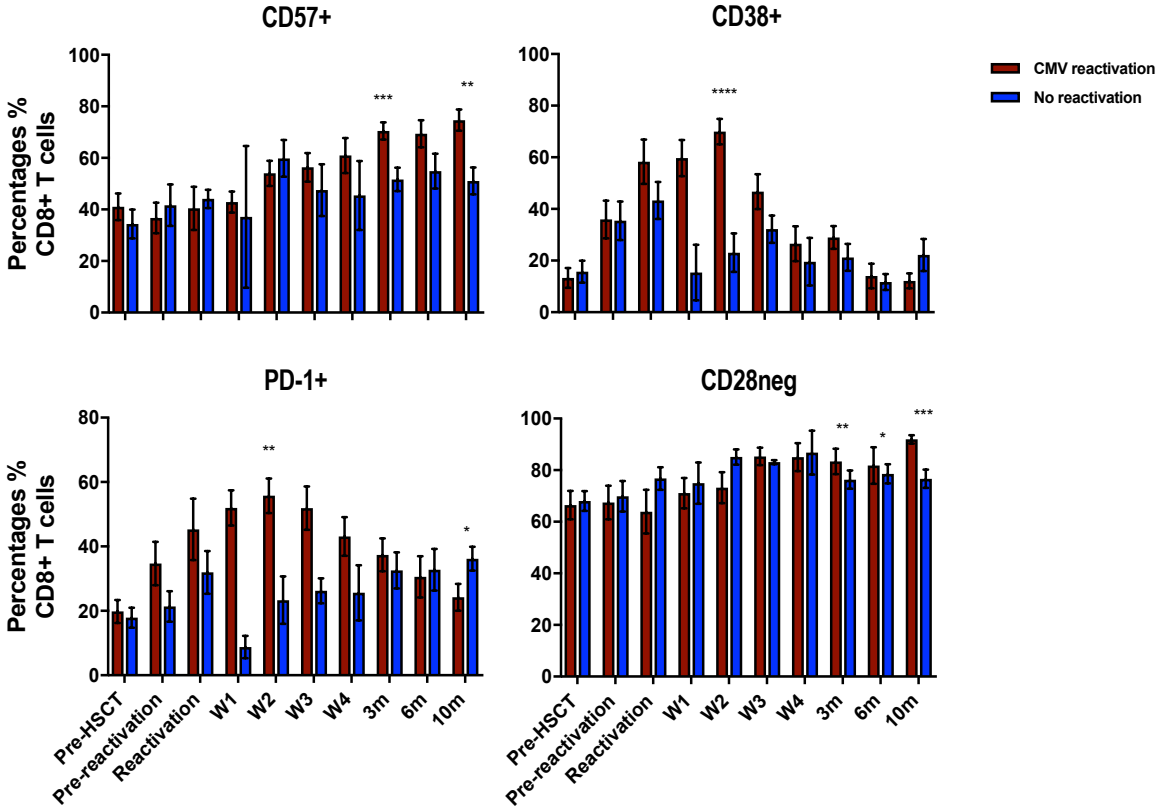


FIGURE 5.3.13. The percentage of CD57$^+$, CD38$^+$, PD-1$^+$ and CD28^{negative} CD8$^+$ T cells in comparison between CMV reactivation (n=37) (red bar) and 'no reactivation' (blue bar) after transplant' (n=26). Analysis was done by Mann Whitney test (*p<0.05, **p<0.01, ***p<0.005). [W: week(s), m: month(s) after CMV reactivation/allo-HSCT].

5.3.1.6. The profile of memory subsets of CD8$^+$ and CD4$^+$ T cells in healthy donors and transplant patients in relation to CMV reactivation

T cells can be separated into four main subsets, naïve T cells, effector memory (EM), effector memory RA (EMRA) and central memory (CM) according to the expression of CCR7 and CD45RA. The examples of flow plots from total CD8$^+$ and CD4$^+$ T cells are shown in **Fig. 5.3.14** and **Fig. 5.3.15**. The flow cytometry plots showed the examples of gating from HDs and CMV reactivation allo-HSCT patient with both total CD8/CD4 and CMV-specific CD8/CD4. Briefly, the CCR7$^+$/CD45RA$^+$ population, CCR7$^+$/CD45RA$^-$ population, CCR7$^-$/CD45RA$^+$

population and CCR7$^-$/CD45RA$^-$ population were classified as Naïve, Central memory, EMRA and Effector memory T cells respectively. The memory phenotypes of CMV seropositive and seronegative HDs, as well as patients with CMV reactivation and without reactivation, were determined by similar gating strategies. However, the analysis for tetramer-positive cells of CD8$^+$ and CD4$^+$ T cells from HDs, and HSCT patients without reactivation, were not included as not enough samples were available for complete statistical analysis.

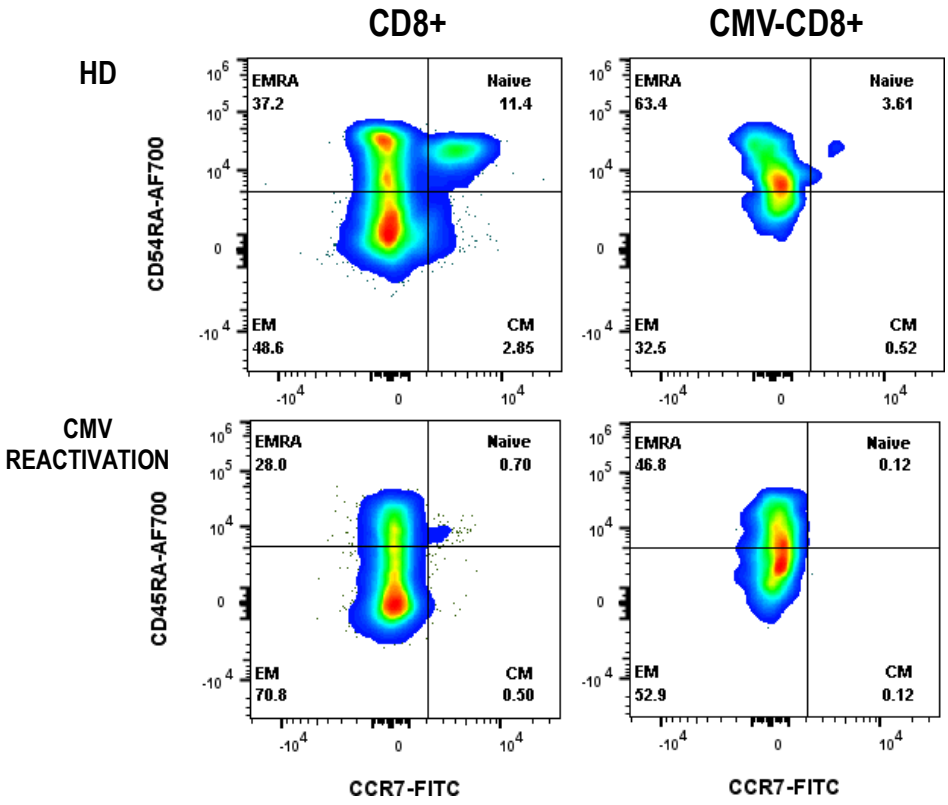


FIGURE 5.3.14. Example of the memory phenotype of total CD8$^+$ and CMV-specific CD8$^+$ T cells in healthy donors and transplant patients according to CCR7 and CD45RA expression. The majority of CD8$^+$ and CMV-CD8$^+$ T cells in CMV seropositive HDs and CMV reactivation allo-HSCT have an effector memory (EM) or EMRA phenotype.

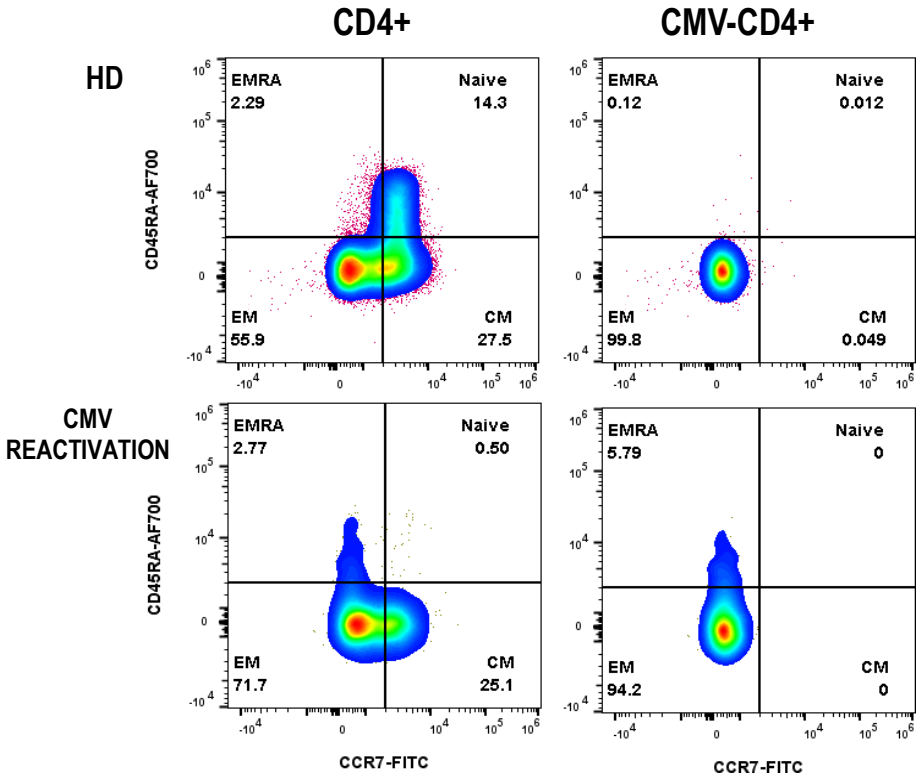


FIGURE 5.3.15. Example of the memory phenotype of total CD4$^+$ and CMV-specific CD4$^+$ T cells in healthy donors and transplant patients according to CCR7 and CD45RA expression. The majority of CD4$^+$ and CMV-CD4$^+$ T cells in CMV seropositive HDs and CMV reactivation allo-HSCT have an effector memory (EM) phenotype.

The proportion of these four subsets was initially compared between CMV negative and CMV positive HDs. As seen from **Fig. 5.3.16**, naïve T cells gated from total CD8$^+$ in HDs have the highest proportion (44.9±3.8%), followed by EM (36.0±3.0%), EMRA (13.4.0±1.4%) and CM (5.7±0.8%) T cells, regardless of CMV serostatus. No differences can be observed from CMV seropositive and seronegative HDs for those phenotypes from total CD8$^+$ T cells **(Fig. 5.3.16)**. Similar to CD8$^+$ T cells, no changes also were seen from memory and naïve phenotypes from CMV seropositive and seronegative HDs on CD4$^+$ T cells. However, in CD4$^+$ T cells CM phenotype constituted majority of the memory subsets with 50.8±3.3%, followed by naïve T cells with 30.3±2.3%, EM

(16.6±1.7%) and EMRA (2.3±1.4%) without taking CMV serostatus into account. It is concluded that proportions and expressions of memory and naïve phenotypes in $CD8^+$ and $CD4^+$ T cells are not markedly affected by CMV serostatus as no changes can be seen between the percentages of CMV positive and CMV negative individuals. Like other analysis, the EM, EMRA, CM and naïve T cell proportions served as a baseline and control for further analysis on CMV reactivation and without reactivation patients, though no data were available on memory and naïve phenotype tetramer positive cells.

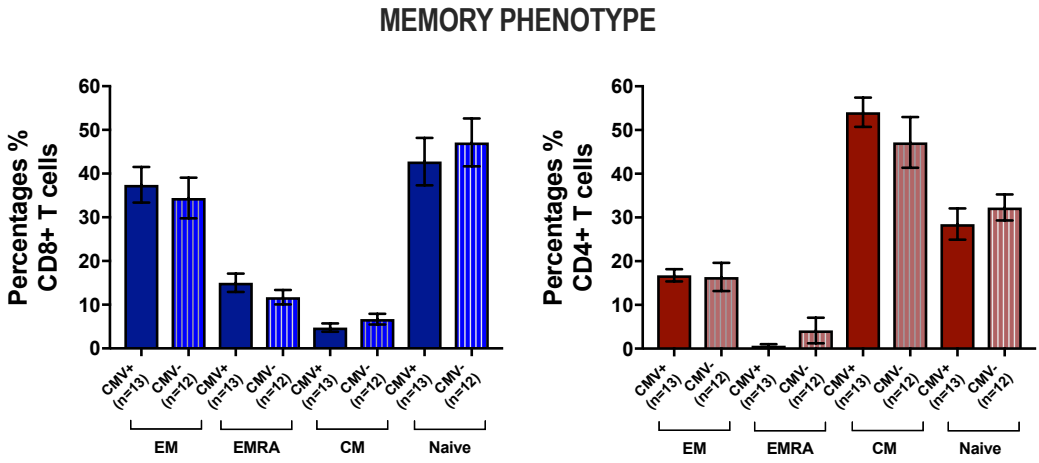


FIGURE 5.3.16. Memory phenotypes of total $CD8^+$ and $CD4^+$ T cells from healthy donors. No differences in the percentages between CMV positive and CMV negative HDs for EM, EMRA, CM and Naïve T cells from both $CD8^+$ and $CD4^+$ T cells. Majority of $CD8^+$ T cells are with Naïve phenotype while most $CD4^+$ T cells are with Central Memory phenotype.

The memory and naïve T cell phenotypes were further investigated in HSCT patients with CMV reactivation or with no CMV reactivation and comparisons were made with the HDs. As shown **(Fig. 5.3.17)**, EM T cells ($CCR7^{-}CD45RA^{-}$) and EMRA T cells ($CCR7\text{-}CD45RA^{+}$) constituted most of $CD8^{+}$ T cells population in HSCT patients with or without CMV reactivation, with 54.8% EM / 28.1% EMRA in patients without CMV reactivation and 66.9% EM / 24.4% EMRA in patients with CMV reactivation. The constitution of the $CD8^{+}$ T cells in HSCT patients was very different from HDs in which naïve T cells comprised the majority of $CD8^{+}$ T cells. The percentage of Naïve CD8 T cells reduced to 5.3% and 14.5% in HSCT patients with CMV reactivation and without reactivation, which was probably due to expansion of EM and EMRA compartments **(Fig. 5.3.17).** Besides, the CMV-specific $CD8^{+}$ T cells in patients with CMV reactivation also contain a high proportion of EM and EMRA T cells.

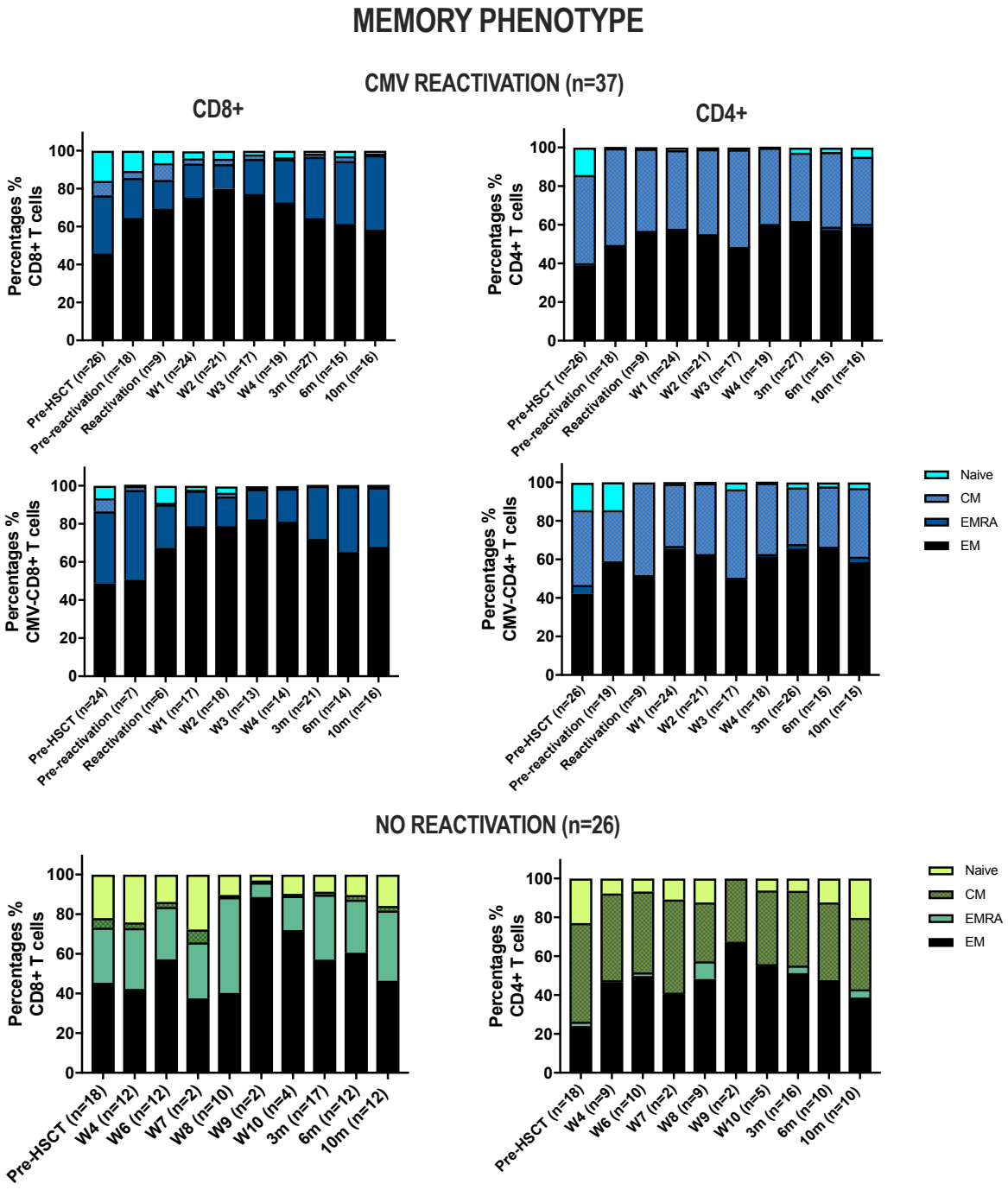


FIGURE 5.3.17. Memory phenotypes of total and CMV-specific CD8$^+$ and CD4$^+$ T cells from healthy donors and HSCT patients with CMV reactivation or no reactivation. [W: week(s), m: month(s) after CMV reactivation/allo-HSCT].

In HDs, most of the $CD4^+$ T cells are those with the CM phenotypes ($CCR7^+CD45RA^-$) and naïve T cells ($CCR7^+CD45RA^+$) having the second highest proportion. But in the HSCT patients with or without CMV reactivation, the $CD4^+$ T cell compartments have shifted into EM, with 54% in patients with CMV reactivation and 46.9% in patients without CMV reactivation. The proportions of naïve CD4 T cells has reduced from 30.3% in HDs to 10.6% in patients with no reactivation and 2.9% in patients with CMV reactivation **(Fig. 5.3.17).**

5.3.1.7. Kinetic changes in naïve and memory phenotypes of $CD8^+$ and $CD4^+$ T cells within HSCT patients in relation to CMV reactivation

The kinetics of change within the memory subsets between the 'reactivation' and 'no-reactivation' groups were next compared. As discussed above, the percentage of naïve T cells is lower compared in transplant patients compared to HDs (grey lines) **(Fig. 5.3.18).** The percentages of CM $CD8^+$ T cells are also downregulated in both patient groups. EM T cells comprise the majority of $CD8^+$ T cells in allo-HSCT patients but a clear trend was observed towards an increase in EM $CD8^+$ T cells after CMV reactivation. This percentage increased immediately after CMV reactivation, peaked around week 3 and decreased until 10 month later. The percentage of EM $CD8^+$ T cells in patients without CMV reactivation varied across the time points with no significant change and was consistently lower compared to those with CMV reactivation **(Fig. 5.3.18).** An increase in the $CD8^+$ EMRA compartment was seen at the later time points in both patient groups **(Fig. 5.3.18).**

For the CMV-specific CD8 T cells in the 'CMV reactivation' patients, the EM subset was the largest proportion, followed by EMRA T cells **(Fig. 5.3.18).** Overall the EM percentage fell over time whilst the EMRA proportion increased from 3 months onwards.

Similar to $CD8^+$ T cells, the proportion of naïve $CD4^+$ T cells is very low in both patient groups **(Fig. 5.3.19).** In those with CMV reactivation the naïve $CD4^+$ T cell pool is hardly detectable (<5%) but it does recover at late time points in those without reactivation. CM cells constituted the major proportion of the $CD4^+$ T cell compartment in both patient groups and were comparable to HDs. EM cells were also a large percentage but were not directly influenced by reactivation status and were broadly stable over time. The percentage of EMRA $CD4^+$ T cells is the lowest among these four subsets (<5%) with no obvious changes over time. Like CMV-$CD8^+$ T cells, the majority of CMV-$CD4^+$ T cells have an EM phenotype although CM cells are also common **(Fig. 5.3.19).**

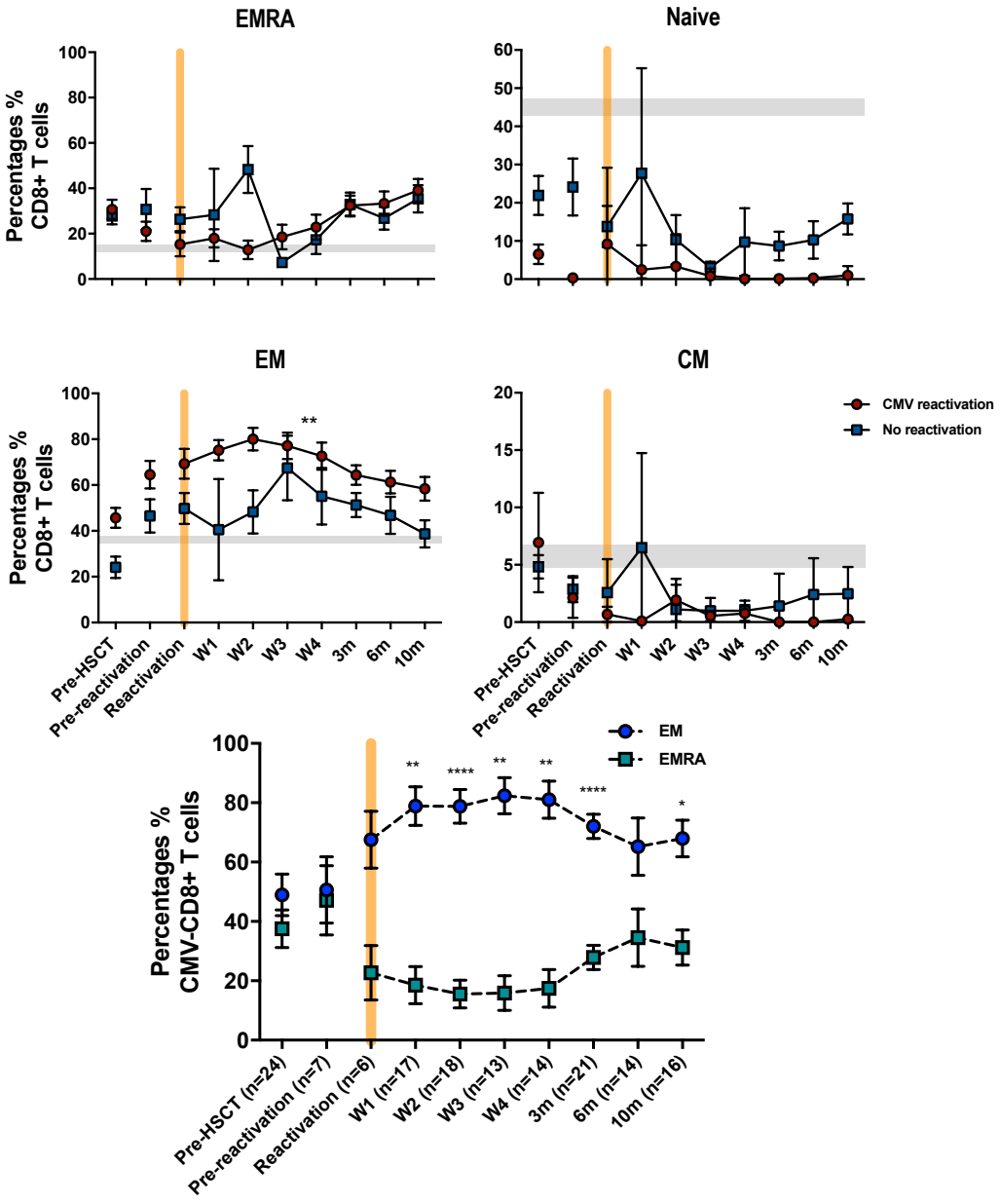


FIGURE 5.3.18. EM, EMRA, CM and naïve T cell proportions within total CD8⁺ from CMV reactivation and without reactivation patients. EM and EMRA T cells percentages were also determined on CMV-specific CD8⁺ T cells percentages from CMV reactivation patients. Range of HDs' memory and naïve T cell percentages are shown in grey lines. Analysis was done by Wilcoxon sign rank test (*p<0.05, **p<0.01, ***p<0.005). [W: week(s), m: month(s) after CMV reactivation/allo-HSCT].

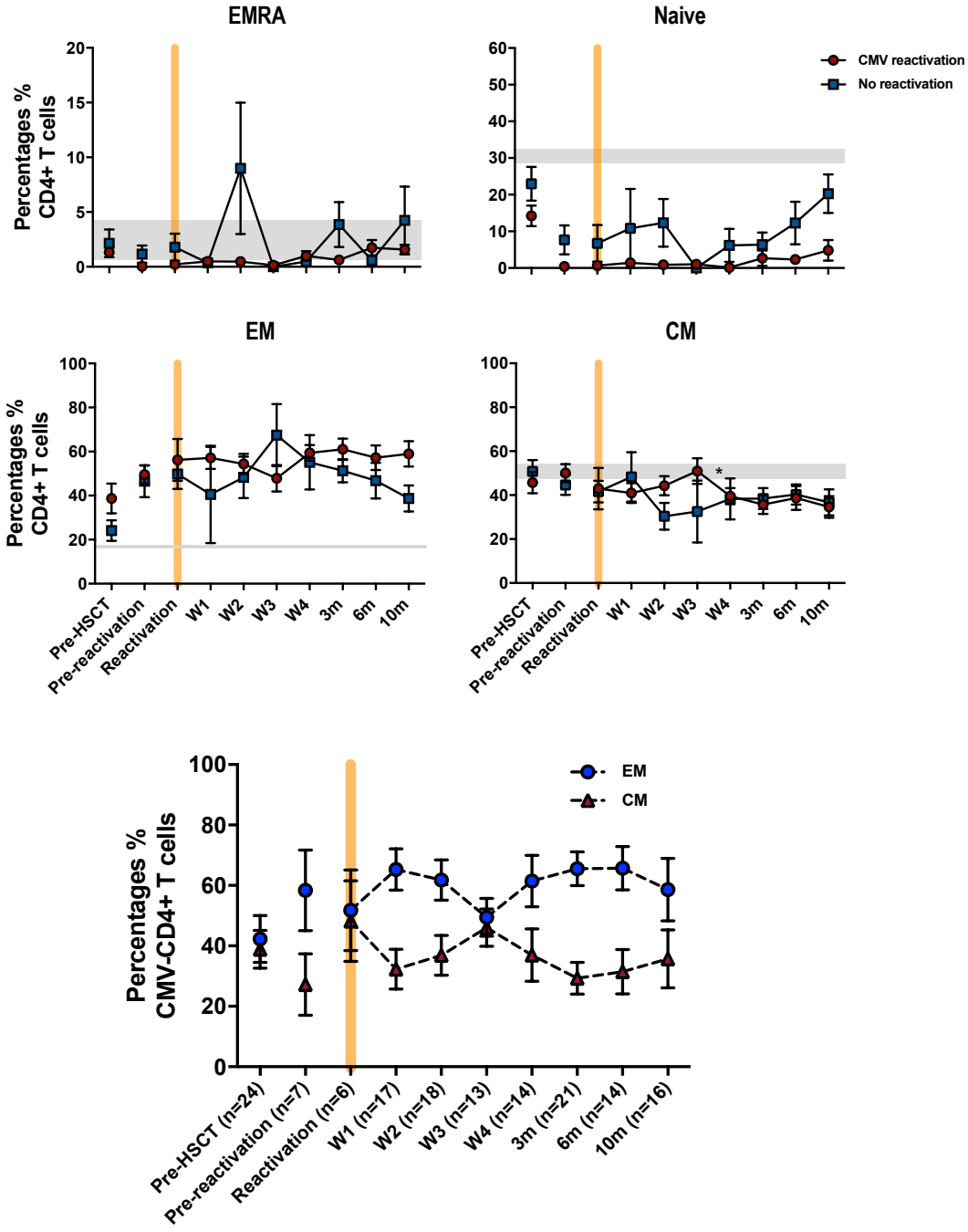


FIGURE 5.3.19. EM, EMRA, CM and naïve T cell proportions within total CD4$^+$ T cells from patients with CMV reactivation or 'no reactivation'. EM and CM T cells percentages were also determined on CMV-specific CD4$^+$ T cells from CMV reactivation patients. Range of HDs' memory and naïve T cell percentages are shown in grey lines. Analysis was done by Wilcoxon sign rank test (*p<0.05, **p<0.01, ***p<0.005). [W: week(s), m: month(s) after CMV reactivation/allo-HSCT].

5.3.1.8. Comparison of memory phenotypes of total $CD8^+$ and $CD4^+$ T cells in relation to CMV reactivation

Comparison also was made of the memory and naïve T cell phenotypes from total $CD8^+$ and $CD4^+$ T cells between patients with CMV reactivation and no reactivation over time. Strikingly, increases can be seen in the proportion of EM T cells within total $CD8^+$ at most time points after CMV reactivation. This indicates that the expansion of EM CD8 T cells is driven by CMV reactivation and could represent both CMV-specific $CD8^+$ T cells and $CD8^+$ T cells with our antigenic specificity. Interestingly, not many changes are seen in the proportions of EM $CD4^+$ T cells until 10 months after reactivation, which implies that the EM $CD4^+$ expansion driven by CMV is a delayed phenotype compared with $CD8^+$ T cells **(Fig. 5.3.20).**

Comparison was also done on EMRA T cells phenotypes from both $CD8^+$ and $CD4^+$ T cells. Within W2 after CMV reactivation, the percentage of the $CD8^+$ EMRA T cells from patients with CMV reactivation showed a decrease but recovered afterward within W3 **(Fig. 5.3.20).** This observation could be due to the big expansion of EM $CD8^+$ T cells at this early stage of CMV reactivation.

No significant differences can be seen within $CD8^+$ and $CD4^+$ in relation to the proportion of CM T cells with or without reactivation. Naïve T cells from both $CD8^+$ and $CD4^+$ are barely detectable in 'CMV reactivation' patients especially after reactivation occurred. However, the total number of T cells is markedly increased by viral reactivation and as such the absolute number of naïve T cells may be less affected.

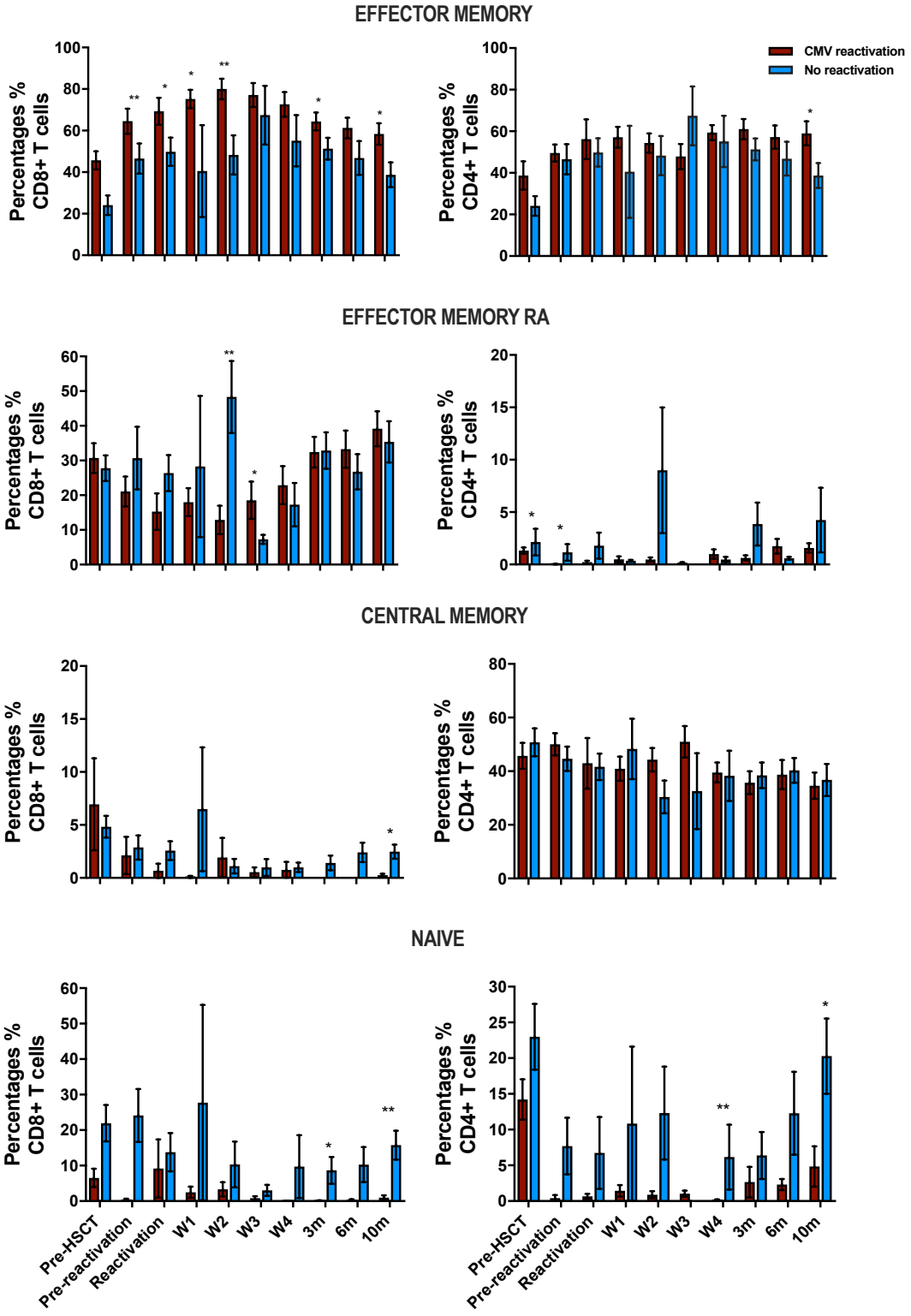


FIGURE 5.3.20. EM, EMRA, CM and naïve T cell percentage within total CD8$^+$ and CD4$^+$ T cells in relation to CMV reactivation or 'no reactivation'. No data is available on tetramer-positive cells from no reactivation patients. Analysis was done by Mann Whitney test (*p<0.05, **p<0.01, ***p<0.005). [W: week(s), m: month(s) after CMV reactivation/allo-HSCT].

5.3.1.9. Memory phenotypes of $CD8^+$ and $CD4^+$ T cells in relation to 'CMV risk group' after allo-HSCT

As has been discussed before, the CMV R+/D- transplant combination poses a risk in allo-HSCT as the donors do not transmit CMV-specific immune memory. Therefore, the EM and EMRA proportion of both total $CD8^+$ T cells and CMV-$CD8^+$ T cells were further investigated in the two 'CMV risk' groups, R+/D- and R+/D+ in relation to CMV reactivation. Interestingly, the percentages of $CD8^+$ EM and $CD8^+$ EMRA T cells were lower in R+/D- CMV reactivation patients at the early time points of CMV reactivation compared (EM at reactivation and EMRA at pre-reactivation) with R+/D+ patients but this difference was lost at later time points **(Fig. 5.3.21).** Also, for the CMV-specific $CD8^+$ T cells, there was less EMRA $CD8^+$ T cells at early time points after CMV reactivation. This fits in with the hypothesis that there are less CMV-specific $CD8^+$ T cells in the R+/D- patients at the early points due to the CMV negative donors, but the CMV reactivation can soon shape the immune cells from CMV negative donors to the same phenotype as R+/D+ patients. No obvious changes were seen with the $CD4^+$ T cells compartment between R+/D+ and R+/D- groups **(Fig. 5.3.22).**

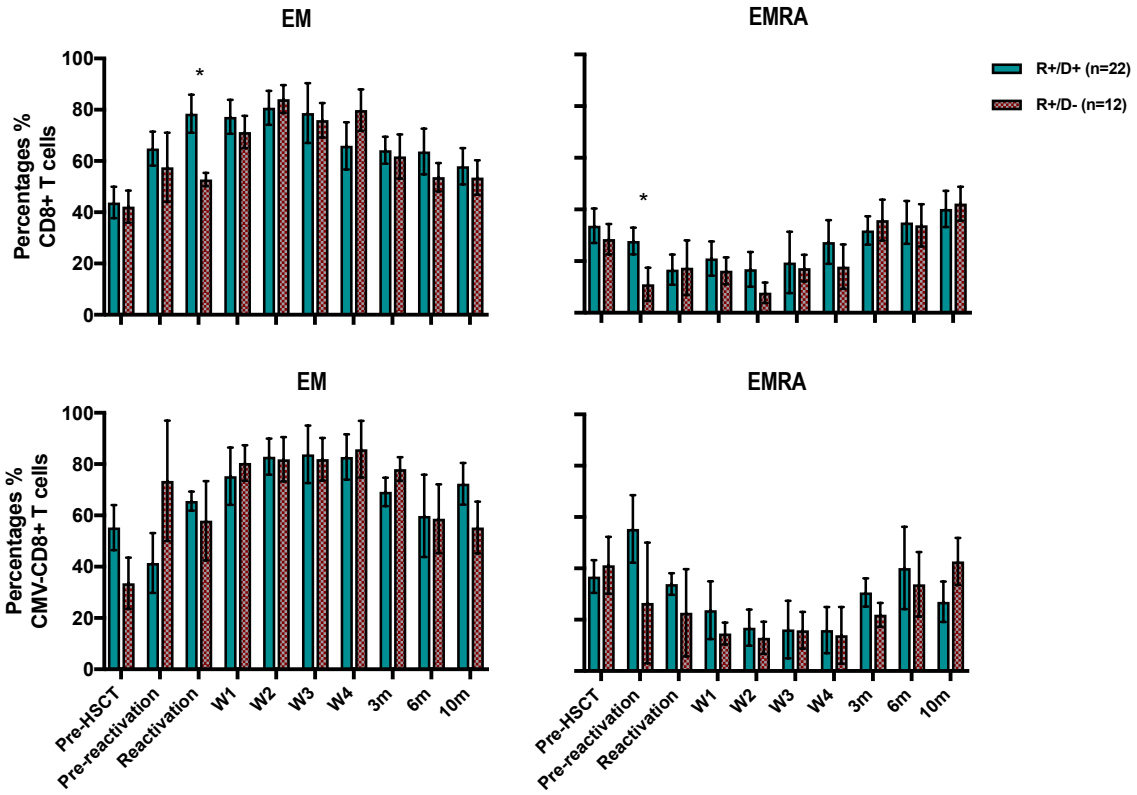


FIGURE 5.3.21. EM and EMRA phenotypes comparison from CD8$^+$ T cells between R+/D- and R+/D+ CMV reactivation patients. Decreases in EM CD8$^+$ T cells can be seen in R+/D- group at week of reactivation as well as EMRA CD8$^+$ T cells at the pre-reactivation week. Analysis was done by Mann Whitney test (*p<0.05, **p<0.01, ***p<0.005). [W: week(s), m: month(s) after CMV reactivation/allo-HSCT].

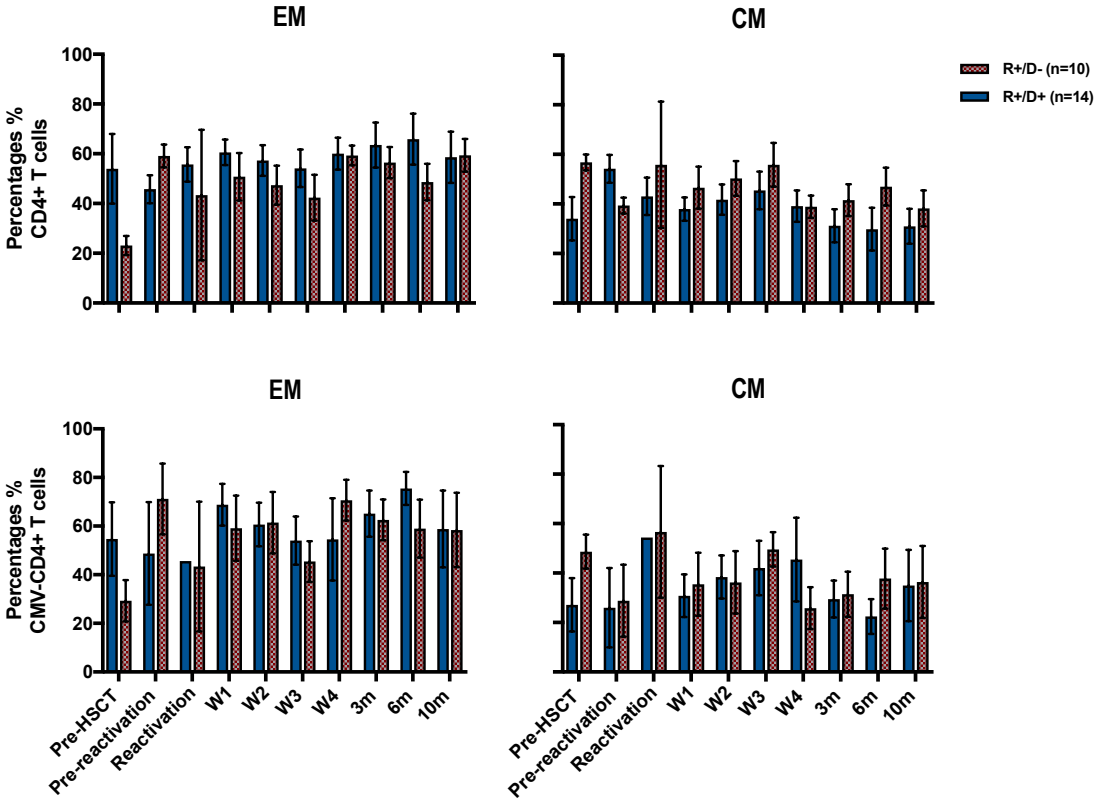


FIGURE 5.3.22. EM and EMRA phenotypes comparison from CD4$^+$ T cells between R+/D- and R+/D+ CMV reactivation patients. Unlike CD8$^+$ T cells, no major changes can be seen in EM and CM T cells from CD4$^+$ T cells as well as CMV-CD4$^+$ T cells. The analysis was done on EM and EM as these are the major CD4$^+$ T cell phenotypes that reside in the peripheral bloods of CMV reactivation patients. The analysis for other phenotypes such as CD8$^+$ CM and naïve T cells, as well as CD4$^+$ EMRA and naïve T cells were not performed due to low percentages. Analysis was done by Mann Whitney test (*p<0.05, **p<0.01, ***p<0.005). [W: week(s), m: month(s) after CMV reactivation/allo-HSCT].

5.3.2. The reconstitution of unconventional T cells including γδ T cells in HSCT patients with CMV reactivation

5.3.2.1. Gating strategies and analysis

It was also our interest to assess how CMV reactivation impacted on the regeneration of 'non-classical' T cells after transplantation. In particular, γδ T cells have been shown to respond to CMV viraemia in other settings.

γδ T cell gating strategy was done in a separate T cell flow cytometry analysis as shown in **Fig. 5.3.23** and **Fig. 5.3.24.** In this panel, both $CD8^+$ and $CD4^+$ T cells antibodies were included thus the analysis were further carried out for the $CD8^+CD4^+$ and $CD8^-CD4^-$ populations. Similar gating strategies were applied as previous chapters such as singlets, lymphocytes and live cells. After the T cells were identified as $CD3^+$ and $CD56^{+/-}$, four different populations of T cells that include $CD8^+CD4^+$, $CD8^+CD4^-$, $CD8^+$ and $CD4^+$ T cells were determined according to their expression of CD4 and CD8.

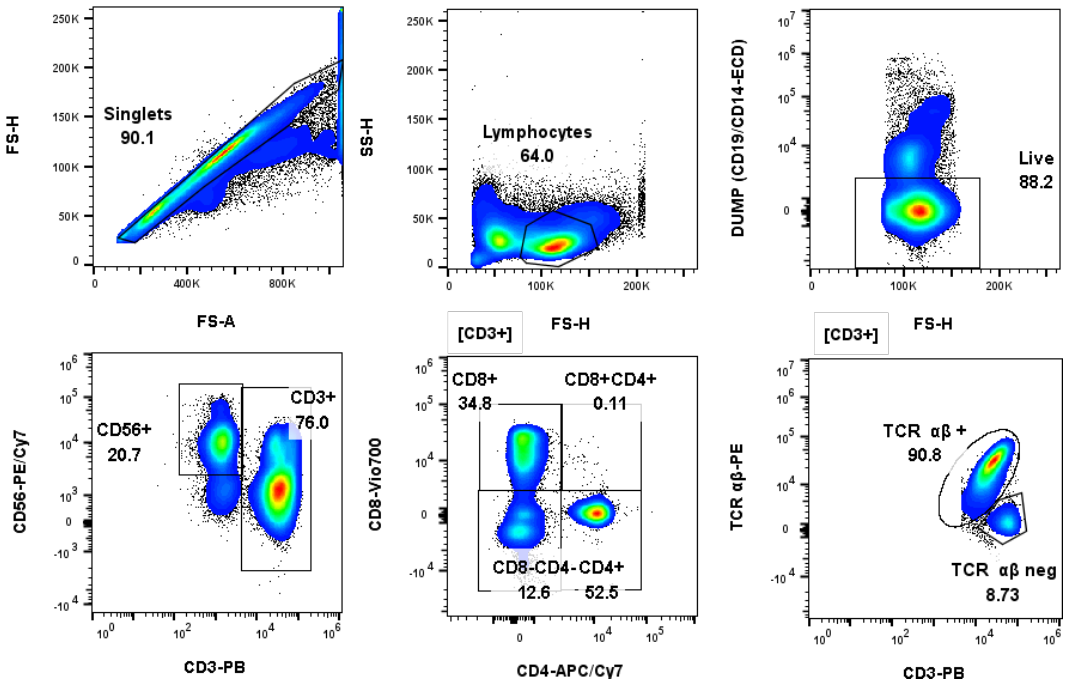


FIGURE 5.3.23. TCRαβ and γδ T cells gating strategy. TCRαβ and γδ T cells were gated from singlets and lymphocytes. Monocytes (CD14), B cells (CD19), and dead cells (stained with PI in dump channel) were excluded from gated T cell populations. $CD8^+$, $CD4^+$ and double negative and double positive cells were determined from $CD3^+$ cells and TCRγδ T cells were gated from αβ negative.

The γδ T cells were determined by TCRαβ-negative phenotype within the total $CD3^+$ population as shown from **Fig. 5.3.23** and **Fig. 5.3.24.** TCRγδ T cells were determined as TCRαβ-negative T cells instead of using pan γδ-specific antibodies as this minimises the interference with other TCR antibodies (such as Vδ1 and Vδ2). **Fig. 5.3.24** showed the further CD4 and CD8 staining of the TCRαβ negative T cells, i.e. γδ T cells. The majority of γδ T cells have a $CD8^-CD4^-$ phenotype.

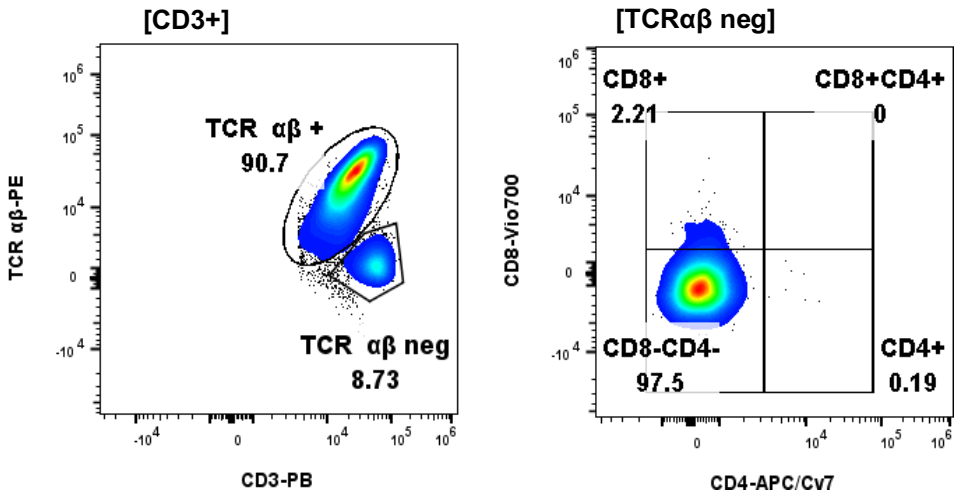


FIGURE 5.3.24. TCRαβ and γδ T cells (gated from αβ negative) CD3$^+$ population from healthy donor. γδ T cells determined by TCRαβ negative population, and majority of γδ T cells are with CD8 and CD4 double negative.

5.3.2.2. Pattern of CD8$^+$ and CD4$^+$ co-expression on T cells in healthy donors

Following the gating strategy that has been described before, the majority of T cells in HDs are CD4$^+$ T cells, followed by CD8$^+$, CD8$^-$CD4$^-$ and then CD8$^+$CD4$^+$ T cells. As shown in **Fig. 5.3.25**, no changes in the composition of different subsets of CD4$^+$ and CD8$^+$ T cells can be seen between CMV seropositive and CMV seronegative HDs. Regardless of CMV serostatus, the double positive CD8$^+$CD4$^+$ T cells constituted 0.6±0.09% of CD3$^+$ T cell compartment while CD8$^-$CD4$^-$ comprised of 7.5±1.0% of total CD3$^+$ T cells in HDs. Moreover, CD8$^+$ T cells analysed from this panel comprised 33±1.7% of T cells, while CD4$^+$ constituted about 59±2.1% of total CD3$^+$ T cells from the same HDs.

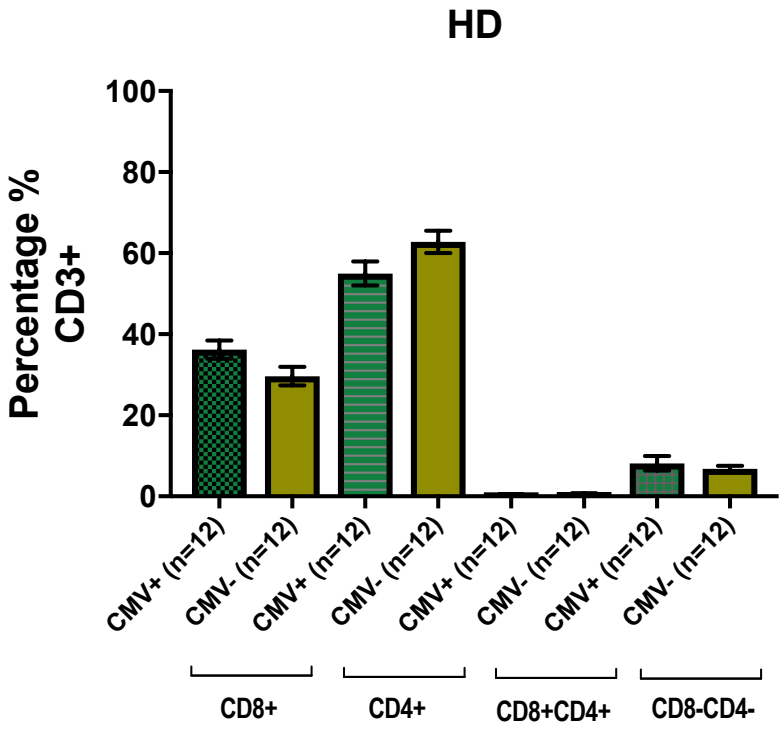


FIGURE 5.3.25. Different T cell subset percentages in healthy donors according to $CD4^+$ and $CD8^+$ expression. Populations of different subsets of T cells which are the $CD8^+$, $CD4^+$, $CD8^-CD4^-$ and $CD8^+CD4^+$ from total $CD3^+$ T cells. Range of $CD8^+$ T cells percentages from CMV seropositive to CMV seronegative HDs are 36.2±2.3% to 29.7±2.3%, $CD4^+$; 55.0±3.0% to 62.8±2.8%, $CD8^+CD4^+$; 0.5±0.08% to 0.6±0.2% and $CD8^-CD4^-$; 8.2±1.8% to 6.9±0.7%. Analysis was done by Mann Whitney test (*p<0.05, **p<0.01, ***p<0.005).

5.3.2.3. Pattern of $CD8^+$ and $CD4^+$ co-expression on T cells in allo-HSCT patients

In HSCT patients without CMV reactivation the average proportion of $CD3^+$ T cells from all time points was 39±18% for $CD8^+$ T cells; $CD4^+$, 52±2.1%; $CD8^+CD4^+$, 0.3±0.07% and $CD8^-CD4^-$; 8.2±1.4% which are comparable to those of HDs. In allo-HSCT patients with CMV reactivation, the proportions of $CD3^+$ T cells changed to 58±4.2% for $CD8^+$ T cells, 37±3.9% for $CD4^+$ T cells, 0.3±0.04% for $CD8^-CD4^-$ T cells and 4.6±0.7% for $CD8^-CD4^-$ T cells. As an increase in the proportion of $CD8^+$ T cells has been seen before in association with CMV

reactivation **(Fig. 5.3.3** and **5.3.4)**, the emphasis here is on $CD8^+CD4^+$ and $CD8^-CD4^-$ T cells, but there are no significant changes that can be seen between patients with CMV reactivation and without CMV reactivation for the proportion of $CD8^-CD4^-$ and $CD8^+CD4^+$T cells.

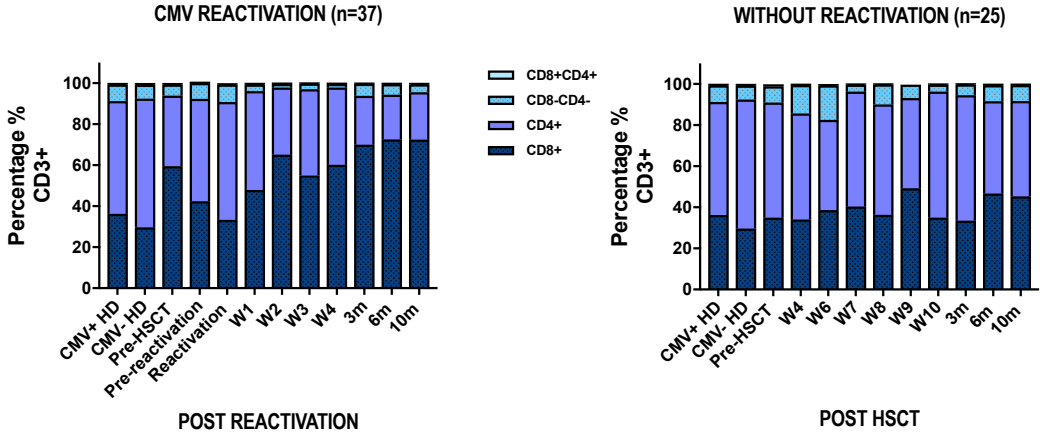


FIGURE 5.3.26. T cells percentages in allo-HSCT patients without reactivation and with reactivation allo-patients according to $CD4^+$ and $CD8^+$ expression. Populations of different subsets of T cells which are the $CD4^+$, $CD8^+$, $CD8^-CD4^-$ and $CD8^+CD4^+$ were acquired from γδ T cell panel. Analysis was done by Mann Whitney and Wilcoxon sign rank test (*p<0.05, **p<0.01, ***p<0.005). [W: week(s), m: month(s) after CMV reactivation/allo-HSCT].

5.3.2.4. γδ T cells in healthy donors and transplant patients

Fig. 5.3.27 showed the example of flow cytometry plots of γδ T cells from CMV seropositive and CMV seronegative HDs, as well as patients with CMV reactivation and no reactivation. The γδ T cells were identified as the TCRαβ-negative $CD3^+$ population. In HDs, TCRαβ-negative or TCRγδ T cells constituted about 6.9±1.0% of peripheral blood with TCRαβ constituted about 93±1.1% **(Fig. 5.3.28).** No changes can be seen in between CMV seropositive and CMV seronegative HDs for TCRαβ T cells [TCRαβ; CMV seropositive: 90.1±2.0% (n=12), CMV

seronegative: 94.4±0.7% (n=12), TCRαβ neg / TCRγδ: CMV seropositive 8.6±1.9% (n=12), CMV seronegative: 5.3±0.7% (n=12)]. **Fig. 5.3.28** showed average proportions of both TCRαβ and TCRγδ T cells in HDs regardless of CMV serostatus (n=24).

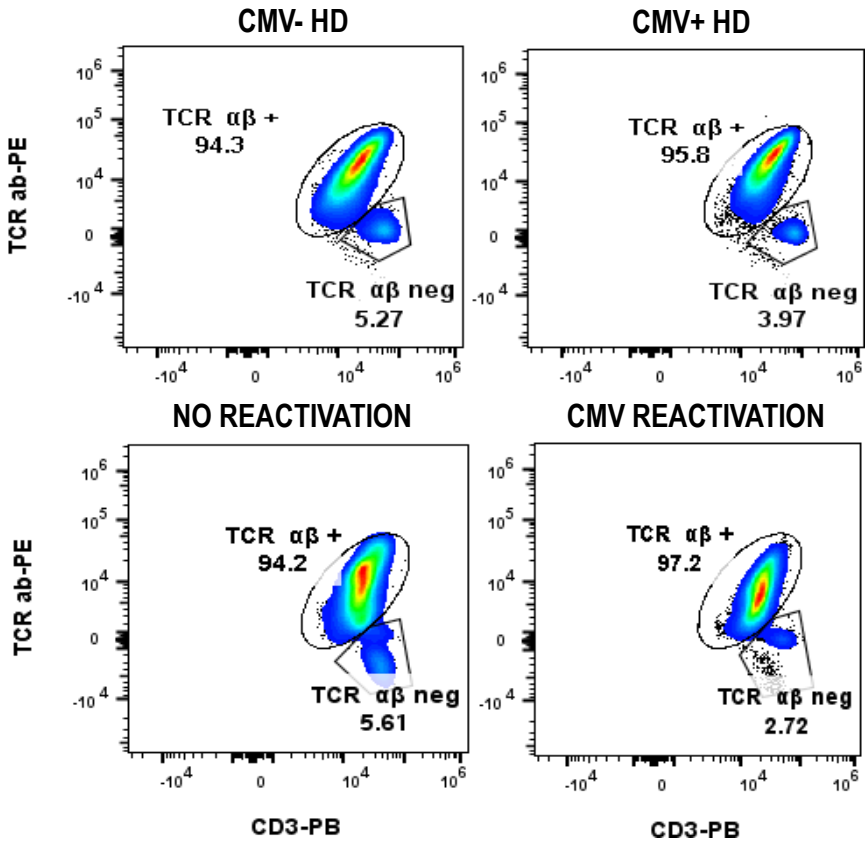


FIGURE 5.3.27. TCRαβ negative or γδ T cells plots gated from total CD3$^+$ population from healthy donors, CMV reactivation and no reactivation patients. γδ T cells were determined by TCRαβ negative population.

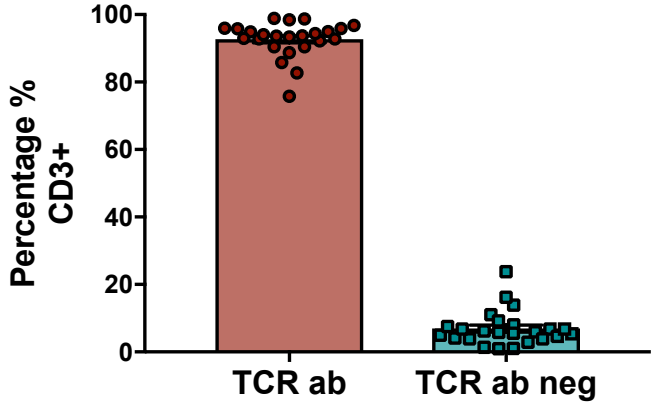


FIGURE 5.3.28. TCRαβ and γδ T cells (gated from αβ negative) CD3$^+$ population from healthy donors. γδ T cells were determined as the TCRαβ-negative population, and majority of γδ T cells are with CD8 and CD4 double negative. TCRαβ percentages are 92.7±1.1% and TCRαβ negative are 6.9±1.0% (n=24). TCRαβ; CMV seropositive: 90.1±2.0% (n=12), CMV seronegative: 94.4±0.7% (n=12), TCRγδ: CMV seropositive 8.6±1.9% (n=12), CMV seronegative: 5.3±0.7% (n=12). Analysis was done by Wilcoxon sign rank test (*p<0.05, **p<0.01, ***p<0.005).

Then the proportion of TCRγδ T cells was analysed in HSCT patients with CMV reactivation. In patients with CMV reactivation, the average percentage of TCRγδ T cells from total CD3$^+$ T cells of all time points is about 8.0±1.8% in peripheral bloods while in no reactivation patients, the percentage is about 5.7±0.9% **(Fig. 5.3.29).** These numbers are not far from the percentages found in HDs.

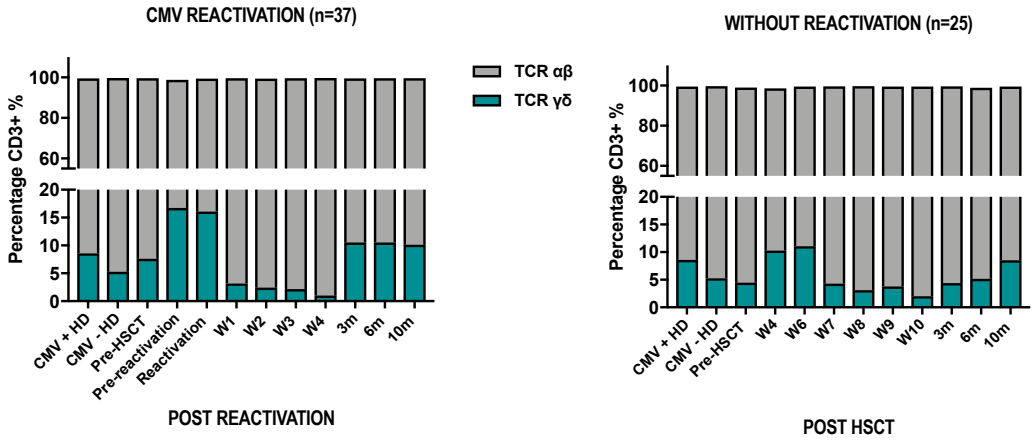


FIGURE 5.3.29. TCRαβ and γδ T cell populations from healthy donors. γδ T cells were determined by TCRαβ-negative population, and the majority of γδ T cells are CD8 and CD4 double negative. [W: week(s), m: month(s) after CMV reactivation/allo-HSCT].

However, when we looked at different time points, it was a different story. In the HSCT patients with no CMV reactivation, there were no significant changes in the proportion of TCRγδ T cells through the time course, although percentages were quite low in the early time points after transplant, equivalent to W1 to W4 after CMV reactivation.

For the patients with CMV reactivation, there was a brief increase in the percentage of TCRγδ T cells straight after the CMV reactivation. Then the percentage went down but picked up in the long-term time points. Significant expansions can be seen from one week to 10 months after reactivation, with a specific increase between 3 to 6 months' time points **(Fig. 5.3.30).** In fact, total TCRγδ T cells in both patients with CMV reactivation and no reactivation were generally lower than HDs (grey lines) from W1 to W4 after CMV and began to reconstitute above the HD threshold at 3 months' time point. At the 3-month time point, the percentage of TCRγδ T cells was significantly higher in patients with CMV reactivation then the patients with no reactivation. This difference became less obvious at later time points. This observation does point to a hypothesis that CMV infection contributes to the expansion of TCRγδ T cells. Interestingly, a significant increase can also be seen in the absolute number of γδ T cells in patients with CMV reactivation after 3 months, with no similar increase seen in patients without reactivation.

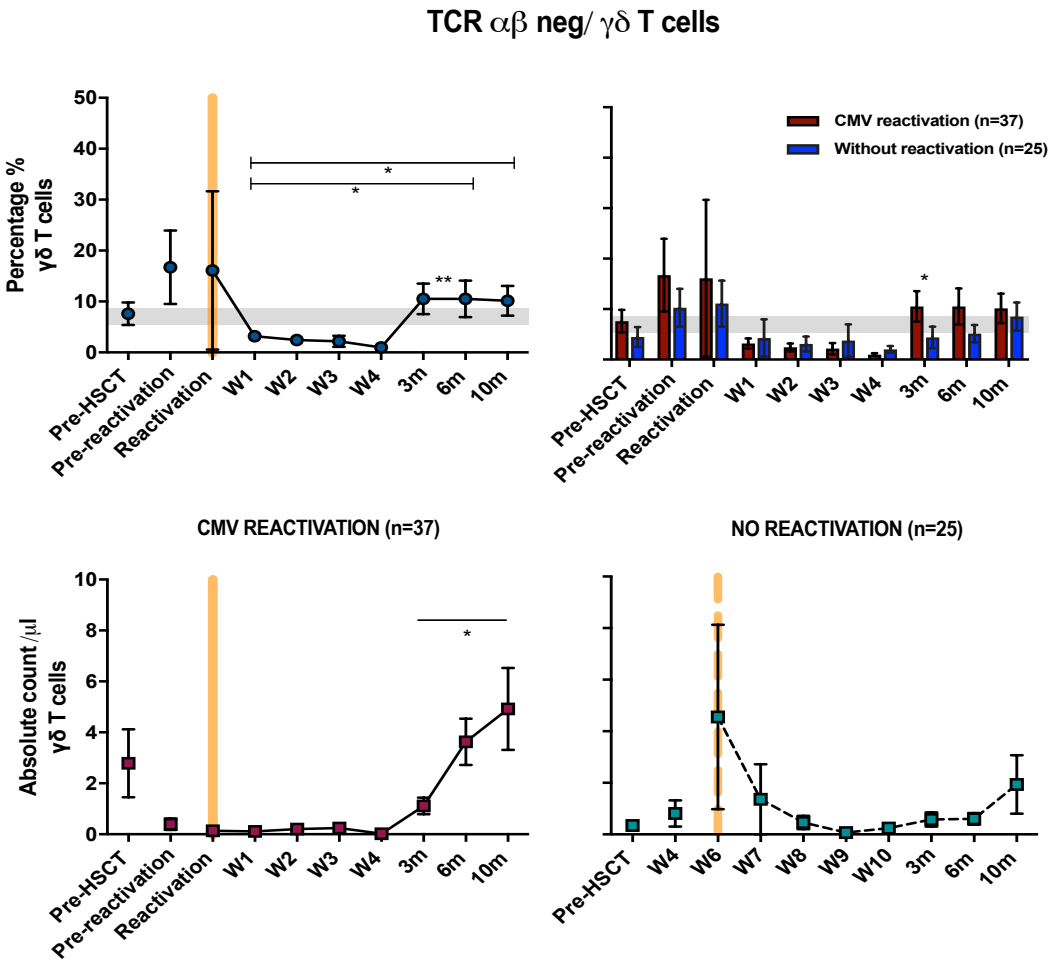


FIGURE 5.3.30. The percentage and absolute count of TCRγδ cells after transplant in relation to CMV reactivation. There is an expansion of TCRγδ T cells percentages following time points after CMV reactivation as compared to HDs represented by dotted grey line (6.9±1.0%), as well as expansion in the absolute count after 3 months of reactivation. Analysis was done by Mann Whitney and Wilcoxon sign rank test (*p<0.05, **p<0.01, ***p<0.005). [W: week(s), m: month(s) after CMV reactivation/allo-HSCT].

5.3.2.5. The percentage distribution of $CD8^+$, $CD4^+$, $CD8^+CD4^+$ and $CD8^-CD4^-$ within TCRγδ cells in healthy donors and HSCT patients with or without CMV reactivation

As can be seen from **Fig. 5.3.24**, the majority of TCRγδ T cells are found within the CD4 and CD8 double negative population. It was therefore considered interesting to see if CMV reactivation would alter the $CD4^+$ and $CD8^+$ profile of TCRγδ T cells. **Fig. 5.3.31** shows the flow cytometry plots to identify $CD8^+$, $CD4^+$, $CD8^+CD4^+$ and $CD8^-CD4^-$ TCRγδ T cells in the various patient cohorts.

In HDs, most TCRγδ T cell are $CD8^-CD4^-$ (72.1±0.9%), with 64.8±6.0% and 79.3±0.3% proportions can be seen from CMV seropositive to CMV seronegative individuals respectively **(Fig. 5.3.32).** Only 22.3±4.0% γδ T cells are $CD8^+$ (CMV positive: 22.3±4.0%, CMV negative: 16.8±4.3%), and 4.2±0.9% are $CD8^+CD4^+$ (CMV negative: 5.4±1.6%, CMV negative: 3.0±0.5%). The γδ T cells with $CD4^+$ are barely detectable in HDs, only around 0.5±0.2%, range from 0.7±0.3% to 0.4±0.1% from CMV positive to CMV negative HDs. There was no significant difference seen between CMV negative and CMV positive HDs.

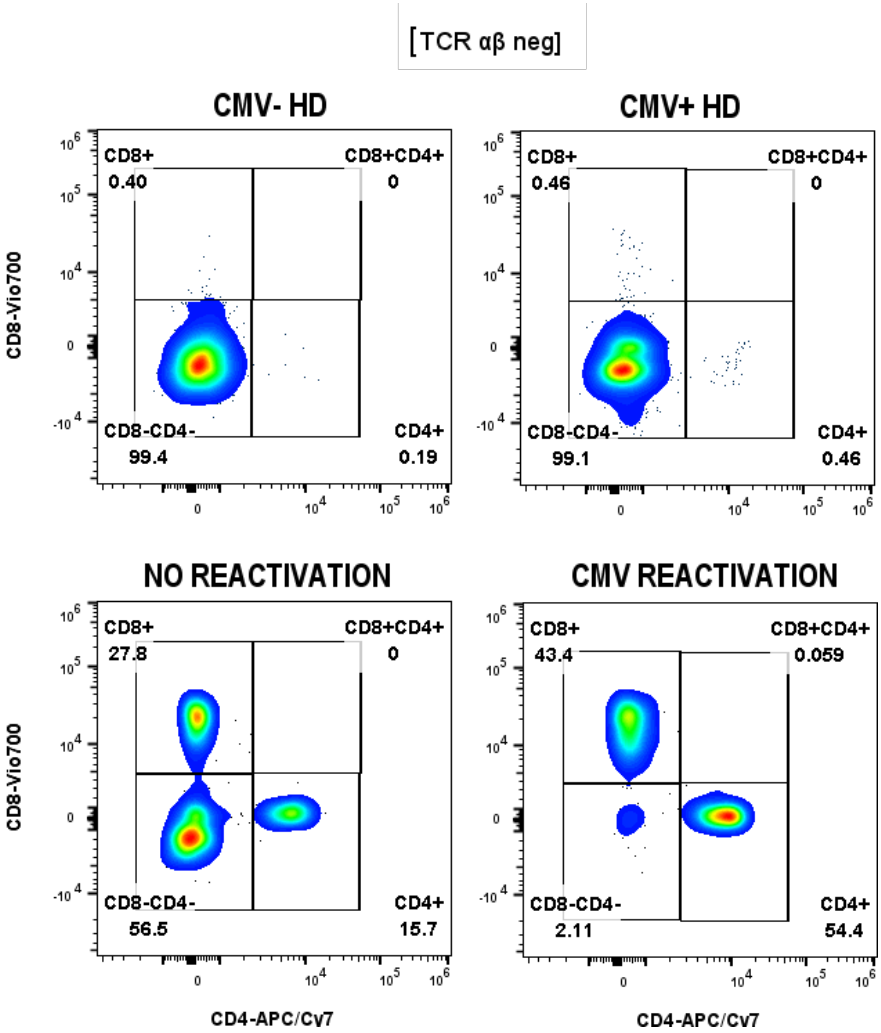


FIGURE 5.3.31. Example of gating strategy of $CD8^+$, $CD4^+$, $CD8^+CD4^+$ and $CD8^-CD4^-$ subsets of TCRγδ T cells in healthy donors and transplant patients, with or without CMV reactivation. The gating strategy is different from previous $CD8^+$ and $CD4^+$ T cells analysis.

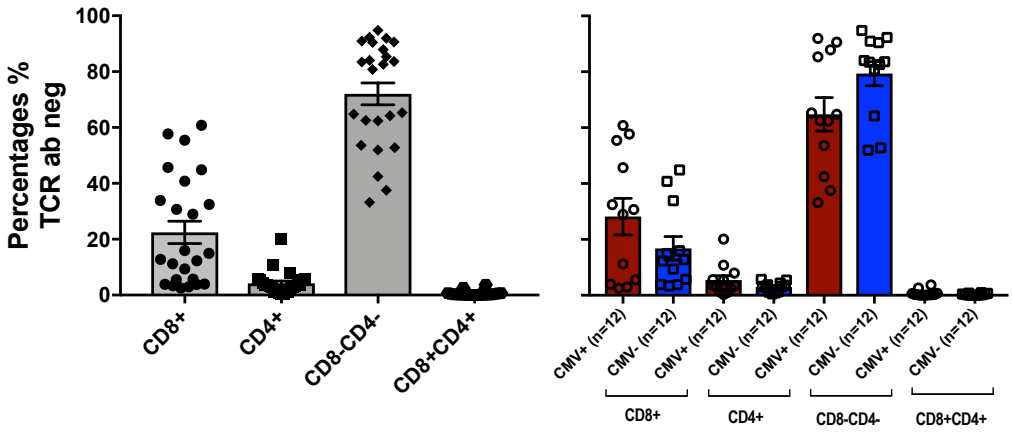


FIGURE 5.3.32. $CD8^+$, $CD4^+$, $CD8^+CD4^+$ and $CD8^-CD4^-$ subsets of TCRγδ cells in healthy donors and HSCT patients, with or without viral reactivation. The average percentages of TCRγδ T cells regardless of CMV serostatus are; 22.3±4.0% for $CD8^+$, 4.2±0.9% for $CD4^+$, 72.1±0.9% for $CD8^-CD4^-$ and 0.5±0.2% for $CD8^+CD4^+$T cells (n=24). Analysis was done by Mann Whitney and Wilcoxon sign rank test (*p<0.05, **p<0.01, ***p<0.005).

Compared to HDs, no significant differences were seen in the percentage of $CD8^+$, $CD4^+$, $CD8^+CD4^+$ and $CD8^-CD4^-$ TCRγδ T cells in patients without viral reactivation (27±3.9%, 5.8 ±0.9%, 0.6±0.2% and 66±4.1% respectively). On the other hand, the average percentages of $CD8^+$, $CD4^+$, $CD8^+CD4^+$ and $CD8^-CD4^-$ TCRγδ T cells in patients with CMV reactivation are 50±1.3%, 6.0±1.3%, 0.7±0.2% and 42±1.9% respectively. As such a significant increase of the percentages of $CD8^+$ γδ T cells in patients with CMV reactivation can be noticed, particularly at W2, 3 months and 10 months' time points **(Fig. 5.3.33).**

Following this increase in the percentage of $CD8^+$ γδ T cells, a simultaneous decrease in the $CD8^-CD4^-$ TCRγδ T cell subset percentage can be seen in patients with CMV reactivation when compared with patients with no reactivation **(Fig. 5.3.33)**. Overall analysis showed a significant decrease in patients with CMV reactivation for $CD8^-CD4^-$ TCRγδ T cells (p=0.0007, Mann Whitney test) and significant increase in $CD8^+$ TCRγδ T cells (p=0.0005, Mann Whitney test), suggesting that CMV reactivation is promoting the expansion of $CD8^+$ γδ T cells following reactivation.

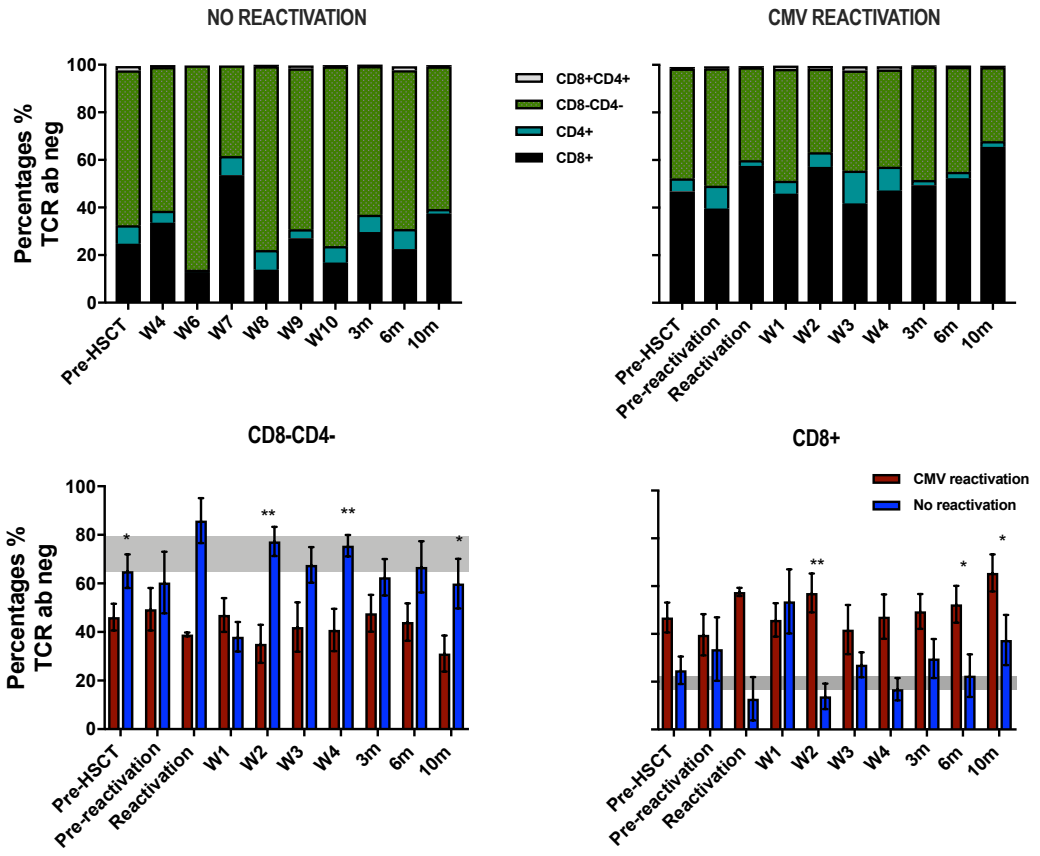


FIGURE 5.3.33. Percentages of $CD8^+$, $CD4^+$, $CD8^+CD4^+$ and $CD8^-CD4^-$ TCRγδ T cells in HSCT patients without CMV reactivation (n=25) or following CMV reactivation patients (n=37). The average percentages of TCRγδ T cells regardless of CMV serostatus are; 22±4.0% for $CD8^+$, 4.2 ±0.9% for $CD4^+$, 72±0.9% for $CD8^-CD4^-$ and 0.5±0.2% for $CD8^+CD4^+$T cells. Analysis was done by Mann Whitney and Wilcoxon sign rank test (*p<0.05, **p<0.01, ***p<0.005). [W: week(s), m: month(s) after CMV reactivation/allo-HSCT].

5.3.2.6. Vδ2 negative and Vδ2 positive γδ T cell subsets in healthy donors

TCRγδ T cells can be broadly divided to two major populations, Vδ2 negative and Vδ2 positive, which are considered to represent broadly adaptive or innate immunity respectively (Davey et al., 2018c). As such it would be informative to analyse the dynamic changes of the different TCRγδ T cells subsets after CMV reactivation.

Fig. 5.3.34 shows the flow cytometry plots of the histograms to distinguish Vδ2 negative and Vδ2 positive populations gated on TCRαβ-negative T cells. In HDs, the main γδ T cell subset circulating within the peripheral blood is the Vδ2 T cells. Regardless of CMV serostatus, the average percentage of Vδ2 negative T cells is 38.7±5.8% while 61.3±5.8% of TCRγδ T cells are Vδ2 positive **(Fig. 5.3.35).** No differences can be observed between CMV negative and CMV positive HDs when Vδ2 positive and negative T cell percentages were compared (Vδ2 negative; CMV seropositive: 46.6±8.5%, CMV seronegative: 30.7±7.3%, Vδ2 positive; CMV seropositive: 53.4±8.5%, CMV seronegative: 69.3±7.3%) **(Fig. 5.3.35).**

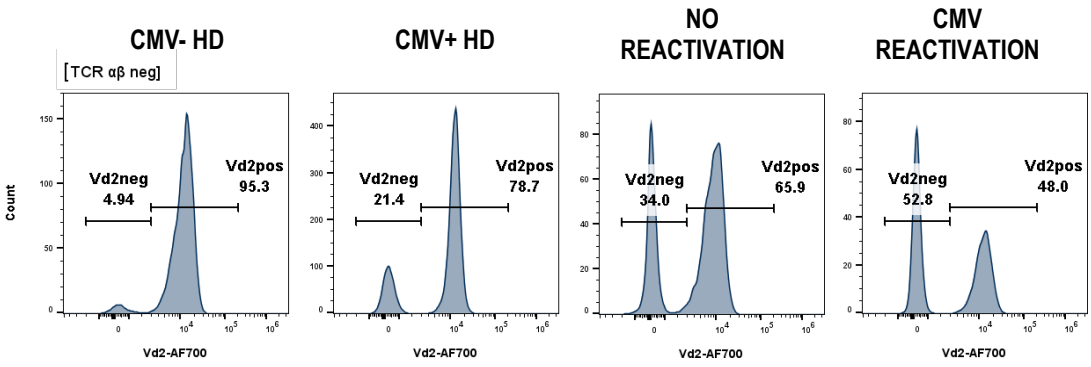


FIGURE 5.3.34. Examples of Vδ2 negative and Vδ2 positive plots in healthy donors, CMV reactivation patients and patients without reactivation. Vδ2 negative and Vδ2 positive populations were determined from TCRγδ or TCRαβ negative T cells.

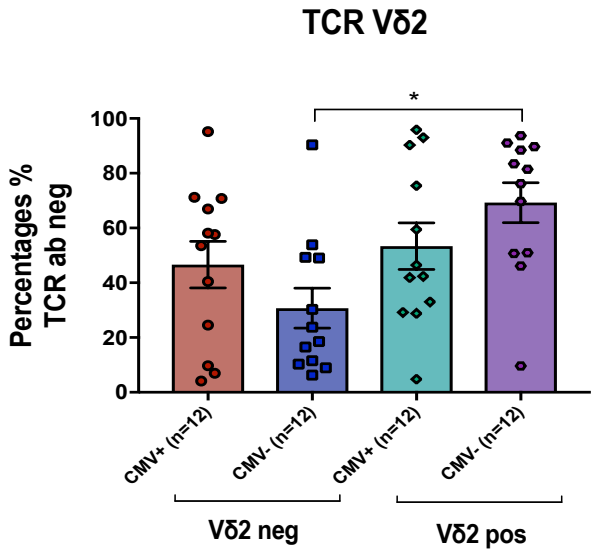


FIGURE 5.3.35. TCR Vδ2 negative and Vδ2 positive T cells in healthy donors (n=24). The average percentages for TCR Vδ2 negative are 38.7±5.8% while Vδ2 positive is 61.3±5.8%. TCR Vδ2 negative; CMV seropositive: 46.6±8.5%, CMV seronegative: 30.7±7.3%, Vδ2 positive; CMV seropositive: 53.4±8.5%, CMV seronegative: 69.3±7.3%. Analysis was done by Mann Whitney and Wilcoxon sign rank test (*p<0.05, **p<0.01, ***p<0.005).

5.3.2.7. Vδ2-negative and Vδ2-positive γδ T cell subsets in HSCT patients with or without CMV reactivation

The composition of TCRγδ T cells between HSCT patients with CMV reactivation or without CMV reactivation was next compared. The proportion of the Vδ2 positive subset in patients with no reactivation was similar to those from HDs **(Fig. 5.3.35)**. In contrast, the percentage of the Vδ2-positive subset was always significantly lower in the patients with CMV reactivation compared with HDs, while the percentages of Vδ2-negative subset were higher **(Fig. 5.3.36).** This implied that CMV infection can induce the expansion of Vδ2-negative TCRγδ T cells. The subsets represented by Vδ2-negative T cells are the $V\delta1^{+}$ subset, which was studied further, and may also include the Vδ3 to Vδ8 subsets although these were not included in the flow cytometry panel and as such, these were not able to be analysed further.

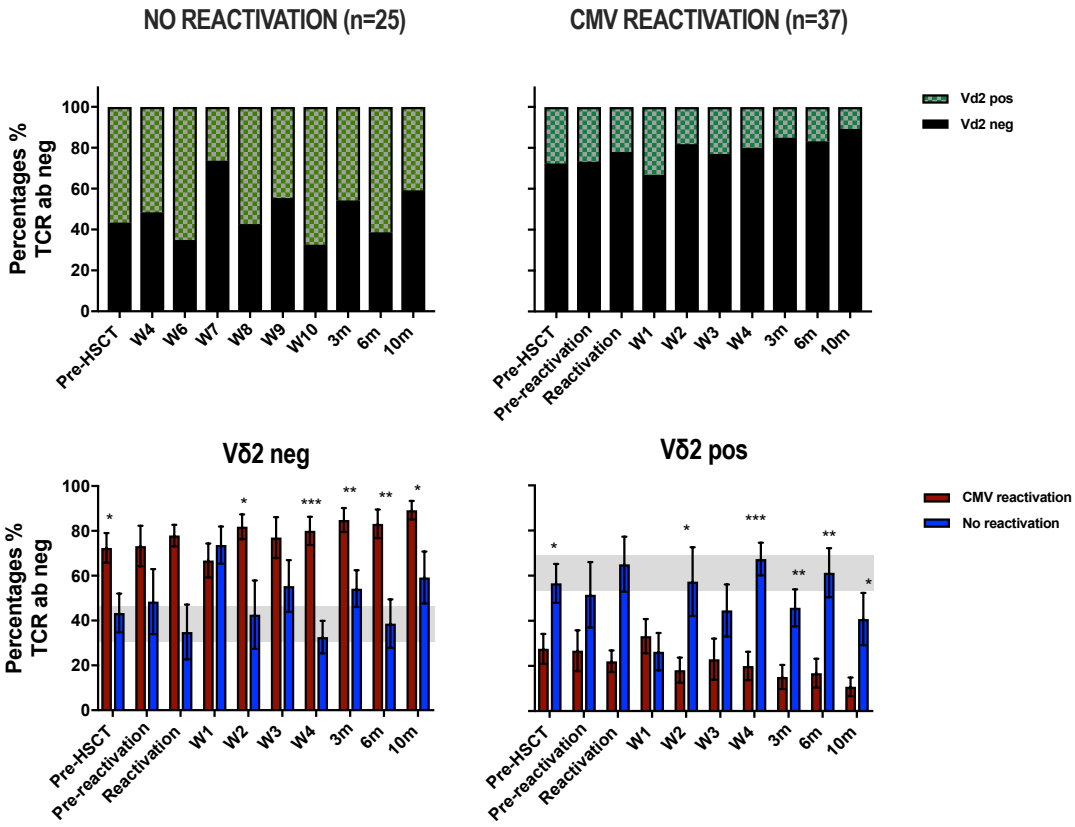


FIGURE 5.3.36. Percentage of TCR Vδ2-negative and Vδ2-positive T cells in HSCT patients with or without CMV reactivation. The average percentages for TCR Vδ2 negative; CMV seropositive: 46.6±8.5%, CMV seronegative: 30.7±7.3%, Vδ2 positive; CMV seropositive: 53.4±8.5%, CMV seronegative: 69.3±7.3% represented by grey lines. Analysis was done by Mann Whitney test (*p<0.05, **p<0.01, ***p<0.005). [W: week(s), m: month(s) after CMV reactivation/allo-HSCT].

5.3.2.8. Vδ1$^+$Vδ2$^-$, Vδ1$^-$Vδ2$^+$ and Vδ1$^-$Vδ2$^-$ subsets in healthy donors and HSCT patients in relation to CMV reactivation

Different gating strategies were further carried out to discriminate TCRγδ T cell subsets. **Fig. 5.3.37** shows examples of Vδ1$^+$Vδ2$^-$, Vδ1$^-$Vδ2$^+$ and Vδ1$^-$Vδ2$^-$ subsets within the TCRαβ-negative flow cytometry plots. No significant populations of Vδ1$^+$Vδ2$^+$ subset would have been expected. As mentioned before, Vδ1$^-$Vδ2$^-$ T cell subsets are likely to represent Vδ3 to Vδ8 subsets, which are not included in this analysis.

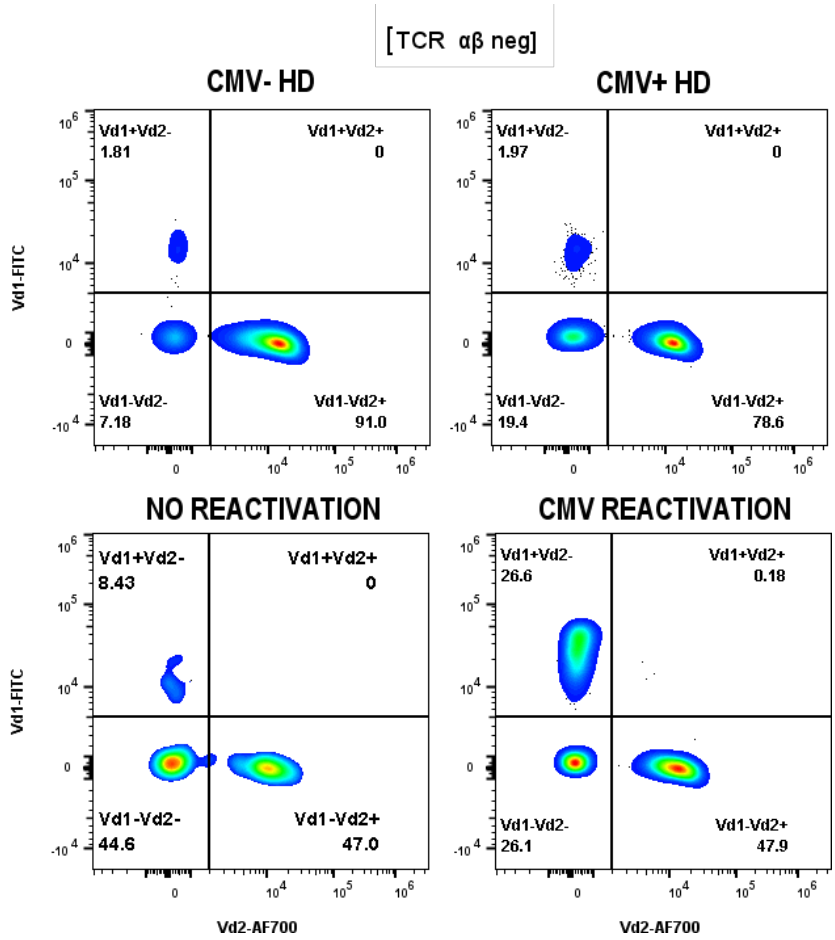


FIGURE 5.3.37. Different TCR Vδ1 and Vδ2 T cells subsets in healthy donors and HSCT patients in relation to CMV reactivation. The subsets were determined from total TCRγδ (TCR αβ-negative) cells, with populations determined from $V\delta1^{+}V\delta2^{-}$, $V\delta1^{-}V\delta2^{+}$ and $V\delta1^{-}V\delta2^{-}$ subsets.

In HDs, the majority of TCRγδ T cells are within the $V\delta1^{-}V\delta2^{+}$ T cell subset (60.4±5.8%), followed by $V\delta1^{+}V\delta2^{-}$ (26.4±4.5%) and $V\delta1^{-}V\delta2^{-}$ T cell (13.1±3.2%) **(Fig. 5.3.38).** No significant differences were observed in these subsets in relation to CMV serostatus in HDs. The average mean of those subsets in HDs are 33.7±7.2% in CMV seropositive and 19.1±4.8% in seronegative for $V\delta1^{+}V\delta2^{-}$ T cells subset, 52.1±8.6% to 68.7 ±7.3% for $V\delta1^{-}V\delta2^{+}$ T cell subset and 13.8±3.3% to 12.2±5.6% for $V\delta1^{-}V\delta2^{-}$ T cell subset.

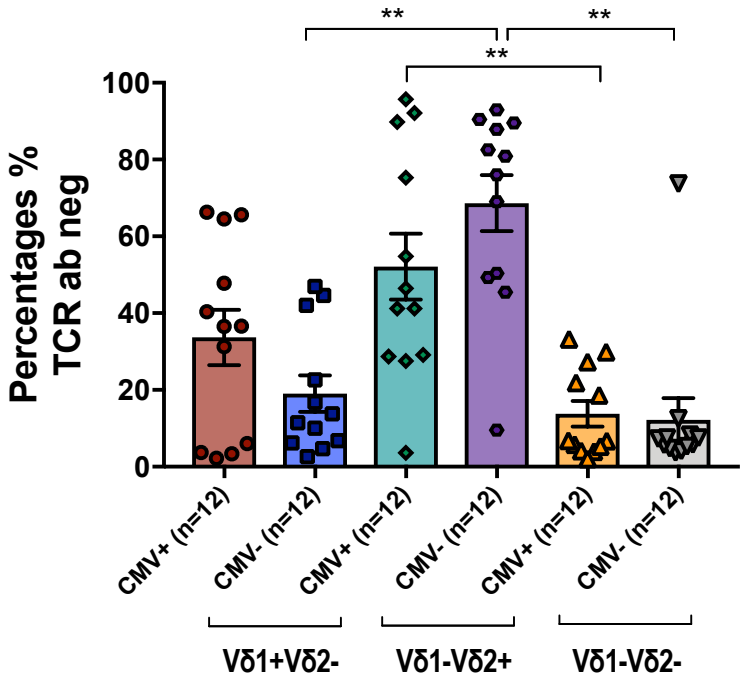


FIGURE 5.3.38. Different TCR Vδ1 and Vδ2 T cells subsets in healthy donors, no reactivation and CMV reactivation patients. The subsets were determined from total TCRγδ or TCRαβ negative T cells, with populations determined from $V\delta1^{+}V\delta2^{-}$ subset, $V\delta1^{-}V\delta2^{+}$ and $V\delta1^{-}V\delta2^{-}$ subsets. The average means in HDs are 33.7±7.2% in CMV seropositive and 19.1±4.8% in seronegative for $V\delta1^{+}V\delta2^{-}$ subset, 52.1±8.6% to 68.7 ±7.3% for $V\delta1^{-}V\delta2^{+}$ subset and 13.8±3.3% to 12.2±5.6% for $V\delta1^{-}V\delta2^{-}$ subset. Analysis was done by Mann Whitney test and Wilcoxon Sign rank test (*p<0.05, **p<0.01, ***p<0.005).

As shown in **Fig. 5.3.39**, a significant increase in the percentage of $V\delta1^{+}V\delta2^{-}$ T cells were seen after reactivation in allo-HSCT patients compared to those without reactivation (p=0.0002, Mann Whiney test) and remained higher at the week 2 and week 4 time points **(Fig. 5.3.39).** Following upregulation of the $V\delta1^{+}$ subset, a downregulation in the $V\delta1^{-}V\delta2^{+}$ subset was seen after CMV reactivation at all time points (p=0.001, Mann Whitney test), whilst $V\delta2^{+}$ cells still constitute the major subset in allo-HSCT and are comparable to HDs (grey lines). The percentage of $V\delta1^{-}V\delta2^{-}$ T cells did not differ in patients with and without reactivation (p=0.28, Mann Whitney test, **Fig. 5.3.39**).

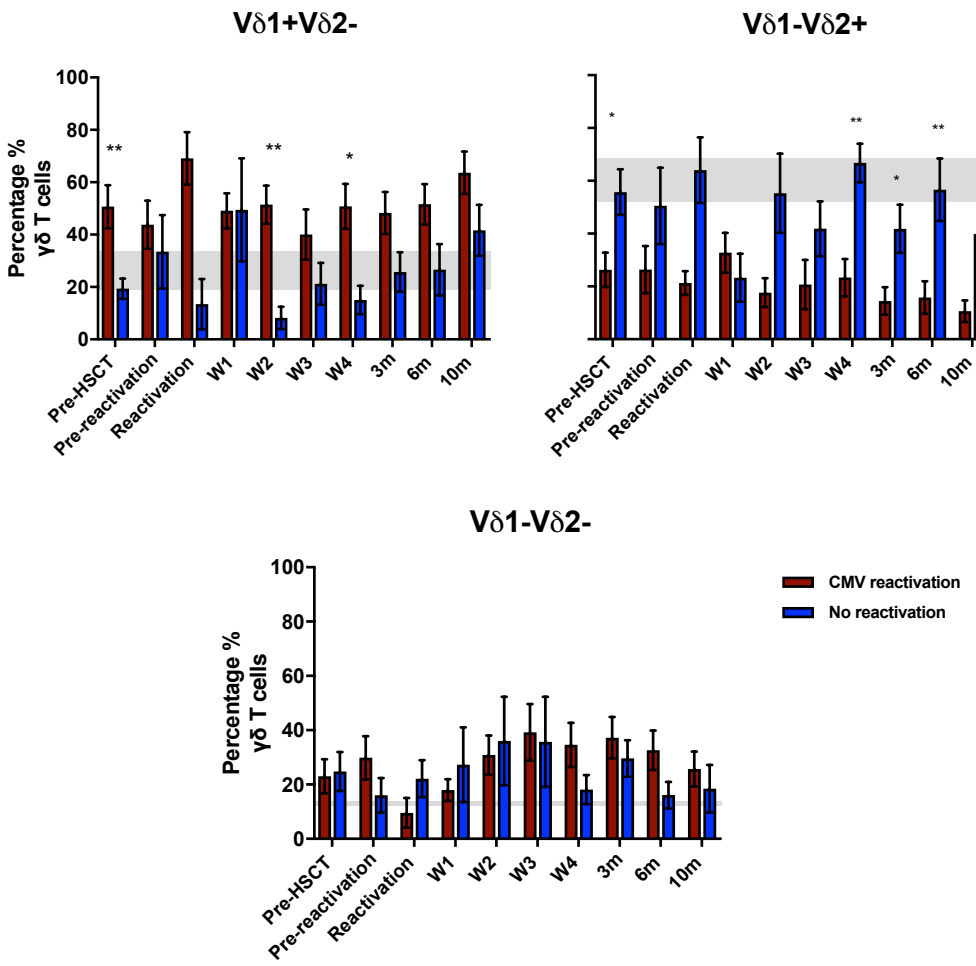


FIGURE 5.3.39. Comparison between TCR Vδ1 and Vδ2 T cells subsets in CMV reactivation and no reactivation patients. The subsets were determined from total TCRγδ or TCRαβ negative T cells, with populations determined from $V\delta1^{+}V\delta2^{-}$ subset, $V\delta1^{-}V\delta2^{+}$ and $V\delta1^{-}V\delta2^{-}$ subsets. Range of the subset percentages in HDs are shown in grey lines. Analysis was done by Mann Whitney test (*p<0.05, **p<0.01, ***p<0.005). [W: week(s), m: month(s) after CMV reactivation/allo-HSCT].

5.4. DISCUSSION

In this chapter the focus is on phenotypic changes on T cells in HSCT patients in relation to CMV reactivation. The findings revealed that the virus has a profound impact on the profile of T cell reconstitution in the first year after transplant. Briefly, the percentage of $CD8^+$ T cells was generally higher in allo-HSCT in patients with CMV reactivation. Indeed, a dramatic expansion of total $CD8^+$ T cells was seen from week 4 to month 10 after reactivation. In addition, elevated numbers of $CD4^+$ T cells were also seen from W3 to 10 months after CMV reactivation.

An increase in CMV-specific $CD8^+$ T cells was also seen immediately after reactivation, and this peaked at week 3 before falling from month 3. The peak time of the CMV-specific $CD8^+$ T cell response corresponded very closely to the profile of CMV virus load. In contrast, the CMV-specific $CD4^+$ T cell response showed delayed kinetics.

The phenotype of T cells populations was also addressed. A $CD57^+$ and $CD28^-$ profile is common on CMV-specific $CD8^+$ T cells and this increased straight after CMV reactivation and continued further for 10 months. In contrast, $CD38^+$ and PD-1^+ expression on CD8 T cells peaked at week 2 and then started to go down to the normal range.

Interestingly, an increase of the percentage of TCRγδ T cells at early time points after viraemia was also seen, but both the percentage and absolute count went up in the long-term time points in patients with CMV reactivation. Also, more detailed study confirmed that there was a significant increase for Vδ2-negative subset and a decrease in the Vδ2-positive subset in patients with CMV reactivation.

$CD8^+$ and $CD4^+$ T cell reconstitution in allo-HSCT with CMV reactivation

Studies on the reconstitution of both $CD8^+$ and $CD4^+$ T cells in allo-HSCT patients are well known and have been described in numerous patient cohorts (Wiegering et al., 2018; Stern et al., 2018; Ogonek et al., 2017a). Also, there have been several reports to study how CMV reactivation can affect the T cells reconstitution after HSCT. Previous data has supported a model that CMV reactivation can drive T-cell reconstitution. Suessmuth et al. (2015) have shown that CMV reactivation can drive a big expansion of Granzyme B^+/CD28null/$CD57^+$ EM phenotype $CD8^+$ T cells (Suessmuth et al., 2015).

In this study we focused on the effect of CMV reactivation on the T cell recovery. By comparing with the same patients without CMV reactivation within the same time point allows us to understand how CMV reactivation can affect the T cell reconstitution. Our study mirrored the previous finding, and we found there is a dramatic expansion of total $CD8^+$ and $CD4^+$ T cells number at later time points 3-10 months post CMV reactivation. Reconstitution of $CD4^+$ T cells is believed to happen with delayed kinetics compared with $CD8^+$ T cells (de Koning et al., 2018). Indeed, from our study, we found the CD8:CD4 ratio is reversed compared to HDs

after transplant. Particularly after CMV reactivation, the percentage of $CD8^+$ increases quickly but the percentage of $CD4^+$ T cells decreases. Nevertheless, the absolute count of $CD4^+$ T cells is still increased in the patients with CMV reactivation **(Fig. 5.3.4).** T cell reconstitution is also vital in controlling CMV reactivation thus monitoring of the $CD8^+$ and $CD4^+$ virus-specific immune response is important (Borchers et al., 2011; Suessmuth et al., 2015; Pourgheysari et al., 2009).

CMV-specific $CD8^+$ and CMV-specific $CD4^+$ T cell reconstitution in CMV reactivation allo-HSCT

In the setting of CMV reactivation, monitoring of the CMV-specific T cell response can be useful in both prediction of outcome and the potential use of adoptive T cell transfer (Neuenhahn et al., 2017). However, the monitoring of these immune cells is determined by the patients' HLA types and the use of appropriate tetramers; as such this is very challenging. Another important factor is the low number of $CD3^+$ T cells at the very early stage of immune reconstitution in the few weeks after CMV reactivation.

In this patient cohort, the tetramer responses from both $CD8^+$ and $CD4^+$ T cells were optimised by pooling the tetramers together in a single staining according to HLA restrictions of the patients. This was done to maximise the chance of detection and to improve the statistical reliability of analysis. Generally, the percentage of tetramer responses seen from $CD8^+$ and $CD4^+$ T cells in these CMV reactivation patients are less than 5% and the responses are varied from one individual to another **(Fig. 5.3.7).**

The tetramer responses from virus specific $CD8^+$ T cells were indeed correlated with CMV viral load in blood of patients **(Fig. 5.3.7)**, signifying the crucial role of these cells in controlling viral burden during reactivation. These CMV-specific $CD8^+$ T cells peaked at week 3 and fell with very similar kinetics as the profile of CMV virus load. Instead, CMV specific $CD4^+$ T cells showed a delayed response to viraemia.

These data reveal the importance of rapid reconstitution of CMV-specific $CD8^+$ T cells and suggest that clinical monitoring of this response is indeed potentially valuable for monitoring the risk of patients for viral replication (Cwynarski et al., 2001). An important consideration in my data is that most HSCT patients with CMV reactivation would have been treated with anti-viral treatment straight after the detection of CMV reactivation and this will affect both the dynamics of the CMV virus load and, potentially, the associated CMV-specific T cell response.

The profile of CD28 and CD57 expression on CMV-specific and total T cells suggests that CMV can exert a bystander effect on T cell activation and differentiation

CD57 is a marker of late differentiated T cells, expressed at a higher level on $CD8^+$ T cells compared to $CD4^+$, whilst CD28 is a co-stimulatory receptor that interacts with CD80 and CD86. CMV infection is the most important factor that drives the expansion of $CD28^-$ ("CD28 null") $CD4^+$ T cells. An increased proportion of $CD57^+$ expression on $CD4^+$ and $CD8^+$ T cells in CMV+ seropositive people was observed, as shown in previous reports (Suessmuth et al., 2015). It was also found that this expansion developed on the total $CD8^+$ population at the very early stage of CMV

reactivation. In contrast the expansion of $CD57^+$ on CMV-specific $CD8^+$ T cells, as determined by tetramer staining, has a delayed kinetic **(Fig. 5.3.11).**

A similar kinetic profile is observed for $CD28^-$ $CD8^+$ T cells in which there is a quick expansion within the total $CD8^+$ population and a delayed expansion for CMV-specific cells. It is interesting to speculate as to the potential reason for this observation. The population of 'total $CD8^+$ T cells' that was studied will include a range of different populations including memory cells against other viruses and bacteria, some naïve cells and also CMV-specific cells that were not identified by the limited availability of HLA-peptide tetramers used in the study. In contrast the 'CMV-specific cells' were clearly a pure population of cells specific for this virus. The data reveals clear differences in the phenotypic profile of these two populations in the early phase after CMV reactivation. Somewhat surprisingly, the CMV-specific pool appears to develop a 'late differentiated' prolife after that of the total $CD8^+$ pool. At first sight this is somewhat surprising. It is suggested that retention of $CD28^+$ and $CD57^-$ T cells within the CMV-specific pool is required to suppress the episode of viraemia before these are lost after this has been controlled. Moreover, we propose that CMV reactivation acts to drive the differentiation of the global $CD8^+$ pool, irrespective of their antigenic specificity. This 'bystander' effect is commonly observed within the immune system and is a major novel observation in this study.

Expansions of $CD57^+$ CMV-specific $CD4^+$ T cells have been seen in allo-HSCT with CMV reactivation (Raeiszadeh et al., 2015) but any difference between expression on the total $CD4^+$ and CMV-specific $CD4^+$ T populations in this patient cohort were not seen. The possible explanation could be this expansion takes longer to be noticed and it is beyond our time course. Interestingly, the expansion of $CD4^+$ $CD28^-$ does not happen until 3 months after reactivation **(Fig. 5.3.22).**

CD38 is an activation marker for T cells and loss of CD38 can lead to impaired immune responses. $CD38^+CD8^+$ T cells are normally found at only a low level in the bloods of HDs, typically around 1.8-3%. PD-1 is of current great interest within cancer immunotherapy, as overexpression of PD-1 on T cells can lead to T-cell exhaustion, but the marker is also seen on cells that have been recently activated (Klenerman and Oxenius, 2016). An increase in $CD38^+$ expression on total and CMV-specific $CD8^+$ and $CD4^+$ cells soon after CMV reactivation were also observed. This remained high for a few weeks before decreasing into the normal range. This supports the suggestion that CMV reactivation can mediate a 'bystander' effect to boost T cell proliferation. The expression pattern of PD-1 also mimicked this profile. Studies have previously described an increase in expression of PD-1 on $CD8^+$ and $CD4^+$ T cells in the weeks after CMV reactivation (Dirks et al., 2013; Gallez-Hawkins et al., 2009), including CMV-specific $CD8^+$ T populations (Poiret et al., 2018). It was confirmed by this finding and also extended to show that this occurs at an early time point after CMV reactivation, primarily within the first four weeks. Of interest, the profile to the same extent on $CD4^+$ cells were not observed.

Viral reactivation leads to expansion of the proportion of effector memory cells

The classic model of T cell differentiation after antigen stimulation is from naïve ($CCR7^+CD45RA^+$) through central memory ($CCR7^+CD45RA^-$) and effector memory ($CCR7^-CD45RA^-$) with regain of a CD45RA phenotype at a late stage (EMRA, $CCR7^-CD45RA^+$) (Lugthart et al., 2014). A marked expansion of the relative proportion of EM $CD8^+$ and $CD4^+$ T cells after CMV reactivation which occurred very early on was found, within the first week. In contrast the expansion of EMRA $CD8^+$ and $CD4^+$ cells are a delayed phenomenon, occurring from 3 months onwards. Within the CMV-specific $CD8^+$ T cells there was a decrease of EMRA phenotype and increase in EM phenotype early after viral reactivation which suggests that the EM pool is required for viral control. Of interest, the EMRA phenotype was lower within the R+/D- group which is likely to reflect the fact that there are no CMV-specific memory T cells within CMV seronegative donors.

$CD8^+$ γδ T cells reconstitution is increased after CMV reactivation

In HDs TCRγδ T cells constitute up to 7.0% of total $CD3^+$ T cells in blood and it has been shown that they reconstitute quickly after HSCT (Ravens et al., 2017) with recovery of the absolute count back to normal after approximately 2 months. Indeed, our own studies revealed that the percentage went back to normal range at the 3-month time point (**Fig. 5.3.29**). The absolute number also increased after 3 months in those patients with CMV reactivation although our findings are somewhat different to what has been reported previously, in which higher proportion of γδ T cells were seen in patients without CMV reactivation (Park et

al., 2018). The reasons for this are not entirely clear but may potentially relate to variation in transplant conditioning regimens.

The majority of TCRγδ T cells in HDs are of $CD8^{-}CD4^{-}$ phenotype and an expansion in $CD8^{+}$ γδ T cells was seen in patients with CMV reactivation with a simultaneous decrease in the $CD8^{-}CD4^{-}$ γδ T cell proportion. This increase in $CD8^{+}$ γδ T cell populations, a novel finding, is in line with the significant expansion of total $CD8^{+}$ T cells upon CMV reactivation as discussed in the previous section. $CD8^{+}$ γδ cells have previously been associated with an increased incidence of GvHD (Gaballa et al., 2019). The reasons for this are not clear as γδ T cells are believed to be able to mediate GvL but not GvHD due to lack of MHC restriction in antigen recognition. Interestingly, depletion of αβ T cells from the stem cell graft does reduce the incidence of GvHD incidence despite retention of γδ T cells (Rådestad et al., 2019).

Vδ1 positive γδ T cells increase after CMV reactivation in allo-HSCT patients

As previously reported, TCRγδ cells can be divided into $Vδ2^{+}$ and Vδ2- populations. $Vδ2^{+}$ is an 'innate-like' subset, and the most abundant subset in blood, whilst $Vδ2^{-}$ cells have more features of adaptive immunity (Davey et al., 2018b; Willcox et al., 2018). After allo-HSCT the majority of TCRγδ cells have been reported to be $Vδ2^{+}$, constituting around 8% of total lymphocytes (de Witte et al., 2018b). Not many studies have shown the recovery of different subsets of γδ T cells upon CMV reactivation in allo-HSCT setting but Ravens, et al. (2017) described the early reconstitution of clonotypic Vδ2 and Vγ9 TCR repertoires over time,

independently of CMV reactivation (Ravens et al., 2017). Our data has shown that there is an expansion of Vδ2^{-} populations after CMV reactivation, comprising of Vδ1^{+} and additional subsets such as Vδ3 to Vδ8 **(Fig. 5.3.32)**.

In order to investigate the Vδ2-negative population expansion, different subsets were analysed by looking at Vδ1^{+}Vδ2^{-}, Vδ1^{-}Vδ2^{+} and Vδ1^{-}Vδ2^{-} cells. In patients with CMV reactivation, expansion of the Vδ1^{+}Vδ2^{-} T cell proportion was seen and these data are similar to a previous study (de Witte et al., 2018), reporting a similar increase within 4 weeks, whilst we have shown that this can even occur within 2 weeks. The CMV-specific activity of Vδ1 cells has not yet been well defined, but they can differentiate from a naïve to effector phenotype, just like the adaptive αβ T cells (Davey et al., 2018a), and it is noteworthy that these cells are believed to bear anti-tumour properties that could potentially mediate GvL and reduce relapse (Hannani et al., 2012). Indeed, they have been suggested as a potential source for cellular immunotherapy.

5.5. CONCLUSION

In conclusion, this chapter has described the impact of CMV reactivation on composition and phenotype of T cell including $CD8^+$, $CD4^+$ and γδ T cells in stem cell transplant patients compared with the HSCT patients without CMV reactivation and HDs. CMV reactivation drives continually expansion of $CD8^+$ and $CD4^+$ T cells, which bear $CD57^+$ $CD28^-$ phenotype. The CMV specific CD8 T cells were generated earlier than CMV specific CD4 T cells, which implied the importance of CMV-CD8 to control CMV infection. Besides, this chapter also has successfully provided the preliminary data on different subsets of γδ T cells, which concluded that CMV can lead to $V\delta2^-$ $V\delta1^+$ γδ T cells in allo-HSCT.

CHAPTER 6:
GENERAL DISCUSSION

6.1. DISCUSSION

In this study the phenotype and kinetics of NK cells and T cells have been studied systematically in HSCT patients with HCMV reactivation. This work has successfully described these features of NK cells, $CD8^+$ T cells, $CD4^+$ T cells and TCRγδ, not only with the early time points within the first four weeks after CMV reactivation, but also at long-term times such as month 3, 6 and 10 post CMV reactivation. The study of immune cells, specifically these cytotoxic subsets, is crucial to understand the significance and impact of CMV reactivation in allo-HSCT patients. Indeed, this is the first to study the simultaneous recovery of NK and T cells upon CMV reactivation in allo-HSCT at the very early time points, as the previous studies mostly focused on the later points (Ogonek et al., 2017; Stern et al., 2018). Also, this study may help to understand the relative importance of innate and adaptive immune control of general CMV infection using allo-HSCT patients with CMV reactivation as a model.

CMV reactivation after transplantation was defined as a viral copy number >200 copies/ml by qPCR although the CMV virus load could reach over 6,000 copies/ml in some patients. This is a massive virus burden compared to levels of virus that are detected within healthy CMV carriers. The peak viral load in HDs with primary infection is not generally known but this is clinically asymptomatic in the great

majority of cases and cases of 'glandular fever', with lymphocytosis, fever and high CMV viral load, are very rare. As such it is highly likely that the viral load is markedly lower in most people during initial infection. Following initial infection, it is thought that the virus reactivates intermittently at low level during persistent infection. However, again it is very difficult to measure viral load within blood within healthy CMV seropositive donors. As such this study identifies a unique situation for studying the immune response against CMV, and one in which the viral challenge is very high. It is likely that this changes the magnitude of the immune response against the virus. However, we would argue that this is unlikely to change the kinetics of the immune response, as reactivation must also be controlled rapidly within HDs.

One major observation was the rapidity with which NK cells and T cells expanded after CMV reactivation in allo-HSCT patients **(Fig. 4.3, Fig. 5.3.3, Fig.5.3.4** and **Fig. 5.3.30).** The summarised figure **(Fig 6.1.1)** has shown that recovery of NK cells upon CMV reactivation are faster than those of $CD8^+$, $CD4^+$ or γδ T cells. The expansion of NK cells started around week 3 after reactivation, but the expansion of $CD4^+$ T cells $CD8^+$ T cells and γδ T cells only became obvious after week 4 or even 3-month post CMV reactivation. An important factor that needs to be taken into account with these studies is that T cell depletion with alemtuzumab was used in many of the transplants, a factor that may act to facilitate NK cell expansion at the expense of T cell regeneration due to reduced competition for the homeostatic cytokines that drive homeostatic proliferation.

The quantitative expansion of the different cell subsets after viral reactivation was remarkable. Indeed, at the 10-month time period the $CD8^+$ pool had expanded by 60-80 fold, NK cells by 30-40 fold and $CD4^+$ T cells by 20 times fold compared to the timepoint pre-reactivation. The γδ T cells show the smallest relative expansion at around 6 times the baseline.

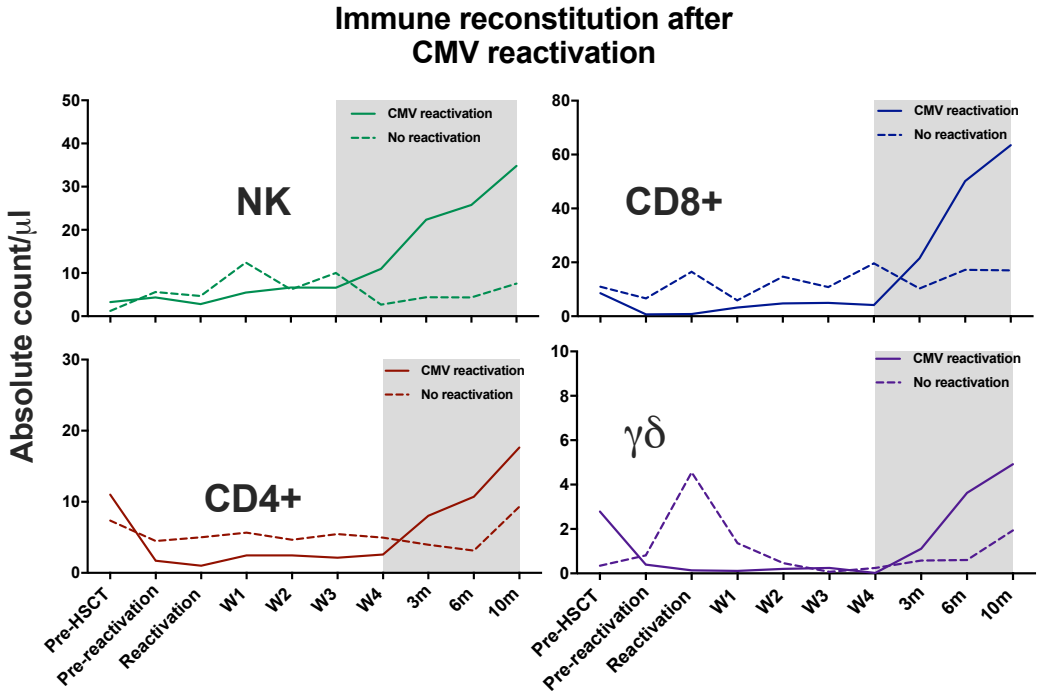


FIGURE 6.1.1. Recovery and reconstitution of NK, $CD8^+$, $CD4^+$ and γδ T cells after CMV reactivation in allo-HSCT patients. NK cells recovery is earlier than $CD8^+$, $CD4^+$ and γδ T cells. [W: week(s), m: month(s) after CMV reactivation/allo-HSCT].

Memory NK population expansion within allo-HSCT patients after CMV reactivation

Many studies have shown expansion of a 'memory-like' or adaptive NK cell pool after CMV reactivation in HSCT patients **(Fig. 4.3.14)** and this was also observed in this study. The expansion of these adaptive NK cells, characterised by simultaneous upregulation of NKG2C and downregulation of NKG2A, within the first week after reactivation has never been shown before and is a novel finding in understanding the kinetics on adaptive NKG2C^{+} NK cell expansion after CMV reactivation. Reports have shown that expansion and differentiation of NKG2C^{+} NK cells is modulated by different CMV strains that encode variable sequences of UL40-derived peptides specifically VMAPRTLIL, VMAPRTLLL and VMAPRTLVL sequences (Hammer et al., 2018), but no enough data available to conclude the association of these peptides with NKG2C^{+} NK cell expansion in this study. NKG2C^{+} NK cell expansion might also be useful as early biomarker of reactivation and might potentially be integrated into immune cell monitoring, although we were not able to show that this increased prior to the development of viraemia. It is possible that *NKG2C* zygosity in allo-HSCT patients also playing a role in causing the expansion of 'memory-like' NK cells, as which both *NKG2C*$^{+/+}$ and *NKG2C*$^{+/-}$ CMV+ individuals have shown variable expansion of the CD56^{bright} NK cells (Muntasell et al., 2013b).

This study has supported previous findings regarding characterisation of the CMV-driven expansion of NKG2C^{+} NK cells in HDs and at later time points in allo-HSCT patients (Bayard et al., 2016; Cichocki et al., 2016; Foley et al., 2012a, 2012b). Very interestingly, our data also showed that adaptive NK population expansion

did not stop after the resolution of CMV reactivation but carries on instead. Indeed, the NKG2C^{+} NK cell pool reached a peak of around 40% of whole NK population 10 months after CMV reactivation, which is a lot higher than the 10% value within CMV seropositive healthy people. The interpretation of this is that the very high viral load in the HSCT patients leads to an 'overshoot' of the NK cell expansion but we predict that the kinetics of this response are likely to be similar in HDs. Certainly, within the patients, this massive CMV reactivation completely changes the peripheral NK phenotype for a long time. Indeed, this may even be for life, but this would require longer follow up samples.

The expression of NKG2C^{+} and loss of NKG2A^{+} on NK cells has been described as the profile of maturation, alongside acquisition of CD57 and KIRs (Cichocki et al., 2016; Foley et al., 2012a, 2012b). The expansion was initially observed in this study within the mature and cytotoxic NK cell population (CD56^{dim} with CD16^{bright}). However, our data shown that the NKG2C^{+} expansion is not seen exclusively in the mature CD56^{dim} NK cell pool, but a rapid expansion can also be seen in the immature CD56^{bright} cells and also in different subsets of NK cells regardless of their cytotoxic properties (based on CD16 expression). The expansion of NKG2C^{+} CD56^{bright} NK cells implies that this NKG2C upregulation could have happened at an early NK precursor stage. Indeed, the NKG2C^{+} CD56^{bright} NK cell expansion peaked earlier than that of NKG2C^{+} CD56^{dim} NK cells, which could hint a transition from immature NK cells to mature NK cells at that point. However, further investigations need to be done to conclude the origin and precursors of

$CD56^{dim/bright}$ $CD16^{bright/negative}$ with high expression and $NKG2C^+$ with loss of $NKG2A^+$ NK cells.

In the $CD56^{dim}CD16^{bright}$ population the CD57 and inhibitory KIR expressions have also significantly increased within the first four weeks after CMV reactivation, with the expansion of KIR^+ $CD57^+$ NK cells be seen in the later time points after months of reactivation. Again, this observation within the early weeks after reactivation is in line with other studies at later time points after CMV reactivation (Della Chiesa et al., 2013b, 2013a). We also analysed the expression of NKG2C, NKG2A, CD57, KIR, PD-1, KLRG1 and CD69 individually. One of the most interesting findings was that expression of the activating receptor CD69 was at its highest level at time of CMV reactivation and then started to decrease in line with CMV viral load.

The comparison of reconstitution from CMV seronegative or seropositive donors allows a unique model to study the impact and significance of CMV-specific immune memory on NK and T cells after CMV reactivation. Within the first 4 weeks we observed that there was a lower proportion of $CD56^{dim}CD16^{bright}$ $NKG2C^+$ cells, and higher percentages of $NKG2A^+$ cells, within the R+/D- patient group compared to R+/D+ patients. This suggests that the CMV-driven 'memory' NK cells are transferrable from seropositive donor to seropositive patient. However, the $NKG2C^+$ NK cell pool then continued to expand in both groups and reached a similar level at 6 months after CMV reactivation.

T cells population expansion upon allo-HSCT patients with CMV reactivation

A dramatic expansion in the total number of $CD8^+$ and $CD4^+$ T cells was also seen at late time points after CMV reactivation. Interestingly the CMV-specific $CD8^+$ and $CD4^+$ T cell pool detected by tetramer staining did not follow the same pattern of expansion as seen by the total $CD8^+$ and $CD4^+$ T cell pool. They started to increase straight after the CMV reactivation happened but then decreased into the normal range at later time points. We propose two potential hypotheses to explain this profile. Firstly, it is possible that all of the expanded T cells that are observed after reactivation are CMV-specific but, for some reason, those that were detected with the use of tetramers do not expand to the same extent. It is not entirely clear why this would be the case, although the tetramer reagents are all specific for T cells that are restricted by HLA-A or HLA-B and it is possible that other CMV-specific cells are restricted by other alleles, such as HLA-C or even non-classical HLA proteins. However, another possible explanation is that the majority of the expanded T cells are actually not actually CMV-specific, but that viral reactivation drives an expansion of the global T cell population. A previous study has also shown that CMV reactivation can drive a 50 fold expansion in the cytotoxic $CD8^+$ T cell compartment with an associated decreased in the naïve pool, although it was assumed in this study that this expansion comprised virus-specific populations (Suessmuth et al., 2015).

It is also of interest to assess the relative expansion profiles of NK cells and T cells. Bayard et al., (2016) described a correlation between the number of $CD56^{dim}NKG2C^+CD57^+$ NK cells and $CD8^+CD57^+$ memory T cells in HDs. $CD8^+$

EMRA T cells are characterised by $CCR7^{-}CD45RA^{+}$ and considered as terminally differentiated memory T cells. In fact, the subject of this terminally differentiation marker is controversial as a study has shown that $CD28^{-}CD45RA^{+}$ $CD8^{+}$ T cells still undergo proliferation upon specific co-stimulatory signal (Waller et al., 2007). Strikingly, when the $CD8^{+}$ EMRA T cells were analysed together with $CD56^{dim}CD16^{bright}$ $NKG2C^{+}$ NK cells, a significant correlation was observed, supporting a hypothesis that these 'memory-like' NK cells expand in similar manner to adaptive or memory T cells (p=0.0077) **(Fig. 6.1.2).**

Overall summary of the phenotype changes of NK and T cells upon allo-HSCT patients with CMV reactivation

In **Table 6.1.1** the phenotype of NK, $CD8^{+}$, $CD4^{+}$ T and TCRγδ T cells in allo-HSCT patients with CMV reactivation have been summarised as compared to HDs (both CMV seronegative or seropositive) and allo-HSCT patients with no reactivation. The CMV negative HDs served as a baseline reference group for this study. Of interest there are some phenotypic changes within the NK and T cell subsets that appear to be related to the HSCT process itself. For NK cells these include an increase in NKG2C expression, a decrease of NKG2A and an increase of CD57 and CD69 expression. However, CMV reactivation is seen to amplify these changes compared with the patients without CMV reactivation. Within the T cell population, we observed an increase of CD57, CD38 and PD-1 expression, together with a loss of CD28, that was more pronounced in the allo-HSCT patients with CMV reactivation compared to those without reactivation. The data from the table suggests that CMV reactivation gives a huge boost to immune reconstitution

after allo-HSCT by imprinting the expansion and phenotype of major cytotoxic populations.

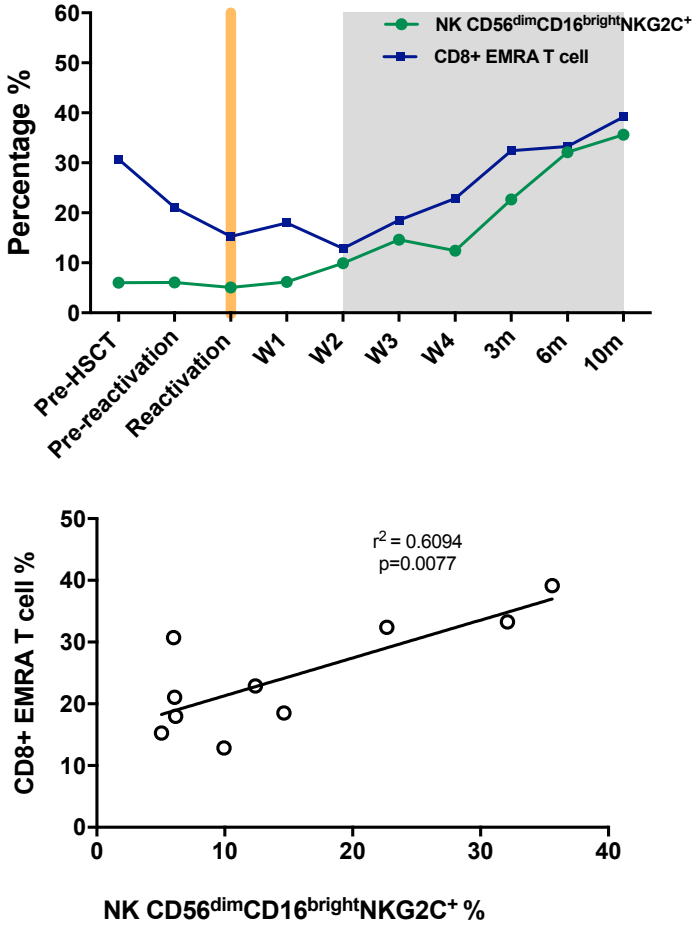


FIGURE 6.1.2. Correlation between NK CD56^{dim}CD16^{bright} NKG2C^{+} cells and CD8^{+} EMRA T cells. The correlation was analysed from the average percentages of both NK and T cells (p=0.0077). Analysis was done by Linear Regression test.

TABLE 6.1.1. Summary of NK and T cell phenotype in allo-HSCT patients after CMV reactivation as compared to control groups. Red arrows represent increase in the phenotype as while blue arrows represent decrease in the phenotype as compared to 'no reactivation' allo-HSCT patients.

	Phenotypes	Markers	Properties	Ligand (Target cells)	CMV - Healthy donors	CMV + Healthy donors	No reactivation allo-HSCT	CMV reactivation allo-HSCT
NK cells	$CD56^{dim}CD16^{bright}$	CD56 / CD16	Mature/cytotoxic		-	-	↓	↓
	$CD56^{dim}CD16^{negative}$		Mature/less cytotoxic		-	-	↑	↑
	$CD56^{bright}CD16^{bright}$		Immature/cytotoxic		-	-	↑	↑
	$CD56^{bright}CD16^{negative}$		Immature/less cytotoxic		-	-	↑	↑
		CD94/NKG2C	Activating	HLA-E	-	↑	↑	↑
		CD94/NKG2A	Inhibiting	HLA-E	-	↓	↓	↓
		CD57	Terminally differentiated	unknown	-	-	↑	↑
		KIR (KIRS2DL1/S1/S5/ KIR2DL2/L3/KIR3 DL2/DL3)	Activating (L) / Inhibitory (S)	HLA-B/C	-	-	-	↑
		PD-1/CD279	Activation/exhaustion	PDL-1	-	-	↑	↑
		KLRG1	Activation/Inhibiting	E/N/R-cadherins	-	-	↑	↑
		CD69	Activation	unknown	-	-	↑	↑
	Inflammatory cytokines:	TNF-α			-	-	↑	↑
		IFN-γ			-	-	↑	↑

	Phenotypes	Markers	Properties	Ligand (Target cells)	CMV - Healthy donors	CMV + Healthy donors	No reactivation allo-HSCT	CMV reactivation allo-HSCT
$CD8^+$ T cells	Memory phenotype	CCR7	Chemokine receptor/Memory		-			
		CD45RA	Memory		-			
	EM ($CCR7^-CD45RA^-$)				-	-	↑	↑
	EMRA ($CCR7^-CD45RA^+$)				-	-	↑	↑
	CM ($CCR7^+CD45RA^-$)				-	-	↓	↓
	Naïve ($CCR7^+CD45RA^+$)				-	-	↓	↓
		CD57	Terminally differentiated	unknown	-	↑	↑	↑
		CD38	Activation	unknown	-	-	↑	↑
		PD-1	Activation/exhaustion	PDL-1	-	-	↑	↑
		CD28	Co-stimulatory	CD80/CD86	-	-	↓	↓
$CD4^+$ T cells	Memory phenotype	CCR7	Chemokine receptor/Memory		-			
		CD45RA	Memory		-			
	EM ($CCR7^-CD45RA^-$)				-	-	↑	↑
	EMRA ($CCR7^-CD45RA^+$)				-	-	-	-
	CM ($CCR7^+CD45RA^-$)				-	-	↓	↓
	Naïve ($CCR7^+CD45RA^+$)				-	-	↓	↓
		CD57	Terminally differentiated	unknown	-	↑	↑	↑
		CD38	Activation	unknown	-	-	-	↑
		PD-1	Activation/exhaustion	PDL-1	-	-	↓	↑
		CD28	Co-stimulatory	CD80/CD86	-	-	-	-
TCRγδ T cells		Vδ1	Subset		-	-	-	↑
		Vδ2	Subset		-	-	-	↓

The potential role of adaptive NK cells in the control of tumour growth

We were not able to demonstrate a correlation between the early increase in $NKG2C^+$ NK cells with the occurrence of leukaemia relapse or GvHD. However this may have been due to the small cohort size of 41 subjects as previous studies have shown that adaptive NK cells have strong cytotoxic properties against some tumour cells (Bigley et al., 2018) and a correlation between CMV reactivation and low rate of disease relapse after HSCT has been seen (Cichocki et al., 2016). It was found that the NK cells that expand in HSCT patients after CMV reactivation retained cytotoxic activity but was not able to demonstrate enhanced function from $NKG2C^+$ cells, although this may have been due to technical difficulties. A particularly interesting finding is that the NK cells from patients after CMV reactivation produce higher TNF-α and IFN-γ compared to those from patients without CMV reactivation. Also, a trend was observed to suggest that $NKG2C^+$ NK cells produce more cytokines than $NKG2C^-$ NK cells after stimulation. This dramatically increased profile of cytokine production may potentially help to control the growth of tumour cells *in vivo*. As such this information supports the idea that the adaptive NK cells driven by CMV might potentially be used to treat patients to avoid relapse or even treat established tumours. Obviously more *in vitro* and *in vivo* studies will be needed to prove this concept.

Future work

Whilst this work has shown a significant impact of CMV reactivation on the subsequent regeneration of immune cells, it will also be important to consider a genome analysis of the virus in order to assess if any polymorphic variants are particularly associated with these findings. During my PhD, we did send samples to Professor Andrew Davison at the MRC-University of Glasgow Centre for Virus Research for sequencing work. However, it was not possible to amplify CMV viral genomes for sequencing due to the low virus copy number. In the future we plan to improve the technique to extract DNA from the patient's urine or serum and potentially increase the chance to successfully sequence the CMV genome. This will give some clues of the relationship of CMV strains, CMV reactivation and shaping of the immune system. This is important as a previous study has shown a relationship between the UL40 peptide sequence and NKG2C^{+} NK cells expansion Hammer et al., (2018). To this end, DNA samples from HCMV reactivated patients' urine and serum have also been sent to Deutsches Rheuma-Forschungszentrum, Germany for viral UL40 peptide sequencing. So far, they have sequenced a small number of patient samples, but not enough data have been collected to build a correlation. In the future, we will carry on this collaboration and sequence more patients' samples to aim for a meaningful result.

A further area of interest would be to assess the impact of CMV reactivation on boosting the immune response to other pathogens, to address the suspicion that the virus may potentiate 'bystander' immune responses in an antigen-nonspecific manner. As such the group are interested in utilizing HLA-peptide tetramers against viruses such as EBV to see if this is indeed the case.

CONCLUSION

In conclusion, my thesis has shown that CMV reactivation makes a profound impact on the profile of immune reconstitution in allo-HSCT patients. This was observed within several lineages, including NK, $CD8^+$, $CD4^+$ and TCRγδ T cells, and was associated with characteristic phenotypic changes. One of the most remarkable observations is the huge expansion of $CD56^{dim}CD16^{bright}$ $NKG2C^+$ NK cells or the controversial 'memory-like' NK cells. Moreover, we elaborated the effect of CMV reactivation on the recovery and expansion of both CMV-specific and global $CD4^+$ and $CD8^+$ T cells repertoires. This work may provide a better understanding of the roles of different immune cells in both controlling CMV reactivation. The broader potential impact of this on the potential eradication of leukaemic blasts requires further study. Our aim has been to provide some insights that might serve to improve the biological understanding and clinical outcome of allo-HSCT and as such we are pleased that we have been at least partially successful in this regard.

REFERENCES

Abel, A.M., Yang, C., Thakar, M.S., et al. (2018) Natural Killer Cells: Development, Maturation, and Clinical Utilization. *Frontiers in Immunology*, 9. doi:10.3389/fimmu.2018.01869.

Airoldi, I., Bertaina, A., Prigione, I., et al. (2015) γδ T-cell reconstitution after HLA-haploidentical hematopoietic transplantation depleted of TCR-αβ+/CD19+ lymphocytes. *Blood*, 125 (15): 2349–58. doi:10.1182/blood-2014-09-599423.

Alejenef, A., Pachnio, A., Halawi, M., et al. (2014) Cytomegalovirus drives Vδ2 ^{neg} γδ T cell inflation in many healthy virus carriers with increasing age. *Clinical & Experimental Immunology*, 176 (3): 418–428. doi:10.1111/cei.12297.

Almehmadi, M., Flanagan, B.F., Khan, N., et al. (2014) Increased numbers and functional activity of CD56 $^{+}$ T cells in healthy cytomegalovirus positive subjects. *Immunology*, 142 (2): 258–268. doi:10.1111/imm.12250.

Amand, M., Iserentant, G., Poli, A., et al. (2017) Human CD56dimCD16dim Cells As an Individualized Natural Killer Cell Subset. *Frontiers in Immunology*, 8: 699. doi:10.3389/fimmu.2017.00699.

Anderlini, P., Rizzo, J.D., Nugent, M.L., et al. (2001) Peripheral blood stem cell donation: an analysis from the International Bone Marrow Transplant Registry (IBMTR) and European Group for Blood and Marrow Transplant (EBMT) databases. *Bone marrow transplantation*, 27 (7): 689–92. doi:10.1038/sj.bmt.1702875.

Angelo, L.S., Banerjee, P.P., Monaco-Shawver, L., et al. (2015) Practical NK cell phenotyping and variability in healthy adults. *Immunological Research*, 62(3): 341–356. doi:10.1007/s12026-015-8664-y.

Atilla, E., Atilla, P.A., Bozdağ, S.C., et al. (2017) A review of infectious complications after haploidentical hematopoietic stem cell transplantations. *Infection*, pp. 1–9. doi:10.1007/s15010-017-1016-1.

Auletta, J.J. and Lazarus, H.M. (2005) Immune restoration following hematopoietic stem cell transplantation: an evolving target. *Bone Marrow Transplantation*, 35 (9): 835–857. doi:10.1038/sj.bmt.1704966.

Barron, M.A., Gao, D., Springer, K.L., et al. (2009) *Relationship of Reconstituted Adaptive and Innate Cytomegalovirus (CMV)-Specific Immune Responses with CMV Viraemia in Hematopoietic Stem Cell Transplant Recipients*., p. 1777. doi:10.1086/648423.

Bayard, C., Lepetitcorps, H., Roux, A., et al. (2016) Coordinated expansion of both memory T cells and NK cells in response to CMV infection in humans. *European Journal of Immunology*, 46 (5): 1168–1179. doi:10.1002/eji.201546179.

Becker, P.S.A., Suck, G., Nowakowska, P., et al. (2016) Selection and expansion of natural killer cells for NK cell-based immunotherapy. *Cancer Immunol Immunother*, 3: 477–484. doi:10.1007/s00262-016-1792-y.

Behrendt, C.E., Nakamura, R., Forman, S.J., et al. (2013) Donor killer immunoglobulin-like receptor genes and reactivation of cytomegalovirus after HLA-matched hematopoietic stem-cell transplantation: HLA-C allotype is an essential cofactor. *Frontiers in Immunology*, 4: 36. doi:10.3389/fimmu.2013.00036.

Behrendt, C.E., Rosenthal, J., Bolotin, E., et al. (2009) Donor and Recipient CMV Serostatus and Outcome of Pediatric Allogeneic HSCT for Acute Leukemia in the Era of CMV-Preemptive Therapy. *Biology of Blood and Marrow Transplantation*, 15 (1): 54–60. doi:10.1016/j.bbmt.2008.10.023.

Bejanyan, N., Brunstein, C.G., Cao, Q., et al. (2018) Delayed immune reconstitution after allogeneic transplantation increases the risks of mortality and chronic GVHD. *Blood Advances*, 2 (8): 909–922. doi:10.1182/bloodadvances.2017014464.

Besse, K., Maiers, M., Confer, D., et al. (2016) On Modeling Human Leukocyte AntigeneIdentical Sibling Match Probability for Allogeneic Hematopoietic Cell Transplantation: Estimating the Need for an Unrelated Donor Source. *Biology of Blood and Marrow Transplantation*, 22: 410–417. doi:10.1016/j.bbmt.2015.09.012.

Beziat, V., Liu, L.L., Malmberg, J.-A., et al. (2013) NK cell responses to cytomegalovirus infection lead to stable imprints in the human KIR repertoire and involve activating KIRs. *Blood*, 121 (14): 2678–2688. doi:10.1182/blood-2012-10-459545.

Bigley, A.B., Baker, F.L. and Simpson, R.J. (2018) Cytomegalovirus: an unlikely ally in the fight against blood cancers? *Clinical & Experimental Immunology*, 193 (3): 265–274. doi:10.1111/cei.13152.

Bigley, A.B., Rezvani, K., Shah, N., et al. (2016) Latent cytomegalovirus infection enhances anti-tumour cytotoxicity through accumulation of NKG2C+ NK cells in healthy humans. *Clinical & Experimental Immunology*, 185 (2): 239–251. doi:10.1111/cei.12785.

Björklund, A.T., Clancy, T., Goodridge, J.P., et al. (2016) Naive Donor NK Cell Repertoires Associated with Less Leukemia Relapse after Allogeneic Hematopoietic Stem Cell Transplantation. *Journal of immunology (Baltimore, Md. : 1950)*, 196 (3): 1400–11. doi:10.4049/jimmunol.1501434.

Blyth, E., Withers, B., Clancy, L., et al. (2016) CMV-specific immune reconstitution following allogeneic stem cell transplantation. *Virulence*, 7 (8): 967–980. doi:10.1080/21505594.2016.1221022.

Boeckh, M. (2017) New insights into cytomegalovirus infection after allogeneic hematopoietic stem cell transplant. *Clinical advances in hematology & oncology : H&O*, 15 (7): 515–517.

Boeckh, M. and Ljungman, P. (2009) How I treat cytomegalovirus in hematopoietic cell transplant recipients. *Blood 11323*, 113 (23): 5711–5719. doi:10.1182/blood-2008-10-143560.

Bonneville, M., O'Brien, R.L. and Born, W.K. (2010) γδ T cell effector functions: a blend of innate programming and acquired plasticity. *Nature Reviews Immunology*, 10 (7): 467–478. doi:10.1038/nri2781.

Borchers, S., Luther, S., Lips, U., et al. (2011) Tetramer monitoring to assess risk factors for recurrent cytomegalovirus reactivation and reconstitution of antiviral immunity post allogeneic hematopoietic stem cell transplantation. *Transplant infectious disease : an official journal of the Transplantation Society*, 13 (3): 222–36. doi:10.1111/j.1399-3062.2011.00626.x.

Byrne, M., Savani, B.N., Mohty, M., et al. (2016) Peripheral blood stem cell versus bone marrow transplantation: A perspective from the Acute Leukemia Working Party of the European Society for Blood and Marrow Transplantation. *Experimental Hematology*, 44 (7): 567–573. doi:10.1016/j.exphem.2016.04.005.

Camargo, J.F. and Komanduri, K. V. (2017) Emerging concepts in cytomegalovirus infection following hematopoietic stem cell transplantation. *Hematology/Oncology and Stem Cell Therapy*,

10 (4): 233–238. doi:10.1016/J.HEMONC.2017.05.001.

Campos, C., Pera, A., Sanchez-Correa, B., et al. (2014) Effect of age and CMV on NK cell subpopulations. *Experimental Gerontology*, 54: 130–137. doi:10.1016/j.exger.2014.01.008.

Cao, K., Marin, D., Sekine, T., et al. (2018) Donor NKG2C Copy Number: An Independent Predictor for CMV Reactivation After Double Cord Blood Transplantation. *Frontiers in Immunology*, 9: 2444. doi:10.3389/fimmu.2018.02444.

Cerwenka, A. and Lanier, L.L. (2016) Natural killer cell memory in infection, inflammation and cancer. *Nature Reviews Immunology*, 16 (2): 112–123. doi:10.1038/nri.2015.9.

Chan, Y.L.T., Zuo, J., Inman, C., et al. (2018) NK cells produce high levels of IL-10 early after allogeneic stem cell transplantation and suppress development of acute GVHD. *European Journal of Immunology*, 48 (2): 316–329. doi:10.1002/eji.201747134.

Chang, C.-J., Osoegawa, K., Milius, R.P., et al. (2018a) Collection and storage of HLA NGS genotyping data for the 17th International HLA and Immunogenetics Workshop. *Human Immunology*, 79 (2): 77–86. doi:10.1016/j.humimm.2017.12.004.

Chang, Y.-J., Zhao, X.-Y. and Huang, X.-J. (2018b) Strategies for Enhancing and Preserving Anti-leukemia Effects Without Aggravating Graft-Versus-Host Disease. *Frontiers in Immunology*, 9: 3041. doi:10.3389/fimmu.2018.03041.

Charoudeh, H.N., Terszowski, G., Czaja, K., et al. (2013) Modulation of the natural killer cell KIR repertoire by cytomegalovirus infection. *European Journal of Immunology*, 43 (2): 480–487. doi:10.1002/eji.201242389.

Chen, C.-T., Gau, J.-P., Liu, J.-H., et al. (2018a) Early achievement of full donor chimerism after allogeneic hematopoietic stem cell transplantation predicts lower relapse risk in patients with acute lymphoblastic leukemia. *Journal of the Chinese Medical Association*, 81 (12): 1038–1043. doi:10.1016/j.jcma.2018.06.005.

Chen, K., Cheng, M.P., Hammond, S.P., et al. (2018b) Antiviral prophylaxis for cytomegalovirus infection in allogeneic hematopoietic cell transplantation. *Blood Advances*, 2 (16): 2159–2175. doi:10.1182/bloodadvances.2018016493.

Della Chiesa, M., Pesce, S., Muccio, L., et al. (2016) Features of Memory-Like and PD-1+ Human NK Cell Subsets. *Frontiers in Immunology*, 7: 351. doi:10.3389/fimmu.2016.00351.

Della Chiesa, M., Falco, M., Bertaina, A., et al. (2014) Human Cytomegalovirus Infection Promotes Rapid Maturation of NK Cells Expressing Activating Killer Ig-like Receptor in Patients Transplanted with NKG2C-/- Umbilical Cord Blood. *The Journal of Immunology*, 192 (4): 1471–1479. doi:10.4049/jimmunol.1302053.

Della Chiesa, M., Falco, M., Muccio, L., et al. (2013a) Impact of HCMV Infection on NK Cell Development and Function after HSCT. *Frontiers in Immunology*, 4: 458. doi:10.3389/fimmu.2013.00458.

Della Chiesa, M., Muccio, L. and Moretta, A. (2013b) CMV induces rapid NK cell maturation in HSCT recipients. *Immunology Letters*, 155 (1–2): 11–13. doi:10.1016/j.imlet.2013.09.020. Della Chiesa, M., Pesce, S., Muccio, L., et al. (2016) Features of Memory-Like and PD-1+ Human NK Cell Subsets. *Frontiers in Immunology*, 7: 351. doi:10.3389/fimmu.2016.00351.

Chiu, Y.-L., Lin, C.-H., Sung, B.-Y., et al. (2016) Cytotoxic polyfunctionality maturation of cytomegalovirus-pp65-specific CD4 + and CD8 + T-cell responses in older adults positively correlates with response size. *Scientific reports*, 6: 19227. doi:10.1038/srep19227.

Ciáurriz, M., Beloki, L., Zabalza, A., et al. (2017) Functional specific-T-cell expansion after first cytomegalovirus reactivation predicts viraemia control in allogeneic hematopoietic stem cell transplant recipients. *Transplant Infectious Disease*, 19 (6): e12778. doi:10.1111/tid.12778.

Cichocki, F., Cooley, S., Davis, Z., et al. (2016) CD56 dim CD57+ NKG2C+ NK cell expansion is associated with reduced leukemia relapse after reduced intensity HCT. *Leukemia*, 30 (2): 456–463. doi:10.1038/leu.2015.260.

Cichocki, F., Taras, E., Chiuppesi, F., et al. (2019) Adaptive NK cell reconstitution is associated with better clinical outcomes. *JCI Insight*, 4 (2). doi:10.1172/jci.insight.125553.

Cockerham, L.R., Siliciano, J.D., Sinclair, E., et al. (2014) CD4+ and CD8+ T Cell Activation Are Associated with HIV DNA in Resting CD4+ T Cells Unutmaz, D. (ed.). *PLoS ONE*, 9 (10): e110731. doi:10.1371/journal.pone.0110731.

Cook, M., Briggs, D., Craddock, C., et al. (2006) Donor KIR genotype has a major influence on the rate of cytomegalovirus reactivation following T-cell replete stem cell transplantation. *Blood*, 107 (3): 1230–1232. doi:10.1182/blood-2005-03-1039.

Cooke, K.R., Luznik, L., Sarantopoulos, S., et al. (2017) The Biology of Chronic Graft-versus-Host Disease: A Task Force Report from the National Institutes of Health Consensus Development Project on Criteria for Clinical Trials in Chronic Graft-Versus-Host Disease HHS Public Access. *Biol Blood Marrow Transplant*, 23 (2): 211–234. doi:10.1016/j.bbmt.2016.09.023.

Cwynarski, K., Ainsworth, J., Cobbold, M., et al. (2001) Direct visualization of cytomegalovirus-specific T-cell reconstitution after allogeneic stem cell transplantation. *Blood*, 97 (5): 1232–40. doi:10.1182/blood.v97.5.1232.

Czerw, T., Labopin, M., Schmid, C., et al. (2016) High CD3+ and CD34+ peripheral blood stem cell grafts content is associated with increased risk of graft-versus-host disease without beneficial effect on disease control after reduced-intensity conditioning allogeneic transplantation from matched unrelate. *Oncotarget*, 7 (19): 27255–66. doi:10.18632/oncotarget.8463.

Davey, M.S., Willcox, C.R., Baker, A.T., et al. (2018a) Recasting Human Vδ1 Lymphocytes in an Adaptive Role. *Trends in Immunology*, 39: 446–459. doi:10.1016/j.it.2018.03.003.

Davey, M.S., Willcox, C.R., Hunter, S., et al. (2018b) The human Vδ2+ T-cell compartment comprises distinct innate-like Vγ9+ and adaptive Vγ9- subsets. *Nature Communications*, 9 (1): 1760. doi:10.1038/s41467-018-04076-0.

Davey, M.S., Willcox, C.R., Hunter, S., et al. (2018c) Vδ2+ T Cells—Two Subsets for the Price of One. *Frontiers in Immunology*, 9 (September): 1–4. doi:10.3389/fimmu.2018.02106.

Davey, M.S., Willcox, C.R., Joyce, S.P., et al. (2017) Clonal selection in the human Vδ1 T cell repertoire indicates γδ TCR-dependent adaptive immune surveillance. *Nature Communications*, 8: 1–15. doi:10.1038/ncomms14760.

Davis, Z.B., Cooley, S.A., Cichocki, F., et al. (2015) Adaptive Natural Killer Cell and Killer Cell Immunoglobulin-Like Receptor-Expressing T Cell Responses are Induced by Cytomegalovirus and Are Associated with Protection against Cytomegalovirus Reactivation after Allogeneic Donor Hematopoietic Cell Transpla. *Biology of Blood and Marrow Transplantation*, 21 (9): 1653–1662. doi:10.1016/j.bbmt.2015.05.025.

Deol, A. and Lum, L.G. (2010) Role of donor lymphocyte infusions in relapsed hematological malignancies after stem cell transplantation revisited. *Cancer Treatmen Review*. doi:10.1016/j.ctrv.2010.03.004.

Dietz, A.C. and Wayne, A.S. (2017) Cells to prevent/treat relapse following allogeneic stem cell transplantation. *Hematology. American Society of Hematology. Education Program*, 2017 (1): 708–715. doi:10.1182/asheducation-2017.1.708.

Dioverti, M.V., Lahr, B.D., Germer, J.J., et al. (2017) Comparison of Standardized Cytomegalovirus (CMV) Viral Load Thresholds in Whole Blood and Plasma of Solid Organ and Hematopoietic Stem Cell Transplant Recipients with CMV Infection and Disease. *Open forum infectious diseases*, 4 (3): ofx143. doi:10.1093/ofid/ofx143.

Dirks, J., Tas, H., Schmidt, T., et al. (2013) PD-1 Analysis on CD28 $^{-}$ CD27 $^{-}$ CD4 T Cells Allows Stimulation-Independent Assessment of CMV Viremic Episodes in Transplant Recipients. *American Journal of Transplantation*, 13 (12): 3132–3141. doi:10.1111/ajt.12480.

Drylewicz, J., M Schellens, I.M., Gaiser, R., et al. (2016) Rapid reconstitution of CD4 T cells and NK cells protects against CMV-reactivation after allogeneic stem cell transplantation. *J Transl Med*, 14: 230. doi:10.1186/s12967-016-0988-4.

Du, W. and Cao, X. (2018) Cytotoxic Pathways in Allogeneic Hematopoietic Cell Transplantation. *Frontiers in Immunology*, 9: 2979. doi:10.3389/fimmu.2018.02979.

Emery, V., Zuckerman, M., Jackson, G., et al. (2013) Management of cytomegalovirus infection in haemopoietic stem cell transplantation. *British Journal of Haematology*, 162 (1): 25–39. doi:10.1111/bjh.12363.

Escudero, A., Martínez-Romera, I., Fernández, L., et al. (2018) Donor KIR Genotype Impacts on Clinical Outcome after T Cell–Depleted HLA Matched Related Allogeneic Transplantation for High-Risk Pediatric Leukemia Patients. *Biology of Blood and Marrow Transplantation*, 24 (12): 2493–2500. doi:10.1016/j.bbmt.2018.08.009.

Fahl, S.P., Coffey, F. and Wiest, D.L. (2014) Origins of γδ T cell effector subsets: a riddle wrapped in an enigma. *Journal of immunology*, 193 (9): 4289–94. doi:10.4049/jimmunol.1401813.

Ferrara, J.L., Levine, J.E., Reddy, P., et al. (2009) Graft-versus-host disease. *The Lancet*, 373 (9674): 1550–1561. doi:10.1016/S0140-6736(09)60237-3.

Feuchtinger, T., Pfeiffer, M., Pfaffle, A., et al. (2009) Cytolytic activity of NK cell clones against acute childhood precursor-B-cell leukaemia is influenced by HLA class I expression on blasts and the differential KIR phenotype of NK clones. *Bone Marrow Transplantation*, 43: 875–881. doi:10.1038/bmt.2008.398.

Fogel, L.A., Sun, M.M., Geurs, T.L., et al. (2013) Markers of Nonselective and Specific NK Cell Activation. *The Journal of Immunology*, 190 (12): 6269–6276. doi:10.4049/jimmunol.1202533.

Foley, B., Cooley, S., Verneris, M.R., et al. (2012a) Cytomegalovirus reactivation after allogeneic transplantation promotes a lasting increase in educated NKG2C+ natural killer cells with potent function. *Blood*, 119 (11): 2665–74. doi:10.1182/blood-2011-10-386995.

Foley, B., Cooley, S., Verneris, M.R., et al. (2012b) Human cytomegalovirus (CMV)-induced memory-like NKG2C(+) NK cells are transplantable and expand in vivo in response to recipient CMV antigen. *Journal of immunology (Baltimore, Md. : 1950)*, 189 (10): 5082–8. doi:10.4049/jimmunol.1201964.

Fry, T.J. and Mackall, C.L. (2005) Immune reconstitution following hematopoietic progenitor cell transplantation: challenges for the future. *Bone Marrow Transplantation*, 35 (S1): S53–S57. doi:10.1038/sj.bmt.1704848.

Gaballa, A., Stikvoort, A., Önfelt, B., et al. (2019) T-cell frequencies of CD8+ γδ and CD27+ γδ cells in the stem cell graft predict the outcome after allogeneic hematopoietic cell transplantation. *Bone Marrow Transplantation*. doi:10.1038/s41409-019-0462-z.

Gallez-Hawkins, G.M., Thao, L., Palmer, J., et al. (2009) Increased Programmed Death-1 Molecule Expression in Cytomegalovirus Disease and Acute Graft-versus-Host Disease after Allogeneic Hematopoietic Cell Transplantation. *Biology of Blood and Marrow Transplantation*, 15 (7): 872–880. doi:10.1016/j.bbmt.2009.03.022.

Ghimire, S., Weber, D., Mavin, E., et al. (2017) Pathophysiology of GvHD and Other HSCT-Related Major Complications. *Frontiers in Immunology*, 8: 79. doi:10.3389/fimmu.2017.00079.

Gokgoz, Z. and Arslan, O. (2018) Haploidentical stem cell transplantation: T cell depleted and repleted. *Transfusion and Apheresis Science*. 57 (2) pp. 171–173. doi:10.1016/j.transci.2018.04.016.

Gordon, C.L., Miron, M., Thome, J.J.C., et al. (2017) Tissue reservoirs of antiviral T cell immunity in persistent human CMV infection. *The Journal of Experimental Medicine*, 214 (3): jem.20160758. doi:10.1084/jem.20160758.

Graff, T.M., Singavi, A.K., Schmidt, W., et al. (2015) Safety of outpatient autologous hematopoietic cell transplantation for multiple myeloma and lymphoma. *Bone Marrow Transplantation*, 50: 947–953. doi:10.1038/bmt.2015.46.

Granados, D.P., Rodenbrock, A., Laverdure, J.-P., et al. (2016) Proteogenomic-based discovery of minor histocompatibility antigens with suitable features for immunotherapy of hematologic cancers. *Leukemia*, 30 (6): 1344–1354. doi:10.1038/leu.2016.22.

Greco, R., Ciceri, F., Noviello, M., et al. (2018) Immune monitoring in allogeneic hematopoietic stem cell transplant recipients: a survey from the EBMT-CTIWP. *Bone Marrow Transplantation*, 53 (9): 1201–1205. doi:10.1038/s41409-018-0167-8.

Green, M.L., Leisenring, W., Stachel, D., et al. (2012) Efficacy of a viral load-based, risk-adapted, preemptive treatment strategy for prevention of cytomegalovirus disease after hematopoietic cell transplantation. *Biology of blood and marrow transplantation : journal of the American Society for Blood and Marrow Transplantation*, 18 (11): 1687–99. doi:10.1016/j.bbmt.2012.05.015.

Green, M.L., Leisenring, W.M., Xie, H., et al. (2013) CMV reactivation after allogeneic HCT and relapse risk: evidence for early protection in acute myeloid leukemia. *Blood*, 122 (7): 1316–1324. doi:10.1182/blood-2013-02-487074.

Guillerey, C., Huntington, N.D. and Smyth, M.J. (2016) Targeting natural killer cells in cancer immunotherapy. *Nature Immunology*, 17 (9): 1025–1036. doi:10.1038/ni.3518.

Guma, M., Budt, M., Sáez, A., et al. (2006) Expansion of CD94/NKG2C+ NK cells in response to human cytomegalovirus-infected fibroblasts. *Blood*, 107 (9): 3624–3631. doi:10.1182/blood-2005-09-3682.

Gyurkocza, B. and Sandmaier, B.M. (2014) Conditioning regimens for hematopoietic cell transplantation: one size does not fit all. *Blood*, 124 (3): 344–353. doi:10.1182/blood-2014-02-514778.

Hammer, Q., Rückert, T., Borst, E.M., et al. (2018a) Peptide-specific recognition of human cytomegalovirus strains controls adaptive natural killer cells. *Nature Immunology*, 19 (5): 453–463. doi:10.1038/s41590-018-0082-6.

Hammer, Q., Rückert, T., Dunst, J., et al. (2018b) Adaptive Natural Killer Cells Integrate Interleukin-18 during Target-Cell Encounter. *Frontiers in Immunology*, 8. doi:10.3389/fimmu.2017.01976.

Hammerstrom, A.E., Lombardi, L.R., Pingali, S.R., et al. (2018) Prevention of Cytomegalovirus Reactivation in Haploidentical Stem Cell Transplantation. *Biology of Blood and Marrow Transplantation*, 24 (2): 353–358. doi:10.1016/j.bbmt.2017.09.018.

Handgretinger, R. and Schilbach, K. (2018) The potential role of γδ T cells after allogeneic HCT for leukemia. *Blood*, 131 (10): 1063–1072. doi:10.1182/blood-2017-08-752162.

Hannani, D., Ma, Y., Yamazaki, T., et al. (2012) Harnessing γδ T cells in anticancer immunotherapy. *Trends in Immunology*, 33: 199–206. doi:10.1016/j.it.2012.01.006.

Harpur, C.M., Stankovic, S., Kanagarajah, A., et al. (2019) Enrichment of cytomegalovirus-induced NKG2C+ Natural Killer cells in the lung allograft. *Transplantation*. doi:10.1097/TP.0000000000002545.

Hayday, A.C. and Pennington, D.J. (2007) Key factors in the organized chaos of early T cell development. *Nature Immunology*, 8 (2): 137–144. doi:10.1038/ni1436.

Heath, J., Newhook, N., Comeau, E., et al. (2016) NKG2C $^{+}$ CD57 $^{+}$ Natural Killer Cell Expansion Parallels Cytomegalovirus-Specific CD8 $^{+}$ T Cell Evolution towards Senescence. *Journal of Immunology Research*, 2016: 1–8. doi:10.1155/2016/7470124.

Helena, S., Paolo, N., Giovanna, P., et al. (2017) Reconstitution of multifunctional CD56 low CD16 low natural killer cell subset in children with acute leukemia given a/b T cell-depleted HLA-haploidentical haematopoietic stem cell transplantation. *OncoImmunology*, 6 (9). doi:10.1080/2162402X.2017.1342024.

Hendricks, D.W., Balfour, H.H., Dunmire, S.K., et al. (2014) Cutting edge: NKG2C(hi)CD57+ NK cells respond specifically to acute infection with cytomegalovirus and not Epstein-Barr virus. *Journal of immunology (Baltimore, Md. : 1950)*, 192 (10): 4492–6. doi:10.4049/jimmunol.1303211.

Hilal, T., Slone, S., Peterson, S., et al. (2017) Cytomegalovirus reactivation is associated with a lower rate of early relapse in myeloid malignancies independent of in-vivo T cell depletion strategy. *Leukemia Research*, 57: 37–44. doi:10.1016/j.leukres.2017.02.009.

Holder, K.A., Lajoie, J. and Grant, M.D. (2018) Natural Killer Cells Adapt to Cytomegalovirus Along a Functionally Static Phenotypic Spectrum in Human Immunodeficiency Virus Infection. *Frontiers in Immunology*, 9: 2494. doi:10.3389/fimmu.2018.02494.

Hosie, L., Pachnio, A., Zuo, J., et al. (2017) Cytomegalovirus-Specific T Cells Restricted by HLA-Cw*0702 Increase Markedly with Age and Dominate the CD8+ T-Cell Repertoire in Older People. *Frontiers in Immunology*, 8: 1776. doi:10.3389/fimmu.2017.01776.

Huenecke, S., Cappel, C., Esser, R., et al. (2017) Development of Three Different NK Cell Subpopulations during Immune Reconstitution after Pediatric Allogeneic Hematopoietic Stem Cell Transplantation: Prognostic Markers in GvHD and Viral Infections. *Frontiers in Immunology*, 8: 109. doi:10.3389/fimmu.2017.00109.

Huygens, A., Dauby, N., Vermijlen, D., et al. (2014) Immunity to cytomegalovirus in early life. *Frontiers in Immunology*, 5 (OCT): 1–11. doi:10.3389/fimmu.2014.00552.

Inagaki, J., Noguchi, M., Kurauchi, K., et al. (2016) Effect of Cytomegalovirus Reactivation on Relapse after Allogeneic Hematopoietic Stem Cell Transplantation in Pediatric Acute Leukemia.

Biology of blood and marrow transplantation : journal of the American Society for Blood and Marrow Transplantation, 22 (2): 300–6. doi:10.1016/j.bbmt.2015.09.006.

Jackson, S.E., Redeker, A., Arens, R., et al. (2017a) CMV immune evasion and manipulation of the immune system with aging. *GeroScience*, 39 (3): 273–291. doi:10.1007/s11357-017-9986-6.

Jackson, S.E., Sedikides, G.X., Okecha, G., et al. (2017b) Latent Cytomegalovirus (CMV) Infection Does Not Detrimentally Alter T Cell Responses in the Healthy Old, But Increased Latent CMV Carriage Is Related to Expanded CMV-Specific T Cells. *Frontiers in Immunology*, 8: 733. doi:10.3389/fimmu.2017.00733.

Jang, J.E., Kim, S.J., Cheong, J.-W., et al. (2015) Early CMV replication and subsequent chronic GVHD have a significant anti-leukemic effect after allogeneic HSCT in acute myeloid leukemia. *Annals of hematology*, 94 (2): 275–82. doi:10.1007/s00277-014-2190-1.

Jaskula, E., Bochenska, J., Kocwin, E., et al. (2012) CMV Serostatus of Donor-Recipient Pairs Influences the Risk of CMV Infection/Reactivation in HSCT Patients. *Bone marrow research*, 2012: 375075. doi:10.1155/2012/375075.

Jethava, Y.S., Sica, S., Savani, B., et al. (2017) Conditioning regimens for allogeneic hematopoietic stem cell transplants in acute myeloid leukemia. *Bone Marrow Transplantation*, 52 (11): 1504–1511. doi:10.1038/bmt.2017.83.

Juárez-Vega, G., Rangel-Ramírez, V., Monsiváis-Urenda, A., et al. (2017) Comparative analysis of NK cell receptor repertoire in adults and very elderly subjects with cytomegalovirus infection. *Human Immunology*, 78 (3): 274–280. doi:10.1016/j.humimm.2017.01.004.

Kared, H., Martelli, S., Ng, T.P., et al. (2016) CD57 in human natural killer cells and T-lymphocytes. *Cancer Immunology, Immunotherapy*, 65 (4): 441–452. doi:10.1007/s00262-016-1803-z.

Kaya, A.H., Tekgunduz, E., Akpinar, S., et al. (2017) Is Cytomegalovirus Surveillance Necessary for Patients With Low Reactivation Risk in an Autologous Hematopoietic Cell Transplantation Setting? *Transplantation Proceedings*, 49 (8): 1911–1915. doi:10.1016/j.transproceed.2017.05.007.

Kennedy, A.E., Ozbek, U. and Dorak, M.T. (2017) What has GWAS done for HLA and disease associations? *International Journal of Immunogenetics*, 44 (5): 195–211. doi:10.1111/iji.12332.

Kinsella, F.A.M., Inman, C.F., Gudger, A., et al. (2019a) Very early lineage-specific chimerism after reduced intensity stem cell transplantation is highly predictive of clinical outcome for patients with myeloid disease. *Leukemia Research*, 83: 106173. doi:10.1016/j.leukres.2019.106173.

Kinsella, F.A.M., Zuo, J., Inman, C.F., et al. (2019b) *Mixed chimerism established by hematopoietic stem cell transplantation is maintained by host and donor T regulatory cells*. doi:10.1182/bloodadvances.2018025502.

Klenerman, P. and Oxenius, A. (2016) T cell responses to cytomegalovirus. *Nature Reviews Immunology*, 16 (6): 367–377. doi:10.1038/nri.2016.38.

Kolb, H.-J. (2008) Graft-versus-leukemia effects of transplantation and donor lymphocytes. *Blood*, 112 (12): 4371–83. doi:10.1182/blood-2008-03-077974.

Kolb, H.-J. (2017) Hematopoietic stem cell transplantation and cellular therapy. *HLA*, 89 (5): 267–277. doi:10.1111/tan.13005.

de Koning, C., Langenhorst, J., van Kesteren, C., et al. (2018) Innate Immune Recovery Predicts CD4+ T Cell Reconstitution after Hematopoietic Cell Transplantation. *Biology of Blood and Marrow Transplantation*. doi:10.1016/j.bbmt.2018.10.013.

de Koning, C., Nierkens, S. and Boelens, J.J. (2016) Strategies before, during, and after hematopoietic cell transplantation to improve T-cell immune reconstitution. *Blood*, 128 (23): 2607–2615. doi:10.1182/blood-2016-06-724005.

Krawczyk, A., Ackermann, J., Goitowski, B., et al. (2018) Assessing the risk of CMV reactivation and reconstitution of antiviral immune response post bone marrow transplantation by the QuantiFERON-CMV-assay and real time PCR. *Journal of Clinical Virology*, 99–100: 61–66. doi:10.1016/j.jcv.2018.01.002.

Lajoie, L., Congy-Jolivet, N., Bolzec, A., et al. (2017) Gradual Increase of FcγRIIIa/CD16a Expression and Shift toward IFN-γ Secretion during Differentiation of CD56dim Natural Killer Cells. *Frontiers in Immunology*, 8: 1556. doi:10.3389/fimmu.2017.01556.

Lanier, L.L. (2008) Up on the tightrope: natural killer cell activation and inhibition. *Nature Immunology*, 9 (5): 495–502. doi:10.1038/ni1581.

Lawand, M., Déchanet-Merville, J. and Dieu-Nosjean, M.-C. (2017) Key Features of Gamma-Delta T-Cell Subsets in Human Diseases and Their Immunotherapeutic Implications. *Frontiers in Immunology*, 8: 761. doi:10.3389/fimmu.2017.00761.

Lian, R.H., Maeda, M., Lohwasser, S., et al. (2002) Orderly and nonstochastic acquisition of CD94/NKG2 receptors by developing NK cells derived from embryonic stem cells in vitro. *Journal of immunology (Baltimore, Md. : 1950)*, 168 (10): 4980–7.

Lidehall, A.K., Sund, F., Lundberg, T., et al. (2005) T Cell Control of Primary and Latent Cytomegalovirus Infections in Healthy Subjects. *Journal of Clinical Immunology*, 25 (5): 473–481. doi:10.1007/s10875-005-5372-8.

Link, C.S., Eugster, A., Heidenreich, F., et al. (2016) Abundant cytomegalovirus (CMV) reactive clonotypes in the CD8 $^{+}$ T cell receptor alpha repertoire following allogeneic transplantation. *Clinical & Experimental Immunology*, 184 (3): 389–402. doi:10.1111/cei.12770.

Litjens, N.H.R., van der Wagen, L., Kuball, J., et al. (2018) Potential Beneficial Effects of Cytomegalovirus Infection after Transplantation. *Frontiers in Immunology*, 9: 389. doi:10.3389/fimmu.2018.00389.

Liu, J., Chang, Y.-J., Yan, C.-H., et al. (2016a) Poor CMV-specific CD8+ T central memory subset recovery at early stage post-HSCT associates with refractory and recurrent CMV reactivation. *The Journal of infection*, 73 (3): 261–70. doi:10.1016/j.jinf.2016.04.033.

Liu, L.L., Landskron, J., Ask, E.H., et al. (2016b) Critical Role of CD2 Co-stimulation in Adaptive Natural Killer Cell Responses Revealed in NKG2C-Deficient Humans. *Cell reports*, 15 (5): 1088–99. doi:10.1016/j.celrep.2016.04.005.

Ljungman, P., Brand, R., Einsele, H., et al. (2003) Donor CMV serologic status and outcome of CMV-seropositive recipients after unrelated donor stem cell transplantation: an EBMT megafile analysis. *Blood*, 102 (13): 4255–4260. doi:10.1182/blood-2002-10-3263.

Ljungman, P., Hakki, M. and Boeckh, M. (2010) Cytomegalovirus in hematopoietic stem cell transplant recipients. *Infectious Disease Clinics of North America*, 24 (2): 319–337. doi:10.1016/j.idc.2010.01.008.

Ljungman, P., Hakki, M. and Boeckh, M. (2011) Cytomegalovirus in Hematopoietic Stem Cell

Transplant Recipients. *Hematology/Oncology Clinics of North America*, 25 (1): 151–169. doi:10.1016/j.hoc.2010.11.011.

Ljungman, P., de la Camara, R., Robin, C., et al. (2019) Guidelines for the management of cytomegalovirus infection in patients with haematological malignancies and after stem cell transplantation from the 2017 European Conference on Infections in Leukaemia (ECIL 7). *The Lancet Infectious Diseases*. doi:10.1016/S1473-3099(19)30107-0.

López-Botet, M., Muntasell, A., Martínez-Rodríguez, J.E., et al. (2016) Development of the adaptive NK cell response to human cytomegalovirus in the context of aging. *Mechanisms of Ageing and Development*, 158: 23–26. doi:10.1016/j.mad.2016.06.010.

López-Botet, M., Vilches, C., Redondo-Pachón, D., et al. (2017) Dual Role of Natural Killer Cells on Graft Rejection and Control of Cytomegalovirus Infection in Renal Transplantation. *Frontiers in Immunology*, 8: 166. doi:10.3389/fimmu.2017.00166.

Lopez-Sejas, N., Campos, C., Hassouneh, F., et al. (2016) Effect of CMV and Aging on the Differential Expression of CD300a, CD161, T-bet, and Eomes on NK Cell Subsets. *Frontiers in Immunology*, 7: 476. doi:10.3389/fimmu.2016.00476.

Lugthart, G., Van Ostaijen-Ten Dam, M.M., Jol-Van Der Zijde, C.M., et al. (2014) Early Cytomegalovirus Reactivation Leaves a Specific and Dynamic Imprint on the Reconstituting T Cell Compartment Long-Term after Hematopoietic Stem Cell Transplantation. *Biology of Blood and Marrow Transplantation*, 20: 655–661. doi:10.1016/j.bbmt.2014.01.018.

Maggs, L., Kinsella, F., Chan, Y.L.T., et al. (2017) The number of CD56 ^{dim} NK cells in the graft has a major impact on risk of disease relapse following allo-HSCT. *Blood Advances*, 1 (19): 1589–1597. doi:10.1182/bloodadvances.2017008631.

Mahaweni, N.M., Ehlers, F.A.I., Bos, G.M.J., et al. (2018) Tuning Natural Killer Cell Anti-multiple Myeloma Reactivity by Targeting Inhibitory Signaling via KIR and NKG2A. *Frontiers in Immunology*, 9: 2848. doi:10.3389/fimmu.2018.02848.

Mahnke, Y.D., Brodie, T.M., Sallusto, F., et al. (2013) The who's who of T-cell differentiation: Human memory T-cell subsets. *European Journal of Immunology*, 43 (11): 2797–2809. doi:10.1002/eji.201343751.

Majhail, N.S., Rizzo, J.D., Lee, S.J., et al. (2012) Recommended Screening and Preventive Practices for Long-Term Survivors after Hematopoietic Cell Transplantation. *Biology of Blood and Marrow Transplantation*, 18 (3): 348–371. doi:10.1016/j.bbmt.2011.12.519.

Malmberg, K.-J., Beziat, V. and Ljunggren, H.-G. (2012) Spotlight on NKG2C and the human NK-cell response to CMV infection. *European journal of immunology*, 42 (12): 3141–5. doi:10.1002/eji.201243050.

Marcenaro, E., Brown, M.G., Carbone, E., et al. (2017) Dual Role of Natural Killer Cells on Graft Rejection and Control of Cytomegalovirus infection in Renal Transplantation. *Front. Immunol*, 8 (8): 1663389–166. doi:10.3389/fimmu.2017.00166.

Marchesi, F., Pimpinelli, F., Gumenyuk, S., et al. (2015) Cytomegalovirus reactivation after autologous stem cell transplantation in myeloma and lymphoma patients: A single-center study. *World journal of transplantation*, 5 (3): 129–36. doi:10.5500/wjt.v5.i3.129.

Markiewicz, M., Siekiera, U., Karolczyk, A., et al. (2009) Immunogenic disparities of 11 minor histocompatibility antigens (mHAs) in HLA-matched unrelated allogeneic hematopoietic SCT. *Bone Marrow Transplantation*, 43: 293–300. doi:10.1038/bmt.2008.326.

Marsh, S.G.E. (2017) Nomenclature for factors of the HLA system, update September 2017. *HLA*, 90 (6): 391–395. doi:10.1111/tan.13169.

Martin, P.J., Levine, D.M., Storer, B.E., et al. (2017) Genome-wide minor histocompatibility matching as related to the risk of graft-versus-host disease. *Blood*, 129 (6): 791–798. doi:10.1182/blood-2016-09-737700.

Masopust, D. and Schenkel, J.M. (2013) The integration of T cell migration, differentiation and function. *Nature Reviews Immunology*, 13 (5): 309–320. doi:10.1038/nri3442.

McKinney, E.F., Lee, J.C., Jayne, D.R.W., et al. (2015) T-cell exhaustion, co-stimulation and clinical outcome in autoimmunity and infection. *Nature*, 523 (7562): 612–616. doi:10.1038/nature14468.

Melandri, D., Zlatareva, I., Chaleil, R.A.G., et al. (2018) The γδTCR combines innate immunity with adaptive immunity by utilizing spatially distinct regions for agonist selection and antigen responsiveness. *Nature Immunology*, 19 (12): 1352–1365. doi:10.1038/s41590-018-0253-5.

Melendez-Munoz, R., Marchalik, R., Jerussi, T., et al. (2018) Cytomegalovirus Infection Incidence and Risk Factors Across Diverse Hematopoietic Cell Transplantation Platforms Using a Standardized Monitoring and Treatment Approach: A Comprehensive Evaluation from a Single Institution. *Biology of Blood and Marrow Transplantation*. doi:10.1016/j.bbmt.2018.10.011.

Michel, T., Poli, A., Cuapio, A., et al. (2016) Human CD56bright NK Cells: An Update. *The Journal of Immunology*, 196 (7): 2923–2931. doi:10.4049/JIMMUNOL.1502570.

Michelo, C.M., van Cranenbroek, B., Touw, P., et al. (2017) Human Cytomegalovirus Infection Increases Both Antibody- and Non–Antibody-Dependent Cellular Reactivity by Natural Killer Cells. *Transplantation Direct*, 3 (12): e335. doi:10.1097/TXD.0000000000000750.

Miller, J.S., Cooley, S., Parham, P., et al. (2007) Missing KIR ligands are associated with less relapse and increased graft-versus-host disease (GVHD) following unrelated donor allogeneic HCT. *Blood*, 109: 5058–5061. doi:10.1182/blood-2007-01.

Minculescu, L. and Sengeløv, H. (2015) The Role of Gamma Delta T Cells in Haematopoietic Stem Cell Transplantation. *Scandinavian Journal of Immunology*, 81 (6): 459–468. doi:10.1111/sji.12289.

Moretta, A., Pende, D., Locatelli, F., et al. (2009) Activating and inhibitory killer immunoglobulin-like receptors (KIR) in haploidentical haemopoietic stem cell transplantation to cure high-risk leukaemiasc ei_3983 325..331. *Clinical and Experimental Immunology REVIEW ARTICLE*. doi:10.1111/j.1365-2249.2009.03983.x.

Morishima, Y., Kashiwase, K., Matsuo, K., et al. (2015) Biological significance of HLA locus matching in unrelated donor bone marrow transplantation. *Blood*, 125 (7): 1189–1197. doi:10.1182/blood-2014.

Moss, P. (2019) 'From immunosenescence to immune modulation': a re-appraisal of the role of cytomegalovirus as major regulator of human immune function. *Medical Microbiology and Immunology*, 208 (3–4): 271–280. doi:10.1007/s00430-019-00612-x.

Muccio, L., Falco, M., Bertaina, A., et al. (2018) Late Development of FcεRγneg Adaptive Natural Killer Cells Upon Human Cytomegalovirus Reactivation in Umbilical Cord Blood Transplantation Recipients. *Frontiers in Immunology*, 9: 1050. doi:10.3389/fimmu.2018.01050.

Muntasell, A., Costa-Garcia, M., Vera, A., et al. (2013a) *Priming of NK cell anti-viral effector*

mechanisms by direct recognition of human cytomegalovirus. doi:10.3389/fimmu.2013.00040.

Muntasell, A., López-Montañés, M., Vera, A., et al. (2013b) NKG2C zygosity influences CD94/NKG2C receptor function and the NK-cell compartment redistribution in response to human cytomegalovirus. *European Journal of Immunology*. doi:10.1002/eji.201343773.

Muntasell, A., Vilches, C., Angulo, A., et al. (2013c) Adaptive reconfiguration of the human NK-cell compartment in response to cytomegalovirus: A different perspective of the host-pathogen interaction. *European Journal of Immunology*, 43 (5): 1133–1141. doi:10.1002/eji.201243117.

Nakasone, H., Tanaka, Y., Yamazaki, R., et al. (2013) Single-cell T-cell receptor-β analysis of HLA-A*2402-restricted CMV- pp65-specific cytotoxic T-cells in allogeneic hematopoietic SCT. *Bone Marrow Transplantation*, 49 (10): 87–94. doi:10.1038/bmt.2013.122.

Nerreter, T., Zeiß, S., Herrmann, T., et al. (2017) Robust 8-color flow cytometry panel reveals enhanced effector function of NKG2C + CD57 + FcεRγ − NK cells in CMV seropositive human blood donors. *Immunobiology*, 222 (5): 719–725. doi:10.1016/j.imbio.2017.01.005.

Neuenhahn, M., Albrecht, J., Odendahl, M., et al. (2017) Transfer of minimally manipulated CMV-specific T cells from stem cell or third-party donors to treat CMV infection after allo-HSCT. *Leukemia*, 31 (10): 2161–2171. doi:10.1038/leu.2017.16.

Newhook, N., Fudge, N. and Grant, M. (2017) NK cells generate memory-type responses to human cytomegalovirus-infected fibroblasts. *European Journal of Immunology*, 47 (6): 1032–1039. doi:10.1002/eji.201646819.

Niederwieser, D., Baldomero, H., Szer, J., et al. (2016) Hematopoietic stem cell transplantation activity worldwide in 2012 and a SWOT analysis of the Worldwide Network for Blood and Marrow Transplantation Group including the global survey. *Bone Marrow Transplantation*, 51 (October 2015): 1–8. doi:10.1038/bmt.2016.18.

Nielsen, C.M., White, M.J., Goodier, M.R., et al. (2013) Functional Significance of CD57 Expression on Human NK Cells and Relevance to Disease. *Frontiers in Immunology*, 4: 422. doi:10.3389/fimmu.2013.00422.

Nunes, E., Heslop, H., Fernandez-Vina, M., et al. (2011) Definitions of histocompatibility typing terms: Harmonization of Histocompatibility Typing Terms Working Group. *Human Immunology*, 72 (12): 1214–1216. doi:10.1016/j.humimm.2011.06.002.

O'Reilly, R.J., Prockop, S., Hasan, A N., et al. (2016) Virus-specific T-cell banks for "off the shelf" adoptive therapy of refractory infections. *Bone marrow transplantation*, 51 (January): 1–10. doi:10.1038/bmt.2016.17.

Oevermann, L., Michaelis, S.U., Mezger, M., et al. (2014) KIR B haplotype donors confer a reduced risk for relapse after haploidentical transplantation in children with ALL. *Blood*, 124 (17): 2744–2747. doi:10.1182/blood-2014-03.

Ogonek, J., Talekar, M.K. and Olson, T. (2017a) Immune reconstitution after hematopoietic stem cell transplantation. *Hematopoietic Stem Cell Transplantation for the Pediatric Hematologist/Oncologist*, 7: 371–383. doi:10.1007/978-3-319-63146-2_26.

Ogonek, J., Verma, K., Schultze-Florey, C., et al. (2017b) Characterization of High-Avidity Cytomegalovirus-Specific T Cells with Differential Tetramer Binding Coappearing after Allogeneic Stem Cell Transplantation. *The Journal of Immunology*, 199 (2): 792–805. doi:10.4049/jimmunol.1601992.

Ozdemir, E., Saliba, R.M., Champlin, R.E., et al. (2007) Risk factors associated with late cytomegalovirus reactivation after allogeneic stem cell transplantation for hematological malignancies. *Bone marrow transplantation*, 40 (2): 125–136. doi:10.1038/sj.bmt.1705699.

Pal, M., Schwab, L., Yermakova, A., et al. (2017) Tumor-priming converts NK cells to memory-like NK cells. *Oncoimmunology*, 6 (6): e1317411. doi:10.1080/2162402X.2017.1317411.

Panch, S.R., Szymanski, J., Savani, B.N., et al. (2017) Sources of Hematopoietic Stem and Progenitor Cells and Methods to Optimize Yields for Clinical Cell Therapy. *Biology of Blood and Marrow Transplantation*, 23 (8): 1241–1249. doi:10.1016/j.bbmt.2017.05.003.

Park, M., Im, H.J., Lee, Y.-J., et al. (2018) Reconstitution of T and NK cells after haploidentical hematopoietic cell transplantation using αβ T cell-depleted grafts and the clinical implication of γδ T cells. *Clinical Transplantation*, 32 (1): e13147. doi:10.1111/ctr.13147.

Parry, H.M., Zuo, J., Frumento, G., et al. (2016) Cytomegalovirus viral load within blood increases markedly in healthy people over the age of 70 years. *Immunity & Ageing*, 13 (1): 1. doi:10.1186/s12979-015-0056-6.

Passweg, J.R., Baldomero, H., Bader, P., et al. (2016) Hematopoietic stem cell transplantation in Europe 2014: more than 40 000 transplants annually. *Bone Marrow Transplantation*, 51: 786–792. doi:10.1038/bmt.2016.20.

Paust, S., Blish, C.A. and Reeves, R.K. (2017) Redefining Memory: Building the Case for Adaptive NK Cells. Pierson, T.C. (ed.). *Journal of virology*, 91 (20). doi:10.1128/JVI.00169-17.

Pegram, H.J., Andrews, D.M., Smyth, M.J., et al. (2011) Activating and inhibitory receptors of natural killer cells. *Immunology and Cell Biology*, 89 (2): 216–224. doi:10.1038/icb.2010.78.

Peric, Z., Wilson, J., Durakovic, N., et al. (2018) Early human cytomegalovirus reactivation is associated with lower incidence of relapse of myeloproliferative disorders after allogeneic hematopoietic stem cell transplantation. *Bone Marrow Transplantation*, 53 (11): 1450–1456. doi:10.1038/s41409-018-0172-y.

Perry, A.R. and Linch, D.C. (1996) The history of bone-marrow transplantation. *Blood Reviews*, 10 (4): 215–219. doi:10.1016/S0268-960X(96)90004-1.

Pical-Izard, C., Crocchiolo, R., Granjeaud, S., et al. (2015) Reconstitution of Natural Killer Cells in HLA-Matched HSCT after Reduced-Intensity Conditioning: Impact on Clinical Outcome. *Biology of Blood and Marrow Transplantation*, 21 (3): 429–439. doi:10.1016/J.BBMT.2014.11.681.

Piper, K.P., Horlock, C., Curnow, S.J., et al. (2007) CXCL10-CXCR3 interactions play an important role in the pathogenesis of acute graft-versus-host disease in the skin following allogeneic stem-cell transplantation. *Blood*, 110 (12): 3827–32. doi:10.1182/blood-2006-12-061408.

Poiret, T., Axelsson-Robertson, R., Remberger, M., et al. (2018) Cytomegalovirus-Specific CD8+ T-Cells With Different T-Cell Receptor Affinities Segregate T-Cell Phenotypes and Correlate With Chronic Graft-Versus-Host Disease in Patients Post-Hematopoietic Stem Cell Transplantation. *Frontiers in Immunology*, 9: 760. doi:10.3389/fimmu.2018.00760.

Pourgheysari, B., Piper, K.P., McLarnon, a, et al. (2009) Early reconstitution of effector memory CD4+ CMV-specific T cells protects against CMV reactivation following allogeneic SCT. *Bone marrow transplantation*, 43 (11): 853–61. doi:10.1038/bmt.2008.403.

Rådestad, E., Sundin, M., Törlén, J., et al. (2019) Individualization of Hematopoietic Stem Cell Transplantation Using Alpha/Beta T-Cell Depletion. *Frontiers in Immunology*, 10: 189. doi:10.3389/fimmu.2019.00189.

Raeiszadeh, M., Pachnio, A., Begum, J., et al. (2015) Characterization of CMV-specific CD4+ T-cell reconstitution following stem cell transplantation through the use of HLA Class II-peptide tetramers identifies patients at high risk of recurrent CMV reactivation. *Haematologica*, 100 (8): e318-22. doi:10.3324/haematol.2015.123687.

Ramanathan, M., Teira, P., Battiwalla, M., et al. (2016) Impact of early CMV reactivation in cord blood stem cell recipients in the current era. *Bone Marrow Transplantation*, 51 (February): 1–8. doi:10.1038/bmt.2016.89.

Ravens, S., Schultze-Florey, C., Raha, S., et al. (2017) Human γδ T cells are quickly reconstituted after stem-cell transplantation and show adaptive clonal expansion in response to viral infection. *Nature immunology*, 18 (4): 393–401. doi:10.1038/ni.3686.

Redondo-Pachón, D., Crespo, M., Yélamos, J., et al. (2017) Adaptive NKG2C+ NK Cell Response and the Risk of Cytomegalovirus Infection in Kidney Transplant Recipients. *Journal of immunology (Baltimore, Md. : 1950)*, 198 (1): 94–101. doi:10.4049/jimmunol.1601236.

Roback, J.D., Drew, W.L., Laycock, M.E., et al. (2003) CMV DNA is rarely detected in healthy blood donors using validated PCR assays. *Transfusion*, 43 (3): 314–21. doi:10.1046/j.1537-2995.2003.00312.x.

Robbins, S.H., Nguyen, K.B., Takahashi, N., et al. (2002) Cutting Edge: Inhibitory Functions of the Killer Cell Lectin-Like Receptor G1 Molecule During the Activation of Mouse NK Cells. *The Journal of Immunology*, 168 (6): 2585–2589. doi:10.4049/jimmunol.168.6.2585.

Robin, C., Hémery, F., Dindorf, C., et al. (2017) Economic burden of preemptive treatment of CMV infection after allogeneic stem cell transplantation: a retrospective study of 208 consecutive patients. *BMC Infectious Diseases*, 17 (1): 747. doi:10.1186/s12879-017-2854-2.

Robinson, J., Mistry, K., McWilliam, H., et al. (2011) The IMGT/HLA database. *Nucleic acids research*, 39 (Database issue): D1171-6. doi:10.1093/nar/gkq998.

Rölle, A. and Brodin, P. (2016) Immune Adaptation to Environmental Influence: The Case of NK Cells and HCMV. *Trends in Immunology*, 37 (3): 233–243. doi:10.1016/j.it.2016.01.005.

Rosenow, F., Berkemeier, A., Krug, U., et al. (2013) CD34+ lineage specific donor cell chimerism for the diagnosis and treatment of impending relapse of AML or myelodysplastic syndrome after allo-SCT. *Bone Marrow Transplantation*, 48 (8): 1070–1076. doi:10.1038/bmt.2013.2.

Sakaguchi, H., Watanabe, N., Matsumoto, K., et al. (2016) Comparison of Donor Sources in Hematopoietic Stem Cell Transplantation for Childhood Acute Leukemia: A Nationwide Retrospective Study. *Biology of Blood and Marrow Transplantation*, 22 (12): 2226–2234. doi:10.1016/j.bbmt.2016.09.020.

Sallusto, F., Lenig, D., Förster, R., et al. (1999) Two subsets of memory T lymphocytes with distinct homing potentials and effector functions. *Nature*, 401 (6754): 708–712. doi:10.1038/44385.

Sansoni, P., Vescovini, R., Fagnoni, F.F., et al. (2014) New advances in CMV and immunosenescence. *Experimental Gerontology*, 55: 54–62. doi:10.1016/j.exger.2014.03.020.

Sanz-Piña, E., Santurtún, A. and Zarrabeitia, M.T. (2019) Forensic implications of the

presence of chimerism after hematopoietic stem cell transplantation. *Forensic Science International*, 302: 109862. doi:10.1016/j.forsciint.2019.06.020.

Scheper, W., Van Dorp, S., Kersting, S., et al. (2013) γδT cells elicited by CMV reactivation after allo-SCT cross-recognize CMV and leukemia. *Leukemia*, 27: 1328–1338. doi:10.1038/leu.2012.374.

Schmidt-Hieber, M., Labopin, M., Beelen, D., et al. (2013) CMV serostatus still has an important prognostic impact in de novo acute leukemia patients after allogeneic stem cell transplantation: a report from the Acute Leukemia Working Party of EBMT. *Blood*, 122 (19): 3359–3364. doi:10.1182/blood-2013-05-499830.

Schneidawind, C., Jahnke, S., Schober-Melms, I., et al. (2019) G-CSF administration prior to donor lymphocyte apheresis promotes anti-leukaemic effects in allogeneic HCT patients. *British Journal of Haematology*, p. bjh.15881. doi:10.1111/bjh.15881.

Servais, S., Dumontier, N., Biard, L., et al. (2016) Response to antiviral therapy in haematopoietic stem cell transplant recipients with cytomegalovirus (CMV) reactivation according to the donor CMV serological status. *Clinical microbiology and infection : the official publication of the European Society of Clinical Microbiology and Infectious Diseases*, 22 (3): 289.e1–7. doi:10.1016/j.cmi.2015.11.006.

Shenoy, S. and Boelens, J.J. (2015) Advances in unrelated and alternative donor hematopoietic cell transplantation for nonmalignant disorders. *Current opinion in pediatrics*, 27 (1): 9–17. doi:10.1097/MOP.0000000000000179.

Simonin, M., Dalissier, A., Labopin, M., et al. (2017) More chronic GvHD and non-relapse mortality after peripheral blood stem cell compared with bone marrow in hematopoietic transplantation for paediatric acute lymphoblastic leukemia: a retrospective study on behalf of the EBMT Paediatric Diseases Working Party. *Bone Marrow Transplantation*, 52 (7): 1071–1073. doi:10.1038/bmt.2017.66.

Sissons, J.G.P. and Wills, M.R. (2015) How understanding immunology contributes to managing CMV disease in immunosuppressed patients: now and in future. *Medical microbiology and immunology*, 204 (3): 307–16. doi:10.1007/s00430-015-0415-0.

Sinclair, J.H. and Reeves, M.B. (2013) Human Cytomegalovirus Manipulation of Latently Infected Cells. *Viruses*, 5: 2803–2824. doi:10.3390/v5112803.

Sivori, S., Vacca, P., Del Zotto, G., et al. (2019) Human NK cells: surface receptors, inhibitory checkpoints, and translational applications. *Cellular & Molecular Immunology*, 16 (5): 430–441. doi:10.1038/s41423-019-0206-4.

Spierings, E. (2014) Minor histocompatibility antigens: past, present, and future. *Tissue Antigens*, 84 (4): 374–360. doi:10.1111/tan.12445.

Stamouli, M., Gkirkas, K. and Tsirigotis, P. (2016) Strategies for improving the efficacy of donor lymphocyte infusion following stem cell transplantation. *Immunotherapy*, 8 (1): 57–68. doi:10.2217/imt.15.100.

Stern, L., McGuire, H., Avdic, S., et al. (2018) Mass Cytometry for the assessment of immune reconstitution after hematopoietic stem cell transplantation. *Frontiers in Immunology*, 9 (JUL): 1672. doi:10.3389/fimmu.2018.01672.

Stiff, P. (2015) What is the role of autologous transplant for lymphoma in the current era? *Hematology. American Society of Hematology. Education Program*, 2015 (1): 74–81. doi:10.1182/asheducation-2015.1.74.

Styczynski, J. (2018) Who Is the Patient at Risk of CMV Recurrence: A Review of the Current Scientific Evidence with a Focus on Hematopoietic Cell Transplantation. *Infectious Diseases and Therapy*, 7 (1): 1–16. doi:10.1007/s40121-017-0180-z.

Suessmuth, Y., Mukherjee, R., Watkins, B., et al. (2015) CMV reactivation drives posttransplant T-cell reconstitution and results in defects in the underlying TCR b repertoire. *Blood*, 125 (25): 3835–3851. doi:10.1182/blood-2015-03-631853.Y.S.

Sureda, A., Bader, P., Cesaro, S., et al. (2015) Indications for allo- and auto-SCT for haematological diseases, solid tumours and immune disorders: current practice in Europe, 2015. *Bone Marrow Transplantation*, 50: 1037–1056. doi:10.1038/bmt.2015.6.

Sylwester, A.W., Mitchell, B.L., Edgar, J.B., et al. (2005) Broadly targeted human cytomegalovirus-specific CD4+ and CD8+ T cells dominate the memory compartments of exposed subjects. *The Journal of experimental medicine*, 202 (5): 673–85. doi:10.1084/jem.20050882.

Szyska, M. and Na, I.-K. (2016) Bone Marrow GvHD after Allogeneic Hematopoietic Stem Cell Transplantation. *Frontiers in immunology*, 7 (March): 118. doi:10.3389/fimmu.2016.00118.

Takaba, H. and Takayanagi, H. (2017) The Mechanisms of T Cell Selection in the Thymus. *Trends in Immunology*, 38 (11): 805–816. doi:10.1016/j.it.2017.07.010.

Takenaka, K., Nishida, T., Asano-Mori, Y., et al. (2015) Cytomegalovirus Reactivation after Allogeneic Hematopoietic Stem Cell Transplantation is Associated with a Reduced Risk of Relapse in Patients with Acute Myeloid Leukemia Who Survived to Day 100 after Transplantation: The Japan Society for Hematopoietic C. *Biology of Blood and Marrow Transplantation*, 21 (11): 2008–2016. doi:10.1016/j.bbmt.2015.07.019.

Teira, P., Battiwalla, M., Ramanathan, M., et al. (2016) Early cytomegalovirus reactivation remains associated with increased transplant-related mortality in the current era: a CIBMTR analysis. *Blood*, 127 (20): 2427–2438. doi:10.1182/blood-2015-11-679639.

Tiercy, J.M. (2016) How to select the best available related or unrelated donor of hematopoietic stem cells? *Haematologica*. 101 (6) pp. 680–687. doi:10.3324/haematol.2015.141119.

Turner, T.R., Hayhurst, J.D., Hayward, D.R., et al. (2018) Single molecule real-time DNA sequencing of HLA genes at ultra-high resolution from 126 International HLA and Immunogenetics Workshop cell lines. *HLA*, 91 (2): 88–101. doi:10.1111/tan.13184.

Ullrich, E., Salzmann-Manrique, E., Bakhtiar, S., et al. (2016) Relation between Acute GVHD and NK Cell Subset Reconstitution Following Allogeneic Stem Cell Transplantation. *Frontiers in Immunology*, 7: 595. doi:10.3389/fimmu.2016.00595.

Vaezi, M., Kasaeian, A., Souri, M., et al. (2017) How Do Donor-Recipient CMV Serostatus and Post-Hematopoietic Stem Cell Transplantation CMV Reactivation Affect Outcomes in Acute Leukemia Patients? *International journal of hematology-oncology and stem cell research*, 11 (3): 199–208.

Vantourout, P. and Hayday, A. (2013) Six-of-the-best: unique contributions of γδ T cells to immunology. *Nature Reviews Immunology*, 13 (2): 88–100. doi:10.1038/nri3384.

Vigorito, A.C., Campregher, P. V, Storer, B.E., et al. (2009) Evaluation of NIH consensus criteria for classification of late acute and chronic GVHD. *Blood*, 114 (3): 702–8. doi:10.1182/blood-2009-03-208983.

Vujanovic, L., Chuckran, C., Lin, Y., et al. (2019) CD56dim CD16- Natural Killer Cell Profiling in Melanoma Patients Receiving a Cancer Vaccine and Interferon-α. *Frontiers in immunology*, 10: 14. doi:10.3389/fimmu.2019.00014.

Wagner, J.A., Rosario, M., Romee, R., et al. (2017) CD56bright NK cells exhibit potent antitumor responses following IL-15 priming. *The Journal of clinical investigation*, 127 (11): 4042–4058. doi:10.1172/JCI90387.

Waller, E.C.P., Mckinney, N., Hicks, R., et al. (2007) *Differential costimulation through CD137 (4-1BB) restores proliferation of human virus-specific "effector memory"; (CD28^{-}CD45RA^{HI}) CD8 T cells*. doi:10.1182/blood-2007.

Waller, E.K., Logan, B.R., Fei, M., et al. (2019) Kinetics of immune cell reconstitution predict survival in allogeneic bone marrow and G-CSF–mobilized stem cell transplantation. *Blood Advances*, 3 (15): 2250–2263. doi:10.1182/bloodadvances.2018029892.

Wang, R., Jaw, J.J., Stutzman, N.C., et al. (2012) Natural killer cell-produced IFN-γ and TNF-α induce target cell cytolysis through up-regulation of ICAM-1. *Journal of leukocyte biology*, 91 (2): 299–309. doi:10.1189/jlb.0611308.

Webb, B.J., Harrington, R., Schwartz, J., et al. (2018) The clinical and economic impact of cytomegalovirus infection in recipients of hematopoietic stem cell transplantation. *Transplant Infectious Disease*, 20 (5): e12961. doi:10.1111/tid.12961.

Widmann, T., Sester, U., Schmidt, T., et al. (2018) Rapid reconstitution of CMV-specific T-cells after stem-cell transplantation. *European Journal of Haematology*, 101 (1): 38–47. doi:10.1111/ejh.13077.

Wiegering, V., Eyrich, M., Winkler, B., et al. (2018) Comparison of Immune Reconstitution after Allogeneic Versus Autologous Stem Cell Transplantation in 182 Pediatric Recipients. *Journal of Pediatric Hematology/Oncology*, 00 (00): 1–6. doi:10.1097/MPH.0000000000001340.

Willcox, C.R., Davey, M.S. and Willcox, B.E. (2018) Development and Selection of the Human Vγ9Vδ2+ T-Cell Repertoire. *Frontiers in Immunology*, 9: 1501. doi:10.3389/fimmu.2018.01501.

Wills, M.R., Poole, E., Lau, B., et al. (2015) The immunology of human cytomegalovirus latency: could latent infection be cleared by novel immunotherapeutic strategies? *Cellular & molecular immunology*, 12 (2): 128–38. doi:10.1038/cmi.2014.75.

de Witte, M.A., Kuball, J. and Miller, J.S. (2017) NK Cells and γδT Cells for Relapse Protection after Allogeneic Hematopoietic Cell Transplantation (HCT). *Current Stem Cell Reports*, 3 (4): 301–311. doi:10.1007/s40778-017-0106-4.

de Witte, M.A., Sarhan, D., Davis, Z., et al. (2018) Early Reconstitution of NK and γδ T Cells and Its Implication for the Design of Post-Transplant Immunotherapy. *Biology of Blood and Marrow Transplantation*, 24 (6): 1152–1162. doi:10.1016/j.bbmt.2018.02.023.

Wu, Y., Tian, Z. and Wei, H. (2017) Developmental and Functional Control of Natural Killer Cells by Cytokines. *Frontiers in immunology*, 8: 930. doi:10.3389/fimmu.2017.00930.

Wu, Z., Sinzger, C., Frascaroli, G., et al. (2013) Human cytomegalovirus-induced NKG2C(hi) CD57(hi) natural killer cells are effectors dependent on humoral antiviral immunity. *Journal of virology*, 87 (13): 7717–25. doi:10.1128/JVI.01096-13.

Yang, J., Cai, Y., Jiang, J., et al. (2018) Early tapering of immunosuppressive agents after HLA-matched donor transplantation can improve the survival of patients with advanced acute myeloid

leukemia. *Annals of Hematology*, 97 (3): 497–507. doi:10.1007/s00277-017-3204-6.

Zook, E.C. and Kee, B.L. (2016) Development of innate lymphoid cells. *Nature Immunology*, 17 (7): 775–782. doi:10.1038/ni.3481.

Zuhair, M., Smit, G.S.A., Wallis, G., et al. (2019) Estimation of the worldwide seroprevalence of cytomegalovirus: A systematic review and meta-analysis. *Reviews in Medical Virology*, 29 (3): e2034. doi:10.1002/rmv.2034.

Zúñiga-Pflücker, J.C. (2004) T-cell development made simple. *Nature Reviews Immunology*, 4 (1): 67–72. doi:10.1038/nri1257.

APPENDIX

Supplementary Table 1a. List of CMV reactivation allo-HSCT patients

No	Patient code	Recipient gender	Age at transplant	Transplant date	Date of reactivation	Days after reactivation	Week post-HSCT	Viral load (copies/ml)	Urine (Y/N)	Serum (Y/N)	Recipient CMV serostatus	Donor CMV serostatus	Second reactivation
1	RW762	Male	70	22/10/2015	06/01/2016	76	13/52	1227	Yes	Yes	Pos	Pos	No
2	AP769	Male	54	01/12/2015	30/12/2015	29	4/52	4293	Yes	Yes	Pos	Neg	Yes
3	CS786	Male	52	26/01/2016	09/03/2016	43	7/52	618	Yes	Yes	Pos	Neg	Yes
4	PF787	Male	61	26/01/2016	16/03/2016	50	8/52	516	Yes	Yes	Pos	Neg	Yes
5	GB788	Male	63	09/02/2016	02/03/2016	22	4/52	462	No	Yes	Pos	Pos	No
6	SD783	Female	51	18/02/2016	23/03/2016	34	6/52	749	Yes	Yes	Pos	Pos	No
7	MV792	Female	59	22/03/2016	06/04/2016	15	3/52	304	Yes	Yes	Pos	Neg	Yes
8	SB789	Female	50	15/03/2016	20/04/2016	36	6/52	2275	Yes	Yes	Pos	Pos	No
9	RF794	Male	65	15/05/2016	06/07/2016	52	9/52	4640	Yes	Yes	Pos	Equi	Yes
10	SA793	Female	35	23/03/2016	06/07/2016	105	18/52	1011	No	Yes	Pos	Neg	Yes
11	DJ802	Male	49	05/07/2016	10/08/2016	36	6/52	677	Yes	Yes	Pos	Neg	Yes
12	KD801	Female	61	05/07/2016	10/08/2016	36	7/52	677	No	Yes	Pos	Pos	Yes
13	RF803	Male	60	07/07/2016	24/08/2016	48	8/52	1178	Yes	Yes	Pos	Neg	Yes
14	DH805	Female	48	26/07/2016	24/08/2016	29	5/52	664	No	Yes	Pos	Pos	Yes
15	PR798	Male	62	28/06/2016	31/08/2016	64	10/52	681	Yes	Yes	Pos	Neg	Yes
16	MW820	Male	66	30/08/2016	05/10/2016	36	6/52	436	Yes	Yes	Pos	Pos	Yes
17	TD828	Male	69	07/06/2016	05/10/2016	120	18/52	1047	Yes	Yes	Pos	Pos	No
18	DR811	Male	54	08/08/2016	05/10/2016	58	9/52	1062	Yes	Yes	Pos	Pos	Yes
19	RH821	Male	65	30/08/2016	12/10/2016	43	7/52	1327	No	Yes	Pos	Neg	Yes
20	MS830	Male	64	04/10/2016	09/11/2016	36	7/52	1233	Yes	Yes	Pos	Pos	No

21	EB831	Male	64	18/10/2016	23/11/2016	36	6/52	294	Yes	Yes	Pos	Neg	No
22	NA825	Female	42	13/09/2016	30/11/2016	78	11/52	387	Yes	Yes	Pos	Neg	Yes
23	MH840	Male	61	17/01/2017	15/03/2017	57	9/52	347	No	Yes	Pos	Neg	No
24	NW853	Female	29	21/03/2017	24/04/2017	34	5/52	25717	No	Yes	Neg	Neg	Yes
25	JC858	Female	58	25/04/2017	03/06/2017	39	6/52	228	No	No	Pos	Pos	No
26	SL865	Male	59	31/05/2017	10/07/2017	40	7/52	1164	Yes	Yes	Pos	Pos	Yes
27	AS866	Male	52	23/05/2017	10/07/2017	48	8/52	3848	Yes	Yes	Pos	Pos	no
28	TR862	Female	51	17/05/2017	19/06/2017	33	5/52	1935	No	No	Pos	Pos	No
29	BJ877	Female	70	11/07/2017	30/08/2017	50	8/52	898	Yes	Yes	Pos	Neg	No
30	FV878	Male	42	25/07/2017	13/09/2017	50	8/52	5269	Yes	Yes	Neg	Pos	No
31	NJ886	Male	42	26/10/2017	15/11/2017	20	3/52	701	Yes	Yes	Pos	Neg	No
32	GM884	Female	63	17/10/2017	08/01/2018	83	13/52	329	No	Yes	Pos	Neg	Yes
33	LW772	Female	35	04/12/2015	14/12/2015	10	2/52	5066	No	No	Pos	Pos	No
34	IV779	Female	68	12/04/2016	25/05/2016	43	6/52	288	No	No	Pos	Pos	No
35	KJ907	Female	60	27/02/2018	04/04/2018	36	5/52	1031	No	No	Pos	Pos	No
36	RH548	Male	61	21/08/2012	26/09/2012	36	5/52	908	No	No	Pos	Neg	No
37	DW505	Male	49	22/11/2011	11/01/2012	50	7/52.	18994	No	No	Pos	Pos	Yes
38	VP921	Female	62	24/04/2018	02/07/2018	69	10/52	923	No	No	Pos	Pos	No
39	SW883	Male	21	10/10/2017	20/11/2017	41	6/52	4131	No	No	Pos	Pos	No
40	GJ923	Male	55	22/05/2018	03/09/2018	104	14/52	283	No	No	Pos	Pos	No
41	RA893	Male	20	14/11/2017	20/12/2017	36	5/52	469	No	No	Pos	Pos	No

Supplementary Table 1b. List of CMV reactivation allo-HSCT patients

No	Patient code	Antiviral treatment	Diagnosis	HLA Types								Conditioning
				HLA-A	HLA-A	HLA-B	HLA-B	HLA-C	HLA-C	HLA-DRB1	HLA-DRB1	
1	RW762	Valganciclovir	MDS	0301	2402	0702	1501	0303	0702	1301	1501	Flu/Melph/CAMPATH
2	AP769	Valganciclovir/Cidofovir/ Foscarnet	AML	2902		4402		0501		1201	1501	FLAMSA/BU
3	CS786	Valganciclovir	ALCL	0201		4402	5701	0501	0602	0401	0404	BEAM/Campath
4	PF787	Valganciclovir	ALL	0101	6801	1302	5701	0602		0701		Flu/Mel/Campath
5	GB788	Valganciclovir	AML	02	24	07	18	07	12	11	15	Flu/Mel/Campath
6	SD783	Valganciclovir	NHL	0101	2501	0801	1801	0701	1203	0301	1501	Flu/Beam/Campath
7	MV792	Valganciclovir	AML	2402	3101	0702	0801	0701	0702	0301	0401	Flu/Bu/ATG
8	SB789	Valganciclovir/Cidofovir	AML	0101	0301	0801	3503	0401	0701	0101	1501	Flu/Melph/Campath
9	RF794	Valganciclovir	AML	0301	2902	0702	4403	0702	1601	0301	0401	FLAMSA/BU
10	SA793	Valganciclovir/Cidofovir	AML	0205	2402	3503	5001	0602	1203	0403	1301	Bu/Cy
11	DJ802	Valganciclovir	ALL	0201	2902	4403	1501	0303	1601	0701	1301	Flu/Melph/Campath
12	KD801	Valganciclovir/Cidofovir/ Foscarnet	AML	0101		0801	3508	0401	0701	0301	0701	FLU/BU/ATG
13	RF803	Valganciclovir	MDS	0205	2902	4403	1402	0802	1601	0102	0701	Flu/Bu/ATG
14	DH805	Valganciclovir	AML	0101	0201	0801	4001	0304	0701	0301	0401	FLAMSA/BU
15	PR798	Cidofovir, Valganciclovir	AML	0201		0702	5301	0401	0702	0701	1501	Cyclo/Flu/TBI
16	MW820	Valganciclovir	MDS	0101	1101	0801	3503	0401	0701	0101	0301	Flu/Bu/ATG
17	TD828	Valganciclovir	MDS	0201	2402	4001	5101	0304	1502	0401	0401	FLU/BU/ATG
18	DR811	Ganciclovir	MDS	0201	0301	4001		0304		0101	1302	FLAMSA/BU
19	RH821	Valganciclovir/Cidofovir	MDS	0301	2601	0702	3801	0702	1203	0101	0901	Flu/Bu/ATG
20	MS830	Valganciclovir/Cidofovir	ALL	0201	1101	1501	4501	0304	0602	0401	0701	Flu/Melph/Campath
21	EB831	Valganciclovir	CMML2	0101	2501	0801	5501	0303	0701	0301	1501	Flu/Melph/Campath

22	NA825	Valganciclovir	CMML	0101	1101	4001	4101	0304	1701	0701	1301	Cyclo/Flu/TBI
23	MH840	none	RCMD	0101	0301	0702		0702		1501		Flu/Melph/Campath
24	NW853	Valganciclovir/Cidofovir	AML	0101	0205	3701	5001	0602		0701	1501	Flu/Bu/ATG
25	JC858	Cidofovir	AML	0201	2902	0702	1501	0303	0702	0701	1501	FLAMSA/BU
26	SL865	Valganciclovir	AML	1101	2501	1501	4402	0303	0501	0407	1103	FLAMSA/BU
27	AS866	Cidofovir	AML	2402	2501	4402	5501	0102	0303	0401	0408	Cyclo/Flu/TBI
28	TR862	Valganciclovir/Cidofovir	AML	0102	2402	2703	3701	0202	0602	0101	0401	Flu/Melph/Campath
29	BJ877	Valganciclovir	CMML2	0101	3301	1402	5102	0802	1502	0102	0402	Flu/Melph/Campath
30	FV878	Valganciclovir	HL	3001	6801	1302	4402	0602	0704	1101	1401	Flu/Melph/Campath
31	NJ886	Valganciclovir/Cidofovir	ALL	2402	2402	3501	3503	0401	0401	1101	1404	Cyclo/TBI
32	GM884	Valganciclovir	MDS	3001	6801	1302	4402	0704	0602	0101	1101	Cyclo/Flu/TBI
33	LW772	Valganciclovir	MF	02	68	44	53	0401	0704	04	13	TLI/ATG
34	IV779	Valganciclovir	ALCL	0201	0301	0702	4402	0501	0702	0407	1401	Flu/Melph/Campath
35	KJ907	Valganciclovir	MDS	0301	3303	0702	5801	0302	0702	1302	1501	FLAMSA/BU
36	RH548	Valganciclovir	AML	2402	3001	3501	4002	0202	0401	1101	1501	FLAMSA/BU
37	DW505	Ganciclovir	TPLL	0201	0301	0702	3908	0702		0101	1301	CY/TBI
38	VP921	Valganciclovir	AML	0101	1101	0801	1501	0303	0701	0301	1301	Flu/Melph/Campath
39	SW883	Valganciclovir	MDS	0201	0301	1501	1801	0304	0501	0301	0401	Flu/Melph/Campath
40	GJ923	Valganciclovir	CML to ALL	0201	NA	4001	5001	0304	0602	0301	1302	Flu/Melph/Campath
41	RA893	Valganciclovir	HL	0211	0301	4006	4701	0602	1502	1301	1501	Cyclo/Flu/TBI

ABBREVIATIONS – ALCL: Anaplastic large cell lymphoma, HL: Hodgkin lymphoma, MF: Mycosis fungoides, MDS: Myelodysplastic syndromes, TPLL: T-cell Prolymphocytic Leukaemia, RCMD: Refractory cytopenia multilineage dysplasia.

Supplementary Table 1c. List of allo-HSCT patients without reactivation

No	Patient code	Donor type	Donor gender	Alive/ deceased	Date of death	Reasons	Relapse	aGvHD (Y/N)	cGvHD (Y/N)	EBV reactivation
1	RW762	MUD	Female	Deceased	18/03/2016	GvHD	No	Yes	No	No
2	AP769	MUD (A mismatch)	Male	Deceased	22/07/2016	Disease	Yes	No	No	No
3	CS786	Sib	Male	Deceased	16/10/2018	unknown	NA	No	No	No
4	PF787	MUD	Male	Deceased	01/12/2016	Disease	Yes	Yes	No	No
5	GB788	MUD	Male	Alive	NA	NA	No	Yes	Yes	No
6	SD783	MUD	Male	Alive	NA	NA	No	Yes	Yes	No
7	MV792	Sib	Female	Alive	NA	NA	No	Yes	Yes	No
8	SB789	Sib	Male	Deceased	21/06/2016	Disease	Yes	No	No	No
9	RF794	MUD	Male	Alive	NA	NA	No	No	No	Yes
10	SA793	Sib	Male	Deceased	31/12/2016	Disease	Yes	Yes	No	No
11	DJ802	Sib	Male	Alive	NA	NA	No	No	No	No
12	KD801	Sib	Male	Deceased	25/03/2017	Disease	Yes	No	No	No
13	RF803	MUD	Male	Alive	NA	NA	No	Yes	Yes	No
14	DH805	MUD	Male	Alive	NA	NA	No	No	No	No
15	PR798	Cord	Male	Deceased	07/11/2018	PML	No	No	No	Yes
16	MW820	MUD	Male	Deceased	14/01/2017	Chest infection with sepsis	No	Yes	No	No
17	TD828	MUD	Female	Deceased	15/04/2017	GvHD	No	Yes	No	No
18	DR811	Sib	Male	Deceased	24/10/2016	GvHD	No	Yes	No	No
19	RH821	MUD	Male	Alive	NA	NA	No	Yes	No	No
20	MS830	Sib	Male	Deceased	09/04/2017	Disease	Yes	No	No	No
21	EB831	MUD	Male	Alive	NA	NA	No	No	No	No
22	NA825	MUD	Unknown	Alive	NA	NA	No	Yes	No	No
23	MH840	Sib	Male	Deceased	24/08/2017	Multiorgan failure/GvHD	No	Yes	No	No

24	NW853	Sib	Female	Alive	NA	NA	Yes	Yes	No	No
25	JC858	MUD	Male	Alive	NA	NA	No	Yes	No	Yes
26	SL865	MUD	Female	Alive	NA	NA	No	Yes	Yes	Yes
27	AS866	Son	Male	Alive	NA	NA	No	Yes	No	Yes
28	TR862	MUD	Male	Alive	NA	NA	No	Yes	No	Yes
29	BJ877	MUD	Male	Deceased	25/05/2018	Pneumonia, MDS	Yes	Yes	No	Yes
30	FV878	Sib	Male	Alive	NA	NA	No	No	No	No
31	NJ886	MUD	Male	Deceased	24/11/2018	Multiorgan failure	No	No	No	No
32	GM884	Cord	Male/Female	Alive	NA	NA	No	Yes	No	No
33	LW772	Sib	Male	Alive	NA	NA	Yes	No	No	No
34	IV779	MUD	Female	Alive	NA	NA	No	No	No	No
35	KJ907	MUD	Female	Alive	NA	NA	Yes	No	No	No
36	RH548	MUD	Female	Deceased	04/01/2014	Brain haemorrhage	No	Yes	No	No
37	DW505	MUD	Male	Deceased	09/06/2013	Sepsis	No	No	Yes	No
38	VP921	MUD	Male	Alive	NA	NA	No	Yes	No	No
39	SW883	MUD	Male	Alive	NA	NA	No	Yes	Yes	Yes
40	GJ923	MUD	Male	Alive	NA	NA	no	no	no	No
41	RA893	Sib	Male	Alive	NA	NA	No	Yes	No	Yes

ABBREVIATIONS – PML: Progressive multifocal leukoencephalopathy, NA: Not available

Supplementary Table 1d. List of allo-HSCT patients without reactivation

No	Patient code	Gender	Age at transplant	Transplant date	Recipient CMV serostatus	Donor CMV serostatus	Diagnosis	HLA types							
								HLA-A	HLA-A	HLA-B	HLA- B	HLA-C	HLA-C	HLA-DRB1	HLA-DRB1
1	AS827	Male	45	20/09/2016	Neg	Neg	CLL	0101	0201	0801	5701	0602	0701	0301	0701
2	JS832	Male	66	01/11/2016	Neg	Neg	AIL	0101	1101	0702	1501	0303	0702	1501	
3	CG833	Male	54	15/11/2016	Neg	Neg	MDS	0301	2301	4403	5701	0401	0602	0701	
4	JG776	Female	60	08/12/2015	Neg	Neg	Pre-B ALL	0201	2402	4001	5501	0303	0304	1302	1401
5	AM778	Female	50	23/12/2015	Neg	Neg	MDS	0201	1101	0702	1518	0702	0704	1301	1501
6	DC780	Male	72	12/01/2016	Neg	Neg	MDS	0101	2402	0801	1402	0701	0802	0102	0301
7	CK782	Male	34	08/02/2016	Neg	Neg	HL	0301	3101	1501	4402			1101	1201
8	ED773	Female	26	01/12/2016	Neg	Neg	AML	0201	2902	4402	4403	0501	1601	0101	0701
9	AS738	Female	35	17/03/2015	Pos	Pos	MDS	0206		3503		0401		1404	
10	JR728	Male	67	16/01/2015	Pos	Pos	MDS	0206		3503		0401		1404	
11	JD757	Female	62	22/09/2015	Pos	Pos	AML	0301	3201	0702	1401	0702	0802	0101	1101
12	GT767	Male	61	17/11/2015	Pos	Pos	AML	03		13	35	04	06	03	07
13	KS725	Female	28	09/12/2014	Pos	Pos	AML	02	03	35	44	0401	0501	04	08
14	DM810	Male	35	02/08/2016	Pos	Neg	ALL	0101	0201	3701	5701	0602		0701	1501
15	DP790	Female	48	22/03/2016	Pos	Neg	ALL	2501	2902	4403	5801	0701	1601	0701	1303
16	CM785	Male	60	23/02/2016	Pos	Pos	Myelofibrosis	0201		0702	1501	0303	0702	0101	1101
17	KC784	Male	64	12/02/2016	Pos	Pos	MDS	0201	0301	0702	0801	0701	0702	0301	1501
18	GP702	Male	55	29/07/2014	Neg	Neg	AML	0101		0801	5601	0102	0701	0101	0301
19	MS714	Male	60	15/10/2014	Neg	Neg	WM	0101	3201	0801	3801	0701	1203	0301	1301
20	BL751	Male	61	09/07/2015	Neg	Neg	AML	0101	2402	3701	4402	0501	0602	1001	1301
21	TT815	Female	49	16/08/2016	Neg	Neg	Follicular NHL	0101	2902	4403	5701	0602	1601	0701	
22	RH746	Female	68	11/06/2015	Neg	Neg	MDS/AML	0301	1101	3501	3503	0401	1203	1301	na

23	SB710	Male	68	30/09/2014	Neg	Neg	AML	0301		0702	5101	0102	0702	1501	0602
24	CC721	Female	62	27/11/2014	Neg	Neg	HL	0301	2501	1801	5501	0303	0701	0801	1401
25	DW703	Male	32	12/08/2014	Neg	Neg	T-ALL	201	301	1516	3501	401	1402	102	103
26	AS738	Female	35	17/03/2015	Pos	Pos	MDS	0206		3503		0401		1404	

ABBREVIATIONS – AIL: Angioimmunoblastic Lymphoma, HL: Hodgkin lymphoma, WM: Waldenstromes macroglobluninaemia

Supplementary Table 1e: List of allo-HSCT patients with no reactivation

No	Patient code	Conditioning	Donor type	Donor gender	Alive/ Deceased	Date of death	Reasons	Relapse	aGvHD Yes/No	cGvHD Yes/No
1	AS827	FLU/CYCLO	Sibling	Male	Alive	NA	NA	No	No	No
2	JS832	Flu/Melph/ Campath	MUD	Male	Alive	NA	NA	No	No	Yes
3	CG833	Flu/Bu/ATG	MUD	Male	Alive	NA	NA	No	Yes	No
4	JG776	Flu/Melph/ Campath	MUD	Male	Alive	NA	NA	No	Yes	No
5	AM778	Flu/Bu/ATG	MUD	Male	Alive	NA	NA	No	Yes	No
6	DC780	Flu/Melph/ Campath	MUD	Male	Alive	NA	NA	No	Yes	Yes
7	CK782	Flu/Melph/ Campath	Sibling	Female	Alive	NA	NA	No	Yes	Yes
8	ED773	Cyclo/TBI	MUD	Male	alive	NA	NA	Yes	Yes	No
9	AS738	Flu/Bu/ATG	Sibling	Male	Deceased	31/05/2016	Disease	Yes	No	No
10	JR728	FLAMSA/BU	MUD	Male	Deceased	12/01/2016	Disease	Yes	No	No
11	JD757	Flu/Melph/ Campath	MUD	Female	Deceased	03/12/2018	Heart Failure	No	Yes	Yes
12	GT767	Flu/Bu/ATG	Sibling	Female	Alive	NA	NA	No	No	No
13	KS725	Cyclo/TBI	Sibling	Male	Deceased	26/10/2015	Disease	Yes	Yes	Yes

14	DM810	Cyclo/TBI	MUD	Male	Alive	NA	NA	No	Yes	No
15	DP790	Flu/Melph/ Campath	MUD	Male	Alive	NA	NA	Yes	Yes	No
16	CM785	Flu/Bu/ATG	MUD	Male	Deceased	23/07/2016	GvHD	No	Yes	No
17	KC784	FLAMSA/BU	MUD	Male	Deceased	06/10/2018	Disease	Yes	No	No
18	GP702	FLAMSA/BU	MUD	Male	Deceased	29/05/2015	Disease	Yes	No	No
19	MS714	Flu/Melph/ Campath	Sibling	Male	Deceased	19/04/2015	GvHD gut	No	Yes	No
20	BL751	FLAMSA/BU	MUD	Male	Alive	NA	NA	No	No	No
21	TT815	BEAM/ Campath	MUD	Male	Deceased	05/09/2017	Disease	Yes	Yes	No
22	RH746	Flu/Bu/ATG	MUD	Female	Deceased	05/11/2015	Disease	Yes	No	No
23	SB710	FLAMSA/BU	MUD	Male	Deceased	14/06/2016	Prostate cancer	No	Yes	No
24	CC721	BEAM/Campath	Sibling	Female	Deceased	26/12/2015	Disease	Yes	Yes	No
25	DW703	Cyclo/TBI	Sibling	Male	Alive	NA	NA	no	No	No
26	AS738	Flu/Bu/ATG	Sibling	Male	Deceased	31/05/2016	Disease	Yes	No	No

Supplementary Table 3: CMV allo-HSCT samples and time points.

Patient code	Pre-HSCT	Pre-reactivation	Reactivation	Week 1	Week 2	Week 3	Week 4	+3m	+6m	+10m
GB788	Yes	Yes	Yes	Yes	Yes	Yes	Yes	Yes	Yes	Yes
Date	03/02/2016	23/02/2016	02/03/2016	09/03/2016	16/03/2016	23/03/2016	30/03/2016	06/07/2016	24/08/2016	08/02/2017
Week		Week 2 post HSCT	Week 3 post HSCT	W4	W5	W6	W7	W21	W28	W52
Lymphocyte count (10^9/L)	0	0.3	0.1	0.1	0.1	0.5	0.7	3.3	4.4	3.2
Viral load (copies/ml)			462	No result	<200	<200	<200	<200	<200	<200
Months (average)								4.2	5.8	10.5
DH805	Yes	Yes	Yes	Yes	Yes	Yes	Yes	Yes	Yes	Yes
Date	15/07/2016	10/08/2016	24/08/2016	01/09/2016	07/09/2016	14/09/2016	21/09/2016	23/11/2016	08/02/2017	05/06/2017
Week		Week 2 post HSCT	Week 4 post HSCT	W5	W6	W7	W8	W17	W28	W45
Lymphocyte count (10^9/L)	0	0.3	0.5	0.2	0.4	0.4	0.4	6.6	7.9	5.4
Viral load (copies/ml)			664	1095	2381	<200	<200	<200	<200	<200
Months (average)								3.0	5.6	9.5
SD783	No	Yes	No	Yes	Yes	Yes	No	Yes	Yes	Yes
Date		17/03/2016	23/03/2016	30/03/2016	07/04/2016	13/04/2016		22/06/2016	24/08/2016	05/07/2017
Week		Week 3 post HSCT	Week 5 post HSCT	W6	W7	W8		W18	W27	W41
Lymphocyte count (10^9/L)		0.1		0.1	0.1	0.2		0.4	1.2	2.9
Viral load (copies/ml)			749	1131	945	0		<200	<200	<200
Months (average)								3.0	5.1	8.4
MW820	Yes	Yes	No	Yes	Yes	No	Yes	No	No	No
Date	24/08/2016	28/09/2016	05/10/2016	12/10/2016	19/10/2016		02/11/2016			
Week		Week 4 post HSCT	Week 5 post HSCT	W6	W7		W9			
Lymphocyte count (10^9/L)	1.4	0.6		0.6	0.9		1.1			

Viral load (copies/ml)			436	654	892		0			
Months (average)										
KD801	No	Yes	No	No	Yes	Yes	No	Yes	No	No
Date		03/08/2016	10/08/2016		24/08/2016	31/08/2016		21/12/2016		
Week		Week 4 post HSCT	Week 6 post HSCT		W7	W8		W24		
Lymphocyte count (10^9/L)		0.5			0.5	1.6		1.2		
Viral load (copies/ml)			677		26275	32021		1480		
Months (average)								4.4		
SB789	Yes	No	No	Yes	Yes	Yes	No	No	No	No
Date	09/03/2016		20/04/2016	27/04/2016	04/05/2016	11/05/2016				
Week			Week 5 post HSCT	W6	W7	W8				
Lymphocyte count (10^9/L)	2.5			0.1	0.2	0.4				
Viral load (copies/ml)			2275	4986	4904	884				
Months (average)										
MS830	No	Yes	No	No	Yes	No	Yes	Yes	No	No
Date		02/11/2016	09/11/2016		23/11/2016		07/12/2016	22/02/2017		
Week		Week 4 post HSCT	Week 5 post HSCT		W7		W9	W20		
Lymphocyte count (10^9/L)		0.1			0.1		0.1	2.8		
Viral load (copies/ml)			1233		32036		13938	<200		
Months (average)								3.5		
MV792	Yes	No	Yes	Yes	Yes	Yes	Yes	Yes	Yes	Yes
Date	16/03/2016		06/04/2016	13/04/2016	20/04/2016	27/04/2016	04/05/2016	10/08/2016	28/09/2016	01/02/2017
Week			Week 2 post HSCT	W3	W4	W5	W6	W20	W27	W45
Lymphocyte count (10^9/L)	0.7		0.2	0.2	0.4	0.4	0.5	2.5	0.8	1.2
Viral load (copies/ml)			304	573	<200	<200	206	<200	329	<200

Months (average)								4.2	5.8	10.0
DJ802	Yes	No	Yes	Yes	Yes	Yes	Yes	Yes	Yes	Yes
Date	29/06/2016		10/08/2016	17/08/2016	24/08/2016	31/08/2016	07/09/2016	01/12/2016	22/02/2017	17/05/2017
Week			Week 5 post HSCT	W6	W7	W8	W9	W21	W33	W45
Lymphocyte count (10^9/L)	0.9		0.3	0.2	0.5	0.3	0.6	1.1	1.2	1.7
Viral load (copies/ml)			667	4860	1032	<200	<200	<200	<200	<200
Months (average)								3.7	6.5	9.3
PR798	Yes	No	No	Yes	Yes	Yes	Yes	Yes	No	Yes
Date	23/06/2016		31/08/2016	07/09/2016	14/09/2016	21/09/2016	28/09/2016	14/12/2016		05/07/2017
Week			Week 9 post HSCT	W10	W11	W12	W13	W24		W49
Lymphocyte count (10^9/L)	0.5			1.6	2.1	1.4	1.5	3.6		2.5
Viral load (copies/ml)			681	1455	6379	27596	85368	<200		<200
Months (average)								3.5		9.3
RF803	Yes	Yes	No	Yes	Yes	Yes	No	Yes	Yes	Yes
Date	29/26/2016	17/08/2016	24/08/2016	31/08/2016	07/08/2016	14/09/2016		23/11/2016	15/02/2017	07/06/2017
Week		Week 6 post HSCT	Week 7 post HSCT	W8	W9	W10		W20	W32	W48
Lymphocyte count (10^9/L)	2.5	0.2		0.9	1.1	1.1		2.0	2.9	2.3
Viral load (copies/ml)			1178	1250	249	0		<200	<200	<200
Months (average)								3.0	5.8	9.5
EB831	Yes	Yes	No	Yes	Yes	Yes	Yes	Yes	Yes	No
Date	12/10/2016	16/11/2016	23/11/2016	01/12/2016	07/12/2016	14/12/2016	21/12/2016	15/03/2017	07/06/2017	
Week		Week 4 post HSCT	Week 5 post HSCT	W6	W7	W8	W9	W21	W33	
Lymphocyte count (10^9/L)	0	1.1		0.7	0.6	0.4	0.5	1.2	1.2	
Viral load (copies/ml)			294	1664	1264	<200	<200	<200	<200	
Months (average)								3.7	6.5	

PF787	Yes	Yes	Yes	Yes	Yes	Yes	Yes	No	Yes	No
Date	26/01/2016	17/02/2016	16/03/2016	23/03/2016	30/03/2016	06/04/2016	13/04/2016		24/08/2016	
Week		Week 3 post HSCT	Week 7 post HSCT	W8	W9	W10	W11		W30	
Lymphocyte count (10^9/L)	0	0.2	0.1	0.1	0.1	0.1	0.1		0.8	
Viral load (copies/ml)			516	858	606	269	<200		<200	
Months (average)									5.3	
RF794	Yes	Yes	Yes	Yes	Yes	No	Yes	Yes	Yes	No
Date	04/05/2016	22/06/2016	06/07/2016	13/07/2016	20/07/2016		03/08/2016	28/09/2016	21/12/2016	
Week		Week 6 post HSCT	Week 8 post HSCT	W9	W10		W12	W20	W32	
Lymphocyte count (10^9/L)	0.3	0.6	0.7	1.2	1.1		0.9	1.1	2.4	
Viral load (copies/ml)			4640	908	<200		<200	<200	<200	
Months (average)								2.8	5.6	
RW762	No	Yes	No	No	Yes	No	Yes	No	No	No
Date		18/11/2015	06/01/2016		20/01/2015		03/02/2016			
Week		Week 4 post HSCT	Week 11 post HSCT		W13		W15			
Lymphocyte count (10^9/L)		0.5			1.2		0.6			
Viral load (copies/ml)			1227		<200		<200			
Months (average)										
LW772	Yes	No	No	Yes	No	No	No	Yes	No	Yes
Date	25/11/2015		14/12/2015	13/01/2016				24/02/2016		19/10/2016
Week			Week 5 post HSCT	W6				W12		W46
Lymphocyte count (10^9/L)	1.9			0.5				0.8		1.7
Viral load (copies/ml)			5066	<200				<200		<200
Months (average)								2.8		10.3
IV779	Yes	Yes	Yes	No	Yes	No	Yes	Yes	Yes	Yes

Date	05/01/2016	11/05/2016	25/05/2016		08/06/2016		22/06/2016	27/07/2016	23/11/2016	12/04/2017
Week		Week 4 post HSCT	Week 6 post HSCT		W8		W10	W15	W32	W52
Lymphocyte count (10^9/L)	1.9	0	0.2		0.2		0.2	0.2	3.6	3.3
Viral load (copies/ml)			854		1424		<200	not done	not done	not done
Months (average)								2.1	6.0	10.7
TD828	No	Yes	No	No	No	No	No	Yes	No	No
Date		15/09/2016	06/07/2016					12/10/2016		
Week		Week 7 post HSCT	Week 7 post HSCT					W18		
Lymphocyte count (10^9/L)		0.4						0.3		
Viral load (copies/ml)			3043					0		
Months (average)								3.2		
AS866	Yes	No	No	Yes	No	No	No	Yes	Yes	Yes
Date	17/05/2017		10/07/2017	17/07/2017				11/10/2017	24/01/2018	28/03/2018
Week			Week 7 post HSCT	W8				W20	W35	W44
Lymphocyte count (10^9/L)	1.5			2.7				3.1	4.3	5.8
Viral load (copies/ml)			3848	37761				<200	<200	<200
Months (average)								3.1	6.6	8.7
DR811	Yes	Yes	No	Yes	No	No	No	No	No	No
Date	27/08/2016	21/09/2016	04/10/2016	13/10/2016						
Week		Week 6 post HSCT	Week 8 post HSCT	W9						
Lymphocyte count (10^9/L)	0.3	0.9		0.2						
Viral load (copies/ml)			1062	<200						
Months (average)										
JC858	No	Yes	No	No	No	No	No	Yes	No	No
Date		23/05/2017	03/06/2017					02/08/2017		

Week		Week 4 post HSCT	Week 6 post HSCT					W14		
Lymphocyte count (10^9/L)		0.4						2		
Viral load (copies/ml)			228					558		
Months (average)								2.8		
SL865	No	No	Yes	Yes	Yes	Yes	No	Yes	Yes	Yes
Date			10/07/2017	17/07/2017	24/07/2017	31/01/2017		04/10/2017	10/01/2017	11/04/2018
Week			Week 7 post HSCT	W8	W9	W10		W21	W32	W45
Lymphocyte count (10^9/L)			0.2	2.6	1.6	1.6		0.8	1.7	2.8
Viral load (copies/ml)			3325	<200	<200	<200		270	<200	<200
Months (average)								2.8	6.1	9.1
SA793	Yes	Yes	No	Yes	Yes	No	No	No	No	No
Date	16/03/2016	18/05/2016	06/07/2016	19/07/2016	27/07/2016					
Week		Week 8 post HSCT	W11 post HSCT	W12	W13					
Lymphocyte count (10^9/L)	2.9	0.1		1.1	0.5					
Viral load (copies/ml)			1011	374	<200					
Months (average)										
TR862	Yes	No	No	No	No	No	No	Yes	Yes	Yes
Date	11/05/2017		26/06/2017					04/10/2017	06/12/2017	18/04/2018
Week			W5 post HSCT					W20	W29	W48
Lymphocyte count (10^9/L)	0							3.2	2.2	3.0
Viral load (copies/ml)			1935					<200	<200	<200
Months (average)								3.3	5.5	9.9
AP769	Yes	No	No	No	Yes	Yes	No	Yes	Yes	No
Date	18/11/2015		30/12/2015		13/01/2016	22/01/2016		20/04/2016	15/06/2016	
Week			W4 post HSCT		W6	W7		W20	W28	

Lymphocyte count (10^9/L)	1.9				0.4	1.2		0.3	0.6	
Viral load (copies/ml)			4293		42867	not done		416	390	
Months (average)								3.7	5.6	
NA825	Yes	Yes	No	No	No	Yes	No	Yes	No	No
Date	07/09/2016	09/11/2016	30/11/2016			21/12/2016		01/02/2017		
Week		Week 8 post HSCT	W11 post HSCT			W14		W19		
Lymphocyte count (10^9/L)	0.9	1.2				0.8		1.9		
Viral load (copies/ml)			387			<200		3245		
Months (average)								2.1		
MH840	No	Yes	Yes	Yes	No	Yes	No	Yes	No	No
Date		11/01/2017	15/03/2017	22/03/2017		05/04/2017		07/06/2017		
Week		Week 6 post HSCT	Week 8 post HSCT	W9		W12		W20		
Lymphocyte count (10^9/L)		0.2	0.9	1.1		1.5		0.8		
Viral load (copies/ml)			347	227		<200		<200		
Months (average)								2.8		
RH821	Yes	Yes	No	Yes	No	No	No	No	No	No
Date	24/08/2016	28/09/2016	12/10/2016	19/10/2016						
Week		W4 post HSCT	Week 6 post HSCT	W7						
Lymphocyte count (10^9/L)	1.5	0.6		1						
Viral load (copies/ml)			1327	8813						
Months (average)										
CS786	Yes	Yes	Yes	Yes	Yes	Yes	Yes	Yes	No	No
Date	20/01/2016	24/02/2016	09/03/2016	16/03/2016	23/03/2016	30/03/2016	06/04/2016	15/06/2016		
Week		W4 post HSCT	Week 6 post HSCT	W7	W8	W9	W10	W20		

Lymphocyte count (10^9/L)	1.3	0.2	0.1	0.1	0.1	0.1	0.1	0.6		
Viral load (copies/ml)			618	2433	2449	5916	1158	<200		
Months (average)								3.2		
GM884	Yes	Yes	Yes	Yes	No	Yes	No	No	No	No
Date	10/10/2017	13/12/2017	08/01/2017	15/01/2017		31/01/2018				
Week		W8 post HSCT	Week 11 post HSCT	W12		W15				
Lymphocyte count (10^9/L)	0.9	0.2	0.4	0.7		1.3				
Viral load (copies/ml)			329	561		<200				
Months (average)										
NJ886	Yes	Yes	No	Yes	No	No	Yes	Yes	No	No
Date	17/10/2017	10/11/2017	15/11/2017	22/11/2017			13/12/2017	28/02/2017		
Week		W2 post HSCT	W3 post HSCT	W4			W7	W18		
Lymphocyte count (10^9/L)	0.9	0		0.7			0.1	0.4		
Viral load (copies/ml)			701	788			380	834		
Months (average)								3.5		
NW853	Yes	No	No	No	Yes	No	No	Yes	Yes	No
Date	21/03/2017		19/04/2017		10/05/2017			19/07/2017	15/11/2017	
Week			W5 post HSCT		W5			W16	W33	
Lymphocyte count (10^9/L)	2.9				0.3			2.8	3.1	
Viral load (copies/ml)			2880		1266			<200	<200	
Months (average)								3.0	7.0	
FV878	No	Yes	No	No	Yes	Yes	Yes	No	No	Yes
Date		06/09/2017	13/09/2017		27/09/2017	04/10/2017	11/10/2017			30/05/2018
Week		W6 post HSCT	W8 post HSCT		W9	W10	W11			W44

Lymphocyte count (10^9/L)		0.1			0.6	1.1	1			3.8
Viral load (copies/ml)			5269		31706	not done	593			<200
Months (average)										8.6
BJ877	No	Yes	No	Yes	Yes	Yes	No	No	No	No
Date		09/08/2017	30/08/2017	04/09/2017	11/09/2017	18/09/2017				
Week		W5 post HSCT	W8 post HSCT	W8	W9	W10				
Lymphocyte count (10^9/L)		0.7		0.8	0.6	0.5				
Viral load (copies/ml)			898	3813	725	270				
Months (average)										
KJ907	Yes	Yes	No	Yes	No	No	Yes	Yes	No	No
Date	15/02/2018	26/03/2018	04/04/2018	09/04/2018			02/05/2018	02/07/2018		
Week		W4 post HSCT	W5 post HSCT	W6			W9	W18		
Lymphocyte count (10^9/L)	0.1	0.3		0.2			0.4	1.2		
Viral load (copies/ml)			1063	1080			<200	<200		
Months (average)								2.9		
VP921	Yes	Yes	No	Yes	Yes	Yes	Yes	Yes	No	No
Date	18/04/2018	18/06/2018	02/07/2018	09/07/2018	16/07/2018	23/07/2018	01/08/2018	17/10/2018		
Week		W8 post HSCT	W10 post HSCT	W11	W12	W13	W14	W25		
Lymphocyte count (10^9/L)	0.3	0.8	0.8	1	1.1	0.7	0.7	0.8		
Viral load (copies/ml)			923	362	<200	<200	<200	474		
Months (average)								3.6		
SW883	Yes	No	Yes	No	Yes	No	No	Yes	No	No
Date	02/10/2017		20/11/2017		04/12/2017			29/01/2018		
Week			W6 post HSCT		W8			W16		
Lymphocyte count (10^9/L)	1.8		0.3		0.6			1.4		

Viral load (copies/ml)			4131		1233			<200		
Months (average)								2.3		
GJ923	No	Yes	No	Yes	Yes	Yes	Yes	No	No	No
Date		13/08/2018	03/09/2018	10/09/2018						
Week		W12 post HSCT	W15 post HSCT	W16	W17	W18	W19			
Lymphocyte count (10^9/L)		0.3		0.7	1.2	1	0.9			
Viral load (copies/ml)			283	<200	<200	<200	<200			
Months (average)										
RA893	No	Yes	No	No	No	Yes	No	Yes	No	Yes
Date		28/11/2017	20/12/2017			10/01/2018		21/03/2018		24/10/2018
Week		W2 post HSCT	W6 post HSCT			W8		W18		W49
Lymphocyte count (10^9/L)		0				0.5		1.5		1.7
Viral load (copies/ml)			469			<200		<200		<200
Months (average)								2.3		2.3
RH548	Yes	No	Yes	No	No	No	Yes	Yes	Yes	Yes
Date	16/08/2012		26/09/2012				24/10/2012	16/10/2012	22/05/2013	24/07/2013
Week			W5 post HSCT				W9	W21	W39	W48
Lymphocyte count (10^9/L)	0		0.2				0.6	0.1	4.3	7.5
Viral load (copies/ml)			908				372	503	2461	218
Months (average)								3.7	7.9	10.0
DW505	Pre	No	No	No	No	No	No	Yes	No	Yes
Date	17/11/2011		11/01/2012					09/05/2012		21/11/2012
Week			W5 post HSCT					W24		W52
Lymphocyte count (10^9/L)	0.1		1.6					5		2.2
Viral load (copies/ml)			18994					<200		44428

Months (average)								14.0		10.5

Supplementary Table 4: 'No reactivation' allo-HSCT samples and time points.

Patient code	Pre-HSCT	W4	W6	W7	W8	W9	W10	+3m	+6m	+10m
AS827	Yes	Yes	Yes	No	No	No	No	Yes	Yes	Yes
Date	15/09/2016	19/10/2016	02/11/2016					14/12/2016	15/02/2017	19/07/2017
Week								W12	W24	W43
Lymphocyte count (10^9/L)	3.0	1.0	1.4					0.8	0.5	1.4
JS832	Yes	Yes	Yes					Yes	Yes	Yes
Date	26/10/2016	01/12/2016	14/12/2016					25/01/2017	29/03/2017	13/01/2017
Week								W12	W21	W45
Lymphocyte count (10^9/L)	0.0	0.1	0.0					0.2	0.3	0.7
CG833	No	Yes					Yes	Yes	Yes	
Date		14/12/2016					25/11/2014	08/02/2017	29/03/2017	
Week								W12	W21	
Lymphocyte count (10^9/L)		0.6					1.8	1.0	0.7	
JG776	Yes	Yes	Yes					Yes	Yes	
Date	03/12/2015	06/01/2016	20/01/2016					02/03/2016	25/05/2016	
Week								W12	W24	
Lymphocyte count (10^9/L)	0.0	0.7	0.6					1.0	0.7	
AM778	Yes	Yes	Yes						Yes	
Date	17/12/2015	20/01/2016	03/02/2016						18/05/2016	
Week									W21	
Lymphocyte count (10^9/L)	0.6	0.6	0.7						1.1	

DC780	Yes	Yes	Yes		Yes			Yes	Yes	Yes
Date	06/01/2016	10/02/2016	24/02/2016		03/02/2016			06/04/2016	29/16/16	12/10/2016
Week								W12	W24	W39
Lymphocyte count (10^9/L)	0	0.1	0.1		0.1			0.3	0.2	0.4
CK782	Yes	Yes	Yes							Yes
Date	01/03/2016	06/04/2016	20/04/2016							14/12/2016
Week										W40
Lymphocyte count (10^9/L)	0.1	0.1	0.1							2.5
ED773	Yes		Yes					Yes		Yes
Date	25/11/2015		13/01/2016					23/02/2016		07/09/2016
Week								W12		W40
Lymphocyte count (10^9/L)	0.1		0.3					0.1		1.3
AS738	Yes	Yes	Yes		Yes			Yes	Yes	Yes
Date	11/03/2015	15/04/2015	29/04/2015		13/05/2015			15/07/2017	02/09/2015	16/03/2016
Week								W17	W24	W52
Lymphocyte count (10^9/L)	1.7	1.7	4.0		3.8			1.3	1.5	1.5
JR728	Yes	Yes	Yes				Yes		Yes	Yes
Date	07/01/2015	11/02/2015	25/02/2015				25/03/2015		23/09/2015	16/12/2015
Week									W36	W48
Lymphocyte count (10^9/L)	0.3	0.4	0.5				0.3		0.6	1.5
JD757	Yes	Yes	Yes		Yes		Yes	Yes	Yes	Yes
Date	16/09/2015	21/10/2015	04/11/2015		18/11/2015		02/12/2015	16/12/2015	16/03/2016	06/07/2016
Week								W12	W25	W40

Lymphocyte count (10^9/L)	0.4	0.5	0.7		0.9		0.8	0.8	1.7	1.9
GT767	Yes	Yes						Yes	Yes	Yes
Date	09/11/2015	09/12/2015						17/02/2016	18/05/2016	16/11/2016
Week		W3						W13	W27	W52
Lymphocyte count (10^9/L)	1.9	0.3						0.3	0.6	1.2
KS725	Yes		Yes		Yes			Yes	Yes	Yes
Date	03/12/2014		21/01/2015		04/02/2015			04/03/2015	03/06/2015	09/09/2015
Week								W12	W24	W39
Lymphocyte count (10^9/L)	0.7		0.2		1			1.2	0.9	1.3
DM810	Yes	Yes	Yes					Yes	Yes	Yes
Date	27/07/2016	01/09/2016	12/10/2016					26/10/2016	18/01/2017	02/08/2017
Week								W12	W24	W52
Lymphocyte count (10^9/L)	0.3	0	0.1					0.1	0.5	0.6
DP790	Yes	Yes	Yes					Yes	Yes	
Date	16/03/2016	20/04/2016	04/05/2016					15/06/2016	14/09/2016	
Week								W12	W25	
Lymphocyte count (10^9/L)	0.5	0	0.4					0.3	0.2	
CM785		Yes		Yes	Yes		Yes	Yes		
Date		16/02/2016		13/04/2016	20/04/2016		04/05/2016	18/05/2016		
Week								W12		
Lymphocyte count (10^9/L)		1.5		0.6	0.5		0.5	0.3		
KC784		Yes	Yes		Yes			Yes	Yes	
Date		09/03/2016	23/03/2016		06/04/2016			04/05/2016	31/01/2018	
Week								W12	W24	
Lymphocyte count (10^9/L)		0.5	0.6		1.7			2.0	2.9	

GP702	Yes	Yes		Yes		Yes		Yes		Yes
Date	16/07/2014	20/08/2014		17/09/2014		02/10/2014		26/11/2014		22/04/2015
Week		W3						W14		W38
Lymphocyte count (10^9/L)	0.3	0.4		1.2		1.2		1.1		1.2
MS714				Yes		Yes		Yes		
Date				03/12/2014		17/12/2014		07/01/2015		
Week								W12		
Lymphocyte count (10^9/L)				0.7		0.4		0.4		
BL751	Yes	Yes	Yes							
Date	01/07/2015	05/08/2015	19/08/2015							
Week										
Lymphocyte count (10^9/L)	0.2	0.4	0.6							
TT815			Yes		Yes			Yes		
Date			28/09/2016		12/10/2016			09/11/2016		
Week								W12		
Lymphocyte count (10^9/L)			0.1		0.2			0.2		
RH746	Yes		Yes		Yes	Yes		Yes		
Date	06/06/2015		22/07/2015		05/08/2015	12/08/2015		09/09/2015		
Week								W13		
Lymphocyte count (10^9/L)	0.2		0.5		1.2	1.5		0.9		
SB710	Yes	Yes				Yes				
Date	17/09/2014	29/10/2014				19/11/2014				
Week										
Lymphocyte count (10^9/L)	0.5	0.6				0.3				
CC721	Yes					Yes	Yes	Yes	Yes	Yes

Date	19/11/2014					28/01/2015	04/02/2015	04/03/2014	20/05/2015	19/08/2015
Week								W14	W24	W38
Lymphocyte count (10^9/L)	0					0.3	0.3	0.5	0.6	0.9
DW703			Yes		Yes		Yes	Yes	Yes	Yes
Date			24/09/2014		08/10/2014		22/10/2014	19/11/2014	04/02/2015	06/05/2015
Week								W14	W24	W38
Lymphocyte count (10^9/L)			1.1		1		0.7	1.2	1.3	2.1

Notes

Yes : Sample available

No : Sample not available

Supplementary Table 5: List of DNA from serum and urine used for qPCR and viral DNA sequencing

DNA extraction from serum and urine by using High Pure Nucleic Acid Kit

NO	PATIENT NO	DNA SERUM ng/µl	DNA URINE ng/µl
1	**SB789**	**295.90**	240.30
2	**SD783**	**313.10**	385.26
3	**PF787**	**219.91**	195.09
4	**RW762**	**218.56**	337.36
5	**AP769**	**291.43**	415.59
6	**CS786**	**247.65**	181.28
7	**GB788**	**425.02**	186.00
8	**RF794**	**232.50**	100.74
9	**PR798**	**412.18**	202.78
10	**RF803**	**255.07**	177.23
11	**BW744**	**322.77**	

DNA extraction from urine by using QIAmp® Viral RNA Kit

NO	PATIENT NO	DNA URINE ng/µl	NO	PATIENT NO	DNA URINE ng/µl
1	**RW762**	**7.23**	14	AP769	0.39
2	**DH805**	**55.12**	15	CS786	-1.40
3	**RF794**	**9.19**	16	DJ802	0.26
4	**MH840**	**10.75**	17	RF803	0.24
5	**BJ877**	**8.90**	18	AS866	2.36
6	**NW853**	**130.23**	19	FV878	3.68
7	**SD783**	**17.50**	20	KD801	0.28
8	**DR811**	**25.06**	21	MW820	0.28
9	**EB831**	**9.98**	22	TD828	-0.94
10	**MV792**	**8.66**	23	GB788	-2.43
11	**AA908**	**80.37**	24	MS830	0.43
12	**VP921**	**5.79**	25	NA825	0.72
13	**GJ923**	**132.16**			

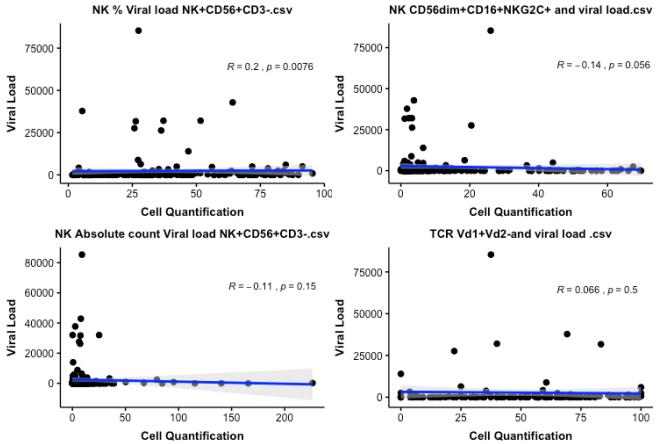
Notes:
UL40 peptide sequencing

SERUM
SD783: VMAPRTLIL
AP769: VMAPRTLIL
CS786: VMAPRTLIL

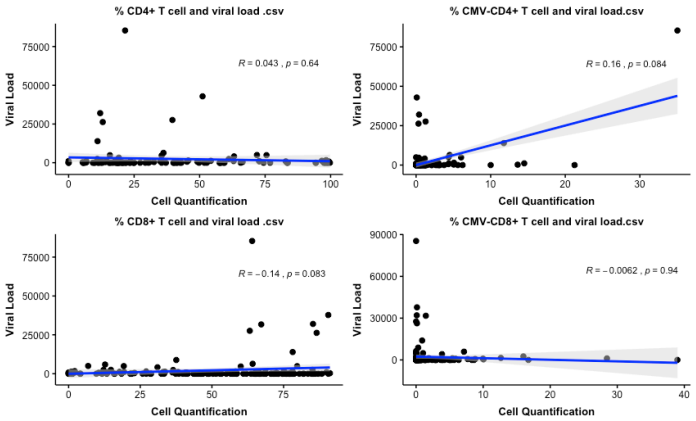
URINE
MH840: VMTPRSLLL
BJ877: VMAPRTLIL
MV792: VMAPRTLIL
AA908: VMAPRTLIL

Supplementary Figure 1: Viral load correlation with NK, CD8$^+$, CD4$^+$ and TCR Vδ1 cell percentages and absolute count

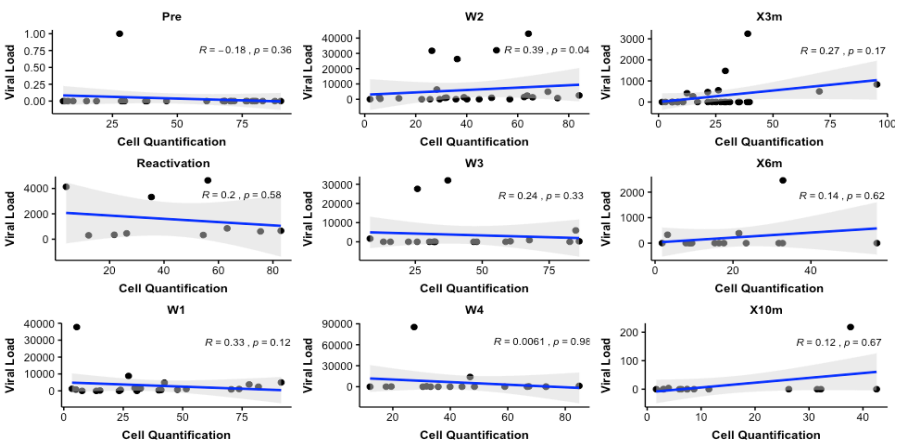
a) Viral load vs absolute cell counts and %: (all time points included) Spearman correlation



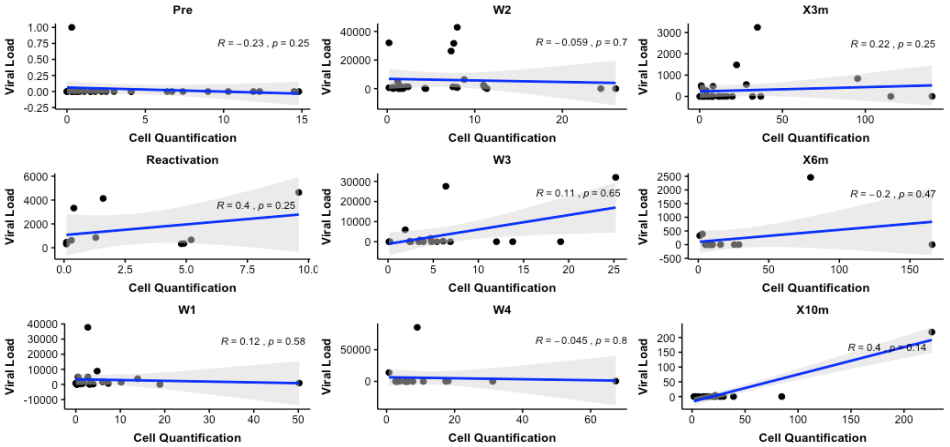
b) Viral load vs absolute cell counts: (all time points included) Spearman correlation



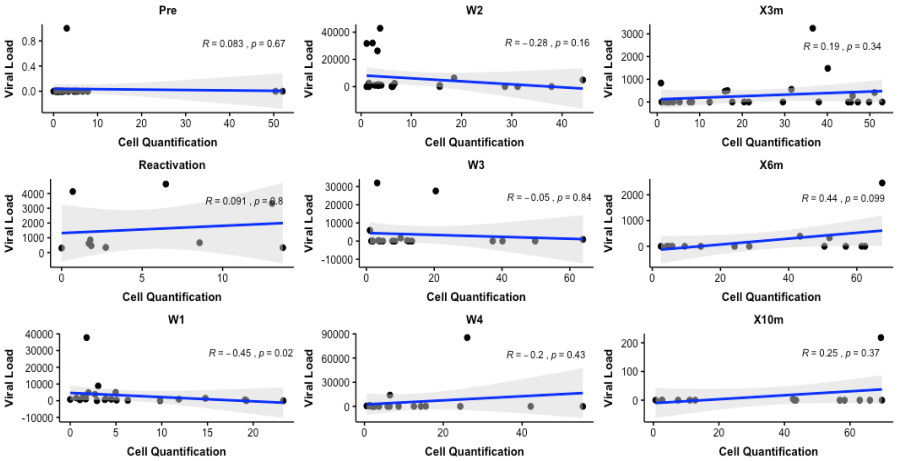
c) NK cell % and Viral load Spearman correlations at each time point



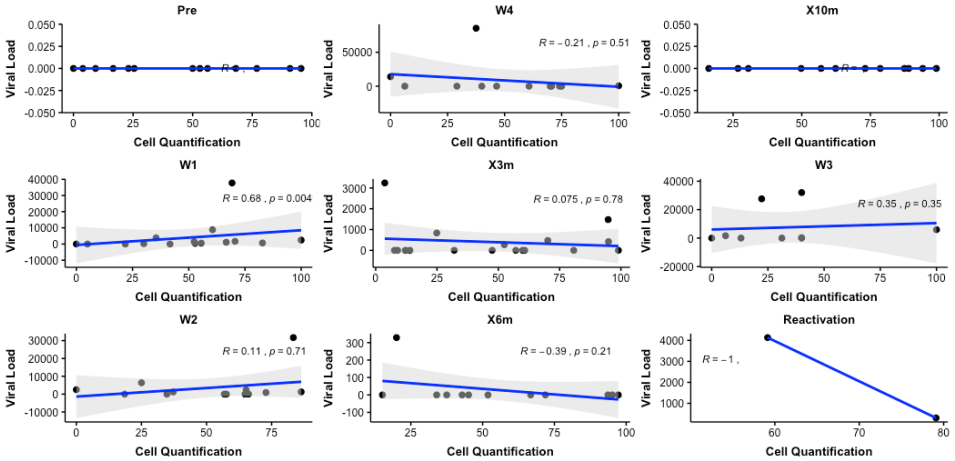
d) NK cell absolute count and Viral load Spearman correlations at each time point



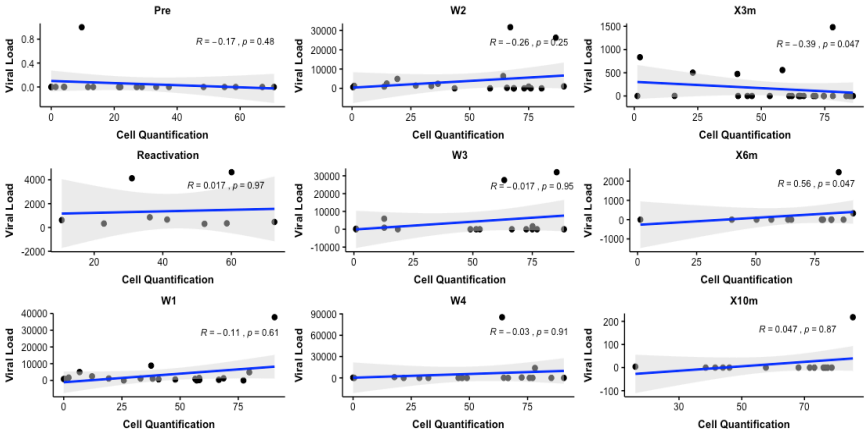
e) NK CD56^{dim}CD16^{bright}NKG2C^{+} cell % and Viral load Spearman correlations at each time point



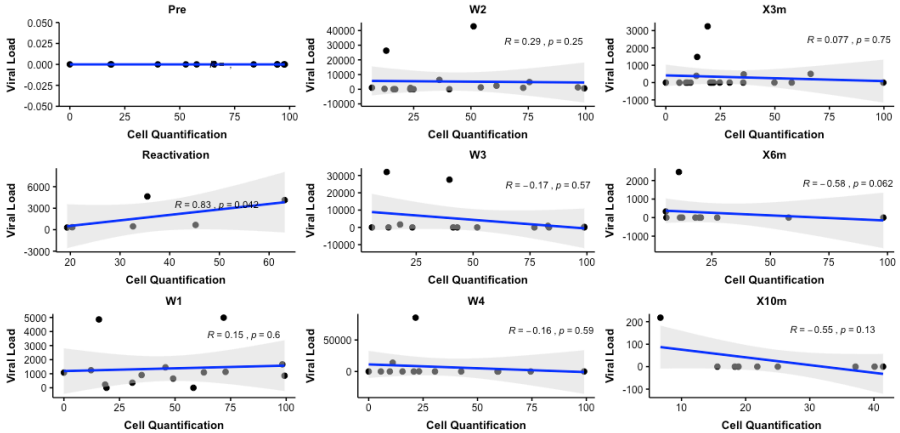
f) TCR Vδ1^{+}Vδ2^{-} % and viral load Spearman correlations at each time point



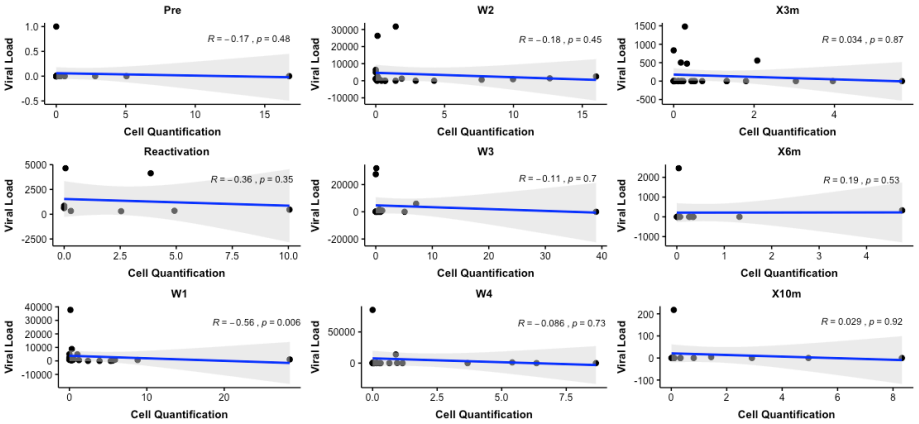
g) CD8^{+} T cells Spearman correlations at each time point



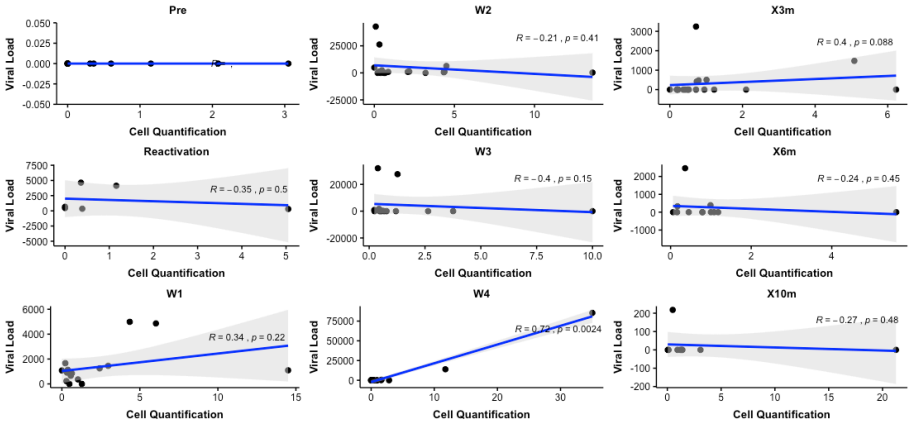
h) CD4^{+} T cells Spearman correlations at each time point



i) CMV-CD8⁺ T cells Spearman correlations at each time point



j) CMV-CD4⁺ T cells Spearman correlations at each time point



Supplementary Table 6. List of samples used for NK killing assay from healthy donors and CMV reactivation allo-HSCT patients

a) Healthy donors

No	CMV+	CMV-
1	TR	AK
2	NH	JM
3	KV	SE
4	DM	JVH
5	DA	LM
6	RP	BM
7	LF	HP
8	PM	
9	II	
10	SB	

b) CMV reactivation allo-HSCT

No	Patient ID	Week post HSCT	% NK NKG2C+
1	DH805	W45	69.7
2	DJ802	W45	12.7
3	PR798	W49	56.8
4	RF794	W15/12	62.4
5	RF803	W49	43.0
6	FV878	W44	0.6
7	GB788	W52	2.7
8	AS866	W41	2.63
9	LW772	W52	11.11
10	IV779	W52	16.11
11	TR862	W48	43.37
12	RH548	W52	69.39
13	DW505	W52	30.49

Supplementary Table 7. List of samples used for NK Intracellular Cytokines Staining from healthy donors, no reactivation and CMV reactivation allo-HSCT patients

No	HD	Allo-HSCT (No reactivation)	CMV reactivation
1	KV	GP702 W14	AP769 W28
2	LM	AS738 W8	NA825 W19
3	GF	KC784 W12	NW853 W19
4	JVH	KC784 W17	PF787 W30
5	NH		TR862 W30
6	SB		
7	DA		

*R statistical analyses were done by Dave Greenwood and Wayne Croft while CMV serum ELISA was performed by Jusnara Begum and Sara Barbieri

Supplementary Table 8. List of Healthy donors

	CMV +	CMV-
1	PM	SE
2	KV	LM
3	DM	JM
4	GF	JVH
5	II	PM2
6	UA	HP
7	SB	EJ
8	SP	AK
9	SW	PC
10	HJ	CI
11	LF	HR
12	MF	BM
13	TR	RB
14	NH	GT
15	RP	RJB
16	DA	AP
17	GM	EH
18	RA	NC
19	CDS	WT
20	SD	AL
21	MD	